Fernanda Mandelli

Estudo dos mecanismos de adaptação ao estresse oxidativo da bactéria termófila *Thermus filiformis*.

Evaluation of the adaptation mechanisms to the oxidative stress of the thermophilic bacterium *Thermus filiformis*.

Campinas, 2014

UNIVERSIDADE ESTADUAL DE CAMPINAS
FACULDADE DE ENGENHARIA DE ALIMENTOS

Fernanda Mandelli

Estudo dos mecanismos de adaptação ao estresse oxidativo da bactéria termófila *Thermus filiformis*.

Tese apresentada à Faculdade de Engenharia de Alimentos da Universidade Estadual de Campinas como parte dos requisitos exigidos para a obtenção do título de Doutora em Ciência de Alimentos.

Orientadora: PROF. DRA. ADRIANA ZERLOTTI MERCADANTE

Co-orientador: PROF.DR. FABIO MARCIO SQUINA

ESTE EXEMPLAR CORREPONDE À VERSÃO FINAL
DA TESE DEFENDIDA PELA ALUNA FERNANDA MANDELLI,
E ORIENTADA PELA PROFA. DRA. ADRIANA ZERLOTTI MERCADANTE.

_____

Campinas, 2014

Ficha catalográfica
Universidade Estadual de Campinas
Biblioteca da Faculdade de Engenharia de Alimentos
Márcia Regina Garbelini Sevillano - CRB 8/3647

M312e

Mandelli, Fernanda, 1984-
Estudos dos mecanismos de adaptaçãoo ao estresse oxidativo da bactéria termófila *Thermus filiformis* / Fernanda Mandelli. – Campinas, SP : [s.n.], 2014.

Orientador: Adriana Zerlotti Mercadante.
Coorientador: Fabio Marcio Squina.
Tese (doutorado) – Universidade Estadual de Campinas, Faculdade de Engenharia de Alimentos.

1. Proteoma. 2. Transcriptoma. 3. Genomas. 4. Estresse oxidativo. 5. Carotenoides. I. Mercadante, Adriana Zerlotti. II. Squina, Fabio Marcio. III. Universidade Estadual de Campinas. Faculdade de Engenharia de Alimentos. IV. Título.

Informações para Biblioteca Digital

Título em outro idioma: Evaluation of the adaptation mechanisms to the oxidative stress of the thermophilic bacterium *Thermus filiformis*
Palavras-chave em inglês:
Proteome
Transcriptome
Genomes
Oxidative stress
Carotenoids
Área de concentração: Ciência de Alimentos
Titulação: Doutora em Ciência de Alimentos
Banca examinadora:
Adriana Zerlotti Mercadante [Orientador]
André Ricardo de Lima Damásio
Camila Caldana
Gabriela Felix Persinoti
Leila Queiroz Zepka
Data de defesa: 07-08-2014
Programa de Pós-Graduação: Ciência de Alimentos

BANCA EXAMINADORA

_____

Profa. Dra. Adriana Zerlotti Mercadante
(orientadora)

_____

Dr. André Ricardo de Lima Damasio
(membro)

_____

Dra. Camila Caldana
(membro)

_____

Dra. Gabriela Felix Persinoti
(membro)

_____

Dra. Leila Queiroz Zepka
(membro)

_____

Dr. Anderson de Souza Sant'Ana
(membro)

_____

Dra. Juliana Pfrimer Falcão
(membro)

_____

Dr. William de Castro Borges
(membro)

Resumo

Espécies reativas de oxigênio (ERO) e nitrogênio (ERN) são comumente geradas dentro das células pela exposição a agentes endógenos e exógenos, estas espécies, quando em níveis normais, encontram-se envolvidas na produção de energia, regulação do crescimento celular, sinalização intercelular e síntese de substâncias biológicas importantes. Por outro lado, se produzidas em excesso, podem provocar oxidação lípidica, de proteínas ou do DNA causando o que conhecemos por estresse oxidativo.

Para combater o excesso de espécies reativas, os organimos produzem moléculas antioxidantes tais como os carotenoides e enzimas como superóxido dismutase e catalase, com alto potencial de aplicabilidade na formulação de alimentos, indústria farmacêutica e de cosméticos.

Diante do exposto, esta pesquisa teve por objetivo avaliar a produção de carotenoides, proteoma e transcriptoma da bactéria termófila *Thermus filiformis* quando submetida à diferentes condições de cultivo: presença e ausência de H_2O_2 e temperatura de crescimento abaixo (63 °C) e acima (77 °C) do seu ótimo (70 °C). Para tanto, os carotenoides e a proteômica foram caracterizados por cromatografia líquida e espectrometria de massas, e o genoma e transcriptoma foram analisados com o emprego de tecnologias de sequenciamento de última geração e ferramentas computacionais.

Algumas diferenças foram observadas na produção de carotenoides de acordo com cada condição de cultivo. Quanto ao perfil de carotenoides, nas condições a 70 °C e a 77 °C os carotenoides majoritários foram termozeaxantinas e termobiszeaxantinas enquanto que para condição a 63 °C foi a zeaxantina livre. A amostra cultivada a 70 °C sem adição de H_2O_2 apresentou a maior quantidade de carotenoides totais (1.516 μg/g), por outro lado o extrato rico em carotenoides que apresentou maior capacidade de desativação do radical peroxila (50,5) foi o da amostra com adição de H_2O_2.

Com o intuito de se obter um banco de dados para as análises de transcriptomica e proteômica, foi realizado o sequenciamento de DNA, o qual apresentou um tamanho total de 2,46MB.

Na análise de transcriptoma, 97,1% dos genes codificadores de proteínas preditos apresentaram expressão com valores detectáveis de RSEM (RNA-Seq by Expectation-Maximization). Através da análise do transcriptoma foram identificados 37% e 5,86% dos genes diferencialmente expressos (p-valor<0,05) nos ensaios com diferentes temperaturas e com e sem adição de H_2O_2, respectivamente.

Através da análise do proteoma, no ensaio com diferentes temperaturas, foi encontrado um total de 27,7% proteínas diferencialmente expressas com um FDR (False Discovery Rate) < 0,05%, sendo 20% significativamente diferentes (p-valor<0,05, teste T) e, no ensaio com e sem adição de H_2O_2, um total de 28,3% com um FDR < 0,05%, sendo 6% significativamente diferentes (p-valor<0,05, teste T).

Os resultados do presente estudo mostram que os principais processos afetados pela mudança de temperatura e adição de peróxido de hidrogênio foram: catabolismo, transcrição e tradução de proteínas. Observou-se também que a alteração na temperatura teve uma maior influencia na expressão diferencial de genes e proteinas do que a adição de peróxido.

Através das análises do trancriptoma e do proteoma de *T. filiformis* foram identificadas enzimas termo-estáveis com potencial de aplicação industrial, como por exemplo alfa-amilases, superóxido dismuatse, alfa-galactosidases e esterases. Além disso, o extrato rico em carotenoides dessa bactéria apresentou capacidade de desativar o radical peroxila superior à capacidade de extratos de frutas e até mesmo de padrões de carotenoides.

Devido à conhecida capacidade antioxidante e potencial de aplicabilidade na indústria, foi feita a clonagem, expressão e caracterização da enzima superóxido dismutase de *Thermus filiformis* (TfSOD). A TfSOD apresentou atividade enzimática utilizando como cofator tanto manganês quanto ferro e termoestabilidade a até 80 °C.

Palavras chave: proteoma, transcriptoma, genoma, estresse oxidativo, carotenoides.

Abstract

Reactive oxygen (ROS) and nitrogen (RNS) species are commonly produced in the cells by exposure to endogenous and exogenous agents, these species, when at normal levels, are involved in energy production, cell growth regulation, intercellular signaling and synthesis of important biological substances. On the other hand, if overproduced, can cause lipid, protein and DNA oxidation, leading to what is known as oxidative stress.

To combat excessive reactive species, organisms produce antioxidant molecules such as carotenoids and enzymes such as superoxide dismutase and catalase, with potential application on food formulations, pharmaceutical and cosmetics.

Therefore the aim of this research was to evaluate the carotenoid production, the proteome and transcriptome of *Thermus filiformis* when submitted to the some cultivation conditions under stress: without and with hydrogen peroxide and temperature below (63 °C) and above (77 °C) the optimum (70 °C). In order to achieve this aim, proteome and carotenoids were characterized by liquid chromatography and mass spectrometry and the genome and transcriptome were analyzed using next generation technology and computational tools.

Regarding to the carotenoid profile, the major carotenoids under conditions at 70 °C (without and with H_2O_2) and at 77 °C were thermozeaxanthins thermobiszeaxanthin while at 63 °C was free-zeaxanthin. The sample cultivated at 70 °C without H_2O_2 showed the highest amount of total carotenoid (1516 μg/g of dry mass), on the other hand the sample with the highest antioxidant capacity was the one cultivated at 70 °C with H_2O_2. The carotenoid rich extract of all conditions studied showed a peroxyl scavenging capacity higher than those carotenoid rich extracts from some fruits and from some carotenoid standards, demonstrating the potential applicability of *T. filiformis* extracts in industry.

In order to obtain a data bank for proteomic and transcriptome analysis, the DNA sequencing was performed, which presented a total size of 2.46MB.

In the transcriptome analysis, 97.1% of predicted protein coding genes showed detectable expression with RSEM values (RNA-Seq by Expectation-Maximization). Through the computational analysis of *T. filiformis* transcriptome 37% and 5.86% of the genes significantly different (p-value < 0.05) in the assays with different temperatures and with and without H_2O_2 were identified, respectivelly.

In the total proteome analysis a total of 27.7% proteins were differentially expressed with a FDR (False Discovery Rate) < 0.05%, being 20% significantly different (p-value < 0.05, T-test) in the temperature assay and 28.3% proteins with a FDR (False Discovery Rate) < 0.05%, being 6% significantly different (p-value < 0.05, T-test) in the H_2O_2 assay. Some changes were observed in the carotenoid production according to the cultivation condition. The results of this study show that the main processes affected by temperature change and addition of H_2O_2 were: catabolism, transcription and protein translation. It was also observed that the change in temperature has greater influence on the differential expression of genes and proteins than the H_2O_2 addition.

Through trancriptome and proteome analysis of *T. filiformis* thermostable enzymes have been identified with potential industrial applications, such as alpha-amylases, superoxide dismutase, alpha-galactosidases and esterases. Moreover, the extract rich in carotenoids of this bacterium had a greater peroxyl radical scavenging capacity than the capacity of fruit extracts and even carotenoids standards.

Due to its known antioxidant capacity and potential application in industry, a superoxide dismutase from *Thermus filiformis* (TfSOD) was cloned, expressed and characterized. The TfSOD showed cambialistic characteristics, once it had enzymatic activity with either manganese or iron as cofactor and thermostability until 80 °C.

Key words: proteome, transcriptoma, genome, oxidative stress, carotenoids.

Sumário

CAPÍTULO III

Dedico este trabalho a minha mãe Marli A. P. Mandelli, ao meu pai Itacir A. Mandelli (in memorian) e a minha irmã Daniela Mandelli pelo amor, incentivo e apoio a mim dedicados. E a todos que de uma forma ou de outra colaboraram para a realização desta pesquisa.

Agradecimentos

A Deus por me amparar nos momentos difíceis, me dar força interior para superar as dificuldades e por me mostrar o caminho nas horas difíceis.

A minha mãe, meu pai (*in memorian*) e minha irmã, pelo amor incondicional.

Aos meus familiares que mesmo distantes sempre me apoiaram na busca desta conquista.

Agradeço a meus mestres, Profa. Dra. Adriana Zerlotti Mercadante e Prof. Dr. Fabio Marcio Squina pela atenção, dedicação e pelas exigências na busca do conhecimento.

À banca examinadora,Dr. Anderson de Souza Sant'Ana, Dr. André Ricardo de Lima Damasio, Dra. Camila Caldana, Dra. Juliana Pfrimer Falcão, Dra. Gabriela Felix Persinoti, Dra. Leila Queiroz Zepka e Dr. William de Castro Borges pelas contribuições, sugestões e atenção dedicadas ao aperfeiçoamento deste trabalho.

A Universidade Estadual de Campinas (Unicamp) e ao Centro Nacional de Pesquisa em Energia e Materiais (CNPEM) por tornar possível a realização desta pesquisa.

A Prof. Dra. Adriana Paes Leme, Romênia Domingues e Carolina Carnielli do Laboratório Nacional de Biociências (LNBio) pela contribuição com as análises de proteômica e interactoma.

Ao Prof. Dr. Igor Polikarpov e Dr. César Camilo do Instituto de Física da Universidade de São Paulo campus de São Carlos por ceder o sequenciador para análise de genômica e transcriptômica.

Ao Prof. Dr. Vitor Leite e Dr. Ronaldo Oliveira da Universidade Estadual Paulista Júlio de Mesquita Filho (Unesp) pela colaboração com a modelagem computacional da enzima superóxido dismutase.

Ao Prof. Dr. Rolf Prade e Brian Couger da Universidade de Oklahoma- USA e Dr. Diego Riaño-Pachón do Laboratório Nacional de Ciência e Tecnologia do Bioetanol (CTBE) pela realização das análises de bioinformática.

A todos os amigos do Laboratório de Química de Alimentos das Unicamp pela amizade, companheirismo e suporte intelectual, em especial ao Eliseu, Renan, Marcella, Lilian, Poliana, Bruno, Naira, Elisângela, Aline, Ana Augusta, Adria, Hugo, Aline e Rosemar.

A todos os amigos do CTBE por terem me recebido com muito carinho, pela amizade e pela ajuda durante todo doutorado, em especial João, Fernanda, Carla, Rosana, Lívia, Thabata, Rodrigo, Ana, Douglas, Rebeca, Evandro, Beto, Thiago, André, Marcelo, Cristiane...

Um agradecimento especial a todos os amigos que fiz durante meu tempo em Campinas, amigos estes que tornaram os dias aqui longe de casa mais leves e felizes. São muitos para mencionar, mas especialmente agradeço a Patrícia, Pollyane, Georgia, Michelle, Fernanda O., Renanta, Carla, Rosana, Silvana, Marcio, Wellington, Renan, Bruno, Elisangela, Fernanda B., Lívia....

A todos que de certa forma contribuíram para a realização deste trabalho.

Agradeço ao CNPq e Fapesp pelo incentivo financeiro para realização deste trabalho.

Por fim agradeço ao CNPq pela concessão da bolsa de fomento que tornou possível a realização deste trabalho.

Lista de Tabelas

CAPÍTULO I

CAPÍTULO II

CAPÍTULO III

SUPPLEMENTARY

Introdução e Justificativa

Micro-organismos extremófilos, tais como termofílicos, pscicrofílicos, acidofilicos, alcalifílicos, halofílicos e barofílicos, estão adaptados a condições extremas consideradas hostis pelo homem. Dentre os micro-organismos extremófilos, os termofílicos têm atraído intensas investigações resultando em um avanço nas pesquisas nos últimos anos. Estes micro-organismos são fontes microbiológicas de recursos com valor científico, como modelos biológicos para estudo dos mecanismos de termoadaptação, e com elevado potencial de aplicabilidade tecnológica em processos industriais conduzidos a altas temperaturas (Morozkina et al., 2010).

A adaptação dos micro-organismos termófilos às condições ambientais extremas a que são submetidos obrigou-os a desenvolver componentes celulares e estratégias bioquímicas para a sua sobrevivência. Dentre esses componentes podemos citar os carotenoides, com estruturas diferentes das comumente encontradas em vegetais, frutas, animais e outros organismos e as proteínas, que englobam as enzimas termoestáveis com características intrínsecas de termoestabilidade e resistência a desnaturação por fatores físicos e químicos (Yokoyama et al., 1995; Burguess et al., 1999; Lutnaes et al., 2004; Li et al., 2010).

Tanto os carotenoides como as proteínas com capacidade antioxidante fazem parte do sistema de defesa antioxidante que os organismos vivos desenvolveram para reduzir ou inibir reações de oxidação, que podem ser causadas por espécies reativas de nitrogênio (ERN) e espécies reativas de oxigênio (ERO). Tais espécies envolvem tanto espécies radicalares, como ânion superóxido ($O_2^{-\bullet}$), radicais hidroxila ($HO^{\bullet}$) e peroxila ($ROO^{\bullet}$), como não radicalares como oxigênio singlete ($^1O_2$) e peróxido de hidrogênio (H_2O_2) (Halliwell, 2012). Os ERO são gerados normalmente durante o metabolismo aeróbio, pois em concentrações fisiológicas eles são necessários para o funcionamento normal das células, no entanto a produção excessiva pode ser prejudicial à célula, uma vez que essas substâncias podem causar oxidação de lipídeos, proteínas e do DNA (Sivapriya e Srinivas, 2007).

É difícil apontar as estratégias de adaptação dos micro-organismos em resposta a diferentes condições de estresse através do estudo individual de moléculas produzidas pelos mesmos. Um dos princípios emergentes da biologia é de que geralmente a resposta de um micro-organismo a uma variedade de estímulos é dada não somente por um gene individual, mas sim por vias e redes biológicas (Quackenbush, 2007).

As moléculas de micro-organismos extremófilos oferecem novas oportunidades para biocatálise e biotransformação como resultado de sua alta estabilidade em condições adversas. Tanto a descoberta de novas espécies extremofílicas quanto a determinação do genoma, transcriptoma e proteoma destes organismos, proporcionam uma via para o descobrimento de novas moléculas, com a possibilidade de que estas conduzirão a novas aplicações industriais.

Estudos prévios com a bactéria *Thermus filiformis* (Mandelli et al. 2012a; Mandelli et al. 2012b) apresentaram a identificação dos carotenoides de *T. filiformis*, otimização das condições de cultivo (fonte de nitrogênio, fonte de carbono, temperatura, pH e quantidade de sais minerais) da bactéria para produção dos mesmos e avaliação da capacidade antioxidante dos extratos ricos em carotenoides. Estes trabalhos demostraram que as condições de cultivo influenciaram no perfil, quantidade e capacidade antioxidante dos carotenoides produzidos.

Diante do exposto, O presente projeto tem como meta a avaliação dos mecanismos de adaptação utilizados pela bactéria termófila *T. filiformis* quando submetidos a diferentes condições de estresse oxidativo - presença (100 μM) e ausência (0 μM) de peróxido de hidrogênio e temperaturas acima (77 °C) e abaixo (63 °C) da ótima (70 °C). Para atingir tais objetivos, foram realizadas as seguintes análises:

- Avaliação do perfil de carotenoides, quantificação de carotenoides totais e capacidade de desativação do radical peroxila pelos extratos de carotenoides, nas diferentes condições de cultivo;
- Sequenciamento do DNA total de *Thermus filiformis*;
- Identificação das proteínas diferentemente expressas nas diferentes condições de cultivo e clonagem e caracterização da enzima antioxidante, superóxido dismutase;
- Identificação dos genes diferencialmente expressos nas diferentes condições de cultivo.

Através da correlação dos dados obtidos pelas análises citadas acima foi possível a elucidação dos principais mecanismos de adaptação utilizados pela bactéria quando cultivada na presença/ausência de peróxido de hidrogênio e em altas/baixas temperaturas. Além disso, com este estudo foi possível apontar possíveis moléculas com potencial para aplicação industrial, como é o caso dos carotenoides e das enzimas, entre elas a enzima antioxidante superóxido dismutase.

CAPITULO I

Revisão Bibliográfica

1.1. Micro-organismos Extremófilos

Organismos extremófilos são aqueles adaptados a ambientes extremos, que por definição são locais onde os parâmetros físico-químicos, como por exemplo temperatura, concentração de sal, pressão, índice de radiação e valores de pH, atingem os limites nos quais a vida ocorre (Gargaud et al. 2005).

Os extremófilos podem ser subdivididos de acordo com a natureza do estresse ao qual são submetidos, como por exemplo: termofílicos/hipertermofílicos (altas temperaturas), psicrofílicos (baixas temperaturas), acidófilos (baixo pH), alcalófilos (alto pH), halófilos (alta concentração de sal), xerófilos (ambientes secos), barofílicos (alta pressão) e radiodúricos (alto índice de radiação). A tabela 1 mostra alguns organismos e as respectivas condições extremas às quais estes estão adaptados (Seckbach 2004).

Tabela 1: Extremófilos e condições ambientais em que estão adaptados.

Fator ambiental	Organismo	Habitat	Filogenia	Tolerância ao estresse
Alta temperatura	*Pyrolobus fumarii*	Fenda marítima	Archea-Crenarchacota	Máximo: 113 °C Ótimo: 106 °C Mínimo: 90 °C
Baixa temperatura	*Polaromonas vacuolata*	Geleiras	Bactéria	Máximo: 12 °C Ótimo: 4 °C Mínimo: 0 °C
Pressão hidrostática	Cepa MT41	Fossa das Marianas	Bactéria	Máximo > 100 MPa Ótimo: 70 MPa Mínimo: 50 MPa
Baixo pH	*Picrophilus oshimae*	Fontes termais ácidas	Archea - Euryarchacota	Máximo: pH 4 Ótimo: pH 0,7 Mínimo: pH -0,06
Alto pH	*Natronobacterium gregoryi*	Lagos alcalinos	Archea - Euryarchacota	Máximo: pH 12 Ótimo: pH 10 Mínimo: pH 8,5
Alta concentração de sal	*Halobacterium salinarum*	Lagos salinos	Bactéria	Maximo: saturação de sal Ótimo: 250 g/L Mínimo: 150 g/L
Radiação ultravioleta e ionizante	*Deinococcus radiodurans*	Carne enlatada	Bactéria	Resitente a 1,5 kGy de radiação gamma e 1500J/m^2 de radiação ultravioleta

Fonte: Seckbach 2004.

O estudo de micro-organismos extremófilos permite aumentar a compreensão da biodiversidade na Terra, além de ser importante na elucidação dos mecanismos de adaptação a condições hostis e conhecer novas moléculas estáveis em condições extremas. Assim sendo, estes estudos não só fornecem uma visão mais profunda do funcionamento das células vivas, mas também pode levar a aplicações biotecnológicas interessantes e exploração econômica destes micro-organismos (Morozkina et al., 2010).

Os micro-organismos extremófilos podem ter aplicação na produção de enzimas com maior atividade e estabilidade e de substâncias biologicamente ativas. Além disso, alguns micro-organismos extremófilos têm a capacidade de destruição e/ou eliminação de xenobióticos (compostos químicos estranhos a um sistema biológico), como é o caso da acumulação de íons de metais pesados e de radionuclídeos (átomos com núcleos instáveis que emitem radiação) em rios e oceanos (Figura 1) (Podar e Reysenbach, 2006).

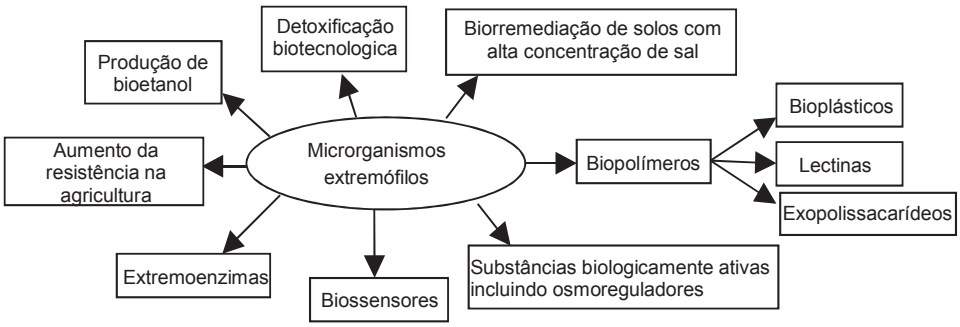

Figura 1: Possíveis aplicações de micro-organismos extremófilos na biotecnologia, medicina e indústria. Fonte: Morozkina et al. (2010).

A indústria de alimentos, farmacêutica e agrícola são as áreas mais promissoras para a aplicação de substâncias biologicamente ativas, como por exemplo, a bactéria ácido-láctica *Tetragenococcus halophila*, que propicia a homofermentação sob alta concentração de NaCl (18,0%), é utilizada na produção de molho de soja (Röling e Van Verseveld, 1997). Além disso, representantes do gênero *Pseudomonas* são intensamente utilizados em processos de biodegradação (Margesin e Schinner, 2001). Bactérias *Shewanella, Colwellia* e alguns outros gêneros, isoladas na Antártica, são fontes potenciais de ácidos graxos poli-insaturados de cadeia longa (Russell e Nichols, 1999).

1.2. Micro-organismos Termófilos

Dentre todos os ambientes extremos existentes, a temperatura é o que mais influencia a função das biomoléculas e a manutenção das estruturas biológicas. Entretanto, a existência de ambientes geotermicamente estáveis permite a seleção de micro-organismos que não apenas resistem, mas também requerem altas temperaturas para sobreviver (Gomes et al., 2007).

Ambientes com temperaturas abaixo de 55 °C são amplamente difundidos na Terra e estão associados com o aquecimento solar; no entanto, temperaturas maiores que 55 - 60 °C são raras e normalmente associadas a ambientes geotérmicos. As áreas geotermais permitem uma grande diversidade de micro-organismos termofílicos e hipertermófilos. Os micro-organismos podem ser classificados de acordo com a faixa de temperatura de seu crescimento conforme apresentado na Figura 2.

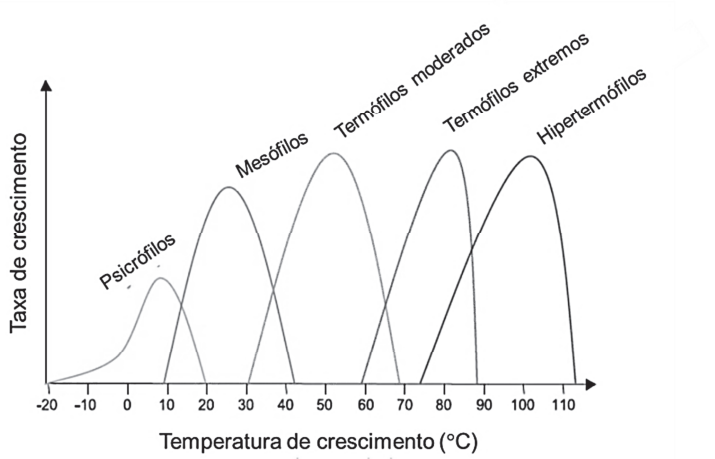

Figura 2: Classificação dos micro-organismos de acordo com sua temperatura de crescimento. Fonte: Gargaud et al. (2005).

Muitos gêneros de micro-organismos termófilos, tais como: *Thermus, Thermoplasma, Rhodothermus, Bacillus, Sulfolobus* e *Hydrogenobacter,* têm uma distribuição mundial. No entanto, a situação no âmbito de espécie é diferente, devido à semelhança fenotípica das espécies e devido à estrutura genética ser desconhecida na maioria dos casos. Através de métodos de sistemática molecular foi possível observar padrões endêmicos claros na distribuição de alguns termófilos (no âmbito de espécie) observando casos de ausência de uma determinada espécie em certas áreas geotérmicas (Stan-Lotter e Fendrihan 2012).

São vários os mecanismos moleculares usados pelos mesmos para se adaptarem às altas temperaturas. Dentre os mecanismos de adaptação a altas temperaturas podemos citar: (a) estrutura/função de macromoléculas e estruturas celulares, (b) fisiologia e metabolismo, e (c) regulação da expressão gênica e manutenção da integridade do DNA. Pelo menos três pontos merecem atenção especial neste contexto: membrana, DNA, e estabilidade e função das proteínas em temperaturas extremas.

No que diz respeito às membranas celulares, sugere-se que a estrutura tetraédrica da monocamada lipídica encontrada em archaeas extremamente termófilas são mais adequadas para sobrevivência em altas temperaturasdo que as bicamadas lipídicas das membranas bacterianas compostas por ésteres. A monocamada lipídica das archeas é considerada mais rígida e possui ligações éteres que são mais resistentes a oxidação a altas temperaturas quando comparadas a ligações ésteres (Van de Vossenberg et al. 1998).

Quanto ao DNA, os mecanismos que contribuem para a manutenção da sua estrutura primária e secundária em temperaturas de crescimento sugerem que fatores como mutação genética, recombinação intramolecular e transferência horizontal de genes entre micro-organismos de diferentes espécies tiveram papel fundamental na adaptação dos micro-organismos termófilos (Grogan 1998; Averhoff and Müller 2010).

As enzimas termófilas, quando comparadas com suas homólogas mesófilas, não são apenas mais resistentes à temperatura, mas também a agentes químicos, propriedades estas que tornam estas termoenzimas interessantes para aplicação em processos industriais (Pantazaki et al. 2002). Os mecanismos específicos envolvidos na termoestabilidade das enzimas variam de enzima para enzima. Comparações estruturais realizadas entre enzimas mesófilas e termófilas validaram mecanismos de estabilização proteica incluindo interações hidrofóbicas, eficiência de empacotamento, pontes salinas, pontes de hidrogênio, redução da tensão conformacional e resistência à destruição covalente (Zeikus et al. 1998).

1.3. Micro-organismos do gênero *Thermus*

O gênero *Thermus* pertence a um dos mais antigos ramos filogenéticos na evolução bacteriana (Willians e Sharp, 1995). Em 1969, Thomas Brock e Hudson Freeze da Universidade de Indiana (EUA) relataram uma nova espécie de bactéria termofílica nomeada *Thermus aquaticus* (Brock e Freeze, 1969), sendo esta a primeira espécie do gênero *Thermus* a ser descoberta.

Atualmente, de acordo com Euzéby (2014), já foram identificadas 16 diferentes espécies pertencentes ao gênero *Thermus*: *T. aquaticus*, *T. antranikianii*, *T. arciformis, T. brockianus*, *T. chliarophilus*, *T. composti*, *T. filiformis*, *T. igniterrae*, *T. islandicus, T. oshimai*, *T. profundus*, *T. ruber*, *T. scotoductus*, *T. silvanus, T. tengchongensis* e *T. thermophilus*. Na tabela 2 são apresentadas algumas das principais características de bactérias do gênero *Thermus*.

Tabela 2: Características de diferentes espécies de *Thermus*.

Espécie	Cor do pigmento	Temperatura	pH	Nutrição	Relação com oxigênio	Local de onde foi isolada	Descobridor (Ano)
Thermus aquaticus	Amarelo	40-79 °C	6,0-9,5	Fontes de nitrogênio, açúcares e ácidos orgânicos. Cresce melhor em meio complexo com 0,1 a 0,3% de triptona e extrato de levedura. Não reduz nitrato.	aeróbia	Parque nacional de Yellowstone - EUA	Brock et al. (1969)
Thermus ruber	Vermelho claro	35-70 °C	6,5-7,3	Meio mínimo suplementado com peptona como fonte de nitrogênio, extrato de levedura e uma fonte de carbono.	aeróbia	Fontes termais da península de Kamchatka - Rússia	Loginova et al. (1975)
Thermus filiformis	Amarelo	37-80 °C	6,0-8,6	Carboidratos, ácidos orgânicos e aminoácidos como fonte de carbono. Não reduz nitrato.	aeróbia	Fontes termais da Nova Zelândia	Hudson et al. (1987)
Thermus igniterrae	Amarelo	45-80 °C	7,5-8,5	Fonte de nitrogênio, extrato de levedura e fonte de carbono. Reduz nitrato.	aeróbia	Fontes termais de Reykyaflot - Islândia	Chung et al. (2000)
Thermus antranikianii	Amarelo	50-80 °C	7,5-8,5	Fonte de nitrogênio, extrato de levedura e fonte de carbono. Reduz nitrato.	aeróbia	Fontes termais de Hruni na Islândia	Chung et al. (2000)

Fonte: adaptado de Chung et al. (2000).

Um padrão particular de distribuição de espécies de acordo com a influência geográfica é encontrado para bactérias do gênero *Thermus* (Figura 3). Estudos anteriores observaram diferenças na composição das espécies de diferentes locais, algumas linhagens apresentaram-se endêmicas a um local e outras se apresentaram mais cosmopolitas (Hreggvidsson et al., 2006).

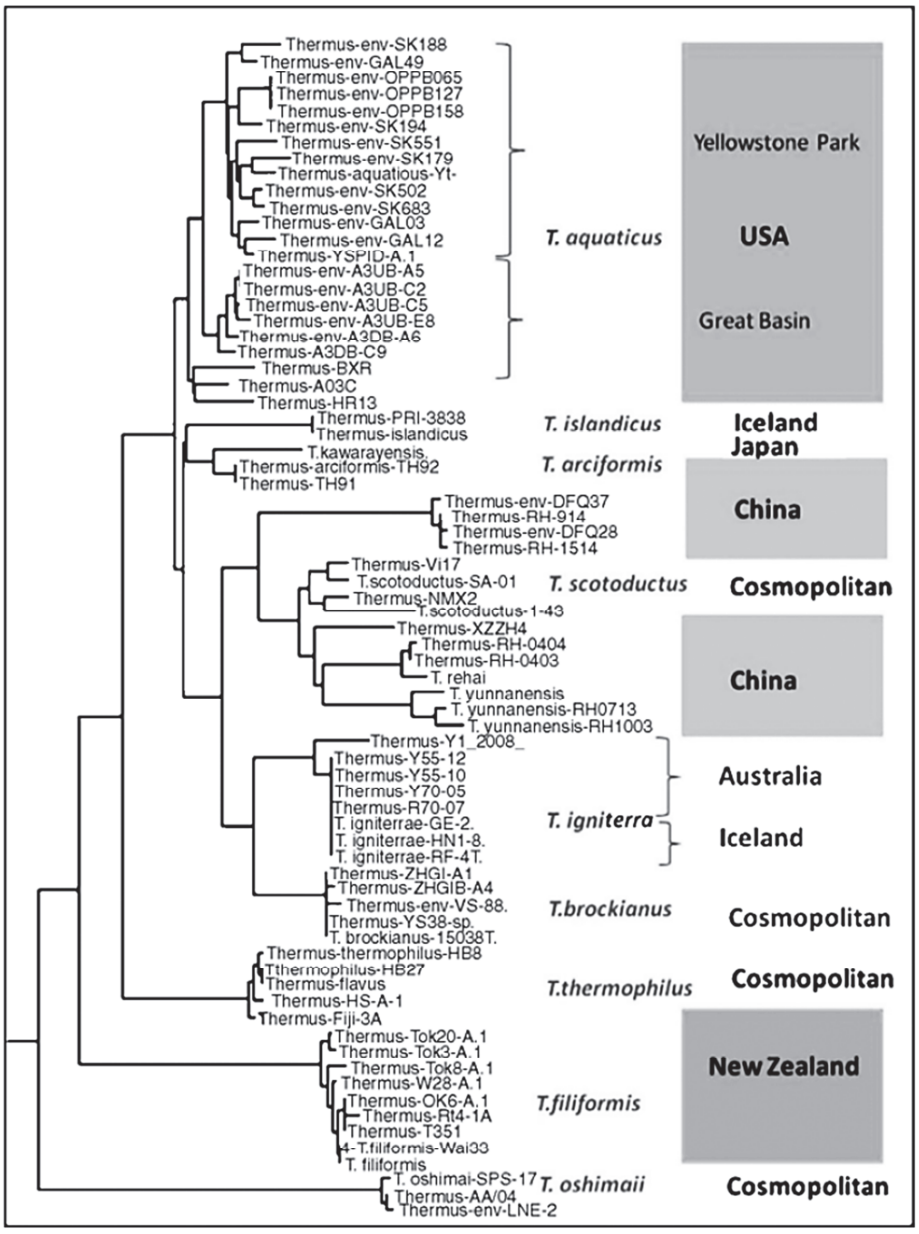

Figura 3: Padrão de distribuição geográfica das bactérias do gênero *Thermus*. Fonte: Stan-Lotter e Fendrihan (2012).

Algumas espécies de *Thermus* possuem seu DNA sequenciado, como pode-se observar na tabela 3, os genomas de bactérias deste gênero tem tamanho em torno de 2Mb e conteúdo de GC variando entre 64,8 e 69,4 %. Recentemente, foram publicados os

genomas completos de *T. oshimai* JL-2 e *T. thermophilus* JL-18. A análise desses genomas revelou que estas bactérias codificam enzimas responsáveis pela redução de nitrato a óxido nítrico, o que é coerente com o elevado fluxo de óxido nítrico presente na fonte termal de onde essas espécies foram isoladas (Senthil et al. 2013).

Tabela 3: Bactérias do gênero *Thermus* com genomas completos sequenciados.

Organismo	Tamanho (Mb)	GC %	Genes	Proteínas
Thermus aquaticus Y51MC23	2,34	68,0	2.593	2.539
Thermus igniterrae ATCC 700962	2,23	68,8	2.345	2.293
Thermus antranikianii DSM 12462	2,17	64,8	-	-
Thermus islandicus DSM 21543	2,26	68,3	2.432	2.330
Thermus oshimai JL-2	2,40	68,6	2.548	2.435
Thermus oshimai DSM 12092	2,26	68,7	2.401	2.341
Thermus scotoductus SA-01	2,36	64,9	2.515	2.458
Thermus scotoductus DSM 8553	2,07	64,8	2.259	2.173
Thermus thermophilus HB8	2,12	69,5	2.245	2.173
Thermus thermophilus HB27	2,13	69,4	2.263	2.210
Thermus thermophilus JL-18	2,31	69,0	2.508	2.402
Thermus thermophilus SG0.5JP17-16	2,30	68,6	2.488	2.339
Thermus thermophilus ATCC33923	2,15	69,4	-	-
Thermus sp. CCB_US3_UF1	2,26	68,6	2.334	2.279
Thermus sp. NMX2.A1	2,29	65,3	2.523	2.449
Thermus sp. RL	2,04	68,6	2.082	1.986

Fonte: NCBI

O interesse no estudo de micro-organismos do gênero *Thermus* começou há anos atrás, quando em 1976, Chien e colaboradores purificaram uma DNA polimerase de *Thermus aquaticus* com temperatura ótima de 80 °C, o que possibilitou a automação das reações de PCR (reação de polimerase em cadeia), revolucionando a biotecnologia. Desde então, além das enzimas termoestáveis, outros compostos interessantes com potencial de aplicabilidade na indústria foram isolados de bactérias do gênero *Thermus*, como por exemplo: vitamina B12, carotenos e poli-hidroxialcanoatos (Pantazaki et al. 2002; Pantazaki et al. 2003; Henne et al. 2004).

1.4. *Thermus filiformis*

Em 1886, cerca de 100 anos antes do descobrimento da bactéria *Thermus filiformis* que foi objeto de estudo desta pesquisa, o vulcão Mount Tarawera, localizado em Rotorua na Nova Zelândia entrou em erupção destruindo toda área ao seu redor. A erupção abriu uma fissura na terra de 17 quilômetros de extensão, que separou o Mount Tarawera em dois, ampliou em 20 vezes o tamanho original do lago Rotomahana e formou 7 crateras que hoje compõem o Vale Vulcânico de Waimangu, que é considerado o sistema geotermal mais recente da Terra.

Waimangu é uma área de atividade hidrotermal diversa e intensa, onde se encontram duas das maiores fontes termais do mundo, nomeadas: Frying Pan Lake, com faixa de temperatura de 44 a 56 °C, e Inferno Crater Lake, com faixa de temperatura de 35 a 84 °C (Waimangu: Geology - Disponível on-line em: http://www.gns.cri.nz/Home/Learning/Science-Topics/Volcanoes/New-Zealand-Volcanoes/Volcano-Geology-and-Hazards/Waimangu-Geology. Acessado em 05 de fevereiro de 2014).

A bactéria *Thermus filiformis* isolada do Vale Vulcânico de Waimangu em 1987, por Hudson et al., (1987) (Figura 4), pertence ao domínio Bactéria, à família Thermaceae e ao gênero *Thermus*, é uma bactéria termófila, Gram negativa, não esporulada, catalase e oxidase positivas e aeróbia. Em geral, as bactérias *Thermus* apresentam crescimento ótimo entre 70°C e 75°C; no entanto algumas espécies apresentam temperaturas de crescimento mais baixas ao redor de 60°C. A faixa ótima de pH para crescimento dessas bactérias é entre 7,5 e 8,0, podendo crescer em valores de pH mais baixo (~ 5,1) ou mais elevado (~ 9,5) (Huber e Stetter, 2004).

Figura 4: Fonte termal do Vale Vulcânico de Waimangu. A coloração amarela é devido à presença da bactéria *Thermus filiformis*. Fonte: True Travel.

Embora a bactéria *T. filiformis* tenha sido descoberta há mais de 20 anos, nenhum estudo sobre seus mecanismos de adaptação foi realizado até o presente momento. As publicações existentes são sobre enzimas termoestáveis (Egas et al. 1998; Choi et al. 2001; Kang et al. 2004) e caracterização de carotenoides (Mandelli et al. 2012a; Mandelli et al. 2012b).

1.5. Extresse Oxidativo

O estresse oxidativo é uma condição biológica em que ocorre desequilíbrio entre a produção de espécies reativas de oxigênio (ERO) ou de nitrogênio (ERN) e a sua desintoxicação através de sistemas biológicos que removam estas espécies ou que reparem os danos por elas causados.

As espécies reativas de oxigênio, como o próprio nome indica, são derivadas do oxigênio molecular com atividade redox e elevada reatividade, já as espécies reativas de nitrogênio são derivadas do óxido nítrico (Tabela 4). As ERO e ERN podem ser geradas dentro das células tanto pela exposição a agentes endógenos como exógenos (Gomes et al., 2005; Gomes et al., 2006).

Tabela 4: Lista de espécies reativas de oxigênio e nitrogênio.

		Estrutura	Descrição
ERO	Peróxido de hidrogênio	H_2O_2	Formado pela dismutação do ânion superóxido ou pela redução direta do O_2. Por ser lipossolúvel pode difundir pela membrana. É substrato da reação de Fenton.
	Oxigênio Singlete	$^1O_2$	Forma altamente reativa de O_2, pode ser produzida in vivo por enzimas peroxidases, durante reações catalisadas por lipoxigenases e também a partir de reações de fotosensibilização através da reação entre o estado triplete excitado de sensibilizadores e o $^3O_2$.
	Ânion Superóxido	$O_2^{\bullet -}$	Formado em muitas reações de auto-oxidação e pela cadeia de transporte de elétrons. Sofre dismutação para formar o H_2O_2 espontaneamente ou por catálise enzimática. Catalisado por metal, é o precursor para formação de $HO^{\bullet}$.
	Radical Hidroxila	$^{\bullet}OH$	Formado pela reação de Fenton ou decomposição do peroxinitrito. Altamente reativo.
	Ácido Hipocloroso	HOCl	Formado a partir do H_2O_2 por mieloperoxidases. Lipossolúvel e altamente reativo. Oxida rapidamente os

			constituintes de proteínas, incluindo grupos tiol, grupos amino e metionina.
	Hidroperóxido orgânico	ROOH	Formado através de reações radicalares com componentes celulares tais como lipídios e nucleobases.
ERN	Óxido Nítrico	$NO^{\bullet}$	Formado de forma endógena pela arginina e oxigênio por várias óxido nítrico-sintase (NOS) e pela redução do nitrato inorgânico. Reage com $O_2^{\bullet -}$ para produzir peroxinitrito. Altamente reativo.
	Ânion Peroxinitrito	$ONOO^-$	Formado pela rápida reação entre $O_2^{\bullet -}$ e $NO^{\bullet}$. Lipossolúvel e reatividade similar ao HOCl. A protonação forma o ácido peroxinitrito, que pode sofrer clivagem homolítica para formar $^{\bullet}OH$ e NO_2.

Mais de 90 % do oxigênio consumido pelos organismos são usados na produção de energia através da fosforilação oxidativa pela cadeia de transporte de elétrons, via mecanismo de quatro elétrons, formando ATP e água. Adições consecutivas de elétrons, um a um, ao oxigênio molecular também levam à obtenção de água, no entanto por esta via ocorre a formação de produtos intermediários tais como: ânion superóxido, peróxido de hidrogênio e radical hidroxila (Figura 5) (Lushchak, 2011).

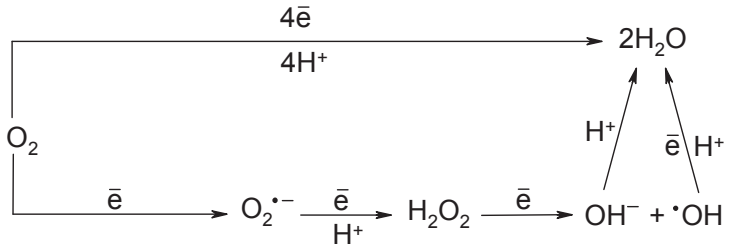

Figura 5: Diferentes vias da redução de oxigênio em sistemas biológicos. A parte superior do esquema mostra a redução por quatro elétrons na cadeia de transporte de elétrons. A parte inferior demonstra a adição consecutiva de elétrons, um a um, com a formação dos produtos intermediários ânion superóxido, peróxido de hidrogênio e radical hidroxila. Fonte: Lushchak (2011).

A maior parte das ERO (normalmente > 90 %) em organismos vivos é gerada pelas cadeias de transporte de elétrons de mitocôndrias, do retículo endoplasmático, das membranas plasmáticas e nucleares e do sistema fotossintético (Starkov, 2008). Adicionalmente, pequenas quantidades de ERO são geradas por algumas enzimas, como

é o caso das oxidases, através da auto-oxidação de diferentes moléculas. As oxidases mais conhecidas por produzirem ERO são: NADPH oxidase, lipo-oxigenases, ciclo-oxigenases e xantina oxidase (Puddu et al., 2008).

A Figura 5 demonstra o metabolismo de algumas ERO. A redução de um elétron do oxigênio molecular pode ao fim produzir água, o que pode ocorrer espontaneamente. No entanto, algumas enzimas podem aumentar em muitas vezes a velocidade de transformação. As superóxido dismutases aceleram a dismutação do ânion superóxido a oxigênio molecular e peróxido de hidrogênio. Catalases decompõem o peróxido de hidrogênio, produzindo água e oxigênio molecular, e as peroxidases, utilizando alguns redutores e peróxidos como co-substratos, produzem água e produtos reduzidos.

Os principais alvos biológicos das ERO/ERN são DNA, RNA, proteínas e lipídeos. De fato, os lipídeos são o principal alvo durante o estresse oxidativo, uma vez que os radicais livres podem atacar diretamente os ácidos graxos poli-insaturados das membranas e iniciar a peroxidação lipídica. O primeiro efeito da peroxidação é uma diminuição na fluidez da membrana, alterando as propriedades da mesma, o que pode levar a um rompimento significativo da ligação membrana-proteína. Este efeito age como um amplificador, no qual mais radicais são gerados, e os ácidos graxos poli-insaturados são degradados em vários compostos de menor massa molecular, tais como os aldeídos, que podem danificar moléculas como proteínas (Humpries e Sweda, 1998).

No que diz respeito ao DNA, as espécies reativas podem atacar tanto suas bases quanto suas ligações de açúcar produzindo quebras tanto na fita simples quanto na dupla, podem levar também a formação de adutos de grupos de base e de açúcar, ligações cruzadas com outras moléculas, lesões que podem bloquear a replicação (Sies e Menck 1992; Sies 1993).

Na oxidação de proteínas, muitos danos já foram documentados, incluindo a oxidação dos grupos sulfidrilas, redução dos dissulfetos, adição oxidativa dos resíduos de amino ácidos próximos a sítios de ligação com metais através de oxidações catalisadas por metais, reações com aldeídos, modificações dos grupos prostéticos ou clusters metálicos, cross-link proteína-proteína e fragmentação de peptídeos (Cabiscol et al., 2000).

Quando o estresse severo é imposto, a sobrevivência celular depende da habilidade da célula em se adaptar ao estresse e reparar ou substituir moléculas danificadas. Caso a célula falhe em se adaptar desta maneira, provavelmente sofrerá apoptose, que é uma forma de resposta ao alto nível de estresse (Ha et al., 2005). A

prevenção da produção de ERO é a forma mais eficiente de proteger as células contra seus efeitos deletérios. Neste contexto, além de enzimas, compostos de baixa massa molecular, tais como vitaminas C e E, glutationas (GSH), carotenoides e ácido úrico, formam um grupo de antioxidantes capazes de neutralizar as ERO/ERN (Lushchak, 2011).

1.6. Mecanismos de Defesa

O aparecimento do oxigênio na atmosfera levou ao desenvolvimento de mecanismos de defesa que tanto mantém a concentração de radicais derivados do oxigênio molecular em níveis aceitáveis quanto reparam danos oxidativos. Algumas moléculas, produzidas pelos organismos, ajudam a manter um ambiente intracelular reduzido ou ainda a desativar as ERO. Entre essas moléculas estão os antioxidantes não enzimáticos, tais como: NADPH, NADH, carotenoides, ácido ascórbico, α-tocoferol e glutationa (GSH) e os enzimáticos tais como: superóxido dismutase, catalase e glutationa peroxidase (Cabiscol et al., 2000).

1.6.1. Carotenoides

Os carotenoides pertencem a um grupo de pigmentos naturais amplamente distribuídos na natureza com grande diversidade de estruturas e funções; possuem como estrutura básica um tetraterpeno de 40 átomos de carbonos, formado por oito unidades isoprenoides de cinco carbonos, ligados de tal forma que a molécula é linear e com simetria invertida no centro. Mais de 700 diferentes carotenoides isolados de fontes naturais já foram caracterizados (Britton et al., 2004).

Os carotenoides apresentam na sua cadeia uma alternância de ligações duplas e simples que geram um sistema de elétrons π que se desloca sobre toda a cadeia poliênica, proporcionando a estas substâncias alta reatividade química e absorção de luz na região do visível. Como consequência, os carotenoides podem facilmente sofrer isomerização e oxidação. Por outro lado, a cadeia poliênica é responsável pela desativação de radicais livres e de oxigênio singlete ($^1O_2$), espécies altamente reativas responsáveis pela iniciação de cadeias de oxidação nas células (Caris-Veyrat, 2007).

O interesse pelos carotenoides tem aumentado consideravelmente nos últimos anos pela evidência dos seus já conhecidos benefícios à saúde humana, devido às suas propriedades antioxidantes, anticarcinogênicas e imunomodulatórias. Uma alternativa

para obtenção natural destes pigmentos é a sua produção por micro-organismos, sendo uma das fontes as bactérias termófilas que em sua maioria possuem carotenoides com estrutura específica para fortalecimento da membrana celular.

Yokoyama et al. (1995; 1996) identificaram ésteres glicosídicos de carotenoides, termozeaxantinas e termocriptoxantinas (Figura 6), na bactéria termófila *Thermus thermophilus*. Mandelli et al. (2012b) identificaram os carotenoides zeaxantina livre, zeaxantina monoglucosilada, e zeaxantinas diglicosiladas e aciladas tais como as termozeaxantinas e termobizeaxantinas em *T. filiformis*.

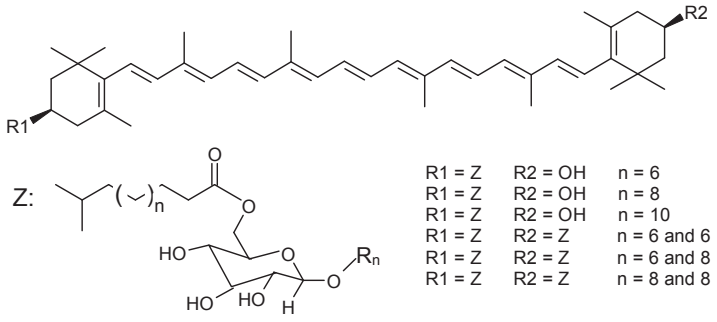

Figura 6: Estrutura das termocriptoxantinas (R1 = Z e R2 = H) e das termozeaxantinas (R1 = Z e R2 = OH).

A influencia na estabilização das membranas se dá pelo posicionamento dos carotenoides em relação a bicamada lipídica. A zeaxanthina é ancorada nas duas regiões polares opostas da bicamada com a cadeia de hicrocarbonetos quase que perpendicular a membrana (Figura 7A) (Havaux 1998). Por outro lado, as termozeaxantinas apresentam uma maior interação com a membrana, devido a presença do açúcar que fica ancorado na região polar da membrana e do ácido graxo que se curva como um gancho para dentro da reagião hidrofóbica da bicamada lipídica proporcionando uma maior rigidez a mesma (Figura 7B) (Hara et al. 1999).

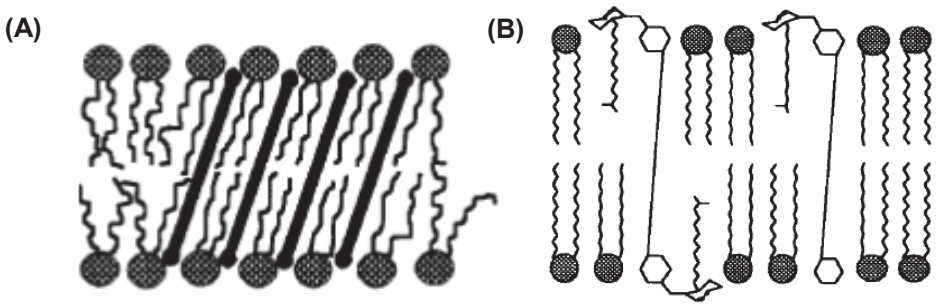

Figura 7: Representação esquemática do posicionamento dos carotenoides zeaxantina (A) , termobiszeaxantinas e termozeaxantinas (B). Fonte: Havaux (1998) e Hara et al. (1999).

1.6.1.1. Carotenogênese em micro-organismos do gênero Thermus

O carotenoide incolor fitoeno, formado pela condensação de duas moléculas de geranil-geranil pirofosfato (GGPP), é o primeiro a ser formado na rota biossintética de carotenoides em bactérias (Armstrong et al., 1990). O gene de uma GGPP sintase (TTHA0013) foi identificado e caracterizado em *T. thermophilus* HB8, esta enzima mostrou-se distinta das GGPP sintases (CrtE) bacterianas por não ter o resíduo de aminoácido de inserção comumente localizado no primeiro domínio rico em aspartato (Ohto et al., 1999). O fitoeno é formado a partir do GGPP pela fitoeno sintase (CrtB), e em *T. thermophilus* esta enzima está localizada em um grande plasmídeo com outros genes responsáveis pela carotenogênese, sendo considerada um fator limitante na velocidade da biossíntese de carotenoides (Hoshino et al., 1993; Tabata et al., 1994).

O fitoeno é convertido em licopeno através de quatro passos de dessaturação, que, em bactérias, é geralmente catalisado pela fitoeno desaturase (CrtI) seguido da ζ-caroteno desaturase (CrtQ) e *cis*-caroteno isomerase (CrtH) (Takaichi e Mochimaru, 2007). Após a síntese do licopeno, a biossíntese dos carotenoides é diversificada em carotenoides acíclicos e cíclicos. A ciclização do licopeno em um ou ambos os lados Ψ-terminais é usualmente catalisada pela enzima licopeno β-ciclase tipo CrtL ou CrtY (Armstrong, 1997). Nas espécies *T. aquaticus* Y51MC23, *T. thermophilus* HB27 e *T. thermophilus* HB8, que possuem genomas sequenciados, foram detectadas apenas homólogos da enzima licopeno ciclase tipo CrtY, responsável pela síntese de carotenoides dicíclicos em *Thermus* (Brüggemann e Chen, 2006).

As modificações que podem ocorrer nos grupos terminais Ψ- e β- dos carotenoides, tais como hidroxilação, dessaturação, cetonização, glicosilação e acilação são responsáveis pelas estruturas únicas dos carotenoides de *Thermus*.

A hidroxilação do anel terminal β- das termozeaxantinas em *T. thermophilus* requerem atividade de uma β-caroteno hidroxilase. Uma mono-oxigenase termoestável (CYP175A1) foi identificada em *T. thermophilus* HB27 como um novo tipo de β-caroteno hidroxilase pertencente à superfamília P450 (Blasco et al., 2004). A CYP175A1 catalisa a introdução de grupos hidroxila ao C-3 e C-3' do anel-β do β-caroteno para formação de zeaxantina.

As etapas de glicosilação e acilação que seguem a etapa de hidroxilação levam à formação de ésteres de zeaxantina mono ou di-glicosilada. A zeaxantina glicosiltransferase responsável pela formação da zeaxantina β-diglicosideo em *T. thermophilus* HB8, *T. thermophilus* HB27 e *T. aquaticus* Y51MC23 é tipo CruC, que apresentou 39 %, 39 % e 40 % de homologia, respectivamente, com a glicosil tranferase tipo CruC de *Clostridium tepidum* (Maresca e Bryant, 2006). Para a etapa de acilação, homólogos de carotenoide aciltransferase foram preditos em *T. thermophilus* HB8 e *T. thermophilus* HB27, no entanto apresentaram baixa identidade (23 %) com o tipo CruD de *C. tepidum* (Tian e Hua, 2010).

A via utilizada para biossíntese de caroteinodes em *T. thermophilus* foi proposta tendo por base a identificação das termozeaxantinas e alguns de seus intermediários (Yokoyama et al., 1996). No entanto, a rota detalhada da carotenogênese não pode ser estabelecida até que todos os genes envolvidos sejam confirmados e analisados funcionalmente.

A rota biossintética de produção de carotenoides mostrada na Figura 8 trata-se de uma via gerada por anatoção automática, com base nos genomas de diferentes organismos, feita pelo banco de dados do KEGG (Kyoto Encyclopedia of Genes and Genomes).

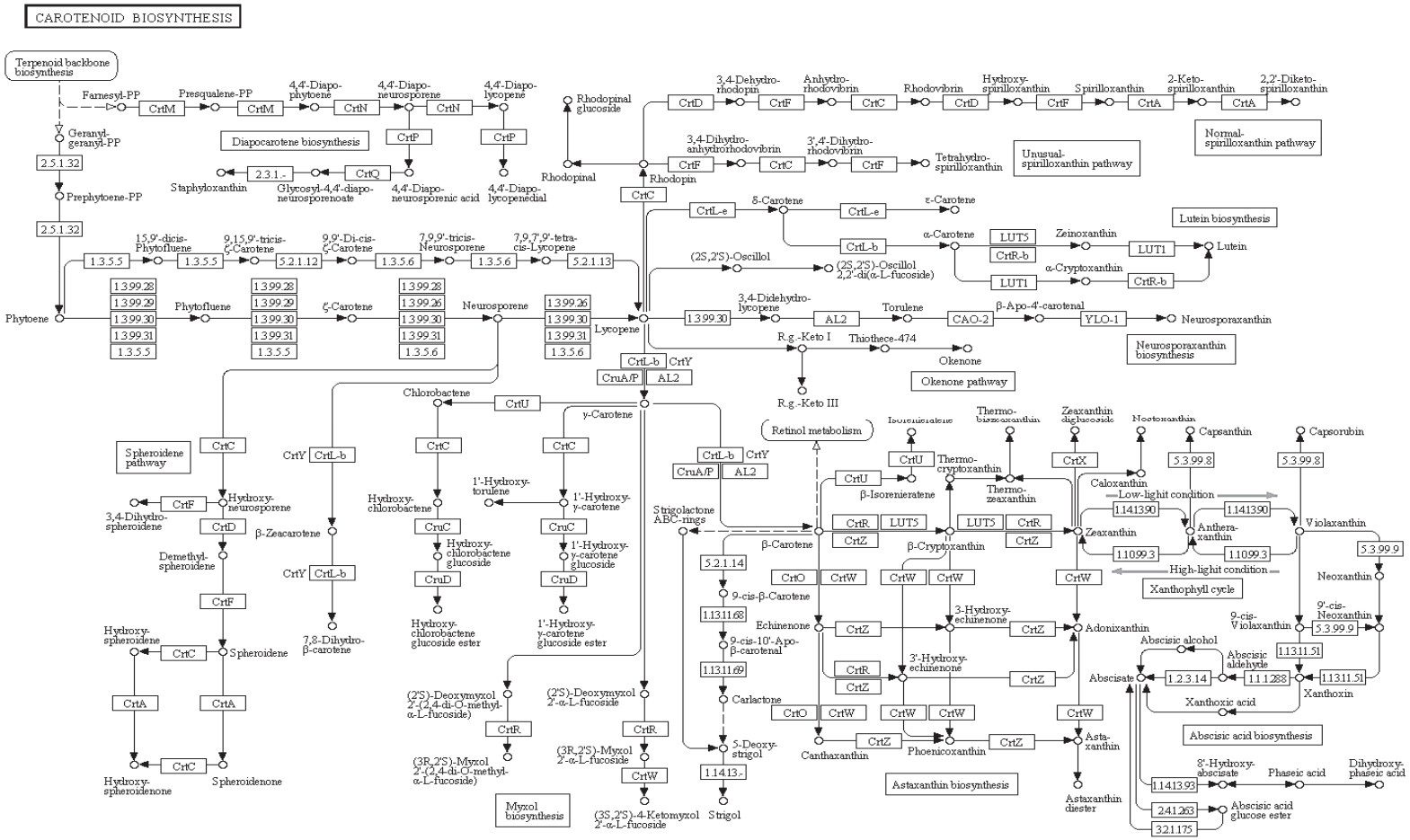

Figura 8: Rota de referência da biossíntese de carotenoides em organismos procariotos e eucariotos. Fonte: www.Kegg.jp.

1.6.2. Superóxido dismutase

Dentre as enzimas produzidas pelos micro-organismos que podem levar à diminuição dos níveis de ROS, destacam-se a superóxido dismutase que converte $O_2^{\bullet-}$ em H_2O_2 e O_2, a catalase que converte H_2O_2 em H_2O e O_2 e a glutationa peroxidase, responsável pela detoxificação de peróxidos orgânicos e inorgânicos.

Das enzimas supracitadas, as superóxidos dismutases (SOD) exercem um papel essencial no metabolismo do ânion superóxido, antecipando reações de oxidação e prevenindo a formação de espécies deletérias como ânion peroxinitrito e radical hidroxila (Miller, 2012). A capacidade de sobreviver ao O_2 é de tal importância que poucos organismos desprovidos de SOD sobrevivem à transição, provocada pela evolução, de um ambiente redutor para um oxidante (Blankenship, 2010). A pressão evolucionária para o desenvolvimento de proteção contra o superóxido foi suficientemente intensa para que as SODs evoluíssem em pelo menos três ocasiões separadas. Uma destas foi suficientemente antiga e importante que esta enzima é encontrada em todos os reinos da vida, o que indica que se desenvolveu antes mesmo da diferenciação das eubactérias de archaeas.

As SODs são divididas em três famílias: as que utilizam níquel, as que utilizam cobre complexado com zinco e por fim as que utilizam manganês ou ferro, ou ambos. No entanto, as famílias não se diferenciam somente pelo íon metálico, mas também pelo enovelamento destas proteínas (Miller, 2012).

Um dos principais requisitos para as SODs comerciais é a termoestabilidade, uma vez que a desnaturação térmica é uma causa comum da inativação enzimática. Por este motivo o interesse por SODs de organismos termofílicos tem aumentado nos últimos anos, com a finalidade de se obter enzimas termoestáveis (Li et al., 2005). SODs já foram isoladas de alguns organismos termofílicos dos gêneros *Aquifex* (Lim et al., 1997), *Aeropyrum* (Yamano et al., 1999), *Sulfolobus* (Yamano e Maruyama, 1999), *Pyrobaculum* (Whittaker e Whittaker, 2000) e inclusive *Thermus* (Liu et al., 2011). Como esperado, todas elas apresentaram termoestabilidade superiores às SODs mesofílicas, apresentando, portanto grande potencial para aplicações industriais.

1.7. Ferramentas para identificação de vias biológicas e moléculas com potencial biotecnológico

Um dos princípios emergentes da biologia é que geralmente, não são genes individuais, mas sim redes e vias biológicas que conduzem a resposta de um organismo a uma vasta gama de estímulo. Neste contexto, para avaliar mecanismos de adaptação e vias de produção de certos metabólitos é essencial o uso de ferramentas, como a proteômica e transcriptômica, que nos forneçam uma visão geral do que está acontecendo com um organismo quando submetido a uma dada condição.

1.7.1. Proteômica

A proteômica é um campo da ciência que se propõe a analisar de forma global o conjunto de proteínas (proteoma) contidas em uma amostra biológica, seja esta um organismo, tecido, célula ou organela celular. Devido à natureza dinâmica do proteoma (ele se altera frente a diferentes condições e estímulos), seu estudo representa, além de uma forma de procurar as possíveis funções das proteínas, uma forma de investigar processos metabólicos em sistemas vivos para melhor entender o seu funcionamento e seus mecanismos de adaptação frente a diferentes estímulos (Anderson e Anderson, 1998).

Muitas das tecnologias hoje utilizadas na proteômica foram desenvolvidas muito antes do início da mesma. No entanto, foi o avanço na tecnologia de sequenciamento de proteínas por meio da espectrometria de massas que possibilitou o seu surgimento e desenvolvimento (Tyers e Mann, 2003). O início da proteômica foi marcado pela caracterização de perfis proteicos, passando, posteriormente, a focar outros aspectos como a quantificação de proteínas, as interações entre proteínas e as modificações pós-traducionais (MPT's).

O fluxo experimental normalmente utilizado na proteômica consiste na extração de proteínas, separação, quantificação e, finalmente identificação. As informações sobre o proteoma de uma amostra podem derivar da análise de proteínas intactas (proteômica *top-down*) ou de seus peptídeos (proteômica *bottom-up*). Na proteômica *bottom-up*, as proteínas de uma mistura são digeridas, e os peptídeos resultantes são analisados por MS. As limitações dessa estratégia podem estar na cobertura incompleta da sequência das proteínas, na perda das MPT's e nas degradações como resultado da digestão proteolítica. Já a análise *top-down* permite deduzir a estrutura primária da proteína e a

maior parte das MPT's. No entanto, essa estratégia é limitada pela energia de colisão necessária na fragmentação da proteína que é insuficiente para proteínas maiores que 50KDa, ficando restrita sua aplicação à análise de proteínas purificadas (Nesaty e Suter, 2008).

Os dados gerados por análise proteômica permitem alcançar diferentes objetivos: esclarecer as proteínas envolvidas em rotas metabólicas relacionadas aos diferentes processos celulares; identificar novos alvos farmacológicos e marcadores biológicos; identificar moléculas bioativas a partir de extratos biológicos naturais, levando ao desenvolvimento de novos fármacos; e, caratcterizar as respostas celulares a determinadas drogas e mudanças ambientais (Silva et al. 2007).

Alguns estudos do proteoma de bactérias já foram realizados no intuito de elucidar os mecanismos utilizados na adaptação ao estresse por estes organismos (Mostertz et al. 2004; Trauger et al. 2008; Li et al. 2010; Hare et al. 2011; Kim et al. 2012). Estes trabalhos, através dos dados de proteômica e analise computacional, demonstram proteinas que tem sua expressão diferenciada de acordo com o tipo de estresse a qual o micro-organismo é submetido.

Em seu estudo sobre termo-adaptação da bactéria *Thermus thermophilus* wl, comparando cultivos acima e abaixo da temperatura ótima de crescimento (65 °C), Li et al. (2010) observaram que as proteínas responsáveis pela adaptação estavam envolvidas em vias metabólicas (via de carboidratos, de amino ácidos e de cofatores e vitaminas) bem como na estabilização e modificação do DNA e de proteínas, sendo que a enzima superóxido dismutase foi considerada crucial na termo-adapatação devido ao seu envolvimento na detoxificação de radicais livres.

Além da função de elucidar os mecanismos de adaptação de organismos, a proteômica também serve como uma ferramenta para prospecção de novas enzimas com potencial de aplicabilidade industrial (Tabela 5). Neste sentido, as enzimas de micro-organismos termofílicos, tornam-se muito interessantes uma vez que estas se apresentam mais estáveis a temperatura, agentes químicos e a mudanças de pH quando comparadas as enzimas de organismos mesofílicos. A principal vantagem dos processos a alta temperatura está na redução do risco de contaminação microbiana, baixa viscosidade, aumento nas taxas de transferência de calor e massa, e melhora na solubilidade dos substratos (Bruins et al. 2001).

Pesquisas realizadas com termoenzimas têm demonstrado que estas são uma ótima fonte de catalisadores com grande atrativo industrial. Enzimas termoestáveis que

degradam polímeros, tais como amilases, pullulanases, xilanases, proteases e celulases, apresentam grande potencial de aplicação nas indústrias de alimentos, química, farmacêutica, de celulose, de papel e de tratamento de efluentes.

Tabela 5: Exemplos de termoenzimas, possíveis aplicações e principais vantagens na sua aplicação industrial.

Enzima	Aplicação	Vantagem
Alcool desidrogenase	Síntese de álcoois quirais	Aumenta estabilidade
Amilase	Produção de xarope de glicose	Compatível com as altas temperaturas utilizadas no processo
Celulase	Processamento de polpa e papel	Compatível com as altas temperaturas utilizadas no processo
	Detergentes industriais	Estável a altos pHs
Ciclodextrina glicosil transferase	Produção de ciclodextrina	Compatível com as altas temperaturas utilizadas no processo
DNA polimerase	Reação de PCR	Compatível com as altas temperaturas utilizadas no processo
Glucoamilase	Conversão de amido	Compatível com as altas temperaturas utilizadas no processo
Glicosidase	Hidrólise da lactose	Menor taxa de crescimento microbiano em altas temperaturas
	Síntese de oligossacarídeos	Melhor solubilidade do substrato em altas temperaturas
	Síntese de detergentes alquil glicosídeos	Compatível com solventes orgânicos
Lacase	Detergentes para lavanderia	Estável em pH alto
Protease	Detergentes	Estável em pH alto
	Síntese do precursor de aspartame	Compatível com solventes orgânicos
Pululanase	Produção de xarope de glicose	Compatível com as altas temperaturas utilizadas no processo
Xilose/glicose isomerase	Produção de xarope de frutose	Equilíbrio deslocado pela alta temperatura

Adaptada de Bruins et al 2001.

Apesar de já serem encontradas em muitos processos, as enzimas termoestáveis apresentam potencial de aplicação ainda mais amplo. Elas podem, por exemplo, substituir enzimas mesofílicas em processos que são beneficiados se operados em alta temperatura. Além disso, termoenzimas podem exercer papel central no melhoramento de

novos processos, a exemplo do ocorrido com as reações de PCR devido ao descobrimento da Taq DNA polimerase de *Thermus aquaticus* (Chien et al. 1976).

Outra vantagem é que as termoenzimas podem ser aplicadas como biocatalisadores nos processos industriais em substituição a reagentes químicos, tornando o processo menos agressivo ao meio ambiente. Este fato pode ser observado na indústria de celulose e de papel, que gera resíduos químicos, danosos ao meio ambiente, oriundos da etapa de branqueamento (Bruins et al. 2001).

A produção de termoenzimas em organismos mesofílicos torna possível a sua obtenção em larga escala, facilita a sua purificação e consequentemente leva a um aumento na disponibilidade e a um menor custo de produção, levando assim, a um crescente aproveitamento das enzimas termoestáveis por parte das indústrias.

1.7.2. Transcriptômica

Transcriptômica é o estudo do transcriptoma que se refere ao conjunto completo de transcritos (RNAs mensageiros, RNAs ribossômicos, RNAs transportadores e os microRNAs) de um dado organismo, órgão, tecido ou linhagem celular. O perfil do transcriptoma pode variar segundo o momento (numa dada fase do ciclo celular, por exemplo), estado fisiológico, estímulos físicos, químicos ou biológicos. O uso da tecnologia de sequenciamento de nova geração para estudar o transcriptoma ao nível dos nucleotídeos é conhecido como RNA-Seq (Wang et al. 2009).

Li et al. (2010) em seu estudo de adaptação térmica da bactéria *T. thermophilus* wl, utilizaram a técnica de Northen blot para confirmar os dados obtidos através da proteômica. Foram avaliados os genes codificadores das proteínas super expressas (total de 17) na condição de cultivo com temperatura acima da ótima (70 °C) e os dados encontrados foram similares ao da proteômica.

O uso da transcriptômica como ferramenta para elucidação dos mecanismos de adaptação a condições adversas também foi demonstrado por Zeller et al. (2005). Neste estudo foi avaliada a expressão gênica da bactéria *Rhodobacter sphaeroides* quando cultivada na presença de H_2O_2. A resposta genética à presença de H_2O_2 envolveu a super expressão de genes envolvidos na detoxificação de H_2O_2, enovelamento de proteínas e proteólise, reparo de DNA danificado, transporte e armazenamento de ferro, reparação de aglomerados de ferro-enxofre e sub expressão de genes para tradução de proteínas, motilidade e síntese de parede celular e lipopolissacarídeos.

Segundo Cabiscol et al. (2000), a magnitude da resposta ao H_2O_2 não depende somente da intensidade e tipo de estímulo, mas também da fase de crescimento do micro-organismo, sendo a resposta máxima na fase logarítmica e a menor na fase estacionária. Culturas em fase estacionária de *Bacillus subtilis* apresentaram alta viabilidade após tratamento com 10 mM de H_2O_2, concentração esta capaz de reduzir a viabilidade celular na fase logarítmica a aproximadamente 0,01% (Dowds, 1994). O mesmo fenômeno foi observado em *E. coli*, onde sugeriu-se que células em fase de crescimento tem sua capacidade de resposta rápida ao estresse severamente comprometida (Eisentark et al., 1996).

A combinação das análises de proteômica e transcriptômica com o intuito de proporcionar uma visão panorâmica das estratégias de adaptação de diferentes organismos a condições de estresse oxidativo tem se mostrado promissora. Além de genes com funções conhecidas, muitos genes com funções desconhecidas são encontrados nestes estudos, sendo estes tanto induzidos quanto reprimidos de acordo com o estímulo ao qual são submetidos. Neste contexto, uma análise sistemática dos produtos codificados por genes induzidos em situações de estresse poderia levar a uma melhor compreensão dos mecanismos de adaptação dos organismos após a sua exposição a espécies reativas de oxigênio e/ou de nitrogênio.

Referências

Anderson, N.L., Anderson, N.G. (1998). Proteome and proteomics: new technologies, new concepts, and new words. *Electrophoresis* 19: 1853–61.

Armstrong, G.A. (1997) Genetics of eubacterial carotenoid biosynthesis: a colorful tale. *Annual Review in Microbiology* 51: 629–659.

Armstrong, G.A., Alberti, M., Hearst, J.E. (1990) Conserved enzymes mediate the early reactions of carotenoid biosynthesis in nonphotosynthetic and photosynthetic prokaryotes. *Proceedings of the National Academy of Sciences U.S.A.* 87: 9975– 9979.

Averhoff, B. and Müller, V. (2010) Exploring research frontiers in microbiology: recent advances in halophilic and thermophilic extremophiles. *Research in Microbiology* 161: 506-514

Blankenship, R. E. (2010) Early evolution of photosynthesis. *Plant Physiology*. 154: 434–438.

Blasco, F., Kauffmann, I., Schmid, R.D. (2004) CYP175A1 from *Thermus thermophilus* HB27, the first beta-carotene hydroxylase of the P450 superfamily. *Applied Microbiology and Biotechnology* 64: 671–674.

Britton, G., Liaaen-Jensen, S. and Pfander, H. *Carotenoids Handbook*; Birkhauser: Basel, Switzerland, 2004.

Brock, T.D. and Freeze, H. (1969) Thermus aquaticus gen. n. and sp. n., a non-sporulating extreme thermophile. *Journal of Bacteriology* 98: 289-297.

Brüggemann, H. and Chen, C. (2006) Comparative genomics of *Thermus thermophilus*: plasticity of the megaplasmid and its contribution to a thermophilic lifestyle. *Journal of Biotechnology* 124: 654–661.

Bruins, M.E., Janssen, A.E., Boom, R.M. (2001) Thermozymes and their applications: a review of recent literature and patents. *Applied Biochemistry and Biotechnology* 90:155-86.

Burguess, M. L., Barrow, K. D., Gao, C., Heard, G. M., Glenn, D. (1999) Carotenoid glycoside esters from thermophilic bacterium Meiothermus rubber. *Journal of Natural Products* 62: 859-863.

Cabiscol, E., Tamarit, J., Ros, J. (2000) Oxidative stress in bacteria and protein damage by reactive oxygen species. *International Microbiology* 3: 3-8.

Caris-Veyrat, C. *Antioxidant and pro oxidant actions and stabilities of carotenoids in vitro and in vivo and carotenoid oxidation products.* In: Food colorants – chemical and functional properties. C. Socaciu (Ed.). CRC, New York, p.177-192, 2007.

Chien, A., Edgar, D.B., J.M. Trela, (1976) Deoxyribonucleic acid polymerase from the extreme thermophile *Thermus aquaticus. Journal of Bacteriology* 127: 1550-1557.

Choi, J.J.; Kim, H.K.; Kwon, S.T. (2001) Purification and characterization of the 5 ' -> 3 ' exonuclease domain-deleted Thermus filiformis DNA polymerase expressed in Escherichia coli. Biotechnology Letters. 23: 1647-1652.

Chung, A.P., Rainey, F.A., Valente, M. (2000) *Thermus igniterrae* sp. Nov. and *Thermus antranikianii* sp. Nov., two new species from Iceland. *International Journal of Systematic and Evolutionary Microbiology* 50: 209-217.

Dowds B.C. (1994) The oxidative stress response in *Bacillus subtilis*. *FEMS Microbiology* 124:155-264.

Egas, M.C.V.; da Costa, M.S.; Cowan, D.A.; Pires, E.M.V. (1998) Extracellular alpha-amylase from Thermus filiformis Ork A2: purification and biochemical characterization. Extremophiles. 2: 23-32.

Eisenstark A.; Calcutt M.J.; Becher-Hapak, M.; Ivanova A. (1996) Role of *Escherichia coli rpoS* and associated genes in defense against oxidative damage. *Free Radical Biology and Medicine* 21: 975-993.

Euzéby (J.P.): List of Prokaryotic names with Standing in Nomenclature. Disponível online: URL: http://www.bacterio.net/thermus.html. Acessado em: 06 de fevereiro de 2014.

Gargaud, M. et al. (Ed.): Lectures in Atrobiology, Vol. I, pp. 657–679 Springer-Verlag Berlin Heidelberg 2005 Chapter 9 Extremophiles. Purificación López-García.

Gomes A., Fernandes E., Lima J.L.F.C. (2005). Fluorescence probes used for detection of reactive oxygen species. *Journal of Biochemical and Biophysical Methods* 65: 45-80.

Gomes A., Fernandes E., Lima J.L.F.C. (2006). Use of fluorescence probes for detection of reactive nitrogen species: a review. *Journal of Fluorescence* 16: 119-139.

Gomes E., Guez M. A. U., Martin N., Silva R. (2007) Enzimas termoestáveis: fontes, produção e aplicação industrial. *Química Nova* 30: 136-145.

Grogan, D.W. (1998). Hyperthermophiles and the problem of DNA instability. *Molecular Microbiology* 28: 1043-1049.

Ha M. K., Chung K. Y., Bang D., Park Y. K., Lee K. H. (2005) Proteomic analysis of the proteins expressed by hydrogen peroxide treated cultured human dermal microvascular endothelial cells. *Proteomics* 5: 1507-1519.

Halliwell, B.B. (2012) Free radicals and antioxidants: updating a personal view. *Nutrition Reviews* 70: 257-65.

Hara M., Yuan H., Yang Q., Hoshino T., Yokoyama A., Miyake J. (1999) Stabilization of liposomal membranes by thermozeaxanthins: carotenoid-glucoside esters. *Biochimica et Biophysica Acta* 1461: 147-154.

Hare, N. J., Scott, N. E., Shin, E. H. H., Connolly, A. M., Larsen, M. R., Palmisano, G. and Cordwell, S. J. (2011), Proteomics of the oxidative stress response induced by hydrogen peroxide and paraquat reveals a novel AhpC-like protein in *Pseudomonas aeruginosa*. *Proteomics* 11: 3056-3069.

Havaux M. (1998) Carotenoids as membrane stabilizers in chloroplasts. *Trends in Plant Science* 3: 147-151.

Henne A., Bruggemann H., Raasch C., Wiezer A., Hartsch T., Liesegang H., Johann A., Lienard T., Gohl O., Martinez-Arias R., Jacobi C., Starkuviene V., Schlenczeck S., Dencker S., Huber R., Klenk H.P., Kramer W., Merkl R., Gottschalk G., Fritz H.J. (2004) The genome sequence of the extreme thermophile *Thermus thermophilus*. *Nature Biotechnology* 22:547-53.

Hoshino T., Fujii R., Nakahara T. (1993) Molecular cloning and sequence analysis of the crtB gene of *Thermus thermophilus* HB27, an extreme thermophile producing carotenoid pigments. *Applied and Environmental Microbiology* 59: 3150-3153.

Hreggvidsson G.O., Skirnisdottir S., Smit B., Hjorleifsdottir S., Marteinsson, V.T., Petursdottir S.K., Kristjansson J.K. (2006) Polyphasic analysis of *Thermus* isolates from geothermal areas in Iceland. *Extremophiles* 10: 563-575.

Huber R. and Stetter K. O. (2004) The Prokaryotes: An Evolving Electronic Resource for the Microbiological Community. New York: Springer-Verlag, pp.959.

Hudson J.A., Morgan H.W., Daniel R.M. (1987) *Thermus filiformis* sp. Nov., a filamentous caldoactive bacterium. *International Journal of Systematic Bacteriology* 37: 431-436.

Humpries K.M. and Sweda L.I. (1998) Selective inactivation of α-ketoglutarate dehydrogenase: reaction of lipoic acid with 4-hydroxy-2-nonenal. *Biochemistry* 37: 15835-15841.

Kang, S.K.; Cho, K.K.; Ahn, J.K.; Kang, S.A.; Hanv, K.H.; Lee, H.G.; Choi, Y.J. (2004) Cloning and expression of thermostable beta-glycosidase gene from *Thermus filiformis* Wai33 A1 in Escherichia coli and enzyme characterization. *Journal of Microbiology And Biotechnology*. 14: 584-592.

Kim K., Okanishi H., Masui R., Harada A., Ueyama N., Kuramitsu S. (2012) Whole-cell proteome reference maps of an extreme thermophile, *Thermus thermophilus* HB8. *Proteomics*. 12, 3063-3068.

Li D. C., Guo J., Li Y. L., Lu J. (2005) A thermostable manganese containing superoxide dismutase from the thermophilic *Thermomyces lanuginosus*. *Extremophiles* 9:1-6.

Li H., Ji X., Zhou Z., Wang Y. and Zhang X. (2010) *Thermus thermophilus* proteins that are differentially expressed in response to growth temperature and their implication in thermoadaptation. *Journal of Proteome Research* 9: 855-864.

Lim J.H., Yu Y.G., Han Y.S., Cho S., Ahn B.Y., Kim S.H., Cho Y. (1997) The crystal structure of an Fe-superoxide dismutase from the hyperthermophile *Aquifex pyrophilus* at 1.9 A resolution: structural basis for thermostability. *Journal of Molecular Biology* 270: 259-274.

Liu J., Yin M., Zhu H., Lu J., Cui Z. (2011) Purification and characterization of a hyperthermostable Mn-superoxide dismutase from *Thermus thermophilus* HB27. *Extremophiles* 15: 221-226.

Loginova L.G. and Egorova L.A. (1975) Obligatno-termofil'nye bacterii *Thermus ruber* v gidrotermakh kamchatki. *Mikrobiologiya* 44: 661-665.

Lushchak V.I. (2011) Adaptive response to oxidative stress: Bacteria, fungi, plants and animals. Comparative Biochemistry and Physiology, Part C 153: 175-190.

Lutnaes B.F., Strand G., Pétursdóttir S.K. and Liaaen-Jensen S. (2004) Carotenoids of thermophilic bactéria — *Rhodothermus marinus* from submarine Icelandic hot springs. *Biochemical Systematics and Ecology* 32: 455-468.

Mandelli F., Miranda V.S., Rodrigues E. and Mercadante A.Z. (2012b) Identification of carotenoids with high antioxidant capacity produced by extremophile microorganisms. *World Journal of Microbiology and Biotechnology* 28:1781-1790.

Mandelli F., Yamashita F., Pereira J.L., Mercadante A.Z. (2012a) Evaluation of biomass production, carotenoid level and antioxidant capacity produced by *Thermus filiformis* using fractional factorial design. *Brazilian Journal of Microbiology* 43: 126-134.

Maresca J.A. and Bryant D.A. (2006) Two genes encoding new carotenoid-modifying enzymes in the green sulfur bacterium Chlorobium tepidum. *Journal of Bacteriology* 188: 6217-6223.

Margesin R., Schinner F. (2001). Biodegradation and bioremediation of hydrocarbons in extreme environments. *Applied Microbiology and Biotechnology* 56: 650-663.

Miller A. F. (2012) Superoxide dismutases: Ancient enzymes and new insights. FEBS Letters 586: 585-595.

Morozkina E.V., Slutskaya E.S., Fedorova T.V., Tugay T.I., Golubeva L.I., and Koroleva O.V. (2010) Extremophilic Microorganisms: Biochemical Adaptation and Biotechnological Application (Review) *Applied Biochemistry* and *Microbiology* 46: 1-14.

Mostertz J., Scharf C., Hecker M., Homuth G. (2004) Transcriptome and proteome analysis of Bacillus subtilis gene expression in response to superoxide and peroxide stress. *Microbiology* 150, 497-512.

Nesaty, V.J.; Suter, M.J.F. (2008) Analysis of environmental stress response on the proteome level. *Mass Spectrometry Reviews* 27: 556-574.

Ohto C., Ishida C., Koike-Takeshita A., Yokoyama K., Muramatsu M., Nishino T., Obata S. (1999) Gene cloning and overexpression of a geranylgeranyl diphosphate synthase of an extremely thermophilic bacterium, *Thermus thermophilus. Bioscience Biotechnology and Biochemistry* 63: 261-270.

Pantazaki A.A., Pritsa A.A., Kyriakidis D.A. (2002) Biotechnologically relevant enzymes from *Thermus thermophilus*. *Applied Microbiology and Biotechnology* 58:1-12

Pantazaki A.A., Tambaka M.G., Langlois V., Guerin P., Kyriakidis D.A. (2003) Polyhydroxyalkanoate (PHA) biosynthesis in *Thermus thermophilus*: Purification and biochemical properties of PHA synthase. *Molecular Cell Biochemistry* 254:173-183.

Podar M., Reysenbach A.L. (2006) New opportunities revealed by biotechnological explorations of extremophiles. *Current Opinion in Biotechnology* 17: 250-255.

Puddu P., Puddu G.M., Cravero E., Rosati M., Muscari A., (2008) The molecular sources of reactive oxygen species in hypertension. *Blood Press* 17: 70-77.

Quackenbush J. (2007) Extracting biology from high-dimensional biological data. *The Journal of Experimental Biology* 210: 1507-1517.

Röling W.F.M., van Verserveld H.W. (1997) Growth, maintenance and fermentation pattern of salt-tolerant lactic acid bacterium *Tetragenonoccus halophile* in anaerobic glucose limited retention cultures. *Antonie van Leeuwenhoek* 72: 239-243.

Russell N. J. and Nichols D. S. (1999). Polyunsaturated fatty acids in marine bacteria – a dogma rewritten. *Microbiology* 145: 767-779.

Seckbach J. (ed.), Origins, 373–393. © 2004 Kluwer Academic Publishers. Printed in the Netherlands. Introduction to The Extremophiles Joseph Seckbach and Aharon Oren.

Senthil K. Murugapiran, S.K., Huntemann, M., Wei, C.L., Han, J., Detter, J. C., Han, C., Erkkila, T.H., Teshima, H., Chen, A., Kyrpides, N., Mavrommatis, K., Markowitz, V., Szeto, E., Ivanova, N., Pagani, I., Pati, A., Goodwin, L., Peters, L., Pitluck, S., Lam, J., McDonald, A.I., Dodsworth, J.A., Woyke, T., Hedlund, B.P. (2013) Thermus oshimai JL-2 and T. thermophilus JL-18 genome analysis illuminates pathways for carbon, nitrogen, and sulfur cycling. *Standards in Genomic Sciences* 7:449-468.

Sies H. (1993) Damage to plasmid DNA by singlet oxygen and its protection. *Mutation Research* 299:183-191.

Sies H., Menck C.F. (1992) Singlet oxygen induced DNA damage. *Mutation Research* 275:367-375.

Silva, A.M.S., Corrêa G.C., Reis, E.M. (2007) Proteomica – Uma Abordagem Funcional do estudo do Genoma. *Saúde e Ambiente em Revista* 2: 1-10.

Sivapriya M., Srinivas. (2007) Isolation and purification of a novel antioxidant protein from the water extract of Sundakai (Solanum torvum) seeds. *Food Chemistry* 104: 510-517.

Stan-Lotter H. and Fendrihan S. (Eds.) Adaption of Microbial Life to Environmental Extremes: Novel Research Results and Application. 2012, XII, 284 p.

Starkov A.A. (2008) The role of mitochondria in reactive oxygen species metabolism and signaling. *Annals of the New York Academy of Sciences* 1147: 37-52.

Tabata K., Hishida S., Nakahara T., Hoshino T. (1994) A carotenogenic gene cluster exists on a large plasmid in *Thermus thermophilus. FEBS Letters* 341: 251-255.

Takaichi S. and Mochimaru M. (2007) Carotenoids and carotenogenesis in cyanobacteria: unique ketocarotenoids and carotenoid glycosides. *Cellular and Molecular Life Science* 64: 2607-2619.

Trauger S. A., Kalisak E., Kalisiak J., Morita H., Weinberg M.V., Menon A. L., Poole F. L., Adams M.W.W., Siuzdak G. (2008) Correlating the Transcriptome, Proteome, and Metabolome in the Environmental Adaptation of a Hyperthermophile. *Journal of Proteome Research*. 7, 1027-1035.

True travel. Disponível on-line em: http://www.truetravel.cz./en/photogallery/geothermal-field-waimangu-new-zealand-photo/. Acessado em 05 de fevereiro de 2014.

Tyers, M.; Mann, M. (2003) From genomics to proteomics. *Nature* 422: 193-197.

Van de Vossenberg J. L. C. M., Driessen A. J. M., and Konings W. N. (1998) The essence of being extremophilic: the role of the unique archaeal membrane lipids. *Extremophiles* 2: 163–170.

Waimangu: Geology. Disponível on-line em: http://www.gns.cri.nz/Home/Learning/Science-Topics/Volcanoes/New-Zealand-Volcanoes/Volcano-Geology-and-Hazards/Waimangu-Geology. Acessado em 05 de fevereiro de 2014.

Wang Z., Gerstein M., Snyder M. (2009) RNA-Seq: a revolutionary tool for transcriptomics. *Nature Reviews Genetics* 10: 57-63.

Whittaker M.M. and Whittaker J.W. (2000) Recombinant superoxide dismutase from a hyperthermophilic archaeon, Pyrobaculum aerophilum. *Journal of Biological Inorganic Chemistry* 5:402-408.

Willians R.A.D. and Sharp R. (1995) The Taxonomic and Identification of Thermus. Biotechnology Handbooks 9: 1-42.

Yamano S. and Maruyama T. (1999) An azide-insensitive superoxide dismutase from a hyperthermophilic archaeon, *Sulfolobus solfataricus*. *Journal of Biochemistry* 125: 186-193.

Yamano S., Sako Y., Nomura N., Maruyama T. (1999) A cambialistic SOD in a strictly aerobic hyperthermophilic archaeon, *Aeropyrum pernix*. *Journal of Biochemistry* 126: 218-225.

Yokoyama A., Sandmann G., Hoshino T., Adachi K., Sakai M. and Shizuri Y. (1995) Thermozeaxanthins, new carotenoid-glicoside-esters from thermophilic Eubacterium *Thermus thermophilus*. *Tetrahedron Letters* 36: 4901-4904.

Yokoyama A., Shizuri Y., Hoshino T. and Sandmann G. (1996) Thermocryptoxanthins: novel intermediates in the carotenoid biosynthetic pathway of *Thermus thermophilus*. *Achives of Microbiology* 165: 342-345.

Zeikus J.G., Vieille C., Savchenko A. (1998) Thermozymes: biotechnology and structure-function relationships. *Extremophiles* 2: 179-183.

Zeller, T., Moskvin, O.V., Li, K., Klug, G., Gomelsky, M. (2005) Transcriptome and Physiological Responses to Hydrogen Peroxide of the Facultatively Phototrophic Bacterium *Rhodobacter sphaeroides. Journal of Bacteriology* 187: 7232-7242.

CAPITULO II

Adaptation strategies of a thermophilic microorganism, *Thermus filiformis*, under different stress conditions and prospection of targets with biotechnological potential

Mandelli, F.[1,2]; Couger, M. B.[3]; Carnielli, C.M. [4]; Paixão, D. A. A.[1]; Machado, C.B.[1]; Camilo, C. M. [5]; Polikarpov, I. [5]; Paes Leme, A.F.[4]; Mercadante, A. Z.[2]; Squina, F. M.[1*]

[1]Brazilian Bioethanol Science and Technology Laboratory (CTBE), Brazilian Centre of Research in Energy and Materials (CNPEM), Campinas, Brazil.

[2] Department of Food Science, Faculty of Food Engineering, University of Campinas (Unicamp), Campinas, Brazil.

[3] Department of Microbiology and Molecular Genetics, Oklahoma State University, OK, USA.

[4] National Laboratory of Biosciences (LNBio), Brazilian Centre of Research in Energy and Materials (CNPEM), Campinas, Brazil.

[5] Physics Institute of São Carlos, University of São Paulo (USP), São Carlos, SP, Brazil.

Manuscrito em preparação para ser submetido à revista

Molecular & Cellular Proteomics

ABSTRACT

Thermus filiformis is an aerobic thermophilic bacterium isolated from a hot spring in New Zealand with optimal growth at 70 °C. In order to evaluate the proteins and genes involved in the adaptation of *T. filiformis* cultivated under different conditions (63 °C, 77 °C, 70 °C without H_2O_2 and 70 °C with H_2O_2) and also to find thermozymes with potential industrial and biotechnological applications we used genomic, transcriptomic and proteomic approaches. Thermozeaxanthins and thermobiszeaxanthin synthetized by *T. filiformis* showed to be responsible for membrane stability at higher temperatures. Moreover, the carotenoid rich extracts of all samples proved to be potent scavengers of the peroxyl radical, being from 14 to 50 times more potent than α-tocopherol. Through proteomic and trancriptomic analysis the main mechanisms involved in the oxidative stress were elucidated. Proteins such as chaperones, aminoacyl-tRNA synthetases, the alarmone ppGpp were up-regulated in response to higher temperatures. On the other hand genes involved in the TCA cycle were down-regulated in respose to an increase in temperature, probably in attempt to avoid an excess in ROS formation. In relation to the addition of H_2O_2, it was observed an up-regulation of the chaperonin 33, which is a protein with highly reactive cysteines that respond quickly to changes in the redox environment. Besides the elucidation of the adaptation strategies, the study of the genome, transcriptome and proteome of *T. filiformis* also allowed the identification of molecules with high biotechnological potential, such as esterases, superoxi dismutase, alpha-galactosidases and alpha-amylase.

Keywords: RNA and DNA sequencing; mass spectrometry; thermozeaxanthin; antioxidant capacity.

INTRODUCTION

Extremophiles microorganisms, such as acidophilies, alcalophiles, barophiles, psychrophiles and thermophilies, are well adapted to unfavorable conditions from a human perspective, and have huge biotechnological potential. As a rule, extremophile molecules present increased stability not to a single, but to range of environmental factors, making possible their use in the industry for a wide range of applications (Topanurak et al. 2005).

Thermal environments are one of the most harmful ones and because the high temperature can transpose physical barriers and can have dramatic effects on the structure of almost all macromolecules (Hickey and Singer 2004). Moreover, thermophiles are also often exposed to oxidative stress, which is very deleterious to the cell, causing cellular damage at both molecular and metabolic levels (Miyoshi et al. 2003). The oxidative stress leads to an excess in generation of reactive oxygen and nitrogen species (ROS/RNS), such as anion superoxide, hydrogen peroxide, hydroxyl radical, peroxynitrite and nitric oxide that are highly reactive and able to cause damage to proteins, nucleic acids, lipids and other biological macromolecules (Topanurak et al. 2005).

Hydrogen peroxide (H_2O_2) can potentially damage enzymes by oxidizing sulfhydryl and iron-sulfur moieties. In addition, hydroxyl radical is fomed through Fenton reaction, which is highly reactive and can produce mutagenic and lethal lesions (Storz and Imlay 1999). Moreover, since H_2O_2 is an uncharged species, it penetrates lipid bilayers, at physiological pH, with a permeability coefficient similar to that of water (Mishra and Imlay 2012). Therefore, organisms typically contain multiple catalases and/or peroxidases to scavenge H_2O_2.

Despite knowing the function of some enzymes to the response of microorganisms exposed to a certain stress condition, it is hard to outline their adaptation strategies only studying the individual proteins (Chen and Chen 2004; Bruno-Bárcena et al. 2010). Therefore, one of the emerging principles in biology is that it is not the individual genes but the biological pathways and networks that drive an organism's response to a wide range of stimuli (Li et al. 2010). In this context it is important to identify the proteins involved in *T. filiformis* metabolism under stress conditions to unveil the mechanisms used in its adaptation to extreme environments.

Besides proteins, other molecules, such as carotenoids, have an important role in the stress adaptation. Carotenoids are known by its antioxidant properties which are closely related to their chemical structure, including aspects such as the number of conjugated double bounds, type of structural end-groups, and oxygen-containing

substituents (Mandelli et al. 2012a; Rodrigues et al. 2012). In *Thermus*, carotenoids can be inserted into lipids bilayers to reinforce the membrane at high temperatures (Yokoyama et al. 1995).

Thermus filiformis (ATCC 43280) is a thermophilic bacterium from *Thermus* genus that belongs to one of the oldest phylogenetic branches of bacterial evolution and that can grow well at temperatures around 70 °C. These microorganisms produce many thermostable enzymes, such as lipases/esterases (Fuciños et al. 2005), laccase (Miyazaki 2005) and superoxide dismutase (Mandelli et al. 2013), all of them can be useful for industrial applications.

Thus, the aim of this study was firstly to identify the carotenoid composition of each cultivation condition and determine the *in vitro* scavenging capacity of carotenoid rich extracts against peroxyl radical (ROO•). Due to the diffente profile and antioxidant capacity obtained for each different cultivation condition, we used genomic, transcriptomic and proteomic approaches to evaluate the mechanisms used by the thermophilic bacterium *T. filiformis* to grown in those differente growing conditions.

EXPERIMENTAL PROCEDURES

Bacterial culture and stress experiments

A strain of *Thermus filiformis* (ATCC 43280), isolated from a hot spring in New Zealand, was obtained from the National Institute for Quality Control in Health (INCQS/FIOCRUZ - Rio de Janeiro, Brazil). The microorganism was reactivated and stored according to Mandelli et al. (2012b).

T. filiformis was cultivated in Petri dishes containing the solid medium Castenholz TYE 1 % at 70 °C (optimum growth temperature) for 24 h (Ramaley and Hixson, 1970). Then, part of the culture from the Petri dishes was transferred to a 250 mL Erlenmeyer flask containing 30 mL of Castenholz TYE 1% and incubated on a shaker at 230 rpm for 24 h at 70 °C (pre-inoculum). After this period, the cell from the pre-inoculum were transferred to a 500 mL Erlenmeyer flask containing 150 mL of Castenholz TYE 1% and incubated under four different conditions: 63 °C, 77 °C, 70 °C without addition of H_2O_2 and 70 °C with addition of 100 μM of H_2O_2 (final concentration). For transcriptomic analysis the microorganim was cultivated for 8h while for carotenoid and proteomic analysis analysis the microorganim was cultivated for 16h.The experiments were performed in triplicates.

After microbial growth under the conditions described above, the suspensions of cells were centrifuged at 8,000 g for 10 min at 10 °C and the supernatant discarded. The pellet obtained was frozen at - 35 °C and afterwards lyophilized (Liobras model K105, Brazil).

Carotenoid extraction and identification

The carotenoids were extracted according to Mandelli et al. (2012). The total carotenoid content was used as the parameter of concentration in the determination of the antioxidant capacity. Total carotenoids were quantified in a diode array spectrophotometer (Agilent model 8453, USA) in the bandwidth from 220 to 700 nm, and the total concentration of carotenoids was calculated using the value obtained at the maximum absorption wavelength (λmax = 449 ± 2). The absorption coefficient value used was 2540 (zeaxanthin in ethanol) (Britton 1995).

The carotenoid extracts were analyzed in a high-performance liquid chromatograph (Shimadzu HPLC, Japan) equipped with quaternary pumps (model LC-20AD), an on-line degasser and a Rheodyne injection valve with 20 μL loop. The equipment included a DAD detector (Shimadzu, model SPD-M20A) connected in series to a mass spectrometer with an atmospheric pressure chemical ionization (APCI) source and an ion-trap analyzer (Bruker Daltonics, model Esquire 4,000, Germany). The carotenoid separation was carried out on a C30 YMC column (5 μm, 4.6 x 250 mm) (Waters, USA) with temperature set at 32 ºC and with a linear gradient of methanol/methyl *tert*-butyl ether (MeOH/MTBE) from 95:5 to 70:30 in 30 min, then to 50:50 in 10 min at 0.9 mL min^{-1} Mandelli et al. (2012a).The mass spectrometer parameters were set as follows: positive mode, current corona: 4,000 nA, source temperature: 450 °C, dry gas: N_2 with a temperature of 350 °C and a flow of 5 L min-1, nebulizer: 60 psi. The MS/MS experiments were run in automatic mode, with fragmentation energy of 1.4 V. The mass spectra were acquired with scan range of *m/z* from 100 to 1,500. The carotenoids were identified as previously mentioned in Mandelli et al. (2012a) and the percentage of each carotenoid was calculated considering the total area of all identified carotenoids.

Peroxyl radical scavenger capacity

Appropriate aliquots of the carotenoid extract were taken to prepare the working solutions in at least five different concentrations for each sample (Figure 4), evaporated under N_2 flow, redissolved in DMSO/MTBE (10:1, v/v) and sonicated for 30 s. The assays were carried out in a microplate reader (Synergy Mx, BioTek, Winooski, VT, USA), equipped

with a thermostat and dual reagent dispenser. The $ROO^{\bullet}$ scavenging capacity was measured by monitoring the effect of the carotenoid rich extract or α-tocopherol standard on the fluorescence decay resulting from $ROO^{\bullet-}$ induced oxidation of C11-BODIPY581/591 (Rodrigues et al., 2012). $ROO^{\bullet}$ was generated by the thermodecomposition of AIBN at 41°C. Reaction mixtures in the wells contained the following reagents at the indicated final concentrations (final volume of 225 μL): 0.18 μM C11-BODIPY581/591 in DMSO, 195 mM AIBN in DMSO/MTBE (10:1, v/v) and the carotenoid extract dissolved in DMSO. The fluorescence was measured until 120 min with excitation at 540 ± 20 nm and emission at 600 ± 20 nm. The $ROO^{\bullet}$ scavenging capacity was calculated according to Rodrigues et al. (2012) and was expressed as an undimensional value that represents how many times the extract is more efficient than α-tocopherol (positive control). The results correspond to analysis performed in triplicate.

DNA Sequencing, Genome Assembly, and Genome Annotation

The genomic DNA of *Thermus filiformis* was extracted with the phenol/chloroform method and then purified with PowerClean® DNA Clean-Up Kit (MoBio laboratories, USA). After that, the libraries for sequencing were prepared using Nextera DNA Sample preparation Kit (Illumina, USA), according to the manufacturer's protocol. These libraries were sequenced using the Illumina MiSeq Sequencing system (MiSeq Reagent Kit v2 of 500 cycles) with 250 base pair end chemistry (250x2bp). All genomic reads were assembled with the De Bruijn short read assembly algorithm Velvet 1.2.08 (Zerbino and Birney 2008). The assembly parameters were a kmer overlap value of 47 (k=47), minimum graph coverage value of (-cov_cutoff 7) and a minimum assembled contig length of 300bp (-min_contig_lgth 300). These parameters were selected based on a kmer optimization sweep. All protein coding genes were predicted using the prokaryotic gene called software Prodigal v2_60 (Hyatt et al. 2010), tRNA coding regions were predicted using tRNAscan-SE 1.21 (Schattner et al. 2005) and secreted proteins and transmembrane proteins were predicted using signalP 4.0 (Petersen et al. 2011). All predicted genes were annotated using homology search with NCBI BLAST 2.2.27+/C++ (Boratyn et al. 2013) against the NR and Uniprot databases. Domain prediction of protein coding genes was achieved using hmmscan (Eddy 2011) against the PFAM 27.0 domain database (Finn et al. 2014). Conserved Carbohydrate Active genes (CAZy) were predicted using hmmscan against the dbCAN database (Yin et al. 2012) CAZy domain profiles.

RNA-Seq Transcriptome Sequencing and Quantitative Transcriptomics

The microorganism was cultivated in Erlenmeyer containing Castenholz TYE 1 % medium at 70 °C for 8 h. After this period, the cultivation was centrifuged as previously described, the cells were recovered and grounded with liquid nitrogen. The *T. filiformis* RNA was extracted using *mir*Vana™ miRNA Isolation Kit (Life technologies, USA), treated with Ribo-Zero™ Magnetic Kit for bacteria, and then the TrueSeq® RNA Sample Preparation (Illumina, USA) was employed to prepare the cDNA libraries for sequencing. The libraries were barcoded and pooled for MiSeq 150x2bp sequencing. All experiments were performed in triplicates. Sequencing was performed on an Illumina MiSeq platform, using MiSeq Reagent Kit v2 of 300 cycles, at the Physics Institute of São Carlos – University of São Paulo, Brazil.

RNA-Seq reads were mapped onto the *de novo* assembly using the Bowtie2 alignment software (Langmead and Salzberg 2012). Quantitative transcription levels were predicted for all predicted protein coding genes in both FPKM (Fragments per kilobase of exon per million fragments mapped) and TPM (Transcripts per million) levels using the quantitative mapping package RSEM version 1.2.1 (Li and Dewey 2011). Differential expressions of all protein coding transcripts between all tested growth conditions were calculated using a significance threshold of $p<0.05$ using the Bioconductor EdgeR package (Robinson et al. 2010; Anders et al. 2013).

The functional classification of the differentially expressed genes (p-value<0.05) was performed according to Pfam. The categories over represented in each of the studied conditions were determined from the enrichment analysis implemented by BayGo algorithm (Vêncio et al. 2006)

Proteome analysis – sample preparation, mass spectrometry and data analysis

The lyophilized bacteria (7.0 ± 0.1 mg) was weighted and transferred to a siliconized microcentrifuge tube (2 mL), 700 μL of MiliQ water were added and the bacterial cells were disrupted by sonication with 10 s pulse for 5 min (Ultrasonic Processor, Sonics Vibracell, USA).

Samples (30 μL) were heated for 5 min at 99 °C in the presence of 15 μL of 6*x* protein loading buffer, followed by protein separation with 12 % sodium dodecyl sulfate polyacrylamide gel (SDS-PAGE) (16 x16 cm). The protein bands were visualized by staining the gel with Coomassie Blue R-250. The analysis was performed in triplicate.

The bands resulting from the SDS-PAGE analysis were excised according to the molecular weight (> 120, 120 to 85, 85 to 50, 50 to 35, 35 to 25, 25 to 20 and < 20 kDa), resulting in 7 gel pieces for each sample replication. The gel pieces were placed in a siliconized microcentrifuge tube, washed and destained in 0.5 mL 50% methanol/5% acetic acid for 3 h at room temperature before dehydration in 200 µL acetonitrile for 5 min and completely dried in a vacuum centrifuge.

The proteins were reduced by addition of 50 µL 10 mM dithiothreitol (DTT) and alkylated by addition of 50 µL 100 mM iodoacetamide (both 30 min at room temperature). To exchange the buffer, the gel pieces were dehydrated in 200 µL acetonitrile, hydrated in 200 µL 100 mM ammonium bicarbonate and dehydrated again with 200 µL acetonitrile. The dehydrated gel pieces were then completely dried in a vacuum centrifuge and rehydrated in 50 µL of 20 ng μL^{-1} ice-cold, sequencing-grade modified porcine trypsin (Promega, USA) for 30 min on ice bath. After that, the digestion was carried out overnight at 37 °C. The peptides produced in the digest were collected using the following solutions: 5 % formic acid in water (1x) and 5 % formic acid in acetonitrile/water (1:1) (2x); the extracts were combined in a siliconized 0.6 mL microcentrifuge tube and the total extract was concentrated in a vacuum centrifuge to 1 µL for analysis (Hanna et al. 2000).

The total extracts were reconstituted in 0.1% formic acid and analyzed on an ETD enabled Orbitrap Velos mass spectrometer (Thermo Fisher Scientific, USA) connected to a nanoflow liquid chromatography (LC-MS/MS) by an EASY-nLC system (Proxeon Biosystem, USA) through a Proxeon nanoelectrospray ion source. Peptides were separated on an analytical column EASY-Column (10 cm x id 75 µm, 3 µm particle size) with a pre-column EASY-Column (2 cm x id 100 µm, 5 µm particle size) and using a 2 - 90% acetonitrile gradient in 0.1% formic acid at a flow rate of 300 nL/min over 20 min. All instrument methods for the Orbitrap Velos were set up according to Souza et al. (2012). Peak lists (mgf) were generated from the raw data files by the software Proteome Discoverer 1.3.0 (Thermo Fisher Scientific, USA) and searched against *Thermus thermophilus* HB27 databases from Uniprot, with carbamidomethylation as fixed modifications and oxidation of methionine as variable modification.

Scaffold (version Scaffold_3.6.1, Proteome Software Inc., Portland, OR) was used to process the data from proteome discoverer. All MS/MS samples were analyzed using Sequest (XCorr Only) (Thermo Fisher Scientific, San Jose, CA, USA; version 1.4.0.288), which was set up to search on *Thermus filiformis* genoma (2402 entries) assuming trypsin as the digestion enzyme. Sequest was searched with a fragment ion mass tolerance of

1.00 Da and a parent ion tolerance of 10.0 PPM. Iodoacetamide derivative of cysteine was specified in Sequest as a fixed modification and oxidation of methionine was specified as a variable modification.

Peptide identifications were accepted only when established with at least 95 % probability as specified by the Peptide Prophet algorithm (Keller et al. 2002). Protein identifications were accepted when established with both at least 95 % probability and contained at least 2 identified peptides. Protein probabilities were assigned by the Protein Prophet algorithm (Nesvizhskii et al. 2003). Proteins that contained similar peptides and could not be differentiated based on MS/MS analysis alone were grouped to satisfy the principles of parsimony.

Functional enrichment analysis

The enrichment analysis was performed to evaluate the over represented biological process, according to Gene Ontology biological processes (GO) (Ashburner et al. 2000) using the Integrated Interactome System (IIS) platform, developed at the National Laboratory of Biosciences (LNBio), Brazil (Carazzolle et al. 2014). Significant biological processes (p-value < 0.05) from proteins/RNA enrichment analysis were assigned as clusters to generate a map of proteins and the corresponding enriched biological process, using the Cytoscape software for visualization (Shannon et al. 2003). The map from proteomic data analysis was merged with the map from RNA data analysis, resulting in one map for each comparison (without and with H_2O_2 and temperature set at 63 and 77 °C). Different colors and shapes were attributed to the corresponding gene of proteomic/RNA data in the proteins and biological process map, according to their expression (up- or down-regulated) and origin data (proteomic or RNA lists).

RESULTS

The carotenoid profile and the antioxidant capacity of the carotenoid extract of *T. filiformis* under different cultivation conditions (63 °C, 77 °C, 70 °C without addition of H_2O_2 and 70 °C with addition of 100 μM of H_2O_2) were evaluated. Due to the differecens presented in those analysis, we used the genomic, proteomic and transcriptomic approach to detect and identify proteins and genes that were differentially expressed by *T. filiformis* in each the mentioned conditions, in an attempt to elucidate the adaptations mechanisms involved in each case, and also to prospect targets with biotechnological potential.

The result from the cultivations were evaluated comparing sample cultivated at 63 °C and 77 °C, below and above the optimum growth temperature of *T. filiformis* (70 °C), to evaluate the thermoadaptation mechanisms used by this bacterium; and sample cultivated with and without H_2O_2, which can penetrates lipid bilayers with a permeability coefficient similar to that of water and be converted into highly reactive and deleterious products such as hydroxyl radical (Mishra and Imlay 2012).

Carotenoid analysis and antioxidant capacity of the carotenoid rich extracts

T. filiformis showed the highest total carotenoid content in the sample cultivated at 70 °C (1516 μg/g freeze-dried bacteria), while low values were obtained under stress conditions: 1272 μg/g freeze-dried bacteria at 70 °C plus H_2O_2, followed by the samples cultivated at 63 °C (981 μg/g freeze-dried bacteria) and at 77 °C (462 μg/g freeze-dried bacteria). The different amount of carotenoid production when submitted to different cultivation condition was already reported by our group (Mandelli et al. 2012b).

The carotenoids of *T. filiformis* were already identified and reported by Mandelli et al. (2012a). The carotenoid profile was similar for all four conditions with thermozeaxanthin-15 and thermozeaxanthin-13 as the major carotenoids in samples cultivated at 70 and 77 °C and thermozeaxanthin-15 and free zeaxanthin as the major carotenoids in sample cultivated at 63 °C (Figure 1).

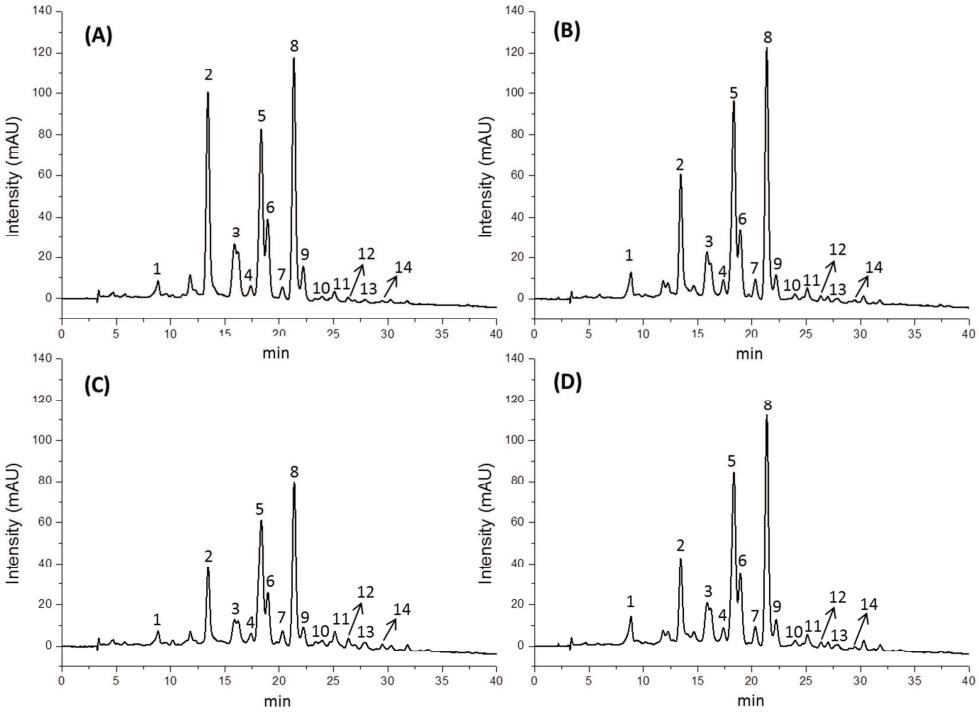

Figure 1. Chromatograms processed at 450 nm, obtained by HPLC-DAD, of the carotenoids from samples cultivated at 63 °C (A), 70 °C (B), 77 °C (C) and 70 °C with 100 μM of H_2O_2 (D). The samples injected on HPLC were resulting from a pool of three extracts for each studied condition. Peak identification: 1) zeaxanthin monoglucoside ($[M+H]^+$ at *m/z* 731); 2) all-*trans*-zeaxanthin ($[M+H]^+$ at *m/z* 569); 3) thermozeaxanthin-11 ($[M+H]^+$ at *m/z* 899); 4) thermozeaxanthin-12 ($[M+H]^+$ at *m/z* 913); 5) thermozeaxanthin-13 ($[M+H]^+$ at *m/z* 927); 6) 9 or 9'-cis-thermozeaxanthin-13 ($[M+H]^+$ at *m/z* 927); 7) thermozeaxanthin-14 ($[M+H]^+$ at *m/z* 941); 8) thermozeaxanthin-15 ($[M+H]^+$ at *m/z* 955); 9) 9 or 9'-cis-thermozeaxanthin-15 ($[M+H]^+$ at *m/z* 955); 10) thermozeaxanthin-16 ($[M+H]^+$ at *m/z* 969); 11) thermozeaxanthin-17 ($[M+H]^+$ at *m/z* 983); 12) thermobiszeaxanthin-13-13 ($[M+H]^+$ at *m/z* 1285); 13) thermobiszeaxanthin-13-15 ($[M+H]^+$ at *m/z* 1313); 14) thermobiszeaxanthin-15-15 ($[M+H]^+$ at *m/z* 1341).

The individual carotenoids were quantified according to the percentage of area obtained in the HPLC chromatogram (Figure 1) in relation to the total carotenoid concentration obtained by UV-visible. Figure 2 shows that no major differences were observed for thermozeaxanthins according to the cultivation condition, while for the sample cultivated at 63 °C a higher amount of all-*trans*-zeaxanthin was observed. The carotenoid extracts from samples submitted to stress conditions (70 °C with H_2O_2 and 77 °C) showed the highest proportions of thermobiszeaxanthins.

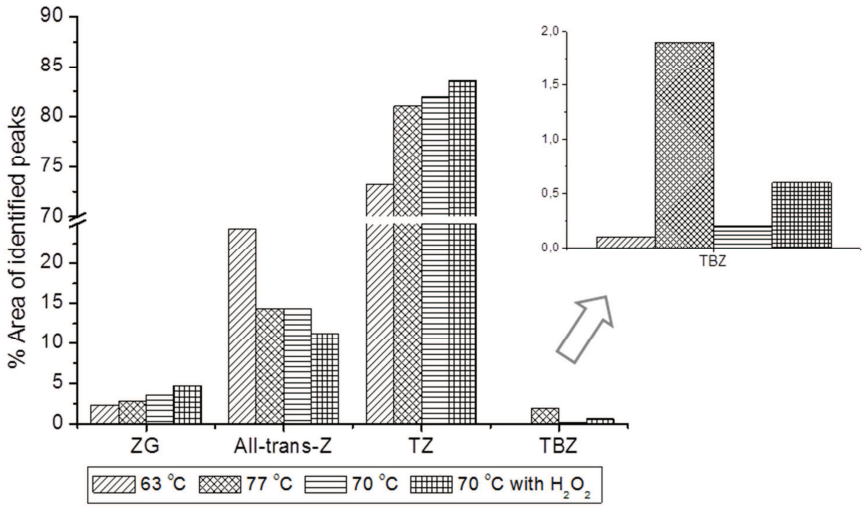

Figure 2. Percentage of carotenoids identified by HPLC-DAD-MS/MS for each cultivation condition. The carotenoids were grouped as: ZG: zeaxanthin monoglucoside (peak 1 on Figure 1); All-*trans*-Z: all-*trans*-zeaxanthin (peak 2 on Figure 1); TZ- thermozeaxanthins (peaks 3 to 11 on Figure 1) and TBZ: thermobiszeaxanthins (peaks 12 to 14 on Figure 1).

The carotenoid rich extract from all samples were able to scavenge $ROO^{\bullet}$ and the net AUC values were linearly dependent to the total carotenoid concentration (Supplementary figure SF1). The highest $ROO^{\bullet}$ scavenger capacity was observed for the extract from *T. filiformis* cultivated at 70 °C with 100 μM H_2O_2 (50.5), followed by that at 70 °C without H_2O_2 (33.7), at 77 °C (25.8) and finally at 63 °C (14.1).

Thermus filiformis genome

The *T. filiformis* genome was sequenced in order to provide a data bank to proteomic and transcriptomic analysis. Further analysis of genome content and comparisons of *T. filiformis* with other microrganims will be theme for future studies.

Adaptor ligated illumina sequencing libraries had a mean insert size of 500bp according to the Agilent Technologies Bioanalyzer 2100. The DNA sequencing produced a total of 9,680,471 paired reads (4.88GB, Table 1) and the produced assembly had an n_{50} = 85.2Kb, n_{90} = 17.1kb, largest contig size = 275.5kb and total size of 2,464,950 bp (2.46MB). Gene prediction resulted in 2,403 protein coding genes (table 1). A total of 2,349 (97.8%) of the predicted protein coding genes contained a NR homolog of e-5 or less. Analysis of protein coding genes using hmmscan against a group of 111 conserved

single copy molecular genes (Albertsen et al. 2013) showed that 95.4% (106/111) were contained in the assembly.

Table 1. Genome parameters obtained by DNA sequencing using an Illumina MiSeq.

Illumina Reads	19360942 bp
Illumina Read Pairs	9680471
Raw Bases	4884023500 bp (4.88GB)
n_{50}	85193 (85.2 kb)
n_{90}	17163 (17.1kb)
Total Size	2464950 (2.46MB)
Largest Contig	275543 (275.54KB)
Number of Contigs	151
Genes Predicted	2403
HMM Conserved Genes Present in the Assembly (e^{-5} of less)	106/111 (95.4%)
Genes with NCBI hit e^{-5} or less	2349 (97.8%)
Genes Predicted with detectable RSEM Value in any condition	2334 (97.1%)
tRNA predicted	45

Transcriptome of *Thermus filiformis*

The value of 97.1% (2334/2403) of predicted protein coding genes showed detectable expression with RSEM (RNA-Seq by Expectation-Maximization) values (Table 1). The reads and the amount of data sequenced for each condition are shown in Supplementary Table 1 and the differential expression of all protein coding transcripts among all tested growth conditions are shown in Supplementary Table 2.

According RNA-Seq analysis, 900 genes were significantly different (p value ≤ 0.05) when comparing samples cultivated at 77 °C and 63 °C, among these, 452 genes were up-regulated at 77 °C being 264 of them with a fold change higher than 2 and 448 genes were down-regulated at 77 °C being 199 of them with a fold change higher than 2 (Supplementary Table 3). Comparing samples cultivated with and without H_2O_2, 141 genes significantly different (p value ≤ 0.05) among these, 81 genes were up-regulated with H_2O_2 being 20 of them with a fold change higher than 2 and 57 genes were down-regulated with H_2O_2 being 15 of them with a fold change higher than 2 (Figure 3; Supplementary Table 4).

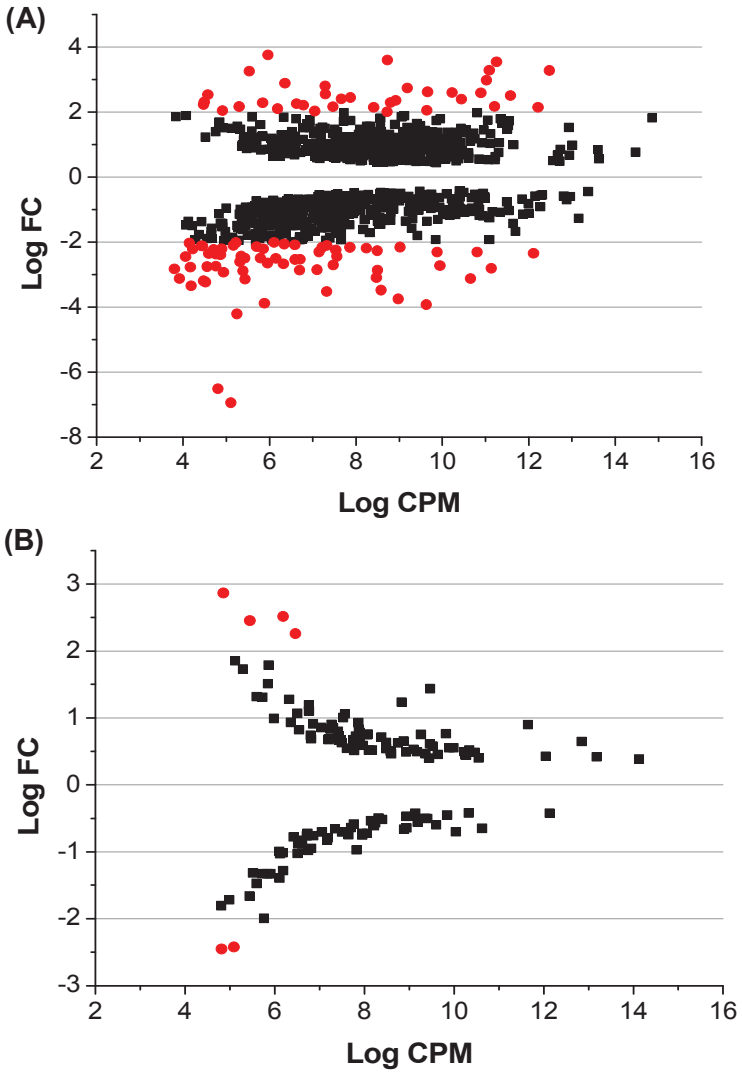

Figure 3. Log of fold change versus log of counts per million. Samples with positive values for log FC are up-regulated; the ones with negative values are down-regulated. (**A**) Comparing samples cultivated at 63 and 77 °C; (**B**) Comparing samples cultivated with and without hydrogen peroxide, both at 70 °C. Red dots represents the genes with log of fold change lower than -2 or higher than 2.

Figure 4 shows the Pfam enrichment analysis, where it is observed that most of the Pfam descriptions higher number of genes up-regulated at 77 °C. The AAA domain (ATPases Associated with diverse cellular Activities) was the annotation with the highest number of genes up-regulated at 77 °C and with H_2O_2. AAA proteins are essential for many cellular functions such as protein degradation, membrane fusion, DNA replication, intracellular transport, transcriptional activation, protein refolding, disassembly of protein complexes and protein aggregates (Hanson and Whiteheart 2005).

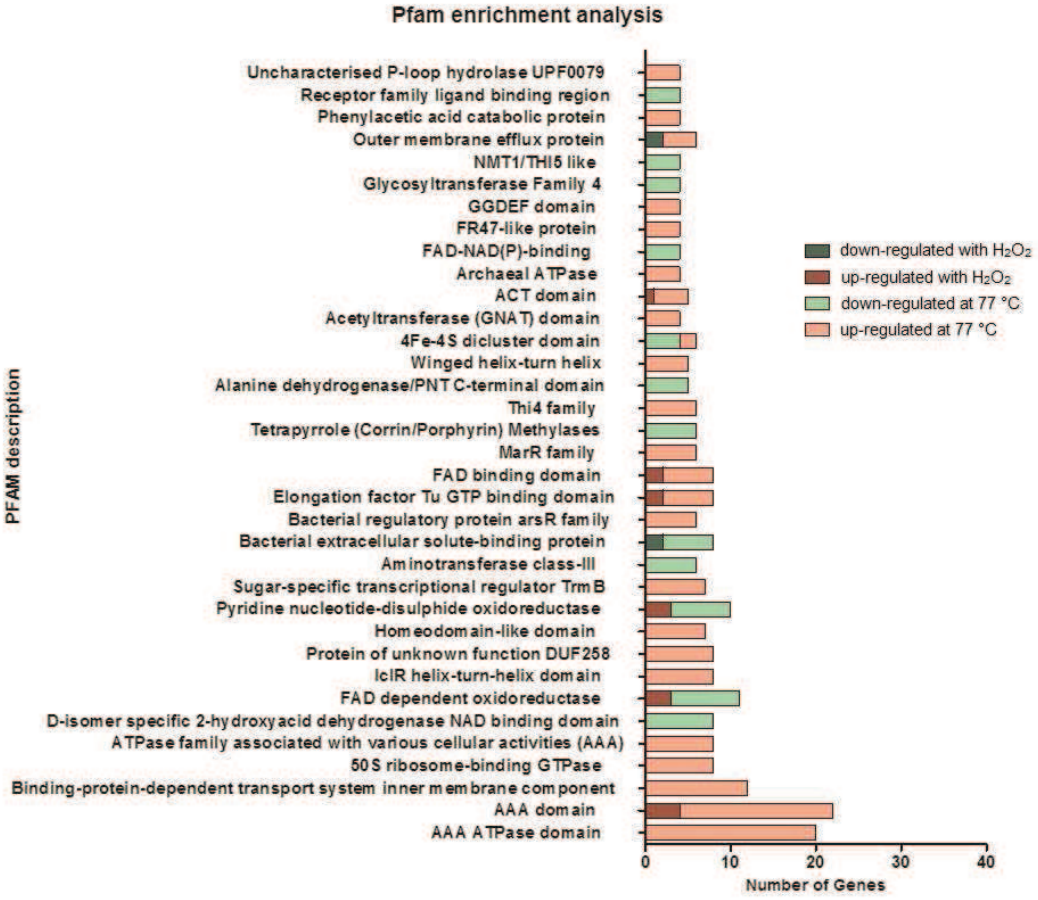

Figure 4: Enrichement analysis according to Pfam familes using software BayGo. The imput data was the significative (p-value <0.05) transcripts founded in temperature and peroxide assays.

Proteomic analysis

The sequenced genome of *T. filiformis* was used as database to identify the proteins from proteome analysis. A total of 666 proteins with an FDR < 0.05 % were identified when comparing conditions at 63 °C and 77 °C; 128 significantly different according to T-test (p value ≤ 0.05), being 31 up-regulated at 63 °C and 97 up-regulated at 77 °C (Supplementary Table 5). On the other hand, comparing conditions with and without H_2O_2, 681 proteins with an FDR < 0.05 % were identified, being 41 significantly different according to T-test (p value ≤ 0.05), among these, 16 were up-regulated at the condition with peroxide and 25 up-regulated at the condition without peroxide (Supplementary Table 6).

Among the proteins up-regulated at 77 °C are: small heat shock protein, chaperonins, superoxide dismutase, elongation factors Tu and G and alpha-glucosidases. On the other hand, proteins like alanine-tRNA ligase, protein GrpE and drug resistance transporter protein were up-regulated with H_2O_2 (Supplementary Tables 7 and 9).

Through proteome analysis some condition-specific proteins for each sample were found. Comparing conditions at different temperatures, one unique protein was identified at 63 °C (E8PKS4_THESS: Cold shock protein, CSD family) and seven at 77 °C (K7R7V5_THEOS: Uncharacterized protein; G8NA19_9DEIN: Two component transcriptional regulator; H9ZUE0_THETH: Putative lactam utilization protein B-like protein; B7AAD3_THEAQ: Putative signal transduction protein with CBS domains; E8PKS5_THESS: Chaperone protein DnaJ; D3PLD6_MEIRD: Uncharacterized protein; H9ZT99_THETH: Hypothetical protein). On the other hand, only one unique protein was identified in each condition when comparing samples with (Q72L28_THET2: Gluconate 5-dehydrogenase) and without H_2O_2 (G8N909_9DEIN: Putative uncharacterized protein).

Functional enrichment analysis

In order to get a more comprehensive understanding of the biological differences between the conditions under study (without and with H_2O_2 and temperature set at 63 and 77 °C), the list of identified proteins or transcripts were submitted to enrichment analysis for the GO biological processes using the IIS (Ashburner et al. 2000; Carazzolle et al. 2014)

Supplementary tables 7 and 8 shows the results of the enrichment by biological process annotation for the proteomic data, while Supplementary tables 9 and 10 shows the result for trancriptomic data, when comparing the conditions at low and high temperatures and with and without hydrogen peroxide, respectively. A protein/gene can be enriched in more than one biological process, although only the process with the lower p-value is shown in the tables. The most relevant biological process are shown in Figures 4A and 4B, for peroxide and temperature assays, respectively.

Based on Supplementary tables 7 to 10 (proteins and genes significantly different, p value ≤ 0.05), a protein map with the biological processe was built for both comparisons, with and without hydrogen peroxide (Figure 5A) and low and high temperatures (Figure 5B). The resultant network combine proteomic and trancriptomic data, and only the clusters with at least three genes are shown in Figure 5.

According to Figure 5A, the main enrriched biological processes involved in H_2O_2 adaptation were translation (ribosomal proteins), where the 5 genes found to be down-

regulated and 1 protein up-regulated with H_2O_2; regulation of transcription, with 2 genes up-regulated (cold shock protein and 16S rRNA) and 1 gene (two component reponse regulator) and 1 protein (DNA-directed RNA polymerase subunit beta) up-regulated with H_2O_2; protein folding, with 3 genes up-regulated (33 kDa chaperonin, Chaperone protein DnaK and Protein GrpE) and 1 protein up (Protein GrpE) and 1 down-regulated (PpiC-type peptidyl-prolyl *cis-trans* isomerase) with H_2O_2 and metabolic process, where all genes were up-regulated with H_2O_2.

In the thermoadaptation (Figure 5B), the main biological processes affected by the higher temperature (77 °C) were: ATP catabolic process, with 10 genes and 1 protein up-regulated, most of then related to the ABC transporter proteins; and transcription, with 11 genes, such as the transcription termination factor Rho and the two component transcriptional regulator and 2 protein up-regulated (Two component transcriptional regulator and Anti-cleavage anti-GreA transcription factor Gfh1).

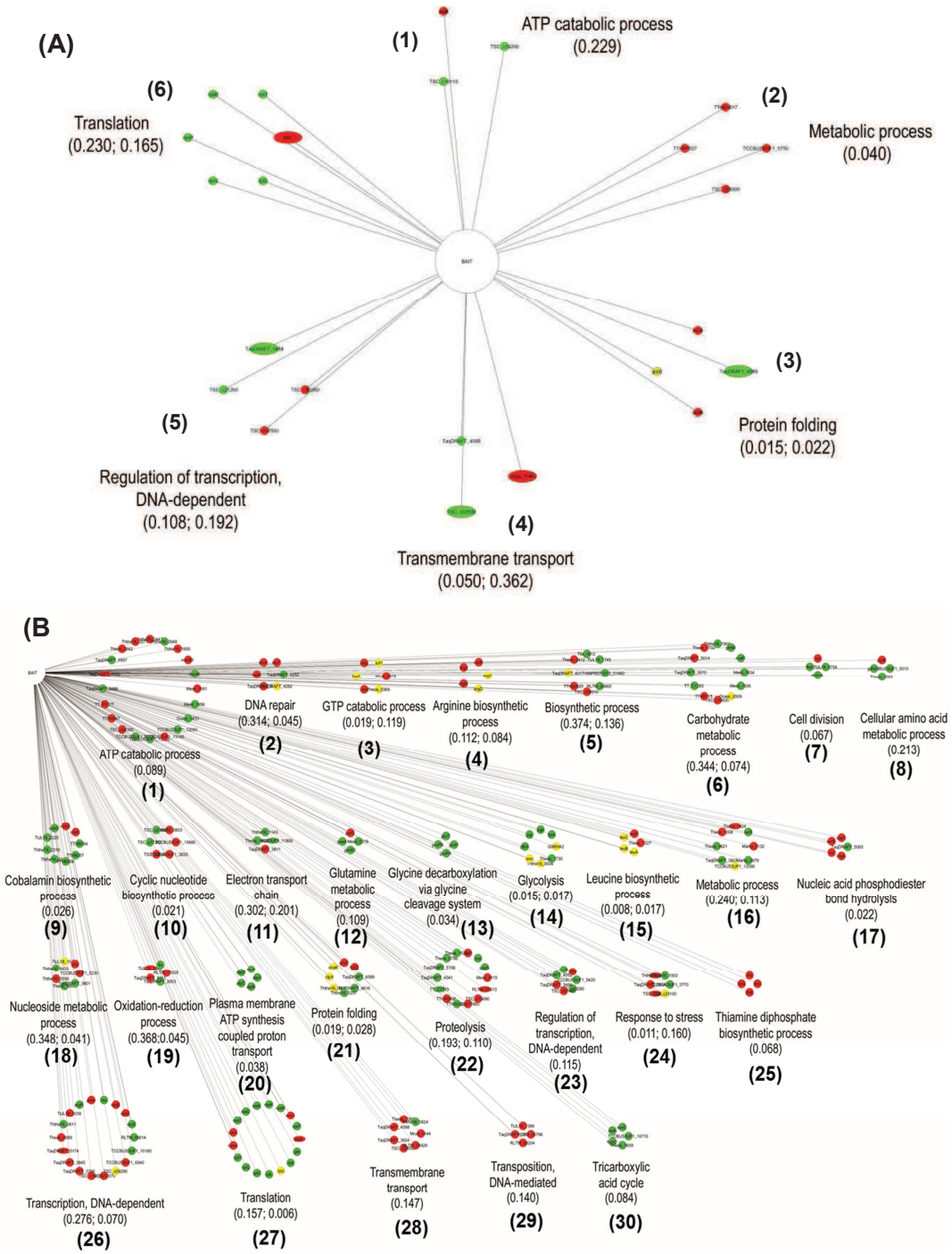

Figure 5. Protein map resultant of the union of proteomic and transcriptomic data built from the IIS platform (**A**) samples cultivated with and without peroxide (**B**) samples cultivated at different temperatures. The enriched biological process ($p \leq 0.05$) is shown for each protein/gene cluster and in parenthesis is the p-value for proteomic and transcriptomic data, respectively. Nodes in red

represent the up-regulated data, node in green the down-regulated data and nodes in yellow are common data of proteomic and transcriptomic analysis. Rounded nodes are from trancriptomic data and oval nodes are from proteomic data. The genes shown on this figure, are listed on the following tables (2 and 3), extra informations can be found in supplementary tables 7 to 10 where are genes/proteins are numbered according to the bold numbers of this figure.

The genes and proteins shown of Figure 5A are listed on Table 2 and genes and proteins shown of Figure 5B are listed on Table 3.

Table 2: Genes of the biological process presented on Figures 5A.

Top enriched Biological Process	Gene	Fig. 5A†
ATP catabolic process	TSC_c19110; TSC_c16200; pstB	1
metabolic process	TSC_c08000; TTHA1327; TTHA1617; TCCBUS3UF1_5750	2
protein folding	hslO; dnaK; grpE; TaqDRAFT_4589	3
transmembrane transport	TaqDRAFT_4588; TSC_c02500; Mrub_0144	4
regulation of transcription, DNA-dependent	TSC_c21260; TSC_c00360; TSC_c17050; TaqDRAFT_3484	5
translation	rpsP; rplQ; rpmI; rpsT; rpsR; rplP	6

†numbered according to figure 5A. Genes in red represent the up-regulated data, genes in green the down-regulated data and genes in yellow are common data of proteomic and transcriptomic analysis.

Table 3: Genes of the biological process presented on Figures 5B.

Top enriched Biological Process	Gene	Fig. 5B†
ATP catabolic process	Mesil_1956; TaqDRAFT_3486; moxR; TCCBUS3UF1_9990; TaqDRAFT_4887; Ththe16_0948; Ocepr_1433; TCCBUS3UF1_12050; TaqDRAFT_4530; TCCBUS3UF1_15950; TCCBUS3UF1_13140; macB1; Theos_0842; Ththe16_0271; Ththe16_0447; Mesil_0181; TT_P0177; TTHV087; Ththe16_1650; TSC_c04350	1
DNA repair	TaqDRAFT_4252; radA; TaqDRAFT_5398; recA; TaqDRAFT_4282; recF	2
GTP catabolic process	Theos_0369; Mrub_0318; obg; tuf1; era; fusA	3
arginine biosynthetic process	argD; argC; argG; argJ; carB	4
biosynthetic process	HMPREF1013_01460; RLTM_00865; Tlie_1812; TtJL18_1745; TaqDRAFT_4317; Theos_0412; TTHA0620; TSC_c09910	5
carbohydrate metabolic process	Ththe16_1904; TaqDRAFT_3070; Mesil_1936; malP; Ocepr_0509; Mesil_1834; TT_C1283; Theos_1732; TTHB115; glmM; TSC_c10830; TaqDRAFT_5014	6
cell division	divIVA; ftsA; TtJL18_0754; int	7
cellular amino acid metabolic process	TCCBUS3UF1_5010; gdhA1; Theos_1523; pyrB	8

cobalamin biosynthetic process	TTHB054; cobD; TTHB057; TTHB058; Ththe16_2318; Ththe16_2319; TtJL18_2225; cobQ; cobS	9
cyclic nucleotide biosynthetic process	TSC_c21880; TSC_c17260; TCCBUS3UF1_15680; TSC_c08960; TCCBUS3UF1_3620; Ththe16_0803	10
electron transport chain	Ththe16_1143; Theos_1499; TCCBUS3UF1_11800; TaqDRAFT_3811	11
glutamine metabolic process	guaA; Mesil_0319; glmS2; pyrG	12
glycine decarboxylation via glycine cleavage system	gcvPB; gcvH; gcvT; gcvPA	13
glycolysis	Q9RHA2; Ththe16_0004; eno; Theos_1730; tpiA; pgi; pfkA; pgk	14
leucine biosynthetic process	leuC; Theos_1227; leuA; leuB; leuD	15
metabolic process	luxS; TaqDRAFT_3803; Marky_0976; TCCBUS3UF1_12090; Theos_0621; Theos_1424; Theos_1008; Marky_0132	16
nucleic acid phosphodiester bond hydrolysis	TaqDRAFT_5093; uvrB; vapC; rnpA; rnr	17
nucleoside metabolic process	Ththe16_1633; TtJL18_1513; Theos_1667; TaqDRAFT_3801; TtJL18_1345; TCCBUS3UF1_5230; Ththe16_0556	18
oxidation-reduction process	Fni; TaqDRAFT_3003; TaqDRAFT_5111; RLTM_11628	19
plasma membrane ATP synthesis coupled proton transport	atpB; atpE; atpD; atpA; atpC	20
protein folding	Ththe16_0257; TaqDRAFT_4616; dnaK; TaqDRAFT_4589; Ththe16_0606; clpX; hslO; groS	21
proteolysis	TaqDRAFT_4341; pepA; TTHA0286; TaqDRAFT_5158; Theos_1520; pcp; Theos_0798; TSC_c17860; Mesil_0115; TTHA0896; TT_C1715; RLTM_07213; TSC_c15690	22
regulation of transcription, DNA-dependent	TCCBUS3UF1_5420; TSC_c03290; TaqDRAFT_4552; nusB; TSC_c07440; TaqDRAFT_3484; rho	23
response to stress	Ththe16_1503; TCCBUS3UF1_3770; TSC_c23100; TSC_c23890; Ththe16_0896; TaqDRAFT_5154	24
thiamine diphosphate biosynthetic process	thiC; thiE; thiI; thiG	25
transcription, DNA-dependent	RLTM_08814; rex; rpoZ; TCCBUS3UF1_10180; argR; Ththe16_0611; TSC_c12070; rpoC; rpoB; TaqDRAFT_3795; TCCBUS3UF1_6540; TSC_c09290; TSC_c18130; TaqDRAFT_5174; Theos_0989; greA; TtJL18_1038; TaqDRAFT_3845	26
translation	rpsK; rpsC; rplI; rpsD; rplJ; rplY; rpsE; rplQ; rpsT; rplO; pth; rplL; rpsA; rpmA; rpsM; rpsO; gatA	27
transmembrane transport	Ththe16_0824; TaqDRAFT_3924; Theos_1382; RLTM_04929; TSC_c20050; TaqDRAFT_4588; Mrub_0144	28
transposition, DNA-mediated	TaqDRAFT_3838; RLTM_05796; TtJL18_1389; RLTM_08204	29
tricarboxylic acid cycle	Mdh; sucC; Theos_1659; TCCBUS3UF1_16710; fumC	30

† numbered according to figure 5B. Genes in red represent the up-regulated data, genes in green the down-regulated data and genes in yellow are common data of proteomic and transcriptomic analysis.

Genes and proteins involved in the stress response

In *T. filiformis* 27 genes of aminoacyl-tRNA synthetases (aaRS) were identified. Among then, 3 presented duplication with one of the genes up-regulated at 77 °C (Suplementary Table 11): a cysteinyl-tRNA synthetase (Thfi_0234 and Thfi_1287), an alanyl-tRNA synthetase (Thfi_0089 and Thfi_1940), an aspartyl-tRNA synthetase (Thfi_2251 and Thfi_1196) and a valyl-tRNA synthetase (Thfi_1644 and Thfi_1505). None of the aaRS identified presented up-regulation in samples cultivated with 100 μM of H_2O_2.

Other proteins involved in translation, such as RelA/SpoT family (p)ppGpp synthetase and some elongation factor of the GTP (guanosine triphosphate) binding elongation factor family also had their expression altered by the stress conditions. The elongation factor EF-Tu and EF-G presented up-regulation at the conditions with H_2O_2 and at 77 °C, respectively, while the elongation factor EF-Ts and EF-P presented no significant difference in expression among the samples.

Genes involved in transcription were also greatly affected by the different growing conditions. Among the 17 genes related to transcription, 11 were up-regulated at 77 °C, such as DNA-directed RNA polymerase, transcriptional regulator - LacI family and MarR family and transcription elongation factor GreA; and in the presence of H_2O_2 a transcriptional regulator, DeoR family, that usually control the expression of genes involved in sugar metabolism was up-regulated (Figure 5 A and B).

Chaperones are proteins that prevent misfolding and promote the refolding and proper assembly of unfolded polypeptides generated under stress conditions (Georgopoulos and Welch 1993). Among the identified chaperones, chaperonin 33, chaperonin 60 (GroL) , chaperonin 10 (GroES) and ATP-dependent chaperone ClpB were up-regulated at 77 °C. In relation to the addition of H_2O_2 up-regulation in the genes encoding a chaperone protein DnaK, chaperonin 33 and a protein GrpE was observed.

Proteins involved in TCA cycle, such as malate dehydrogenase, succinyl-CoA ligase, succinate dehydrogenases and fumarate hydratase were all down-regulated at 77 °C. On the other hand, no significative differences in protein and gene expression of TCA cycle was observed for hydrogen peroxide assays.

A total of 562 and 62 hypothetical/uncharacterized proteins were identified by transcriptome and proteome analysis, respectively. The amino acid sequences of these proteins were submitted to Pfam analysis in order to check their domain. It was found ferrodoxins, AAA proteins, ABC transporters, acetyltransferase, elongation factors G, TU

and P, glycosyl transferases and hydrolases, major facilitators, methyltransferases, thioredoxins among others.

Carotenogenesis

Genes involved in the synthesis of geranylgeranyl pyrophosphate (GGPP) and carotenoid biosynthesis were identified. Figure 6 shows the FPKM of the identified genes involved in terpenoid (Figure 6A) and carotenoid (Figure 6B) biosynthesis. No major differences in gene expression were observed when comparing samples with and without H_2O_2. On the other hand most of the genes involved in GGPP biosynthesis were up-regulated at the highest temperature (77 °C). Another significative difference is the highest level of expression of the gene encoding phytoene dehydrogenase at 70 °C.

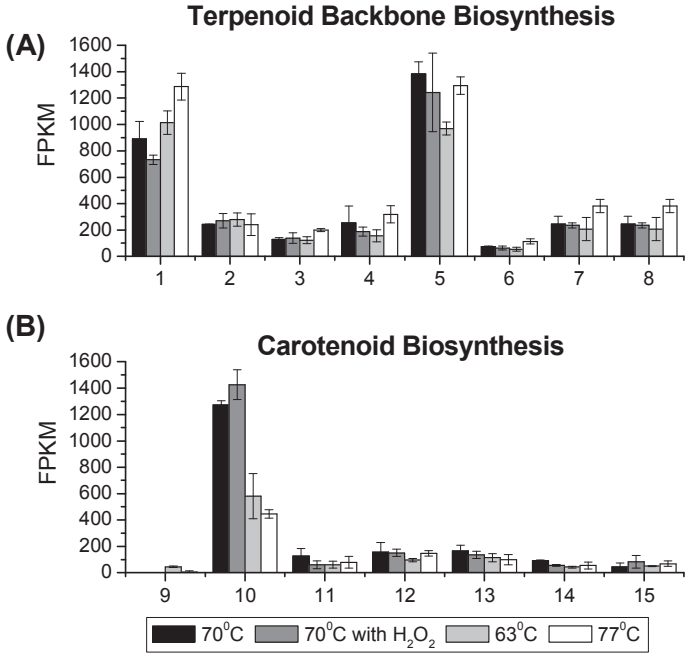

Figure 6. FPKM (Fragments per kilobase of exon per million fragments mapped) of the identified genes belonging to terpenoid backbone (**A**) and carotenoid biosynthesis (**B**) for each condition analyzed. 1) 1-deoxy-D-xylulose-5-phosphate synthase; 2) 2-C-methyl-D-erythritol 4-phosphate cytidylyltransferase; 3) 4-diphosphocytidyl-2-C-methyl-D-erythritol kinase; 4) 2-C-methyl-D-erythritol 2,4-cyclodiphosphate synthase ; 5) 4-hydroxy-3-methylbut-2-enyl diphosphate reductase; 6) isopentenyl-diphosphate delta-isomerase; 7) Dimethylallyltranstransferase; 8) geranylgeranyl pyrophosphate synthase; 9) phytoene/squalene synthetase; 10) phytoene dehydrogenase; 11) lycopene cyclase; 12) cytochrome P450; 13) deoxyribodipyrimidine photolyase; 14) glycosyltransferase; 15) phospholipid/glycerol acyltransferase. For further information see Figure 8 on page 20 of this thesis.

DISCUSSION

Bacteria stress can be defined as a physiological perturbation caused by environmental modifications (physical, chemical and/or nutritional) that can have many consequences for the microorganism, such as retarded growth, molecular damage, metabolic pathway disruptions and cell death (Farr and Kogoma 1991; Fridovich 1998). Proteome and transcriptome are powerful tools for identifying differentially expressed profiles of proteins and genes in response to bacterial adaptation to extreme environments. Thus, we used these methods to investigate the mechanisms of *T. filiformis* adaptation under different cultivation conditions.

Translation

The duplication of some aaRS,, which are key enzymes in the translation of the genetic code, presented by *T. filiformis* presented one of the two genes (Thfi_0234, Thfi_0089, Thfi_2251 and Thfi_1644) induced by heat shock (Suplementary Table 11).

In most organisms, 20 aaRS, each with a particular specificity, provide the various aminoacyl-tRNA involved in protein synthesis. Although there are a few exceptions, where two genes encode aaRS of the same specificity (Becker and Kern, 1998). Duplication of synthetases was first exemplified with the discovery of two lysyl-tRNA synthetases (LysRS) encoded by distinct genes in *Escherichia coli* (Hirshfield et al. 1981). Later it was discovered that one of the two LysRS from *E. coli* was induced by heat shock, anaerobiosis, or low pH and is involved in adaptation of the organism to stress conditions (Lévêque et al 1991).

The ppGpp (guanosine pentaphosphate) nucleotide, found as a heat response, is synthetized in the ribosome by the RelA protein upon activation by the presence in the A site of the ribosome of deacylated-tRNA and is considered an “alarmone” which is involved in the stringent response in bacteria (Srivatsan and Wang 2008; Katz and Orellana 2012). During the stringent response, ppGpp accumulation affects replication, transcription, and translation in the cells. ppGpp bind to RNA polymerase redirecting the transcription profile, so that genes important for stringent response are favoured at the expense of those required for growth and proliferation (Magnusson et al. 2005). Additionally, the initiation of new rounds of replication is inhibited and the cell cycle arrests until nutrient conditions improve (Srivatsan and Wang 2008).

Other proteins involved in translation and induced by heat were the elongation factors EF-Tu, which interact with an aminoacyl-tRNA to begin the protein synthesis cycle

and EF-G which promotes the GTP-dependent translocation of the nascent protein chain from the A-site to the P-site of the ribosome (Kovtun et al 2006).

Transcription

Among the proteins annotated in the transcription process, two of them are highlighted due to their role in thermoadaptation: the transcription elongation factor GreA (Q8VQD6), which plays multiple roles in transcriptional elongation and may be implicated in the resistance to various stresses, besides being involved in protection of cellular proteins against aggregation (Li et al 2012); and, two-component response regulator (B7A5R7), which together with a membrane-bound histidine kinase comprises the two-component regulatory system and is responsible to mediate the cellular response, mostly through the differential expression of target genes (Stock et al 2000).

Chaperones and Protein Folding

The combining action of GroL and GroES are required for the proper folding of many proteins, and demonstrated to be necessary for thermoadaptation. The central cavity of the cylindrical GroL provides an isolated environment for protein folding, while the co-chaperone, GroES, binds to GroL and synchronizes the release of the folded protein in an ATP-dependent manner (Hartl 1996). Further on these chaperones recover unfolded and misfolded proteins in the stress condition.

The other chaperone involved in the cell recovery from heat-induced damage was the ATP-dependent chaperone ClpB, which is part of a stress-induced multi-chaperone system, belonging to the AAA family (Figure 4) (Lee et al. 2004).

In relation to the addition of H_2O_2 adaptation, the chaperonin 33 called especial attention once it is a molecular chaperone, distinguished from all other known chaperones by its mode of functional regulation. This chaperonin is a cytoplasm-localized protein with highly reactive cysteines that respond quickly to changes in the redox environment. Oxidizing conditions such as H_2O_2 causes disulfide bonds that lead to the activation of the chaperonin 33 function (Jakob et al. 1999), as found in the present study.

Tricarboxylic acid cycle

In general, all aerobic organisms produce NADH and $FADH_2$ in the TCA cycle, where these reducing equivalents are oxidized in the respiratory chain, and the electrons generated are subsequently transferred to cytochromes where O_2 is converted to H_2O. The proton motive force created by the electrons movement is harnessed to produce ATP with

the participation of ATP synthase (Shimizu 2014). The inefficient transfer of electron via the respiratory complexes results in the one electron reduction of diatomic oxygen, a phenomenon known to generate toxic ROS (Mailloux et al. 2007).

The TCA cycle acts both as a scavenger and generator of ROS, so its modulation is an important strategy in O_2-dependent organisms to regulate the intracellular levels of ROS (Mailloux et al. 2007). A reduced activity of the TCA cycle leads to a decrease in the oxygen level and consequently less ROS is generated (Shimizu 2014).

Once oxygen diffusion trhough the membrane increases with an increase in temperature, problably, the microorganim uses the down regulation of TCA cycle in attempt to avoid the increase in the oxygen concentration and consequently increase in ROS formation.

Terpenoid Backbone and Carotenoids Biosynthesis

Carotenoids are a diverse class of natural pigments that are of interest as food colorants and nutrient supplements as well as for pharmaceuticals (Sandman 2001). According to Henne et al. (2004) in *T. thermophilus* HB27, the terminal steps of carotenoid biosynthesis are encoded on the plasmid, whereas precursor synthesis, the formation of geranylgeranyl pyrophosphate (GGPP) via MEP/DOXP (2-C-methyl-D-erythritol 4-phosphate/1-deoxy-D-xylulose 5-phosphate) pathway, is accomplished by enzymes encoded on the chromosome. The MEP/DOXP pathway is an alternative to mevalonate pathway that leads to the formation of isopentenyl pyrophosphate and dimethylallyl pyrophosphate. These compounds are converted into geranyl pyrophosphate, followed by (*trans*,*trans*)-farnesyl pyrophosphate and finally to geranyl-geranyl pyrophosphate, the precursor of carotenoid biosynthesis

Proteome and transcriptome analysis reveal that the terpenoid biosynthesis follows the MEP/DOXP pathway in *T. filiformis*. Among the eight transcripts involved on this pathway, no significative difference was observed for sample with and without H_2O_2. On the other hand, seven genes involved on this pathway were up-regulated at 77 °C, indicating that GGPP biosynthesis is favored at high temperatures (Figure 6A).

The identified genes involved in carotenoid biosynthesis were all located at the same gene cluster, as observed by genome analysis. These genes encodes a phytoene synthase responsible for the convertion of GGPP in phytoene; a phytoene desaturase that catalyzes four successive desaturation reactions beginning with the colorless carotenoid phytoene and producing the colored carotenoid lycopene; a lycopene cyclase responsible

for the cyclization of lycopene on one or both Ψ-ends and a cytochrome P450 which has a sequence identity of 68 % with a P450 monooxygenase from *T. thermophilus* HB27 (CYP175A1). According to Blasco et al. (2004) the CYP175A1 encodes a type of β-carotene hydroxylase that is capable of introducing OH groups into the β-ionone rigns of β-carotene producing zeaxanthin via β-cryptoxanthin. This type of β-carotene hydroxylase shows little similarity to other known β-carotene hydroxylases, including CrtZ and CrtR, and the histidine rich iron-binding motifs that are typical of CrtZ are not detected in CYP175A1 (Tian and Hua 2011).

A glycosyltranferase and an acyltranferase, responsible for the glucosylation and acylation steps follow hydroxylations on C-3 and C-3′ of β-carotene to form zeaxanthin monoglucoside esters and diglucoside esters were also identified. The glycosyltranferase (Thfi_1229) and acyltranferase (Thfi_1230) of *T. filiformis* showed identity of 65 % and 76 % with a glycosyltranferase (TTHB103) and an acyltranferase (TTHB105) of *T. thermophilus* HB8.

In addition, the carotenoid genes were interlocked with deoxyribodipyrimidine photolyase, which can repair DNA damages caused by UV light. According to Brüggemann and Chen (2006) carotenoid production and repair of UV-induced DNA damage are co-evolved protection mechanisms against the photo-oxidative damage caused by UV light.

The highest amount of phytoene dehydrogenase found in the samples cultivated at 70 °C (figure 6B) indicates a high rate of carotenoids synthesis, which corroborates with the highest amount of total carotenoids obtained in these conditions.

Although no major differences in expression of the genes involved in carotenoid biosynthesis, biochemical analysis showed a greater tendency for the synthesis of thermobiszeaxanthins at 77 °C than in the other conditions studied (Figure 2). This result agrees with the fact that *Thermus* carotenoids reinforce the membranes leading to a decrease in membrane fluidity and an increase in membrane stability, what are essential for its survival at high temperatures (Yokoyama et al. 1995). Another result that reinforces this hypothesis is the highest amount of free-zeaxanthin presented at 63 °C, where the membrane lipids are more stable and more fluid (Figure 2).

The carotenoid rich extract from *T. filiformis* cultivated at the most stressful condition (77 °C and with H_2O_2) showed higher antioxidant capacity than those obtained under the less stressful condition (63 °C and without H_2O_2). This results is probably related

to the fact that, besides its role in membrane reinforce, carotenoids are also known as efficient ROS scavengers and protect DNA from oxidative damage, proteins from carbonylation and membranes from lipid peroxidation (Stahl et al. 1998; Zhang and Omaye 2000; Stahl and Sies 2003; Astley et al. 2004).

The carotenoid rich extract of all conditions studied (cultivation at 63 °C, 77 °C and 70 °C with and without addition of H_2O_2) showed a ROO• scavenging capacity higher than those carotenoid rich extracts from some fruits, such as mamey (6.9), peach palm (7.8), murici (12.8) and mana-cubiu (9.80) (Rodrigues et al. 2012; Mariutti et al. 2013; Rodrigues et al. 2013). The carotenoid rich extract from *T. filiformis* was also more potent as ROO• scavenger than authentic standards of (all-*trans*)-lycopene (8.67), (all-*trans*)-lutein (1.90) and (all-*trans*)-zeaxanthin (3.52) (Rodrigues et al. 2012), suggesting the synergy among the type of carotenoids or the presence of other compounds in the bacteria extract.

Hypothetical/Uncharacterized proteins

Among the hypothetical/uncharacterized proteins found in *T. filiformis* some of them presented a chaperone domain, which may be involved in thermoadaptation, and a thioredoxin domain, which plays a role in redox signaling and can catalyze the reduction of H_2O_2 and thereby prevent the oxidative stress and the apoptosis induction (Arnér and Holmgren 2000). This result shows that there is an amount of proteins involved in the adaptation of several environmental stimuli that still remain uncharacterized.

Metabolic features of *Thermus filiformis* with biotechnological potential

A termostable pyrophosphatase was identified in *T. filiformis*, with a FPKM for the gene encoding this enzyme, was 2 times greater at 77 °C than at 63 °C. This is an enzyme commercially available due to its biotechnological applications in protein, DNA and RNA synthesis (Pantazaki et al. 2002). This enzyme eliminates organic pyrophosphate which is created during incorporation of nucleotide triphosphates. The presence of pyrophosphate is reported to inhibit DNA polymerase activity and causes DNA and RNA degradation at elevated temperatures (Tabor and Richardson 1990). By eliminating pyrophosphate, pyrophosphatase removes these threats of inhibition and degradation.

An α-amylase was also identified by RNA-Seq. A *T. filiformis* α-amylase was already purified and characterized by Egas et al. (1998). Termostable α-amylases from *Bacillus* has been used in the industrial degradation of starch to glucose.

Enzymes involved in oligosaccharide degradation were also found in *T. filiformis.* Two glycosidase, that can be used in biomass degradation due to its ability to hydrolyze glycosidic bonds in complex sugars (Sinnott 1990). One alpha-galactosidase responsible to hydrolyze simple and complex α-D-galactosides was also detected. This enzyme has a wide industrial application, such as, in the paper industry, sugar beet refining, and replacement therapy for Fabry disease (Benitez and Sanchez 2009).

Genes encoding proteins belonging to the esterase family (total of 15 genes) were also found in *T. filiformis*. The esterases attract increasing attention because they plays a major role in the degradation of natural materials and industrial pollutants besides being useful in the synthesis of optically pure compounds, perfums and antioxidants (Panda and Gowrishankar 2005).

Cobalamin (vitamin B12) is an important vitamin involved in the metabolism of every cell of the human body; however fungi, plants and animals are not capable to produce vitamin B12. This vitamin is industrially produced only through fermentation of selected microorganisms (Martens et al. 2002). Once the genes related to cobalamin biosynthesis were found in the *T. filiformis*, this bacterium can also be exploited as a thermophilic source of enzymes involved in the biosynthesis of this vitamin.

Antioxidant enzimes such as superoxide dismutase, catalase and thioredoxins were also synthetized by *T. filiformis*. Besides the medical appeal, the antioxidant enzymes can also have many industrial uses, such as preservatives in food and cosmetics (Hamid et al. 2010).

Thermophilic DNA polymerases of various *Thermus* species are of indispensable value in PCR techniques. The genes encoding DNA polymerases (a total of 13) were identified in *T. filiformis*. Moreover, 4 DNA-directed RNA polymerase were identified, which could be an interesting tool in molecular biology for *in vitro* transcription assays, for example.

CONCLUSION

Exposure of *T. filiformis* to oxidative stress caused changes in carotenoid, proteome and trancriptome pattern. The differentially expressed proteins and genes provide information to understand the mechanisms used in the stress adaptation.

In relation to thermoadaptation it was observed that *T. filiformis* favor the synthesis of thermozeaxanthins and thermobiszeaxanthin at higher temperature in order to increase the membrane stability.

Some genes involved in translation were also affected by high temperatures. In *T. filiformis* some aminoacyl-tRNA synthetases presented duplication, being one of them induced by the heat shock to participate in the amino acid biosynthesis. Besides, the alarmone ppGpp was also up-regulated at 77 °C favoring the synthesis of the genes involved in the stringent response.

The two-component response regulator, which enable the microorganism to sense, respond, and adapt to a wide range of environments, stressors, and growth conditions; and GreA, involved in protection of cellular proteins against aggregation, are genes involved in transcription and also demonstrated to be important in the adaptation to high temperature.

Another important class of protein involved in *T. filiformis* thermoadaptation was the chaperones. Chaperonins 33, 60, 10 and the chaperone ClpB were up-regulated at 77 °C, where their main role is to prevent misfolding and promote the refolding and proper assembly of unfolded polypeptides.

To deal with the oxidative stress, the genes involved in the TCA cycle were down-regulated at 77 °C, what is probably an attempt of the microorganism to avoid the O_2 accumulation and consequently avoid the increase in ROS formation.

The addition of H_2O_2, at least in the amount studied (100 μM), did not seem to have a great influence on carotenoid profile, protein and gene expression of *T. filiformis*. Although some changes were observed: the carotenoid rich extract of the sample cultivated with H_2O_2, was the one with the greatest antioxidant capacity among the samples studied, suggesting that, in this case, carotenoid also plays an antioxidant role due to the presence of H_2O_2. Another feature to highlight, for the sample cultivated with H_2O_2, is the up-regulation of the chaperonin 33, which is a protein with highly reactive cysteines that respond quickly to changes in the redox environment.

The highest quantity of genes/proteins differentially expressed when comparing growth temperature and hydrogen peroxide addition indicates that changes in temperature had grater influence in *T. filiformis* metabolism than the hydrogen peroxide addition.

Finally, this work also allowed us to point out some thermostable macromolecules produced by *T. filiformis*, such as amylases, pyrophosphatases, glycosidases and galactosidases, all them with a wide range of industrial applications.

Acknowledgment: This work was financially supported by grants from CNPq (474022/2011-4 and 310177/2011-1) and FAPESP (2008/58037-9 and 2011/17658-3). FM

received fellowship from CNPq (142685/2010-0). We gratefully acknowledge the provision of time on the MAS facilities (LNBio) at the National Center for Research in Energy and Materials.

REFERENCES

Albertsen, M.; Hugenholtz, P.; Skarshewski, A.; Nielsen, K. L.; Tyson, G. W.; Nielsen, P. H. Genome sequences of rare, uncultured bacteria obtained by differential coverage binning of multiple metagenomes. *Nature Biotechnology* **2013**, 31, 533-538.

Anders, S.; McCarthy, D. J.; Chen, Y.; Okoniewski, M.; Smyth, G. K.; Huber, W.; Robinson, M. D. Count-based differential expression analysis of RNA sequencing data using R and Bioconductor. *Nature Protocols* **2013**, 8, 1765-1786.

Arnér, E.; Holmgren, A. Physiological functions of thioredoxin and thioredoxin reductase. *European Journal of Biochemistry* **2000**, 267, 6102–6109.

Ashburner, M.; Ball, C.A.; Blake, J.A.; Botstein, D.; Butler, H.; Cherry, J.M.; Davis, A.P.; Dolinski, K.; Dwight, S.S.; Eppig, J.T.; Harris, M.A.; Hill, D.P.; Issel-Tarver, L.; Kasarskis, A.; Lewis, S.; Matese, J.C.; Richardson, J.E.; Ringwald, M.; Rubin, G.M.; Sherlock, G. Gene Ontology: tool for the unification of biology. *Nature Genetics* **2000**, 25: 25-29.

Astley, S. B.; Hughes, D. A.; Wright, A. J.; Elliott, R. M.; Southon, S., DNA damage and susceptibility to oxidative damage in lymphocytes: effects of carotenoids in vitro and in vivo. *British Journal of Nutrition* **2004**, 91, 53-61.

Becker, H.D.; Kern D.; *Thermus thermophilus*: A link in evolution of the tRNA-dependent amino acid amidation pathways. *PNAS* **1998**, 95, 12832–12837.

Benitez, A.; Sanchez, O. Evaluation of agro-industrial by products for α-galactosidase production by *Aspergillus oryzae* in submerged culture. *Chemical Engineering Transactions* **2009**, 17, 1155-1160.

Blasco, F.; Kauffmann, I.; Schimid, R.D. CYP175A1 from *Thermus thermophiles* HB27, the first β-carotene hydroxylase of the P450 superfamily. Applied Microbiology and Biotechnology **2004**, 64: 671-674.

Boratyn, G. M.; Camacho, C.; Cooper, P. S.; Coulouris, G.; Fong, A.; Ma, N…. Zaretskaya, I. BLAST: a more efficient report with usability improvements. *Nucleic Acids Research* **2013**, 41(Web Server issue), W29-33.

Britton G **1995** UV/Vis Spectroscopy. In: Carotenoids: Spectroscopy, vol 1B. Britton, G.; Liaaen-Jensen, S.; Pfander, H. (Eds.). Birkhauser, Basel, Switzerland.

Brüggemann, H.; Chen, C. Comparative genomics of *Thermus thermophilus*: Plasticity of the megaplasmid and its contribution to a thermophilic lifestyle. Journal of Biotechnology **2006**, 124: 654–661.

Bruno-Bárcena, J. M.; Azcárate-Peril, M. A.; Hassan, H. M., Role of Antioxidant Enzymes in Bacterial Resistance to Organic Acids. *Applied Environmental and Microbiology* **2010**, 76, 2747-2753.

Carazzolle, M.F.; de Carvalho L.M.; Slepicka, H.H.; Vidal, R.O.; Pereira, G.A.G.; Kobarg, J.; Meirelles, G.V. IIS – Integrated Interactome System: A Web-Based Platform for the Annotation, Analysis and Visualization of Protein-Metabolite-Gene-Drug Interactions by Integrating a Variety of Data Sources and Tools. *PLoS ONE* **2014**, 9, e100385.

Chen, K. Y.; Chen, Z. C., Heat shock proteins of thermophilic and thermotolerant fungi from Taiwan. *Botanical Bulletin of Academia Sinica* **2004**, 45, 247-257.

Eddy, S. R. Accelerated Profile HMM Searches. *PLoS Computional Biology* **2011**, 7(10), e1002195.

Egas, M.C.V.; da Costa, M.S.; Cowan, D.A.; Pires, E.M.V. Extracellular α-amylase from Thermus filiformis Ork A2: purification and biochemical characterization. *Extremophiles* **1998**, 2: 23-32.

Farr, S. B.; Kogoma, T., Oxidative stress responses in *Escherichia coli* and *Salmonella typhimurium*. *Microbiology Reviews* **1991**, 55, 561–585.

Finn, R. D.; Bateman, A.; Clements, J.; Coggill, P.; Eberhardt, R. Y.; Eddy, S. R.…Punta, M. Pfam: the protein families database. *Nucleic Acids Research* **2014**. 42(Database issue), D222-230.

Fridovich I., Oxygen Toxicity: A Radical Explanation. *The Journal of Experimental Biology* **1998**, 201, 1203–1209.

Fuciños, P.; Abadín, C. M.; Sanromán, A.; Longo, M. A.; Pastrana, L.;l Rúa, M. L., Identification of extracellular lipases/esterases produced by *Thermus thermophilus* HB27: partial purification and preliminary biochemical characterisation. *Journal of Biotechnology* **2005** 17, 233-41.

Georgopoulos, C.; Welch, W. J., Role of the major heat shock proteins as molecular chaperones. *Annual Review of Cell and Developmental Biology* **1993**, 9, 601–34.

Hamid, A.A.; Aiyelaagbe, O.O.; Usman, L.A.; Ameen, O.M.; Lawal, A. Antioxidants: Its medicinal and pharmacological applications. *African Journal of Pure and Applied Chemistry* **2010**, 4, 142-151.

Hanna, S. L.; Sherman, N. E.; Kinter, M.; Goldberg, J. B., Comparison of proteins expressed by *Pseudomonas aeruginosa* strains representing initial and chronic isolates from a cystic fibrosis patient: an analysis by 2-D gel electrophoresis and capillary column liquid chromatography–tandem mass spectrometry. *Microbiology* **2000**, 146, 2495–2508.

Hanson, P.I.; Whiteheart, S.W. AAA+ proteins: have engine, will work. *Nature Reviews Molecular Cell Biology* **2005**, 6, 519–29.

Hartl FU. Molecular chaperones in cellular protein folding. *Nature* **1996**, 381:571.

Henne, A.; Brüggemann, H.; Raasch, C.; Wiezer, A.; Hartsch, T.; Liesegang, H.; Johann, A.; Lienard, T.; Gohl, O.; Martinez-Arias, R.; Jacobi, C.; Starkuviene, V.; Silke Schlenczeck, S.; Dencker, S.; Huber, R.; Klenk, H.P.; Kramer, W.; Merkl, R.; Gottschalk, G.; Fritz, H.J. The genome sequence of the extreme thermophile *Thermus thermophiles*. *Nature Biotechnology* **2004**, 22: 547-553.

Hickey, D. A.; Singer, G. A. C., Genomic and proteomic adaptations to growth at high temperature. *Genome Biology* **2004**, 5, 117.

Hirshfield I.N.; Bloch, P.L.; Van Bogelen, R.A.; Neidhardt, F.C.. Multiple forms of lysyl-transfer ribonucleic acid synthetase in *Escherichia coli*. *Journal of Bacteriol*ogy **1981**, 146, 345–351.

Hyatt, D.; Chen, G. L.; Locascio, P. F.; Land, M. L.; Larimer, F. W.; Hauser, L. J. Prodigal: prokaryotic gene recognition and translation initiation site identification. *BMC Bioinformatics* **2010**, 11, 119.

Jakob, U.; Muse, W.; Eser, M.; Bardwell, J.C. Chaperone activity with a redox switch. *Cell* **1999**, 96: 341–352.

Katz, A.; Orellana, O. **2012**. Protein Synthesis and the Stress Response, Cell-Free Protein Synthesis, Prof. Manish Biyani (Ed.), ISBN: 978-953-51-0803-0, InTech, DOI: 10.5772/50311.

Keller, A.; Nesvizhskii, A.I.; Kolker, E.; Aebersold, R., Empirical Statistical Model to Estimate the Accuracy of Peptide Identifications Made by MS/MS and Database Search. *Analytical Chemistry* **2002**, 74, 5383-92.

Kovtun, A. A.; Minchenko, A. G.; Gudkov, A. T., Mutation analysis of functional role of amino acid residues in domain IV of elongation factor G. *Molecular Biology (Moscow, Russ. Fed., Engl. Ed.)* **2006**, 40, 850-856.

Langmead, B.; Salzberg, S. L. Fast gapped-read alignment with Bowtie 2. *Nature Methods* **2012**, 9(4), 357-359.

Lee S, Sowa ME, Choi JM, Tsai Francis TF. The ClpB/Hsp104 molecular chaperone-a protein disaggregating machine. *Journal of Structural Biology* **2004**, 146: 99–105.

Lévêque, F.; Gazeau, M, Fromant, M.; Blanquet, S.; Plateau, P.; Control of Escherichia coli lysyl-tRNA synthetase expression by anaerobiosis. *Journal of Bacteriol*ogy **1991**, 173, 7903–7910.

Li, B.; Dewey, C. N. RSEM: accurate transcript quantification from RNA-Seq data with or without a reference genome. *BMC Bioinformatics* **2011**, 12, 323.

Li, H.; Ji, X.; Zhou, Z.; Wang, Y.; Zhang, X., *Thermus thermophilus* Proteins That Are Differentially Expressed in Response to Growth Temperature and Their Implication in Thermoadaptation. *Journal of Proteome Research* **2010**, 9, 855–864.

Li, K.; Jiang, T.; Yu, B.; Wang, L.; Gao, C.; Ma, C.; Xu, P.; Ma, Y. Transcription Elongation Factor GreA Has Functional Chaperone Activity. *PLOS One* **2012**, 7: e47521.

Magnusson L.U.; Farewell, A.; Nyström, T. ppGpp: a global regulator in *Escherichia coli*. *Trends in Microbiology* **2005**, 13, 236-242.

Mailloux, R.J.; Beriault, R.; Lemire, J.; Singh, R.; Chenier, D.R.; Hamel, R.D.; Appanna, V.D. The Tricarboxylic Acid Cycle, an Ancient Metabolic Network with a Novel Twist. *PLoS ONE* **2007**, 2: e690.

Mandelli, F.; Franco-Cairo, J. P. L.; Citadini, A. P. S.; Büchli, F.; Alvarez, T. M.; Oliveira, R. J.; Leite, V. B. P.; Paes-Leme, A. F.; Mercadante, A. Z.; Squina, F. M., The characterization of a thermostable and cambialistic superoxide dismutase from *Thermus filiformis*. *Letters in Applied Microbiology* **2013**, 57, 40-46.

Mandelli, F.; Miranda, V. S.; Rodrigues, E.; Mercadante, A. Z., Identification of carotenoids with high antioxidant capacity produced by extremophile microorganisms. *World Journal of Microbiology and Biotechnology* **2012a**, 28, 1781-90.

Mandelli F., Yamashita F., Pereira J.L., Mercadante A.Z. Evaluation of biomass production, carotenoid level and antioxidant capacity produced by *Thermus filiformis* using fractional factorial design. *Brazilian Journal of Microbiology* **2012b**, 43: 126-134.

Mariutti, L.R.B.; Rodrigues, E.; Mercadante, A.Z. Carotenoids from Byrsonima crassifolia: Identification, quantification and in vitro scavenging capacity against peroxyl radicals. *Journal of Food Composition and Analysis* **2013**, 31: 155-160.

Martens, J.H., Barg, H., Warren, M.J., Jahn, D., Microbial production of vitamin B12. *Applied Microbiology and Biotechnology* **2002**, 58, 275–85.

Mishra, S.; Imlay, J. A., Why do bacteria use so many enzymes to scavenge hydrogen peroxide? *Archives of Biochemistry and Biophysics* **2012**, 525, 145-160.

Miyazaki, K., A hyperthermophilic laccase from *Thermus thermophilus* HB27. *Extremophiles* **2005**, 9, 415-25.

Miyoshi, A.; Rochat, T.; Gratadoux, J. J.; Le Loir, Y.; Oliveira, S. C.; Langella, P.; Azevedo, V., Oxidative stress in *Lactococcus lactis*. *Genetics and Molecular Research* **2003**, 30, 348-359.

Nesvizhskii A.I.; Keller, A; Kolker, E.; Aebersold, R., A statistical model for identifying proteins by tandem mass spectrometry. *Analytical Chemistry* **2003**, 75, 4646-58.

Panda, T., Gowrishankar, B.S. Production and applications of esterases. *Applied Microbiology and Biotechnology* **2005**, 67:160-9.

Pantazaki, A.A., Pritsa, A.A. & Kyriakidis, D.A. Biotechnologically relevant enzymes from *Thermus thermophilus*. *Applied Microbiology and Biotechnology* **2002**, 58, 1-12.

Petersen, T.N.; Brunak, S.; von Heijne, G.; Nielsen, H. SignalP 4.0: discriminating signal peptides from transmembrane regions. *Nature Methods* **2011**, 8(10), 785-786.

Ramaley, R.F.; Hixson, J. Isolation of a nonpigmented, thermophilic bacterium similar to *Thermus aquaticus*. *Journal of Bacteriology* **1970**, 103, 527-528

Robinson, M.D.; McCarthy, D.J.; Smyth, G.K. edgeR: a Bioconductor package for differential expression analysis of digital gene expression data. *Bioinformatics* **2010**, 26, 139-40.

Rodrigues, E., Mariutti, L. R. B., Mercadante, A. Z. Carotenoids and phenolic compounds from Solanum sessiflorum, an unexploited Amazonian fruit, and their scavenging capacity against reactive oxygen and nitrogen species. *Journal of Agricultural and Food Chemistry* **2013**, 61: 3022-3029.

Rodrigues, E.; Mariutti, L. R. B.; Chisté, R. C.; Mercadante, A. Z., Development of a novel micro-assay for evaluation of peroxyl radical scavenger capacity: Application to carotenoids and structure–activity relationship. *Food Chemistry* **2012**, 135, 2103–2111.

Sandmann, G. Carotenoid biosynthesis and biotechnological application. *Achieves of Biochemistry and Biophysics* **2001**, 385, 4–12.

Schattner, P.; Brooks, A. N.; Lowe, T. M. The tRNAscan-SE, snoscan and snoGPS web servers for the detection of tRNAs and snoRNAs. *Nucleic Acids Research* **2005**, 33(Web Server issue), W686-689.

Shannon, P.; Markiel, A.; Ozier, O.; Baliga, N.S.; Wang, J.T.; Ramage, D.; Amin, N.; Schwikowski, B.; Ideker, T. Cytoscape: A Software Environment for Integrated Models of Biomolecular Interaction Networks. *Genome Research* **2003**, 13: 2498-2504.

Shimizu, K. Regulation Systems of Bacteria such as *Escherichia coli* in Response to Nutrient Limitation and Environmental Stresses. *Metabolites* **2014**, 4, 1-35.

Sinnott, M. L., Catalytic mechanisms of enzymatic glycosyl transfer. *Chemical Reviews* **1990**, 90, 1171-1202.

Souza, T. A.; Soprano, A. S.; de Lira, N. P.; Quaresma, A. J.; Pauletti, B. A.; Paes Leme, A. F.; Benedetti, C. E., The TAL effector PthA4 interacts with nuclear factors involved in RNA-dependent processes including a HMG protein that selectively binds poly(U) RNA. *PLoS One* **2012**, 7, 32305.

Srivatsan, A.; Wang, J.D. Control of bacterial transcription, translation and replication by (p)ppGpp. *Current Opinion in Microbiology* **2008**, 11, 100–105.

Stahl, W.; H. Sies., Antioxidant activity of carotenoids. *Molecular Aspects of Medicine* **2003**, 24, 345–351.

Stahl, W.; Junghans, A.; de Boer, B.; Driomina, E. S.; Briviba, K.; Sies, H., Carotenoid mixtures protect multilamellar liposomes against oxidative damage: synergistic effects of lycopene and lutein. *FEBS Letters* **1998**, 427, 305-308.

Stock, A.M.; Robinson, V. L.; Goudreau, P. N. Two-Component Signal Transduction. *Annual Review of Biochemistry* **2000**, 69:183–215.

Storz, G.; Imlay, J. A., Oxidative stress. *Current Opinion on Microbiology* **1999**, 2, 188-194.

Tabor, S. and Richardson, C.C. DNA sequence analysis with a modified bacteriophage T7 DNA polymerase. *The Journal of Biologycal Chemistry* **1990**, 265, 8322–8328.

Tian, B. and Hua, Y. Carotenoid biosynthesis in extremophilic Deinococcus–Thermus bacteria. *Trends in Microbiology* **2011**, 18, 512 - 520.

Topanurak, S.; Sinchaikul, S.; Phutrakul, S.; Sookkheo, B.; Chen, S. T., Proteomics viewed on stress response of thermophilic bacterium *Bacillus stearothermophilus* TLS33. *Proteomics* **2005**, 5, 3722-30.

Vencio, R.Z.; Koide, T.; Gomes, S.L.; Pereira, C.A. BayGO: Bayesian analysis of ontology term enrichment in microarray data. *BMC Bioinformatics* **2006**, 7, 86.

Yin, Y.; Mao, X.; Yang, J.; Chen, X.; Mao, F.; Xu, Y. dbCAN: a web resource for automated carbohydrate-active enzyme annotation. *Nucleic Acids Research* **2012**, 40(Web Server issue), W445-451.

Yokoyama, A.; Sandmann, G.; Hoshino, T.; Adachi, K.; Sakai, M.; Shizuri, Y., Thermozeaxanthins, new carotenoid-glycoside-esters from thermophilic eubacterium Thermus thermophiles. *Tetrahedron Letters* **1995**, 36, 4901-4904.

Zerbino, D. R.; Birney, E. Velvet: algorithms for de novo short read assembly using de Bruijn graphs. *Genome Research* **2008**, 18(5), 821-829.

Zhang, P.; Omaye, S. T., Beta-carotene and protein oxidation: effects of ascorbic acid and alpha-tocopherol. *Toxicology* **2000**, 146, 37-47.

CAPITULO III

The characterization of a thermostable and cambialistic superoxide dismutase from *Thermus filiformis*

F. Mandelli, J.P.L. Franco Cairo, A.P.S. Citadini, F. Büchli, T.M. Alvarez, R.J. Oliveira, V.B.P. Leite, A.F. Paes Leme, A.Z. Mercadante and F.M. Squina

Reprinted from Letters in Applied Microbiology, volume 57, issue 1, F. Mandelli, J.P.L. Franco Cairo, A.P.S. Citadini, F. Büchli, T.M. Alvarez, R.J. Oliveira, V.B.P. Leite, A.F. Paes Leme, A.Z. Mercadante, F.M. Squina, The characterization of a thermostable and cambialistic superoxide dismutase from *Thermus filiformis*, 40-46, Copyright © 2013 The Society for Applied Microbiology (License number: 3365441250429).

Letters in
Applied Microbiology

Letters in Applied Microbiology ISSN 0266-8254

ORIGINAL ARTICLE

The characterization of a thermostable and cambialistic superoxide dismutase from *Thermus filiformis*

F. Mandelli[1,2], J.P.L. Franco Cairo[1], A.P.S. Citadini[1], F. Büchli[1], T.M. Alvarez[1], R.J. Oliveira[3], V.B.P. Leite[3], A.F. Paes Leme[4], A.Z. Mercadante[2] and F.M. Squina[1]

1 Laboratório Nacional de Ciência e Tecnologia do Bioetanol (CTBE), do Centro Nacional de Pesquisa em Energia e Materiais (CNPEM), Campinas, Brazil
2 Departamento de Ciência de Alimentos da Faculdade de Engenharia de Alimentos, UNICAMP, Campinas, Brazil
3 Departamento de Física, Instituto de Biociências, Letras e Ciências Exatas, Universidade Estadual Paulista, São José do Rio Preto, Brazil
4 Laboratório Nacional de Biociências (LNBio), do Centro Nacional de Pesquisa em Energia e Materiais (CNPEM), Campinas, Brazil

Significance and Impact of the Study: This manuscript describes the expression and characterization of a superoxide dismutase (SOD) from *Thermus filiformis* with thermophilic and cambialistic characteristics. The SODs are among the most potent antioxidants known in nature, and their stability and pharmacokinetics can vary widely in accordance to their biological source. Although the currently clinical research work has been focused on human and bovine SODs, alternative sources may become more biotechnological attractive in the near future. Our study brings new insights for the research field of antioxidant enzymes with potential application on pharmaceutical, cosmetics and food formulations.

Keywords
3-D model, cambialistic enzyme, circular dichroism, nitroblue tetrazolium, pyrogallol autoxidation.

Correspondence
F.M. Squina, Laboratório Nacional de Ciência e Tecnologia do Bioetanol (CTBE), do Centro Nacional de Pesquisa em Energia e Materiais (CNPEM), Rua Giuseppe Máximo Scolfaro, nº 10000, Campinas, SP-13083-970, Brazil.
E-mail: fabio.squina@bioetanol.org.br

2012/2317: received 27 December 2012, revised 15 March 2013 and accepted 15 March 2013

doi:10.1111/lam.12071

Abstract

The superoxide dismutase (TfSOD) gene from the extremely thermophilic bacterium *Thermus filiformis* was cloned and expressed at high levels in mesophilic host. The purified enzyme displayed approximately 25 kDa band in the SDS-PAGE, which was further confirmed as TfSOD by mass spectrometry. The TfSOD was characterized as a cambialistic enzyme once it had enzymatic activity with either manganese or iron as cofactor. TfSOD showed thermostability at 65, 70 and 80°C. The amount of enzyme required to inhibit 50% of pyrogallol autoxidation was 0·41, 0·56 and 13·73 mg at 65, 70 and 80°C, respectively. According to the circular dichroism (CD) spectra data, the secondary structure was progressively lost after increasing the temperature above 70°C. The 3-dimensional model of TfSOD with the predicted cofactor binding corroborated with functional and CD analysis.

Introduction

Antioxidant enzymes such as superoxide dismutase (SOD) and catalase protect living cells from reactive oxygen and nitrogen species that are responsible for oxidative damage of essential components of cell structure (Pantazaki *et al.* 2002). Superoxide dismutases are a class of antioxidant defence metalloenzymes that disproportionate superoxide radical ion into molecular oxygen and hydrogen peroxide (Whittaker and Whittaker 1999). Due to its antioxidative effects, SOD has been widely applied in medical treatments, as well as cosmetic, food, agricultural and chemical industries (Liu *et al.* 2011). SODs have recently found applications as supplementation to prevent or reverse the adverse effect of cardiovascular diseases, ageing, infertility, neurological disorders, ischaemia–reperfusion injury, transplant rejection, autoimmune diseases, rheumatoid arthritis, diabetes, asthma, septic shock-induced tissue injury and cancer, as well as in the pharmaceutical and cosmetic industries (Bafana *et al.* 2011).

Once thermal denaturation is a common cause of enzyme inactivation in the industry, one of the major

requirements for commercial SOD is the thermal stability. This fact has stimulated a widespread interest in the biochemistry and molecular biology of extremophiles organisms (Morozkina *et al.* 2010). However, the extreme conditions required for growth and maintenance of these organisms present a problem for large-scale isolation of proteins from their native sources. Thus, gene cloning and heterologous expression can be used to achieve high levels of recombinant thermophilic protein production in a mesophilic host (Hough and Danson 1999). Thermozymes display higher stability and activity than their counterparts currently used in the biotechnology industry. Thermozymes are not only more thermostable, but also more resistant to chemical agents than their mesophilic homologues, these properties that make them extremely interesting for application in industrial processes (Pantazaki *et al.* 2002; dos Santos *et al.* 2011).

In this study, we report gene cloning and expression, followed by purification and functional characterization of a cambialistic thermostable superoxide dismutase from *Thermus filiformis* (TfSOD). Thus, our main goal was to characterize the thermostability potential of this enzyme throughout biochemical and biophysical analysis targeting novel biotechnological applications.

Results and discussion

Thermophilic SOD was successfully expressed in mesophilic host

The amplified sequence of TfSOD was sequenced in 3500xL Genetic Analyzers (Applied Biosystems, Foster City, CA, USA) and then the amino acid sequence (KC768706) was compared with others SOD on NCBI. The TfSOD showed 96% of identity with SOD from *T. oshimai* (AAM93203) and *T. thermophilus* JL-18 (YP006059182) and 94% of identity with SOD from *T. antranikianii* (AAM93199) and *T. brockianus* (AAM93200).

Superoxide dismutase (SOD) was expressed in *E. coli* BL21 (DE3) cells in the soluble fraction at 37°C. The enzyme was purified using two chromatographic steps (Figs 1a,b) yielding approximately 0·1 mg of purified enzyme per ml. The purified SOD presented a single band near 25 kDa (Fig. 1c) in the SDS-PAGE analysis. This isolated band was trypsin digested and the peptide analysis by LC-MS/MS confirmed the expression of the recombinant SOD from *T. filiformis* with FDR (false discovery rate) of 1·35% (Table 1).

A cambialistic SOD with high thermostability

Despite the high expression level of the thermophilic protein by the mesophilic host, the recombinant protein was

Table 1 Protein identification by LC-MS/MS

Protein	Accession number organism	Peptide	*m/z*	*z*
Superoxide dismutase	gi|22135443 *Thermus filiformis*	LLTPGGAK	378·7057	+2
		LTQAAMGR	424·1778	+2
		EPVGELKK	450·2169	+2
		EKLTQAAMGR	552·758	+2
		FGSGWAWLVK	575·7892	+2
		AVDEQFGGFAALK	676·8151	+2
		KAVDEQFGGFAALK	494·2526	+3
		HLAALPQDIQTAVR	766·8825	+2
		HHGAYVNNLNAALEK	550·9493	+3
		FGSGWAWLVKDPFGK	565·6015	+3
		FGSGWAWLVKDPFGK	847·9043	+2

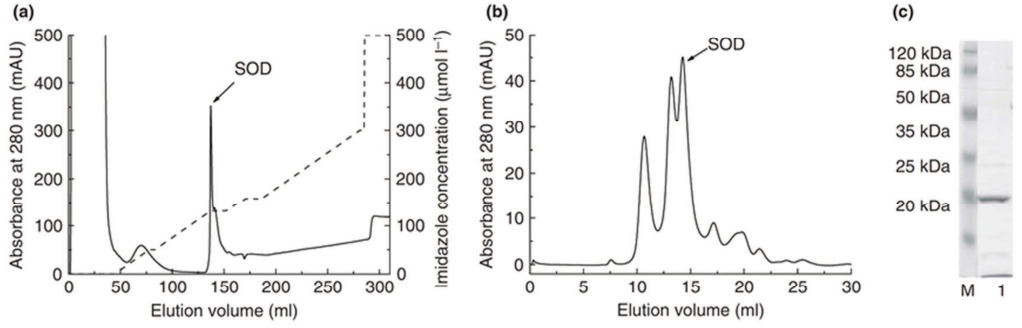

Figure 1 (a) Elution profile of superoxide dismutase (SOD) on 5 ml HiTrap Chelating HP column. Bound fractions were eluted using nonlinear imidazole gradient (dashed line) ranging from 5 to 500 mmol l^{-1} at 1 ml min^{-1}. (b) Size-exclusion chromatogram of SOD on a Superdex 200 10/300 column in 20 mmol l^{-1} sodium phosphate buffer pH 7·5 containing 100 mmol l^{-1} NaCl at 0·5 ml min^{-1}. (c) SDS–PAGE analysis of SOD samples where: M: Molecular weight marker (Thermo Scientific, Milwaukee, WI, USA), 1: Purified Mn-SOD.

not active at ambient temperatures. However, it regained activity in the presence of a metal ion after heating at the physiological growth temperature of the source organism (approximatly 70°C). This effect was previously described by Whittaker and Whittaker (1999). The thermostability was further investigated after preincubating the enzyme with 10 mmol l^{-1} of $MnCl_2$ or $FeCl_2$ for 30 min at temperatures ranging from 65 to 90°C. The enzyme was highly active at 65 and 70°C with both metals, as shown by the white halo in the NBT-PAGE (riboflavin-nitroblue tetrazolium assay in nondenaturing polyacrylamide gel) (Fig. 2a,b). As TfSOD regained enzymatic activity after incubation with either Mn^{2+} or Fe^{2+}, this enzyme can be considered as a cambialistic SOD. This property was not previously reported for other recombinant SOD enzymes from *Thermus* genera (Liu *et al.* 2011; Yanbing *et al.* 2011).

The Mn-dependent SOD activity of *T. filiformis* was quantified by the pyrogallol assay and shown to be thermostable in the range from 65 to 80°C. At 65 and 70°C, the enzyme presented higher stability with IC_{50} values of 0·41 mg and 0·56 mg, respectively, whilst at 80°C, the activity considerably decreased requiring 13·73 mg of the enzyme to inhibit 50% of pyrogallol autoxidation (Fig 2c).

The thermostability shown by TfSOD was lower than the MnSOD previously isolated from *T. thermophilus*, which was demonstrated to be highly stable until 90°C (Liu *et al.* 2011). On the other hand, the TfSOD was active at higher temperatures than SODs from *Thermus* sp. JM1 and *Thermomyces lanuginosus,* which were stable up to 60°C (Yanbing *et al.* 2011; Li *et al.* 2005), as well as, SODs from *Aspergillus flavus, A. niger, A. nidulans and A. terreus,* which were stable only until 50°C (Holdom *et al.* 1996).

The TfSOD α-helix content was disarranged along the thermal denaturation

Far-UV circular dichroism (CD) spectrum of SOD showed a positive band at approximatly 190 nm and negative bands at approximatly 208 nm and approximatly 222 nm, characteristic of the α-helix spectrum (Fig. 3a) (Corrêa and Ramos 2009). Deconvolution of CD data using K2d method available in the Dichroweb server (Whitmore and Wallace 2004) showed that the secondary structure (SS) is formed by 58% α-helix, 8% *β*-sheet and 34% random coil (at 20°C). These values are similar to the SS contents observed for superoxide dismutase of *T. thermophilus* (Liu *et al.* 2011). As well as, regarding the SS, this result also validated properly folding of the recombinant TfSOD expressed in the *E. coli*.

The SOD thermal stability was assessed by monitoring the effect of temperature over the range 20–100°C on protein SS, as measured by the changes in the far-UV CD spectrum (Fig. 3b). According to CD spectral data, the SS was progressively lost after increasing the temperature above 70°C. The structural changes of the enzyme SS were in agreement with decrease in enzyme activity at temperatures higher than 70°C (Fig 2c). The unfolding transition was determined by monitoring the wavelength at 209 nm, the wavelength that characterizes the α-helix protein content. Therewith, a curve of temperature versus molar ellipticity at 209 nm was plotted and through the equation generated by its sigmoidal adjustment, as a result the denaturation temperature was calculated to be 75·7°C (Fig. 3b). The main SS change after the thermal treatment was in the α-helix contents, varying from 41% at 65°C to 26% at 80°C and to 15% at 100°C. According to the structure of MnSOD from *T. thermophilus* (Ludwig *et al.* 1991; Liu *et al.* 2011), which shares high identity of

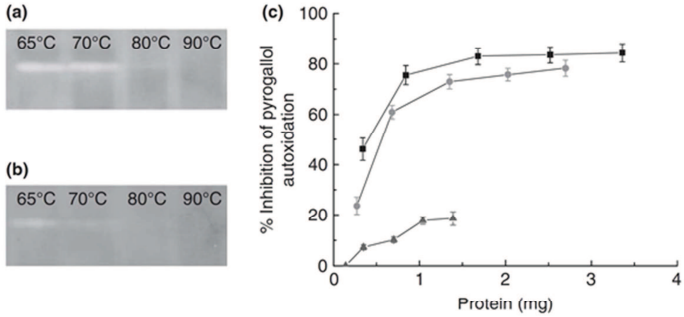

Figure 2 Effect of temperature (65–90°C) on MnSOD (a) and FeSOD (b) activities based on the Nitroblue tetrazolium reduction on native PAGE. White halos correspond to positive activity. Inhibition percentage of pyrogallol autoxidation by different amounts of SOD heated at 65°C (■), 70°C (●) and 80°C (▲) with 10 mmol l^{-1} of $MnCl_2$ (c). Analyses were done in triplicate.

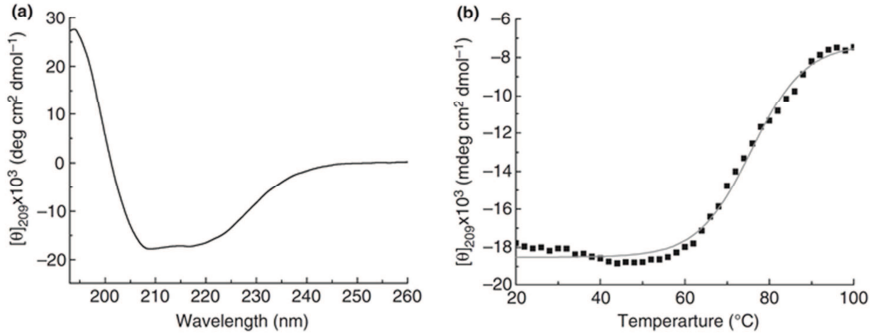

Figure 3 Far-UV circular dichroism (CD) spectra of recombinant TfSOD. The experiment was carried out with 0·15 mg ml^{-1} of SOD in sodium phosphate buffer at 20°C (a), and the sigmoidal adjustment with R-squared: 0·9915 ($y = -7.3 \cdot 10^3 + (-1.9 \cdot 10^4 + 7.3 \cdot 10^3)/(1 + \exp(x - 75.7)/6.3)$) of the monitored wavelength at 209 nm (b).

amino acid sequence with TfSOD, the manganese is directly in contact with amino acids of two different α-helix and one ß-sheet. Based on this previous report, it was suggested that the alteration of the α-helix conformation could lead to the loss of the redox-active metal ion in the catalytic pocket responsible for catalysing the dismutation of superoxide radical ion into molecular oxygen and hydrogen peroxide. The denaturation temperature found for TfSOD was close to the optimum growth temperature of the micro-organism (70°C). Recombinant enzymes may be less stable than the native ones, because it might require post-translational modifications or specific chaperones to reach their fully functional and stable folded state (Vieille and Zeikus 2001).

The TfSOD predicted structure was closely correlated with experimental data

The best-ranked protein used as a template was the manganese SOD from *Thermus thermophilus* (TtSOD) (PDB code 3MDS) from residue 11–189, which has 95% identity and 98% similarity between the two sequences. The final minimized structure of TfSOD has root-mean deviation of 0·2 Å from TtSOD (Fig. 4a). The initial tertiary structure model obtained from I-TASSER was also compared with the TfSOD model obtained from another protein structure prediction program, RaptorX (Källberg *et al.* 2012) with a very good agreement between the two models (root-mean deviation of 1·0 Å). The SS prediction content from the bioinformatics tools I-TASSER, RaptorX, Psi-Pred (Jones 1999) and PredictProtein (Rost *et al.* 2004) was closely correlated with the experimental CD analysis. The manganese binding site predicted by COFACTOR program (Roy *et al.* 2012) (residues H18, H73, W122, D156, H160 in Fig. 4b) has similar binding site as TtSOD and the manganese SOD from *Bacillus anthracis* (PDB code 1XRE), both enzymes were used as top-ranked templates by COFACTOR and has very high confidence score. It was observed for TfSOD sequence in the HHpred server (Biegert *et al.* 2006) that its sequence is conserved and its SS has high probability (80–99%) to be similar to 37 manganese and iron SOD enzymes. Regarding these computational biology analysis, the predicted model (Fig. 4a) has a good confidence to represent the 3-dimensional structure model of TfSOD studied in this manuscript.

Antioxidative enzymes and their role in health are an emerging field in research and industry. The results described in this study can be considered as a new addition to the pool of industrial antioxidant enzymes with biotechnological application. It is important to highlight that this group of enzymes is now surpassing many other biotechnological enzymes in terms of the volume of research and production. For these reasons, we expect that our findings bring relevant insights for the research field of antioxidant enzymes with potential application in drugs, cosmetics and food formulations.

Material and methods

Cloning of the SOD coding sequence

The *T. filiformis* (ATCC 43280) strain was obtained from the National Institute for Quality Control in Health (INCQS/FIOCRUZ - Rio de Janeiro, Brazil) and the cultivation of the micro-organism was conducted according to Mandelli *et al.* (2012).

The coding sequence of SOD was amplified from a genomic DNA of *T. filiformis* by a standard PCR method using two oligonucleotide primers (forward,

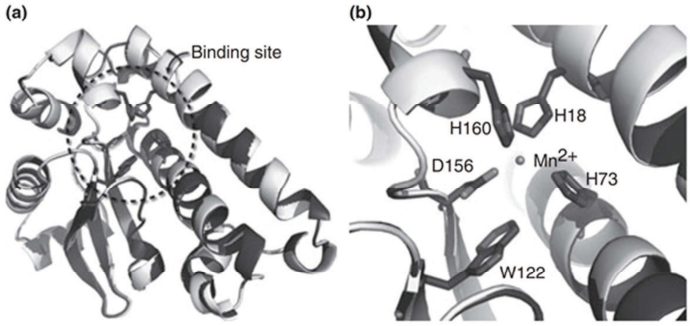

Figure 4 Ribbon representation of the 3-dimensional homology model of TfSOD with manganese as cofactor. The model was created by I-TASSER server with the side chains minimized by the foldX software. TfSOD (dark colour) was superimposed to manganese SOD from *Thermus thermophilus* (PDB code 3MDS) (light colour) (a). Zoom at the predicted five residues coordinating the active site (H18, H73, W122, D156 and H160) and the manganese atom (Mn^{2+}) in the centre of the figure (b).

5′- TATATCATATGCCGTACACGGCCCTCGAG-3′; reverse, 5′- TATGGATCCTTAGTTCCAGACCGCCTGGAG-3′) where underlined sequence indicates the recognition site of the restriction enzymes. The PCR product was recovered after agarose electrophoresis and further digested with *Nde*I and *Bam*HI enzymes, according to the manufacturer's instruction. Finally, the double-digested PCR product was ligated between the *Nde*I and *Bam*HI sites in pET-28a (Novagen) vector treated with the same two enzymes. This approach allowed the insertion of a 6X-His Tag sequence at N-terminal position of SOD from *T. filiformis*.

Protein expression

E. coli BL21 (DE3) was transformed with pET28a/SOD plasmid and plated in selective solid LB medium containing kanamycin (50 μg mg^{-1}). Cells from a single colony were grown in liquid LB-kanamycin (at the same previous concentration) for 16 h at 37°C and 250 rpm. After that, this culture was diluted in 500 ml of fresh medium of LB-kanamycin and grown under the same conditions until an optical density at 600 nm reached 0·6. Afterwards, $MnCl_2$ was added to a final concentration of 2 mmol l^{-1}, and the recombinant protein expression was induced by adding 0·1 mmol l^{-1} IPTG. After 4 h, the cells were harvested at 8500***g*** and stored at −20°C.

Protein purification

Stored cells were resuspended in a mixture 1 : 1 of lysis buffer (20 mmol l^{-1} sodium phosphate pH 7·5, 500 mmol l^{-1} NaCl, 5 mmol l^{-1} imidazole, 80 μg of egg lysozyme ml^{-1} and 5 mmol l^{-1} PMSF) and of TE buffer (10 mmol l^{-1} Tris–HCl containing 1 mmol l^{-1} EDTA, pH 8·0) for 30 min in Nutating Mixer (Labnet, Edison, NJ, USA). Cell disruption was performed in ice bath by an ultrasonic processor (7 pulses of 10 s at 500 W; VC750 Ultrasonic Processor, Sonics Vibracell). The extract was centrifuged at 10 000 ***g*** for 30 min at 4°C, the lysate was heated at 65°C for 30 min in the presence of 10 mmol l^{-1} $MnCl_2$, to bound the metal and thereby restore the enzyme activity, and then centrifuged at the same conditions described above. The SOD from the supernatant was purified by chromatography using an ÄKTA FPLC system (GE Healthcare, Waukesha, WI, USA). Firstly, the supernatant was loaded onto a 5 ml HiTrap Chelating HP column (GE Healthcare) charged with Ni^{2+} and pre-equilibrated with buffer A (20 mM sodium phosphate pH 7·5, 100 mmol l^{-1} NaCl, 5 mmol l^{-1} imidazole) at 1 ml min^{-1}. The column was washed with five column volumes (CVs) of buffer A to remove unbound fractions, and the bound fractions were eluted with a nonlinear, imidazole gradient from 5 to 500 mmol l^{-1} (buffer B) in 20 CVs. Fractions containing SOD were pooled and concentrated to 2 ml by filtration using a 30 kDa-pore Amicon before passage through a Superdex 200 10/300 GL column (GE Healthcare), which was pre-equilibrated and eluted with 20 mmol l^{-1} sodium phosphate buffer pH 7·5 containing 100 mmol l^{-1} NaCl at 0·5 ml min^{-1}; elution was monitored at 280 nm. The purified SOD was analysed by sodium dodecyl sulfate polyacrylamide gel (SDS-PAGE), and protein concentration was measured by the Bradford method.

Mass spectrometry

The isolated protein band was excised, reduced, alkylated and submitted to in-gel digestion with trypsin. An aliquot (4·5 μl) of the resulting peptide mixture was separated on

a C18 (100 μm × 100 mm) RP-nanoUPLC (nanoAcquity, Waters) column using a gradient from 2 to 90% (v/v) acetonitrile in 0·1% formic acid (v/v) over 60 min at 0·6 μl min^{-1}. The HPLC was coupled to a Q-Tof Ultima mass spectrometer (Waters, Milford, MA, USA) with nano-electrospray source, operated in the 'top three' mode, which means one MS spectrum is acquired followed by MS/MS of the top three most intense peaks detected. The spectra were acquired using software MassLynx v.4.1 (Waters) and the raw data files were converted to a peak list format (mgf) by the software Mascot Distiller v.2.3.2.0, 2009 (Matrix Science Ltd., Boston, MA, USA). This list was searched against NCBI database (12 780 006 sequences; 4 363 582 260 residues) using engine Mascot v.2.3 (Matrix Science Ltd.), with carbamidomethylation as fixed modification, oxidation of methionine as variable modification, one trypsin missed cleavage and a tolerance of 0·1 Da for both precursor and fragment ions. The FDR was calculated for estimate the confidence of the peptide identification.

Enzyme activity assay

Superoxide dismutase (SOD) activity was determined by a modified procedure of pyrogallol autoxidation (Marklund and Marklund 1974). Different amounts of the enzyme solution (0·3–3·4 mg) were added in a 50 mmol l^{-1} Tris buffer containing 1 mmol l^{-1} EDTA, at pH 8·2. After vortexing for 1 min, the reaction was initiated by the addition of 0·2 mmol l^{-1} pyrogallol (final concentration). The change of absorbance at 325 nm was measured every 30 s for 5 min at ambient temperature. The results were expressed as the amount of enzyme in mg required for 50% of inhibition of pyrogallol autoxidation (IC_{50}).

Metal incorporation and Thermostability

To determine the metal specificity and thermostability of TfSOD, the enzyme was incubated in 75 mmol l^{-1} sodium phosphate buffer (pH 7·4) with 10 mmol l^{-1} of $MnCl_2$ or $FeCl_2$ at 65, 70, 80 and 90°C. The remaining enzyme activity was observed with riboflavin-nitroblue tetrazolium assay with nondenaturing polyacrylamide gel (NBT-PAGE) (Boonmee *et al.* 2011).

Circular dichroism spectroscopy and thermal denaturation

Far-UV CD spectra were recorded on a Jasco J-810 spectropolarimeter (Jasco International Co. Ltd., Tokyo, Japan), equipped with a Peltier temperature control unit, from 190 to 260 nm in a 1 mm quartz cuvette. The purified band of SOD (0·15 mg ml^{-1}) was measured in 75 mmol l^{-1} of sodium phosphate buffer, pH 7·5. The data collection parameters were set to scan rate of 100 nm/min, response time of 0·5 s, scan step of 0·1 nm and accumulation of 8. The CD data are shown as mean residue ellipticity units (deg cm^2 dmol^{-1}). The SS contents were evaluated by deconvolution of the CD spectrum using the DichroWeb K2d database (Whitmore and Wallace 2004).

For thermal scans, the protein samples (0·15 mg ml^{-1}) were heated from 20 to 100°C and subsequently cooled to 20°C with a heating/cooling rate of 1°C min^{-1} controlled by a Jasco programmable Peltier element. Far-UV CD spectra were recorded every 2°C, and all the spectra were corrected by discounting the solvent contribution.

Structure modelling of TfSOD

The TfSOD amino acid sequence was sent to I-TASSER web server (Zhang 2008; Roy *et al.* 2010) to create the 3-dimensional model for the enzyme. The side chain energy minimization was performed in the predicted model from I-TASSER using the foldX software (Schymkowitz *et al.* 2005a,b). Moreover, the manganese binding site was predicted by the COFACTOR program (Roy *et al.* 2012).

Acknowledgements

This work was financially supported by grants from CNPq (474022/2011-4 and 310177/2011-1) and FAPESP (2008/58037-9, 2011/17658-3). JPC, TMA and RJO have received fellowship from FAPESP (2010/11469-1, 2011/20977-3 and 2011/08609-9) and FM, and FB has received fellowship from CNPq (142685/2010-0 and 131992/2012-0). We gratefully acknowledge the provision of time on the MAS facilities (LNBio) at the National Center for Research in Energy and Materials.

References

Bafana, A., Dutt, S., Kumar, S. and Ahuja, O.S. (2011) Superoxide dismutase: an industrial perspective. *Crit Rev Biotechnol* **31**, 65–76.

Biegert, A., Mayer, C., Remmert, M., Söding, J. and Lupas, A. (2006) The MPI Toolkit for protein sequence analysis. *Nucleic Acids Res* **34**, W335–W339.

Boonmee, A., Srisomsap, C., Karnchanatat, A. and Sangvanich, P. (2011) Biologically active proteins from Curcuma comosa Roxb. Rhizomes. *J Med Plants Res* **5**, 5208–5215.

Corrêa, D.H.A. and Ramos, C.H.I. (2009) The use of circular dichroism spectroscopy to study protein folding, form and function. *Afr J Biochem Res* **3**, 164–173.

Holdom, M.D., Hay, R.J. and Hamilton, A.J. (1996) The Cu, Zn superoxide dismutases of *Aspergillus flavus, Aspergillus niger, Aspergillus nidulans*, and *Aspergillus terreus*: purification and biochemical comparison with the *Aspergillus fumigatus* Cu, Zn superoxide dismutase. *Infec Immun* **64**, 3326–3332.

Hough, D.W. and Danson, M.J. (1999) Extremozymes. *Curr Opin Chem Biol* **3**, 39–46.

Jones, D.T. (1999) Protein secondary structure prediction based on position-specific scoring matrices. *J Mol Biol* **292**, 195–202.

Källberg, M., Wang, H., Wang, S., Peng, J., Wang, Z., Lu, H. and Xu, J. (2012) Template-based protein structure modeling using the RaptorX web server. *Nat Protoc* **7**, 1511–1522.

Li, D.C., Gao, J., Li, Y.L. and Lu, J. (2005) A thermostable manganese-containing superoxide dismutase from the thermophilic fungus *Thermomyces lanuginosus*. *Extremophiles* **9**, 1–6.

Liu, J., Yin, M., Zhu, H., Lu, J. and Cui, Z. (2011) Purification and characterization of a hyperthermostable Mn-superoxide dismutase from *Thermus thermophilus* HB27. *Extremophiles* **15**, 221–226.

Ludwig, M.L., Metzger, A.L., Pattridge, K.A. and Stallings, W.C. (1991) Manganese superoxide dismutase from *Thermus thermophiles* a structural model refined at l.8 a resolution. *J Mol Biol* **219**, 335–358.

Mandelli, F., Miranda, V.S., Rodrigues, E. and Mercadante, A.Z. (2012) Identification of carotenoids with high antioxidant capacity produced by extremophile microorganisms. *World J Microbiol Biotechnol* **28**, 1781–1790.

Marklund, S. and Marklund, G. (1974) Involvement of the superoxide anion radical in the autoxidation of pyrogallol and a convenient assay for superoxide dismutase. *Eur J Biochem* **47**, 469–474.

Morozkina, E.V., Slutskaya, E.S., Fedorova, T.V., Tugay, T.I., Golubeva, L.I. and Korolev, O.V. (2010) Extremophilic microorganisms: biochemical adaptation and biotechnological application (Review). *Appl Biochem Microbiol* **46**, 1–14.

Pantazaki, A.A., Pritsa, A.A. and Kyriakidis, D.A. (2002) Biotechnologically relevant enzymes from *Thermus thermophilus*. *Appl Microbiol Biotechnol* **58**, 1–12.

Rost, B., Yachdav, G. and Liu, J. (2004) The PredictProtein server. *Nucleic Acids Res* **32**, W321–W326.

Roy, A., Kucukural, A. and Zhang, Y. (2010) I-TASSER: a unified platform for automated protein structure and function prediction. *Nat Protoc* **5**, 725–738.

Roy, A., Yang, J. and Zhang, Y. (2012) COFACTOR: an accurate comparative algorithm for structure-based protein function annotation. *Nucleic Acids Res* **40**, W471–W477.

dos Santos, C.R., Squina, F.M., Navarro, A.M., Oldiges, D.P., Leme, A.F., Ruller, R., Mort, A.J., Prade, R. *et al.* (2011) Functional and biophysical characterization of a hyperthermostable GH51 α-L-arabinofuranosidase from *Thermotoga petrophila*. *Biotechnol Lett* **33**, 131–137.

Schymkowitz, J., Borg, J., Stricher, F., Nys, R., Rousseau, F. and Serrano, L. (2005a) The FoldX web server: an online force field. *Nucleic Acids Res* **33**, W382–W388.

Schymkowitz, J.W.H., Rousseau, F., Martins, I.C., Ferkinghoff-Borg, J., Stricher, F. and Serrano, L. (2005b) Prediction of water and metal binding sites and their affinities by using the Fold-X force field. *PNAS* **102**, 10147–10152.

Vieille, C. and Zeikus, G.J. (2001) Hyperthermophilic enzymes: sources, uses, and molecular mechanisms for thermostability. *Microbiol Mol Biol Rev* **65**, 1–43.

Whitmore, L. and Wallace, B.A. (2004) DICHROWEB, an online server for protein secondary structure analyses from circular dichroism spectroscopic data. *Nucleic Acids Res* **32**, W668–W673.

Whittaker, M.M. and Whittaker, J.W. (1999) Thermally triggered metal binding by recombinant *Thermus thermophilus* manganese superoxide dismutase, expressed as the apo-enzyme. *J Biol Chem* **274**, 34751–34757.

Yanbing, Z., Hebin, L., Xuqin, Z., Chunyan, Z., Jionghua, C. and Guangming, L. (2011) Characterization of a thermostable manganese-containing superoxide dismutase from inshore hot spring thermophile *Thermus* sp. JM1. *Acta Oceanol Sin* **30**, 95–103.

Zhang, Y. (2008) I-TASSER server for protein 3D structure prediction. *BMC Bioinformatics* **9**, 40.

Conclusão Geral

Através da análise de carotenoides observou-se a formação de zeaxantinas glicosiladas e aciladas em todas as condições; no entanto, houve uma maior produção de zeaxantina livre a 63 °C e de termobiszeaxantinas a 77 °C quando comparadas com as demais condições, o que indica que os carotenoides produzidos por *T. filiformis* tem por principal papel a estabilização da membrana lipidica. Por outro lado, no que diz respeito à capacidade de desativação do radical peroxila, dos extratos ricos em carotenoides, o melhor resultado foi obtido pelo extrato da condição com H_2O_2. Como neste caso não foi observado um perfil diferenciado de carotenoides quando comparado ao das demais amostras, provavelmente outros compostos produzidos pela bactéria quando na presença de peróxido podem estar presentes no extrato e terem influenciado positivamente na capacidade antioxidante do mesmo. No entanto, é interessante ressaltar que os extratos de todas as condições apresentaram capacidade de desativar o radical peroxila superior à capacidade de extratos de frutas e até mesmo de padrões de carotenoides, evidenciando o potencial dos extratos de *T. filiformis* de aplicabilidade em indústrias farmacêuticas, de cosméticos e de alimentos.

Com o intuito de se obter uma banco de dados para as análises de trancriptômica e proteômica, o genoma de *T. filiformis* foi sequenciado. O genoma apresentou um tamanho total de 2,46 Mb, similar ao tamanho encontrado para outras espécies de *Thermus*.

Com a comparação dos dados de transcriptoma, proteoma foi possível apontar diferenças tanto na expressão gênica quanto na expressão de proteínas de acordo com o estímulo a qual a bactéria foi submetida. Além disso, a análise do interactoma possibilitou apontar os processos biológicos mais influenciados na adaptação da bactéria *Thermus filiformis* quanto a mudanças na temperatura e adição de peróxido de hidrogênio.

Os processos biológicos mais relevantes envolvidos nos processos de termoadaptação da bactéria *T. filiformis* foram: tradução, transcrição, enovelamento de proteínas e ciclo do ácido tricarboxílico.

A bactéria *T. filiformis* apresenta duplicidade de genes codificadores de algumas aminoacil- tRNA sintetases, sendo que uma representante de cada aminoacil- tRNA sintetase teve sua expressão aumentada quando submetidas a um choque térmico. Além disso, o regulador de expressão genética ppGpp, se mostrou super expresso a 77 °C

favorecendo a síntese dos genes envolvidos na resposta ao estresse gerado pala falta de amino ácidos.

Os genes envolvidos na transcrição que se mostraram super expressos em altas temperaturas foram: o regulador de resposta dois-componentes, reponsável por permitir que o micro-organismo sinta, responda e se adapte a uma ampla faixa de condições ambientais, de estresse e de crescimento, e o gene GreA, envolvido na proteção celular das proteínas contra a agregação.

As chaperonas também se mostraram importantes no processo de termoadaptação. As chaperonas 33, 60, 10 e a ClpB foram super expressas a 77 °C, onde exercem papel fundamental na prevenção do enovalamento errôneo das proteínas além de prover o re-enovelamento e correta montagem de polipeptídeos desonovelados.

Outro processo biológico envolvido na adaptação de *T. filiformis* ao estresse oxidativo foi o ciclo do ácido tricarboxílico. Os genes envolvidos nesse processo tiveram sua expressão reprimida a 77 °C, este comportamento pode ser uma tentativa do micro-organismo para evitar o acúmulo de O_2, o que poderia ocosionar um aumento na formação de espécies reativas de oxigênio.

Em relação a adição de H_2O_2, foi observado que a quantidade de H_2O_2 utilizada neste estudo não teve grande influência na expressão genética e de proteínas. A principal alteração observada foi a super expressão da chaperona 33, que é uma proteína com cisteínas reativas que respondem rapidamente a mudanças no ambiente redox, sendo ativadas na presença de H_2O_2.

Quanto a produção de carotenoides, as analises de transcriptômica e proteômica oportunizaram a elucidadção da via de produção destes pigmentos. A bactéria *T. filiformis* utiliza a via MEP/DOXP, alternativa a do mevalanonato, para na síntese do geranil-geranil pirofosfato, precursor da via de carotenoides. Já na biossíntese de carotenoides, foi observado que a hidroxilaçao dos anéis β-ionona do β-caroteno, para formação de zeaxantina é feita pelo citocromo P450, um tipo de β-caroteno hidroxilase que apresenta pouca similaridade com outras β-caroteno hidroxilase conhecidas, incluindo CrtZ e CrtR.

Além da elucidação dos mecanismos de adaptação da bactéria *T. filiformis* quando submetida a condições de estresse, este trabalho mostrou que esta bactéria pode ser explorada como fonte de moléculas termo-estáveis de interesse industrial, como por exemplo, pirofosfatases, alfa-amilases, superóxido dismutase, alfa-galactosidases, esterases, enzimas envolvidas na síntese da vitamina B12 e polimerases, dentre outras.

Por fim, através de técnicas de clonagem e expressão de proteínas foi possível a caracterização da enzima superóxido dismutase produzida por *Thermus filiformis* (TfSOD). A TfSOD apresentou massa molecular de aproximadamente 25 kDa, estrutura secundária predominantemente na conformação de alfa-hélice (58%) e termo-estabilidade a até 80 °C, sendo que sua maior capacidade antioxidante foi a 65 °C onde apresentou IC_{50} de 0,41 mg. Além disso, a TfSOD apresentou características cambialisticas por ter atividade tanto utilizando manganês quanto ferro como cofator. Devido a estas características, principalmente a termo-estabilidade é que esta enzima se mostra com potencial de aplicabilidade nas indústrias farmacêutica e de formulações alimentícias.

Supplementary

Table S1: Data obtained in the RNA sequencing by Ilumina MiSeq to the diferent cultivation conditions.

Transcriptome Conditon	Illumina Reads	Illumina Read Pairs	Raw Bases	Raw Bases
70 °C	3766434	1883217	564965100	565MB
70 °C 100 uM H_20_2	5197032	2598516	779554800	779MB
63 °C	12901310	6450655	1935196500	1.9GB
77 °C	7611736	3805868	1141760400	1.1GB
Total	29476512	14738256	4421476800	4.4GB

Table S2: Differential expression of all protein coding transcripts between all tested growth conditions.

edgeR Differential Expression	p Value 0.01 or Less	p Value 0.05 or less
63 °C vs 70 °C H_20_2	109	247
77 °C vs 63 °C	638	900
70 °C H_20_2 vs 77 °C	611	841
70 °C vs 63 °C	30	138
70 °C vs 70 °C H_20_2	15	141
70 °C vs 77 °C	586	824

Table S3: Genes differently expressed in temperature assay.

					FPKM						
Gene code	**logCPM**	**logFC**	**PValue**	**FDR**	**63 degrees**			**77 degrees**			**Top Hit Uniprot**
Thfi_0003	7,051	1,369	0,002	0,009	1402,38	1576,99	1689,52	511,95	576,63	1103,36	tr|K7R797|K7R797_THEOS Uncharacterized protein OS=Thermus oshimai JL-2
Thfi_0011	6,067	-1,939	0,000	0,000	20,29	14,27	29,03	98,41	74,6	124,38	tr|Q72JR9|Q72JR9_THET2 Riboflavin biosynthesis protein RibD OS=Thermus thermophilus
Thfi_0012	8,587	-0,955	0,000	0,003	1116,96	723,84	968,87	1829,49	1395,5	1560,35	tr|K7QZC0|K7QZC0_THEOS Ribosome maturation factor RimP
Thfi_0016	9,737	-0,970	0,000	0,000	564,75	359,12	519,35	1036	1108,03	839,05	tr|G8N8I1|G8N8I1_9DEIN Transcription termination factor Rho OS=Thermus sp. CCB_US3_UF1 GN=rho PE=3 SV=1
Thfi_0018	11,312	1,059	0,000	0,000	1088,93	1728,13	1401,7	881,27	833,72	780,1	tr|K7R5J4|K7R5J4_THEOS Protein-export membrane protein, SecD/SecF family (Precursor)
Thfi_0020	6,237	-1,353	0,000	0,002	129,99	104,33	72,41	255,63	376,25	354,28	tr|E8PKP2|E8PKP2_THESS Death-on-curing family protein OS=Thermus scotoductus
Thfi_0021	8,084	-0,559	0,019	0,060	110,93	127,84	135,64	194,56	261,04	237,21	tr|B7A719|B7A719_THEAQ D-3-phosphoglycerate dehydrogenase
Thfi_0029	8,419	-0,996	0,000	0,000	1671,22	1177,28	1358,01	2841,05	2758,75	2407,48	tr|F2NM77|F2NM77_MARHT 30S ribosomal protein S15 OS=Marinithermus hydrothermalis
Thfi_0030	10,608	-0,989	0,000	0,000	546,26	444,28	476,95	1075,31	1078,79	1081,2	tr|E8PPC3|E8PPC3_THESS Polyribonucleotide nucleotidyltransferase OS=Thermus scotoductus
Thfi_0034	8,065	0,738	0,012	0,042	940,06	834,19	764,44	405,93	699,33	757,61	tr|B7AAD3|B7AAD3_THEAQ Putative signal transduction protein with CBS domains
Thfi_0036	6,407	-0,736	0,031	0,085	169,22	58,07	75,91	124,31	133,32	130,37	tr|H7GG11|H7GG11_9DEIN Uncharacterized protein OS=Thermus sp. RL GN=RLTM_04929 PE=4 SV=1
Thfi_0038	10,404	-0,428	0,048	0,121	379,98	386,31	313,41	502,15	562,47	574,5	tr|H9ZRD2|H9ZRD2_THETH Isoleucine--tRNA ligase OS=Thermus thermophilus JL-18 GN=ileS PE=3 SV=1
Thfi_0043	9,368	1,395	0,000	0,000	627,07	632,12	707,21	263,52	340,93	252,07	tr|F6DEJ8|F6DEJ8_THETG Probable glycine dehydrogenase [decarboxylating] subunit 2
Thfi_0044	8,570	1,810	0,000	0,000	435,24	439,47	411,24	138,76	167,63	116,62	tr|H7GFD6|H7GFD6_9DEIN Probable glycine dehydrogenase [decarboxylating] subunit 1
Thfi_0045	8,252	1,557	0,000	0,000	1993,24	1488,93	1654,97	534,15	665,55	451,08	tr|B7A6K6|B7A6K6_THEAQ Glycine cleavage system H protein OS=Thermus aquaticus Y51MC23
Thfi_0046	8,224	1,292	0,000	0,000	436,43	410,33	410,37	155,76	180,79	284,18	tr|H9ZSX1|H9ZSX1_THETH Aminomethyltransferase OS=Thermus thermophilus JL-18 GN=gcvT PE=3 SV=1
Thfi_0049	8,131	0,566	0,035	0,093	493,89	309,79	363,26	222,1	245,83	314,2	tr|B7A692|B7A692_THEAQ Peptidase M24 OS=Thermus aquaticus Y51MC23 GN=TaqDRAFT_4341 PE=4 SV=1
Thfi_0054	6,350	-1,559	0,000	0,001	106,63	63,88	21,22	220,71	155,97	274,45	tr|E8PKN3|E8PKN3_THESS Membrane metalloprotease OS=Thermus scotoductus (strain ATCC 700910 / SA-01) GN=TSC_c15690 PE=4 SV=1
Thfi_0058	5,915	-1,079	0,020	0,063	167,82	91,89	118,1	142,37	281,1	514,51	tr|E4U9X7|E4U9X7_OCEP5 Uncharacterized protein (Precursor) OS=Oceanithermus profundus
Thfi_0060	11,527	1,582	0,000	0,000	3103,48	3900,05	3546,35	1335,27	1123,3	1615,44	tr|K7R1F0|K7R1F0_THEOS ABC-type sugar transport system, periplasmic component (Precursor)
Thfi_0062	6,717	-0,993	0,002	0,010	48,34	69,24	98,07	159,22	201,11	228,26	tr|E8PJL0|E8PJL0_THESS ABC transporter, permease protein, MalFG family OS=Thermus scotoductus (strain ATCC 700910 / SA-01)
Thfi_0063	8,744	0,549	0,030	0,085	224,76	243,99	163,93	165,67	171,9	143,34	tr|E4U6W5|E4U6W5_OCEP5 Alpha-glucosidase OS=Oceanithermus profundus (strain DSM 14977 / NBRC 100410 / VKM B-2274 / 506)

					FPKM						
Gene code	logCPM	logFC	PValue	FDR	63 degrees			77 degrees			Top Hit Uniprot
Thfi_0064	10,614	0,584	0,008	0,030	1476,01	1048,16	925,83	812,14	848,11	626,79	tr|B7ABE7|B7ABE7_THEAQ PpiC-type peptidyl-prolyl cis-trans isomerase (Precursor)
Thfi_0065	7,205	-1,568	0,000	0,000	62,9	34,88	75,49	227,25	200,08	186,57	tr|B7ABE6|B7ABE6_THEAQ Major facilitator superfamily MFS_1 OS=Thermus aquaticus Y51MC23
Thfi_0067	7,339	-0,879	0,003	0,012	428,39	343,49	193,93	696,64	554,55	651,39	tr|K7RL84|K7RL84_THEOS Putative signal-transduction protein containing cAMP-binding and CBS domains
Thfi_0068	6,295	-1,379	0,005	0,020	207,64	84,24	282,82	461,7	464,93	257,66	tr|B7ABE3|B7ABE3_THEAQ Putative uncharacterized protein OS=Thermus aquaticus Y51MC23
Thfi_0069	6,695	-1,843	0,001	0,007	24,45	21,07	14,03	186,18	180,5	180,53	tr|H0BHA6|H0BHA6_9ACTO Putative integral membrane protein OS=Streptomyces sp. W007
Thfi_0071	6,001	-1,506	0,002	0,008	37,57	29,51	24,92	128,47	92,49	160,64	tr|D3PLD6|D3PLD6_MEIRD Uncharacterized protein OS=Meiothermus ruber
Thfi_0072	7,003	-0,809	0,022	0,066	282,43	121,11	217,28	280,65	271,58	233,03	tr|H9ZRH6|H9ZRH6_THETH Transcriptional regulator OS=Thermus thermophilus JL-18
Thfi_0080	8,365	1,016	0,000	0,000	353,22	326,43	454,71	210,98	183,54	264,48	tr|K7R7Y9|K7R7Y9_THEOS Pyruvate/2-oxoglutarate dehydrogenase complex, dihydrolipoamide acyltransferase component OS=Thermus oshimai JL-2
Thfi_0081	7,047	2,027	0,000	0,000	140,58	112,15	160,6	14,53	60,6	80,84	tr|B7A642|B7A642_THEAQ Putative uncharacterized protein
Thfi_0083	7,347	1,026	0,000	0,003	399,08	295,35	356,5	183,26	155,6	263,27	tr|B7A618|B7A618_THEAQ ABC transporter related OS=Thermus aquaticus Y51MC23
Thfi_0086	7,710	-0,975	0,002	0,009	230,31	286,5	249,52	575,46	747,69	1048,28	tr|E8PLJ2|E8PLJ2_THESS Transposase family protein OS=Thermus scotoductus
Thfi_0087	5,840	-1,051	0,012	0,043	60,75	54,49	57,34	105,85	193,34	176,39	tr|H9ZTT4|H9ZTT4_THETH Transposase OS=Thermus thermophilus JL-18
Thfi_0089	9,744	-0,526	0,019	0,059	349,01	243,1	281,22	423,71	353,48	512,65	tr|H9ZTY0|H9ZTY0_THETH Alanine--tRNA ligase OS=Thermus thermophilus JL-18 GN=alaS PE=3 SV=1
Thfi_0094	6,607	1,102	0,000	0,002	487,32	298,91	413	229,96	156,21	163,41	tr|E8PQ68|E8PQ68_THESS Uncharacterized protein OS=Thermus scotoductus
Thfi_0097	8,556	-0,695	0,019	0,060	585,3	347,08	634,58	642,73	989,56	652,25	tr|Q72H04|Q72H04_THET2 23S rRNA methyltransferase OS=Thermus thermophilus
Thfi_0105	4,062	-1,479	0,031	0,087	2,87	9,01	0	12,74	28,97	35,41	tr|G8NC45|G8NC45_9DEIN Putative uncharacterized protein OS=Thermus sp. CCB_US3_UF1
Thfi_0107	4,866	-2,390	0,002	0,010	4,3	1,11	4,07	13,73	9,46	17,37	tr|E8PQF9|E8PQF9_THESS Hypothetical membrane spanning protein
Thfi_0108	6,796	-1,368	0,000	0,001	157,03	69,97	137,75	277,6	202,24	317,77	tr|K7QVG1|K7QVG1_THEOS Uncharacterized protein (Precursor) OS=Thermus oshimai JL-2
Thfi_0110	8,099	0,590	0,025	0,074	391,31	324,34	269,39	194,42	289,75	209,92	tr|E8PJI0|E8PJI0_THESS Phosphate-binding protein OS=Thermus scotoductus (strain ATCC 700910 / SA-01)
Thfi_0116	5,314	-1,140	0,029	0,083	113,07	91,79	0	135,65	242,4	260,75	tr|E4U9X7|E4U9X7_OCEP5 Uncharacterized protein (Precursor) OS=Oceanithermus profundus
Thfi_0123	10,021	0,745	0,002	0,010	3063,01	3421,74	3252,85	1914,8	2335,82	2032,83	tr|E8PQQ9|E8PQQ9_THESS Bacterioferritin OS=Thermus scotoductus
Thfi_0129	7,969	0,889	0,003	0,014	188,73	170,45	217,85	92,23	124,53	193,28	tr|F2NN31|F2NN31_MARHT Acyl-CoA dehydrogenase domain-containing protein OS=Marinithermus hydrothermalis (strain DSM 14884 / JCM 11576 / T1)
Thfi_0130	9,845	-1,924	0,000	0,000	255,68	158,89	223,35	819,73	804,34	843,16	tr|K7QUP2|K7QUP2_THEOS Thioredoxin domain protein OS=Thermus oshimai JL-2 GN=Theos_1008 PE=4 SV=1

					FPKM						
Gene code	logCPM	logFC	PValue	FDR	63 degrees			77 degrees			Top Hit Uniprot
Thfi_0131	7,859	-2,163	0,000	0,000	128,24	175,22	413	1379,76	1048,82	1225,55	tr|E8PQ66|E8PQ66_THESS Uncharacterized protein OS=Thermus scotoductus (strain ATCC 700910 / SA-01)
Thfi_0133	7,364	-1,233	0,000	0,001	127,32	115,43	78,78	309,58	201,12	353,43	tr|E8PNX5|E8PNX5_THESS Diguanylate cyclase OS=Thermus scotoductus (strain ATCC 700910 / SA-01)
Thfi_0140	8,516	1,390	0,000	0,000	952,6	1162,59	1140,44	736,31	654,34	472,37	tr|B7A934|B7A934_THEAQ Putative uncharacterized protein (Precursor) OS=Thermus aquaticus Y51MC23
Thfi_0142	4,173	-2,771	0,001	0,007	1,54	2,4	0	10,84	12,84	37,68	tr|E8PNY9|E8PNY9_THESS Feruloyl-CoA synthetase OS=Thermus scotoductus (strain ATCC 700910 / SA-01)
Thfi_0150	5,373	0,990	0,030	0,085	168,66	173,74	210,47	83,38	173,52	57,66	tr|H9ZVC9|H9ZVC9_THETH Putative transcriptional regulator OS=Thermus thermophilus JL-18
Thfi_0156	12,930	1,527	0,000	0,000	13650	21738,9	22344,4	7558,69	7640,42	9980,43	tr|E8PMF8|E8PMF8_THESS Uncharacterized protein OS=Thermus scotoductus (strain ATCC 700910 / SA-01)
Thfi_0157	6,054	-1,889	0,000	0,000	24,46	16,91	11,62	40,48	67,7	115,91	tr|F6DDV3|F6DDV3_THETG Transposase OS=Thermus thermophilus (strain SG0.5JP17-16)
Thfi_0162	6,749	-1,185	0,002	0,008	229,04	173,89	90,51	431,73	537,5	314,91	tr|Q82UB3|Q82UB3_NITEU Probable ribonuclease VapC OS=Nitrosomonas europaea
Thfi_0164	5,327	-0,992	0,019	0,060	61,36	56,29	13,7	89,7	129,39	118,53	tr|H9ZVD1|H9ZVD1_THETH Uncharacterized protein OS=Thermus thermophilus JL-18 GN=TtJL18_2470
Thfi_0181	4,429	-1,378	0,049	0,124	22,69	24,49	22,28	63,25	93,08	145,95	tr|B7A5V0|B7A5V0_THEAQ Putative uncharacterized protein OS=Thermus aquaticus Y51MC23
Thfi_0187	6,450	-1,060	0,002	0,009	51,21	72,21	105,57	176,94	229,62	204,75	tr|B7A7J5|B7A7J5_THEAQ DNA repair protein RecO OS=Thermus aquaticus Y51MC23
Thfi_0190	8,314	1,073	0,000	0,000	1112,27	1129,46	1133,43	509,45	654,99	588,7	tr|F6DGV0|F6DGV0_THETG Thioesterase superfamily protein OS=Thermus thermophilus (strain SG0.5JP17-16)
Thfi_0195	8,731	0,568	0,013	0,043	632,68	880,55	929,67	687,72	852,86	809,3	tr|E8PLG3|E8PLG3_THESS Ribosome-recycling factor OS=Thermus scotoductus
Thfi_0199	6,269	-1,018	0,003	0,013	102,88	70,6	47,82	136,3	185,21	164,62	tr|H9ZRX5|H9ZRX5_THETH Glycosyl transferase OS=Thermus thermophilus JL-18
Thfi_0200	6,263	-0,767	0,015	0,048	144,46	126,42	111,85	205	231,21	242,06	tr|G8N8S8|G8N8S8_9DEIN Putative uncharacterized protein OS=Thermus sp. CCB_US3_UF1 GN=TCCBUS3UF1_15440 PE=4 SV=1
Thfi_0201	7,117	0,807	0,014	0,046	251	140,3	347,95	183,08	147,91	74,81	tr|H9ZRX7|H9ZRX7_THETH Pyrroline-5-carboxylate reductase OS=Thermus thermophilus JL-18
Thfi_0204	7,722	1,977	0,000	0,000	959,19	1104,63	2184,02	467,54	530,95	502,41	tr|E8PLH1|E8PLH1_THESS Stage V sporulation protein S OS=Thermus scotoductus (strain ATCC 700910 / SA-01)
Thfi_0208	4,757	1,393	0,022	0,067	417,01	128,55	248,92	69,34	74,98	0	tr|D7BFL6|D7BFL6_MEISD Transcriptional regulator, AsnC family OS=Meiothermus silvanus
Thfi_0210	8,406	-1,107	0,001	0,008	83,02	52,95	73,49	248,73	154,14	218,39	tr|F6DGA7|F6DGA7_THETG Putative serine protein kinase, PrkA OS=Thermus thermophilus
Thfi_0211	7,216	-2,162	0,000	0,000	108,41	59,2	34,65	380,65	314,85	335,17	tr|K7R4R6|K7R4R6_THEOS Putative Ser protein kinase OS=Thermus oshimai JL-2 GN=Theos_0873 PE=4 SV=1
Thfi_0212	5,284	-1,559	0,005	0,019	22,11	12,11	12,67	44,92	55,52	67,87	tr|B7A6C6|B7A6C6_THEAQ Putative uncharacterized protein OS=Thermus aquaticus Y51MC23
Thfi_0213	7,379	-1,356	0,000	0,001	77,02	43,42	56,16	203	171,92	170,18	tr|G8N8T9|G8N8T9_9DEIN SpoVR OS=Thermus sp. CCB_US3_UF1 GN=TCCBUS3UF1_15550 PE=4 SV=1
Thfi_0214	7,174	1,495	0,000	0,001	222,57	322,25	329,96	84,71	204,72	40,57	tr|A5UV18|A5UV18_ROSS1 Putative uncharacterized protein (Precursor)
Thfi_0223	8,419	0,718	0,010	0,036	527,69	371,18	690,41	275,19	360,65	398,37	tr|F6DEZ9|F6DEZ9_THETG PpiC-type peptidyl-prolyl cis-trans isomerase (Precursor)

					FPKM						
Gene code	logCPM	logFC	PValue	FDR	63 degrees			77 degrees			Top Hit Uniprot
Thfi_0229	8,068	1,313	0,000	0,000	413,56	246,51	397,78	145,67	128,63	161,11	tr|K7QXK2|K7QXK2_THEOS Leucyl aminopeptidase (Aminopeptidase T) OS=Thermus oshimai JL-2
Thfi_0230	4,523	1,221	0,029	0,082	86,62	56,45	76,94	56,85	46,1	0	tr|K7QVH5|K7QVH5_THEOS O-acetylhomoserine sulfhydrylase (Precursor) OS=Thermus oshimai JL-2
Thfi_0233	7,170	-0,563	0,044	0,112	108,05	125,05	80,8	180,76	208,66	202,15	tr|H9ZRT7|H9ZRT7_THETH 33 kDa chaperonin OS=Thermus thermophilus JL-18 GN=hslO PE=3 SV=1
Thfi_0235	9,188	0,551	0,032	0,087	276,77	384,99	300,06	266,28	306,32	364,05	tr|E8PRA9|E8PRA9_THESS Acyl-CoA dehydrogenase OS=Thermus scotoductus (strain ATCC 700910 / SA-01)
Thfi_0236	6,784	2,208	0,000	0,000	386,38	487,68	218,78	72,87	112,07	126,35	tr|E4U957|E4U957_OCEP5 Putative nitrous oxidase accessory protein NosL (Precursor)
Thfi_0237	7,808	0,810	0,005	0,020	203,26	241,84	160,57	146,68	177,78	130,42	tr|Q5SJW1|Q5SJW1_THET8 Acetyl-CoA acetyltransferase OS=Thermus thermophilus
Thfi_0241	4,477	2,223	0,009	0,032	31,19	49,51	25,82	8,04	15,23	27,91	tr|E8PRB6|E8PRB6_THESS Pyrrolidone-carboxylate peptidase OS=Thermus scotoductus
Thfi_0242	6,481	1,095	0,004	0,017	127,06	85,67	119,21	40,63	91,66	40,34	tr|H7GDR7|H7GDR7_9DEIN Lipopolysaccharide core biosynthesis protein rfaG OS=Thermus sp.
Thfi_0243	6,520	1,396	0,000	0,001	174,45	100,15	160	43,2	77,96	42,89	tr|Q72KB8|Q72KB8_THET2 UDP-galactopyranose mutase OS=Thermus thermophilus
Thfi_0245	7,702	1,081	0,001	0,004	377	312,56	437,59	142,34	206,77	197,8	tr|D3PSF4|D3PSF4_MEIRD Glycosyl transferase family 2 OS=Meiothermus ruber
Thfi_0247	8,412	2,147	0,000	0,000	539,42	820,68	712,44	230,28	277,03	86,44	tr|G8N8P3|G8N8P3_9DEIN Putative uncharacterized protein OS=Thermus sp.
Thfi_0248	9,610	0,881	0,000	0,001	1973,95	1481	1782,11	792,3	1126,99	948,64	tr|D7BG10|D7BG10_MEISD Glycosyl transferase family 2 OS=Meiothermus silvanus
Thfi_0250	7,392	0,805	0,005	0,019	223,46	166,76	148,42	114,32	140	85,59	tr|D7BG08|D7BG08_MEISD Polysaccharide deacetylase (Precursor) OS=Meiothermus silvanus
Thfi_0254	8,374	1,214	0,000	0,000	468,59	375,87	401,77	165,71	289,88	139,23	tr|B7A7E3|B7A7E3_THEAQ Mandelate racemase/muconate lactonizing protein OS=Thermus aquaticus Y51MC23
Thfi_0255	7,299	0,981	0,004	0,015	310,21	322,23	223,22	127,16	199	172,82	tr|K7QZZ6|K7QZZ6_THEOS Uncharacterized protein OS=Thermus oshimai JL-2 GN=Theos_1557 PE=4 SV=1
Thfi_0258	5,842	1,271	0,015	0,048	122,79	120,27	47,8	32,59	78,57	41,15	tr|E4U959|E4U959_OCEP5 ABC transporter related protein (Precursor) OS=Oceanithermus profundus
Thfi_0260	7,024	-1,217	0,000	0,001	311,13	263,57	283,37	549,85	858,27	618,57	tr|F6DGD0|F6DGD0_THETG Chorismate mutase OS=Thermus thermophilus
Thfi_0263	7,154	-0,548	0,048	0,121	345,56	246,11	294,05	372,58	503,73	503,29	tr|H9ZRR4|H9ZRR4_THETH Phosphopantetheine adenylyltransferase OS=Thermus thermophilus JL-18
Thfi_0267	6,403	0,717	0,034	0,092	99,56	138,58	105,17	94,81	123,47	61,73	tr|D7BGL5|D7BGL5_MEISD ABC transporter related protein (Precursor) OS=Meiothermus silvanus
Thfi_0274	5,496	-1,783	0,001	0,006	18,87	11,74	7,17	18,73	43,85	76,61	tr|E8PLA7|E8PLA7_THESS ABC transporter, permease/ATP-binding protein, HlyB family
Thfi_0278	6,943	-0,927	0,003	0,013	97,49	72,9	78,88	134,67	145,33	260,03	tr|B7AAC2|B7AAC2_THEAQ Putative uncharacterized protein OS=Thermus aquaticus Y51MC23 GN=TaqDRAFT_3407 PE=4 SV=1
Thfi_0279	11,493	-0,762	0,002	0,008	1273,39	843,61	1070,54	1265,31	1924,8	2364,28	tr|Q72K93|Q72K93_THET2 Ribonuclease R OS=Thermus thermophilus (strain HB27 / ATCC BAA-163 / DSM 7039) GN=rnr PE=3 SV=1
Thfi_0280	6,155	1,093	0,005	0,020	31,2	31,32	39,17	13,61	25,81	22,28	tr|B7A5I6|B7A5I6_THEAQ UvrD/REP helicase OS=Thermus aquaticus Y51MC23 GN=TaqDRAFT_5093 PE=4 SV=1

					FPKM						
Gene code	logCPM	logFC	PValue	FDR	63 degrees			77 degrees			Top Hit Uniprot
Thfi_0281	10,837	-0,719	0,002	0,009	1482,25	1146,63	1314,06	1704,55	2242,03	2462,69	tr|H9ZRS1|H9ZRS1_THETH Acetylornithine/acetyl-lysine aminotransferase OS=Thermus thermophilus JL-18
Thfi_0284	7,675	0,979	0,000	0,002	135,91	153,55	229,04	105,73	119,08	138,5	tr|K7QYX6|K7QYX6_THEOS Phosphoglucosamine mutase OS=Thermus oshimai JL-2 GN=glmM PE=3 SV=1
Thfi_0290	8,461	0,749	0,002	0,011	224,48	368,43	424,5	297,96	320,34	323,08	tr|G8N809|G8N809_9DEIN UPF0365 protein TCCBUS3UF1_14350 OS=Thermus sp. CCB_US3_UF1
Thfi_0298	9,227	-1,051	0,000	0,001	1282,12	713,57	1261,14	2637,17	1767,81	2424,06	tr|E8PP08|E8PP08_THESS Anti-cleavage anti-GreA transcription factor Gfh1 OS=Thermus scotoductus
Thfi_0299	10,044	-1,159	0,000	0,000	449,66	390,99	457,15	1362,48	1004,35	958,7	tr|E8PP07|E8PP07_THESS Lysine--tRNA ligase OS=Thermus scotoductus
Thfi_0300	7,376	-1,305	0,001	0,004	173,72	72,42	132,52	407,17	241,94	217,62	tr|G8N817|G8N817_9DEIN Cadmium-zinc resistance protein czrB OS=Thermus sp.
Thfi_0301	7,533	-1,395	0,000	0,000	302,2	211,16	282,89	929,01	660,57	408,99	tr|Q8VQD6|Q8VQD6_THEAQ Transcription elongation factor GreA OS=Thermus aquaticus GN=greA PE=3 SV=1
Thfi_0303	8,329	0,737	0,007	0,028	1456,66	1086,26	959,52	599,99	696,07	704,6	tr|E8PP34|E8PP34_THESS Conserved protein/domain typically associated with flavoprotein oxygenase, Dim6/ntab family OS=Thermus scotoductus
Thfi_0304	6,291	-0,885	0,008	0,029	40,77	27,03	17,09	54,56	51,71	65,68	tr|Q5SKM3|Q5SKM3_THET8 Alternative anthranilate synthase component I+II (TrpEG)
Thfi_0305	7,114	-0,916	0,025	0,075	370,78	168,56	279,62	571,38	371,58	211,8	tr|H9ZSM2|H9ZSM2_THETH Uncharacterized protein OS=Thermus thermophilus JL-18
Thfi_0307	11,093	-1,259	0,000	0,000	306,98	315,47	318,88	767,37	1113,3	987,52	tr|E8PJR6|E8PJR6_THESS Methionine synthase OS=Thermus scotoductus
Thfi_0309	10,413	-0,617	0,013	0,045	710,25	829,13	752,06	1641,54	1860,57	1475,55	tr|F6DF87|F6DF87_THETG ATP-dependent Clp protease ATP-binding subunit ClpX OS=Thermus thermophilus
Thfi_0310	10,386	-0,925	0,000	0,001	995,68	1287,25	1672,99	3370,28	3532,65	4588,42	tr|F6DF86|F6DF86_THETG ATP-dependent Clp protease proteolytic subunit OS=Thermus thermophilus
Thfi_0313	9,479	-0,438	0,050	0,124	206,32	172,51	200,19	302,98	300,75	254,34	tr|K7QZP1|K7QZP1_THEOS Carbamoyl-phosphate synthase large chain (Precursor) OS=Thermus oshimai JL-2
Thfi_0316	8,400	0,718	0,013	0,044	547,66	391,32	751,22	297,5	380,36	386,51	tr|B7A7K8|B7A7K8_THEAQ DSBA oxidoreductase (Precursor) OS=Thermus aquaticus Y51MC23 GN=TaqDRAFT_5411 PE=4 SV=1
Thfi_0320	7,214	-0,765	0,009	0,031	88,54	108,6	135,12	218,69	270,01	273,14	tr|K7QZP2|K7QZP2_THEOS Putative 4-hydroxybenzoate polyprenyltransferase OS=Thermus oshimai JL-2 GN=Theos_1357 PE=4 SV=1
Thfi_0321	5,702	-2,146	0,000	0,001	73,01	20,43	49,75	193,55	124,6	107,45	tr|U2PKX6|U2PKX6_9ACTO Uncharacterized protein OS=Actinomadura madurae LIID-AJ290 GN=AMLIID_05805 PE=4 SV=1
Thfi_0323	5,521	-1,793	0,000	0,000	14,57	27,47	16,75	98,45	73,63	89,99	tr|F6DGR1|F6DGR1_THETG Nicotinate-nucleotide pyrophosphorylase OS=Thermus thermophilus
Thfi_0324	9,927	-0,630	0,003	0,014	1960,44	2096,43	2254,82	4274,19	3717,27	4000,4	tr|Q72GH6|Q72GH6_THET2 Pseudocatalase OS=Thermus thermophilus
Thfi_0325	10,222	-0,672	0,001	0,007	1305,29	2011,53	2224,04	4037,63	3687,2	4164,02	tr|K7QTP0|K7QTP0_THEOS Mn-containing catalase OS=Thermus oshimai JL-2
Thfi_0330	7,410	-0,732	0,027	0,078	219,75	204,22	245,03	470,54	425,9	216,17	tr|E8PJU2|E8PJU2_THESS Uridine kinase OS=Thermus scotoductus (strain ATCC 700910 / SA-01)
Thfi_0338	6,502	-1,330	0,001	0,005	209,94	72,86	152,04	248,53	216,61	410,63	tr|K7QZR4|K7QZR4_THEOS Thymidine kinase OS=Thermus oshimai JL-2
Thfi_0343	6,240	-1,437	0,000	0,001	200,8	82,97	88,92	306,82	316,71	309,28	tr|B7AA78|B7AA78_THEAQ Transcriptional regulator, MarR family (Precursor) OS=Thermus aquaticus Y51MC23

					FPKM						
Gene code	logCPM	logFC	PValue	FDR	63 degrees			77 degrees			Top Hit Uniprot
Thfi_0344	7,775	-0,888	0,030	0,084	121,41	78,23	100,57	284,78	281,61	107,61	tr|G8N8D1|G8N8D1_9DEIN Putative uncharacterized protein OS=Thermus sp. CCB_US3_UF1
Thfi_0345	7,948	-1,056	0,001	0,004	271,09	134,61	187,4	407,06	479,04	238,22	tr|B7AA76|B7AA76_THEAQ Putative uncharacterized protein (Precursor) OS=Thermus aquaticus Y51MC23
Thfi_0346	6,650	-0,807	0,045	0,116	85,64	48,64	66,81	116,62	139,76	59,61	tr|F2NMA1|F2NMA1_MARHT Efflux transporter, RND family, MFP subunit OS=Marinithermus hydrothermalis (strain DSM 14884 / JCM 11576 / T1)
Thfi_0351	6,348	-1,352	0,000	0,001	35,62	18,45	27,06	55,05	70,88	65,02	tr|K7QZ72|K7QZ72_THEOS Uncharacterized protein OS=Thermus oshimai JL-2 GN=Theos_1080 PE=4 SV=1
Thfi_0354	5,457	-0,931	0,031	0,087	32,36	30,37	24,71	51,44	36,1	92,69	tr|H7GFT9|H7GFT9_9DEIN Dehydrogenase (Alcohol) OS=Thermus sp. RL GN=RLTM_05404 PE=4 SV=1
Thfi_0356	7,961	0,641	0,016	0,052	288,79	236,44	410,45	209,68	217,41	219,97	tr|K7QV95|K7QV95_THEOS Uncharacterized protein (Precursor) OS=Thermus oshimai JL-2
Thfi_0358	3,838	1,850	0,050	0,124	8,74	16,02	25,13	5,18	4,91	0	tr|K7QWW6|K7QWW6_THEOS Putative ornithine cyclodeaminase, mu-crystallin OS=Thermus oshimai JL-2
Thfi_0367	7,488	0,606	0,049	0,122	81,03	117,49	113,72	101,58	58,17	88,32	tr|K7QZQ6|K7QZQ6_THEOS AMP-forming long-chain acyl-CoA synthetase OS=Thermus oshimai JL-2
Thfi_0370	4,559	-2,758	0,000	0,002	4,35	6,9	12,59	70,56	51,96	54,4	tr|F2NQR9|F2NQR9_MARHT Integrase catalytic region OS=Marinithermus hydrothermalis
Thfi_0372	7,560	-0,845	0,005	0,019	844,1	379,45	387,06	954,78	678,91	561,32	tr|D3PRL8|D3PRL8_MEIRD Fe-S metabolism associated SufE OS=Meiothermus ruber
Thfi_0373	7,287	0,813	0,017	0,054	152,13	211,45	260,37	119,49	148,2	150,97	tr|K7QWI0|K7QWI0_THEOS Zn-dependent dipeptidase, microsomal dipeptidase OS=Thermus oshimai JL-2
Thfi_0374	12,727	0,852	0,000	0,002	11366,6	11262,4	10677,8	8359,14	5663,08	6148,17	tr|Q72JV2|Q72JV2_THET2 Thiosulfate sulfurtransferase OS=Thermus thermophilus
Thfi_0375	9,315	-1,281	0,000	0,000	812,29	573,98	580,58	1737,94	1214,84	1952,62	tr|Q5SJV6|Q5SJV6_THET8 Zn-dependent protease OS=Thermus thermophilus
Thfi_0376	5,333	-1,572	0,001	0,004	86,82	102,87	74,63	322,22	293,78	494,33	tr|E8PJN4|E8PJN4_THESS Uncharacterized protein OS=Thermus scotoductus
Thfi_0378	7,529	0,627	0,017	0,056	63,13	67,68	68,86	54,99	43,65	57,84	tr|Q5SJV3|Q5SJV3_THET8 Chromosome segregation SMC protein OS=Thermus thermophilus
Thfi_0379	6,473	1,197	0,000	0,001	366,31	223,85	291,7	127,52	146,56	94,76	tr|Q72KA3|Q72KA3_THET2 Uncharacterized protein OS=Thermus thermophilus
Thfi_0380	5,133	1,491	0,007	0,025	27,78	26,35	45,41	10,49	23,2	12,16	tr|B7A7H2|B7A7H2_THEAQ Cell wall hydrolase/autolysin (Precursor) OS=Thermus aquaticus Y51MC23
Thfi_0381	5,657	0,897	0,042	0,108	139,95	151,3	177,85	78,1	137,24	77,32	tr|F6DGG4|F6DGG4_THETG SsrA-binding protein (Precursor) OS=Thermus thermophilus
Thfi_0382	10,141	0,947	0,000	0,000	856,43	1443,2	1558,43	936,98	1040,28	702,82	tr|F6DGG7|F6DGG7_THETG Glyceraldehyde-3-phosphate dehydrogenase, type I OS=Thermus thermophilus
Thfi_0383	8,538	0,948	0,000	0,003	382,66	435,24	460,32	245,57	203,2	324,59	tr|B7A7G6|B7A7G6_THEAQ Phosphoglycerate kinase OS=Thermus aquaticus Y51MC23 GN=pgk PE=3 SV=1
Thfi_0384	6,774	1,155	0,001	0,004	242,68	249,71	265,31	118,59	155,97	45,74	tr|D7BHM2|D7BHM2_MEISD Peptidase C26 OS=Meiothermus silvanus
Thfi_0385	8,413	1,153	0,000	0,000	560,94	671,84	618,81	316,56	394,53	250,74	tr|H7GG75|H7GG75_9DEIN Triosephosphate isomerase OS=Thermus sp. RL GN=tpiA PE=3 SV=1
Thfi_0388	6,261	1,159	0,019	0,060	66,42	68,73	129,22	46,17	35,79	116,69	tr|H9ZRQ6|H9ZRQ6_THETH Pyruvate/2-oxoglutarate dehydrogenase complex, dehydrogenase component beta subunit OS=Thermus thermophilus JL-18
Thfi_0391	7,627	-0,817	0,001	0,006	133,68	115,33	137,01	223,37	250	281,21	tr|H9ZS71|H9ZS71_THETH Homoserine O-acetyltransferase OS=Thermus thermophilus JL-18

					FPKM						
Gene code	logCPM	logFC	PValue	FDR	63 degrees			77 degrees			Top Hit Uniprot
Thfi_0392	8,047	-0,735	0,008	0,028	173,18	163,26	170,16	220,65	388,12	275,91	tr|B7A7F5|B7A7F5_THEAQ O-acetylhomoserine/O-acetylserine sulfhydrylase
Thfi_0395	6,866	0,812	0,006	0,023	236,32	141,87	187,52	104,68	130,83	30,95	tr|E8PKR5|E8PKR5_THESS Cell wall endopeptidase, family M23/M37 OS=Thermus scotoductus
Thfi_0404	8,131	0,510	0,042	0,110	345,56	222,08	317,28	203,21	262,74	109,52	tr|Q72JS4|Q72JS4_THET2 ADP-ribosylglycohydrolase OS=Thermus thermophilus
Thfi_0416	7,085	-1,046	0,001	0,003	67,88	62,18	48,48	119,34	166,82	176,32	tr|G8N9W5|G8N9W5_9DEIN Binding-protein-dependent transport system inner membrane component
Thfi_0417	7,197	-0,723	0,017	0,054	73,3	94,42	122	169,43	253,67	203,51	tr|B7A6T4|B7A6T4_THEAQ Binding-protein-dependent transport systems inner membrane component
Thfi_0418	11,107	1,036	0,000	0,000	1032,04	1512,03	1407,59	812,41	1057,64	896,62	tr|E8PMW8|E8PMW8_THESS Oligopeptide-binding protein AppA OS=Thermus scotoductus
Thfi_0427	6,134	-1,861	0,000	0,000	23,26	42,91	56	240,07	151,55	144,92	tr|B7A7W7|B7A7W7_THEAQ GCN5-related N-acetyltransferase
Thfi_0428	8,783	0,905	0,000	0,001	623,51	908,9	868,68	486,13	639,27	473,04	tr|H7GHA4|H7GHA4_9DEIN Long-chain-fatty-acid-CoA ligase OS=Thermus sp. RL GN=RLTM_08162 PE=4 SV=1
Thfi_0429	7,776	0,854	0,004	0,016	484,64	683,9	441,31	361,3	480,43	208,87	tr|E8PMH9|E8PMH9_THESS Long-chain-fatty-acid--CoA ligase OS=Thermus scotoductus
Thfi_0430	7,291	-0,825	0,004	0,018	147,29	146,82	162,79	281,91	257,52	297,28	tr|G8N8B8|G8N8B8_9DEIN Bile acid-inducible operon protein F
Thfi_0432	8,315	-0,707	0,002	0,008	173,24	199,23	183,76	322,12	375,25	360,5	tr|Q72JW9|Q72JW9_THET2 ABC transporter permease protein OS=Thermus thermophilus
Thfi_0433	7,565	-1,284	0,000	0,000	259,09	128,82	143,32	485,9	457,15	418,99	tr|E8PKC9|E8PKC9_THESS Macrolide export ATP-binding/permease protein MacB
Thfi_0436	7,019	-1,048	0,017	0,055	67,79	32,53	79,47	172,73	130,38	95,65	tr|E8PKC6|E8PKC6_THESS Outer membrane efflux protein OS=Thermus scotoductus
Thfi_0438	11,132	-2,804	0,000	0,000	331,94	375,78	335,17	4967,03	2876,29	2703,89	tr|E8N0U9|E8N0U9_ANATU Putative ABC transporter substrate binding protein
Thfi_0439	7,393	-1,873	0,000	0,001	51,18	52,16	51,4	442,27	313,71	110,32	tr|D7BAB3|D7BAB3_MEISD Binding-protein-dependent transport systems inner membrane component (Precursor) OS=Meiothermus silvanus
Thfi_0440	7,658	-1,928	0,000	0,000	73,93	80,98	74,04	564,78	439,89	457,97	tr|O54314|O54314_9DEIN Permease OS=Thermus sp. T2 PE=3 SV=1
Thfi_0446	9,898	0,902	0,000	0,003	2231,44	1906,36	2322,58	848,66	1483,21	1478,78	tr|G7V8Z4|G7V8Z4_THELD Glycosyl transferase group 1 OS=Thermovirga lienii (strain ATCC BAA-1197 / DSM 17291 / Cas60314) GN=Tlie_1812 PE=4 SV=1
Thfi_0448	9,619	-0,545	0,016	0,051	1650,47	1437,71	1879,08	2952,06	2734,99	2432,87	tr|G8N9G7|G8N9G7_9DEIN Phospho-2-dehydro-3-deoxyheptonate aldolase OS=Thermus sp. CCB_US3_UF1 GN=TCCBUS3UF1_4170 PE=4 SV=1
Thfi_0449	9,102	-0,635	0,005	0,020	710,32	594,55	644,49	1163,27	1178,51	884,29	tr|K7R021|K7R021_THEOS Sec-independent protein translocase protein TatC (Precursor) OS=Thermus oshimai JL-2 GN=tatC PE=3 SV=1
Thfi_0451	8,648	-0,483	0,035	0,094	651,41	402,22	625,96	739,43	805,32	919,98	tr|Q5SH76|Q5SH76_THET8 Demethylmenaquinone methyltransferase OS=Thermus thermophilus
Thfi_0461	8,411	0,509	0,023	0,071	474,95	302,55	380,31	301,19	253,7	209,38	tr|K7RF25|K7RF25_THEOS ABC-type sugar transport system, periplasmic component (Precursor)
Thfi_0462	6,233	0,679	0,027	0,078	190,72	101,63	132,76	101,38	72,67	38,06	tr|K7QVC4|K7QVC4_THEOS Sugar phosphate isomerase/epimerase OS=Thermus oshimai JL-2
Thfi_0467	7,173	-1,232	0,001	0,005	71,4	81,96	87,8	332,19	184,12	172,73	tr|K7QYG2|K7QYG2_THEOS Uncharacterized protein OS=Thermus oshimai JL-2 GN=Theos_2055 PE=4 SV=1

					FPKM						
Gene code	logCPM	logFC	PValue	FDR	63 degrees			77 degrees			Top Hit Uniprot
Thfi_0470	5,431	-3,143	0,000	0,000	19,66	7,82	0	178,23	151,84	92,72	tr|B7A5X6|B7A5X6_THEAQ Putative uncharacterized protein OS=Thermus aquaticus Y51MC23
Thfi_0471	6,695	-2,865	0,000	0,000	13,67	17,32	14,65	177,31	113,92	114,92	tr|B7A5X5|B7A5X5_THEAQ Polysulphide reductase NrfD OS=Thermus aquaticus Y51MC23
Thfi_0472	6,708	-2,526	0,000	0,000	7,74	8,67	4,89	90,79	38,41	78,3	tr|Q5SHG6|Q5SHG6_THET8 Molybdopterin oxidoreductase, iron-sulfur binding subunit
Thfi_0473	5,954	-2,646	0,000	0,000	26,56	20,99	10,96	231,39	122,44	141,74	tr|K7QYG4|K7QYG4_THEOS Class III cytochrome C family protein (Precursor)
Thfi_0474	7,555	-2,441	0,000	0,000	259,99	139,11	90,51	1045,25	935,25	905,37	tr|G8NB56|G8NB56_9DEIN ATP/GTP hydrolase
Thfi_0475	7,149	-2,304	0,000	0,000	182,11	55,59	124,76	775,4	424,62	574,86	tr|G8NB57|G8NB57_9DEIN Thiol:disulfide interchange protein
Thfi_0476	6,846	-0,809	0,013	0,044	118,77	161,55	186,91	408,42	280,38	342,44	tr|D7BE64|D7BE64_MEISD Putative uncharacterized protein OS=Meiothermus silvanus
Thfi_0479	8,774	1,312	0,000	0,000	1660,77	1258,54	1729,2	624,02	731,66	613,64	tr|K7R7R4|K7R7R4_THEOS CarD-like transcriptional regulator
Thfi_0484	7,378	-1,424	0,000	0,000	184,38	93,51	153,93	396,94	305,81	312,5	tr|D7BBZ8|D7BBZ8_MEISD Undecaprenyl-diphosphatase OS=Meiothermus silvanus
Thfi_0487	9,416	0,981	0,000	0,000	10998,8	5839,48	6270,09	3927,7	3465,09	3744,38	tr|E8PKS4|E8PKS4_THESS Cold shock protein, CSD family OS=Thermus scotoductus
Thfi_0488	6,753	-1,291	0,001	0,004	282,88	117,01	213,41	476,43	315,64	297,35	tr|K7RKW9|K7RKW9_THEOS Acetyltransferase OS=Thermus oshimai JL-2 GN=Theos_2075 PE=4 SV=1
Thfi_0489	7,468	1,331	0,000	0,001	3142,88	1829,22	1607,97	901,66	707,59	266,69	tr|B7A5V7|B7A5V7_THEAQ 4Fe-4S ferredoxin iron-sulfur binding domain protein OS=Thermus aquaticus Y51MC23
Thfi_0493	9,782	-0,897	0,000	0,001	345,15	466,25	373,05	980,31	955,93	817,57	tr|H9ZPD0|H9ZPD0_THETH PEGA domain-containing protein (Precursor)
Thfi_0494	7,932	0,834	0,000	0,003	345,97	301,8	401,11	234,63	209,95	166,07	tr|K7QTP7|K7QTP7_THEOS Acetyl-coenzyme A carboxylase carboxyl transferase subunit alpha OS=Thermus oshimai JL-2 GN=accA PE=3 SV=1
Thfi_0495	7,872	0,628	0,024	0,071	426,67	270,48	377,07	237,96	211,63	337,42	tr|E8PKR7|E8PKR7_THESS Acetyl-coenzyme A carboxylase carboxyl transferase subunit beta
Thfi_0499	8,842	0,765	0,001	0,005	466,62	477,74	790,19	399,98	445,3	471,07	tr|Q9RHA2|Q9RHA2_THEAQ Fructose-1,6-bisphosphate aldolase OS=Thermus aquaticus PE=1 SV=1
Thfi_0504	8,807	-1,078	0,000	0,001	726,38	480,02	850,12	1662,48	1211,23	1244,01	tr|E8PKQ8|E8PKQ8_THESS Uncharacterized protein OS=Thermus scotoductus
Thfi_0505	8,523	0,577	0,022	0,067	3316,39	1426,49	2219,7	1281,54	1284,47	1213,98	tr|B7A5U2|B7A5U2_THEAQ Ribosomal silencing factor RsfS OS=Thermus aquaticus Y51MC23
Thfi_0509	10,012	-1,149	0,000	0,000	438,9	447,02	462	1430,55	1084,53	1413,84	tr|B7A5T8|B7A5T8_THEAQ GTPase obg OS=Thermus aquaticus Y51MC23 GN=obg PE=3 SV=1
Thfi_0510	9,808	-0,698	0,002	0,010	3679,53	3687,93	4035,28	8072,86	5929,31	7338,95	tr|K7RFL5|K7RFL5_THEOS 50S ribosomal protein L27 OS=Thermus oshimai JL-2 GN=rpmA PE=3 SV=1
Thfi_0517	10,963	1,447	0,000	0,000	15469,1	10745,1	10870,8	4385,46	4148,62	4378,39	tr|K7QV57|K7QV57_THEOS Prepilin-type N-terminal cleavage/methylation domain-containing protein
Thfi_0520	8,550	-1,247	0,000	0,000	246,25	225,94	250,12	632,99	596,01	508,68	tr|E8PLA1|E8PLA1_THESS ABC transporter
Thfi_0523	6,500	-1,504	0,000	0,001	86,94	79,3	88,14	321,43	274,62	136,01	tr|H9ZTW0|H9ZTW0_THETH Ribulose-5-phosphate 4-epimerase-like epimerase or aldolase
Thfi_0525	12,004	-1,110	0,000	0,000	458,95	503,01	482,16	1607,69	1286,12	1084,71	tr|H9ZTW1|H9ZTW1_THETH DNA-directed RNA polymerase subunit beta' OS=Thermus thermophilus JL-18

					FPKM						
Gene code	logCPM	logFC	PValue	FDR	63 degrees			77 degrees			Top Hit Uniprot
Thfi_0526	11,695	-1,672	0,000	0,000	391,86	414,93	420,11	2195,15	1385,29	1315,39	tr|K7RFC6|K7RFC6_THEOS DNA-directed RNA polymerase subunit beta OS=Thermus oshimai JL-2
Thfi_0527	8,648	-0,485	0,027	0,078	759,24	551,69	564,91	956,49	899,2	835,99	tr|G8NAR5|G8NAR5_9DEIN Putative uncharacterized protein OS=Thermus sp.
Thfi_0531	9,219	-0,593	0,024	0,073	527,03	557,06	431,47	1004,35	783,45	616,73	tr|E7CG24|E7CG24_THEFI Protein RecA OS=Thermus filiformis GN=recA PE=3 SV=1
Thfi_0534	7,546	-0,554	0,041	0,107	329,56	203,54	205,63	376,42	379,5	337,29	tr|K7R309|K7R309_THEOS Folate-binding protein YgfZ OS=Thermus oshimai JL-2 GN=Theos_0177 PE=3 SV=1
Thfi_0537	5,669	1,013	0,006	0,023	160,19	87,43	132,2	58,17	77,76	0	tr|H9ZTX2|H9ZTX2_THETH Haloacid dehalogenase superfamily enzyme, subfamily IA
Thfi_0538	9,718	1,103	0,000	0,001	381,44	496,01	411,74	334,39	258,48	318,42	tr|G8NCJ8|G8NCJ8_9DEIN Putative uncharacterized protein OS=Thermus sp.
Thfi_0546	9,823	-0,945	0,000	0,001	1434,43	1276,17	1323,09	2466,03	2681,62	2568,57	tr|B7A5D2|B7A5D2_THEAQ YceI family protein (Precursor) OS=Thermus aquaticus Y51MC23
Thfi_0551	6,237	-1,389	0,000	0,001	24,4	31,23	44,47	111,68	103,96	108,94	tr|H9ZU17|H9ZU17_THETH AAA ATPase OS=Thermus thermophilus JL-18 GN=TtJL18_1968 PE=4 SV=1
Thfi_0552	9,065	0,558	0,035	0,094	1057,23	1085,34	980,44	680,6	780,17	689,75	tr|F6DFM1|F6DFM1_THETG Uncharacterized protein (Precursor) OS=Thermus thermophilus
Thfi_0553	10,858	-0,993	0,000	0,000	1070,77	623,38	860,21	1385,09	1481,56	1860,53	tr|D3PLY5|D3PLY5_MEIRD GTP-binding protein TypA OS=Meiothermus ruber
Thfi_0557	4,572	2,530	0,000	0,001	129,37	180,19	130,64	69,9	0	0	tr|E5WG85|E5WG85_9BACI Putative uncharacterized protein
Thfi_0561	6,249	-1,259	0,001	0,005	101,77	81,24	109,17	292,6	212,31	304,34	tr|E8PQG0|E8PQG0_THESS Putative lipoprotein OS=Thermus scotoductus
Thfi_0567	5,362	0,947	0,043	0,110	36,2	97,87	158,67	71,88	62,78	114,95	tr|K7QVQ1|K7QVQ1_THEOS Haloacid dehalogenase superfamily enzyme, subfamily IA
Thfi_0568	7,354	0,703	0,037	0,097	942,78	1058,89	809,71	615,57	678,03	571,6	tr|H7GHG2|H7GHG2_9DEIN 2-haloalkanoic acid dehalogenase-like protein
Thfi_0570	10,325	-0,666	0,003	0,012	1015,48	765,76	911,11	1738,26	1489,26	1312,44	tr|G8NA00|G8NA00_9DEIN Amidophosphoribosyltransferase
Thfi_0573	7,076	-1,208	0,000	0,000	672,99	412,42	417,61	1211,1	1051,71	1074,23	tr|E8PP63|E8PP63_THESS Uncharacterized protein OS=Thermus scotoductus
Thfi_0574	9,323	1,201	0,000	0,000	3070,12	2248,26	2623,75	1195,85	1222,54	1073,11	tr|D7BFA0|D7BFA0_MEISD Cytochrome c class I (Precursor) OS=Meiothermus silvanus
Thfi_0575	10,416	0,819	0,000	0,002	1347,43	1556,29	1475,3	837,12	1056,66	937,15	tr|B7A5B7|B7A5B7_THEAQ Serine hydroxymethyltransferase
Thfi_0576	7,318	-1,070	0,008	0,029	315,21	124,67	250,53	566,24	348,5	221,1	tr|H9ZQF3|H9ZQF3_THETH 1-acyl-sn-glycerol-3-phosphate acyltransferase
Thfi_0577	10,105	-1,005	0,000	0,001	911,49	496,81	819,64	1400,69	1193,93	1291,27	tr|K7QY54|K7QY54_THEOS GTPase Der OS=Thermus oshimai JL-2 GN=der PE=3 SV=1
Thfi_0578	7,076	-0,800	0,005	0,020	181,84	199,53	242,7	396,57	455,51	370,89	tr|G8NAH7|G8NAH7_9DEIN Putative uncharacterized protein
Thfi_0582	5,593	1,412	0,001	0,005	330,21	321,96	460,16	180,9	149,84	0	tr|R6V3D5|R6V3D5_9FIRM Uncharacterized protein OS=Erysipelotrichaceae bacterium CAG:64
Thfi_0585	9,341	0,728	0,002	0,010	5655,54	3682,87	4341,28	2694,34	2840,32	2062,11	tr|E8PNN6|E8PNN6_THESS 30S ribosomal protein S20 OS=Thermus scotoductus
Thfi_0597	5,706	1,016	0,006	0,023	80,07	103,44	105,02	65,19	55,56	22,63	tr|G8NAF9|G8NAF9_9DEIN Cytochrome c-type biogenesis protein, heme exporter protein B OS=Thermus sp. CCB_US3_UF1

					FPKM						
Gene code	logCPM	logFC	PValue	FDR	63 degrees			77 degrees			Top Hit Uniprot
Thfi_0599	5,255	-1,494	0,007	0,025	41,22	29,38	35,77	55,63	119,39	180,18	tr|B7A5K4|B7A5K4_THEAQ Cytochrome c biogenesis protein transmembrane region
Thfi_0602	10,158	0,702	0,003	0,014	872,17	1234,78	1053,77	904,46	709,35	683,04	tr|E8PNQ1|E8PNQ1_THESS Sulfide dehydrogenase flavocytochrome C OS=Thermus scotoductus
Thfi_0611	4,831	-1,130	0,024	0,071	21,26	23,88	0	37,86	46,1	75,13	tr|H9ZQC3|H9ZQC3_THETH SoxAX cytochrome complex subunit A (Precursor)
Thfi_0612	5,301	2,167	0,000	0,002	213,97	285,66	126,64	48,11	75,85	0	tr|K7RJS1|K7RJS1_THEOS Sulfur oxidation protein SoxZ (Precursor) OS=Thermus oshimai JL-2
Thfi_0616	7,283	1,503	0,000	0,000	468,95	607,18	506,86	243,48	170,3	366,9	tr|K7R063|K7R063_THEOS Cytochrome c, mono-and diheme variants family (Precursor)
Thfi_0620	6,689	-0,918	0,003	0,012	341,39	394,06	366,52	714,78	820,91	1213,5	tr|H7GF52|H7GF52_9DEIN Uncharacterized protein OS=Thermus sp. RL GN=RLTM_03696 PE=4 SV=1
Thfi_0621	10,172	-1,181	0,000	0,000	441,24	479,18	466,29	1452,52	1048,99	1146,08	tr|K7R067|K7R067_THEOS Inosine-5'-monophosphate dehydrogenase
Thfi_0628	6,047	1,190	0,002	0,009	89,59	115,03	120,23	53,15	60,42	55,38	tr|F6DD86|F6DD86_THETG 2-nitropropane dioxygenase NPD OS=Thermus thermophilus (strain SG0.5JP17-16)
Thfi_0632	4,913	2,041	0,001	0,007	166,42	85,72	245,04	42,17	26,59	48,65	tr|B7A6V3|B7A6V3_THEAQ Response regulator receiver protein (Precursor) OS=Thermus aquaticus Y51MC23
Thfi_0640	8,181	0,677	0,004	0,016	138,04	131,9	127,45	102,1	99,82	94,34	tr|Q72LN0|Q72LN0_THET2 Hypothetical conserved protein OS=Thermus thermophilus
Thfi_0646	7,121	-0,739	0,012	0,040	95,2	104,06	129,36	175,32	256,51	200,48	tr|G8N9G8|G8N9G8_9DEIN Putative uncharacterized protein
Thfi_0649	7,349	-1,569	0,000	0,001	73,65	78,57	70,32	124,22	340,03	397,43	tr|Q1AV60|Q1AV60_RUBXD Benzoate-CoA ligase OS=Rubrobacter xylanophilus
Thfi_0654	5,166	-2,106	0,000	0,000	13,62	32,45	0	86,14	116,49	170,76	tr|H7GI01|H7GI01_9DEIN Orotate phosphoribosyltransferase OS=Thermus sp.
Thfi_0655	7,573	-0,521	0,033	0,091	106,46	144	152,47	195,93	259,9	313,21	tr|D3PMZ6|D3PMZ6_MEIRD Uncharacterized protein OS=Meiothermus ruber
Thfi_0662	9,334	0,848	0,000	0,002	471,29	506,82	843,49	393,67	421,05	488,32	tr|E8PK41|E8PK41_THESS Cell division protein ftsA OS=Thermus scotoductus
Thfi_0663	9,748	0,712	0,002	0,008	1144,85	922,95	1107,7	611,37	722,62	876,84	tr|Q72JP4|Q72JP4_THET2 Cell division protein FtsZ OS=Thermus thermophilus
Thfi_0669	9,772	1,388	0,000	0,000	1352,47	1390,37	1369,16	548,03	721,39	421,57	tr|E8PMQ8|E8PMQ8_THESS Malate dehydrogenase OS=Thermus scotoductus
Thfi_0671	7,477	-2,708	0,000	0,000	85,37	29,29	41,72	358,25	247,2	293,71	tr|F6DEK4|F6DEK4_THETG Methyltransferase small OS=Thermus thermophilus
Thfi_0672	10,856	-1,177	0,000	0,000	953,17	757,15	733,88	2552,05	1761,51	2076,28	tr|B7A6J9|B7A6J9_THEAQ RNA polymerase sigma factor OS=Thermus aquaticus Y51MC23
Thfi_0673	6,232	-1,920	0,000	0,003	83,91	21,1	99,15	253,2	136,08	213,78	tr|Q72L97|Q72L97_THET2 Hypothetical cytosolic protein OS=Thermus thermophilus
Thfi_0684	7,106	1,404	0,003	0,014	766,12	743,01	768,83	110,39	529,08	305,57	tr|F6DHY7|F6DHY7_THETG Uncharacterized protein OS=Thermus thermophilus
Thfi_0690	12,145	-0,584	0,008	0,030	1891,1	1637,64	1635,09	3406,45	2923,23	2394,27	tr|B7A552|B7A552_THEAQ Elongation factor G OS=Thermus aquaticus Y51MC23 GN=fusA PE=3 SV=1
Thfi_0693	10,483	0,684	0,002	0,009	988,39	1028,02	1074,08	627,75	882,46	843,78	tr|F6DGP0|F6DGP0_THETG Lipopolysaccharide biosynthesis protein OS=Thermus thermophilus
Thfi_0700	5,128	-1,891	0,004	0,018	12,17	9,51	11,61	51,89	20,35	74,63	tr|G8NDX5|G8NDX5_9DEIN Putative uncharacterized protein OS=Thermus sp. CCB_US3_UF1 GN=TCCBUS3UF1_13340 PE=4 SV=1

					FPKM						
Gene code	logCPM	logFC	PValue	FDR	63 degrees			77 degrees			Top Hit Uniprot
Thfi_0705	5,826	-0,779	0,043	0,110	49,33	35,44	28,22	64,35	65,92	48,36	tr|G8NDX6|G8NDX6_9DEIN CRISPR-associated protein, TM1812 OS=Thermus sp.
Thfi_0716	7,409	0,775	0,015	0,050	536,98	654,38	425,93	357,69	404,14	333,04	tr|G8NCQ4|G8NCQ4_9DEIN Putative uncharacterized protein OS=Thermus sp. CCB_US3_UF1
Thfi_0717	11,574	2,502	0,000	0,000	7534,19	11645,2	10187,6	1673,06	2421,51	2288,37	tr|B7AAU3|B7AAU3_THEAQ DOMON domain protein (Precursor) OS=Thermus aquaticus Y51MC23
Thfi_0728	10,891	2,589	0,000	0,000	9240,63	6681,13	8123,08	1574,58	1428,53	907,72	tr|G8NC04|G8NC04_9DEIN 50S ribosomal protein L10 OS=Thermus sp. CCB_US3_UF1 GN=rplJ PE=3 SV=1
Thfi_0729	9,188	2,738	0,000	0,000	3243,65	2911,13	3364,94	664,86	448,38	546,99	tr|F6DI90|F6DI90_THETG 50S ribosomal protein L7/L12 OS=Thermus thermophilus (strain SG0.5JP17-16)
Thfi_0730	8,501	1,001	0,001	0,004	1579,34	910,08	1926,9	844,98	625,77	618,47	tr|F6DD49|F6DD49_THETG Uncharacterized protein OS=Thermus thermophilus
Thfi_0741	5,790	1,613	0,001	0,006	44,35	72,97	181,36	43,05	43,91	68,98	tr|G8NE34|G8NE34_9DEIN Cobyrinic acid a,c-diamide synthase OS=Thermus sp.
Thfi_0746	8,327	-0,667	0,017	0,054	67,6	99,84	94,69	208,28	233,24	188,67	tr|Q5SLU3|Q5SLU3_THET8 Molybdopterin oxidoreductase OS=Thermus thermophilus
Thfi_0754	8,299	-0,688	0,013	0,043	444,28	459,22	270,27	745,28	602,99	1020,16	tr|E8PLD1|E8PLD1_THESS Uncharacterized protein OS=Thermus scotoductus
Thfi_0755	9,034	-0,497	0,030	0,084	703,82	784,51	810,88	1181,67	1620,12	1470,2	tr|K7R7Y4|K7R7Y4_THEOS Uncharacterized protein OS=Thermus oshimai JL-2 GN=Theos_2155 PE=4 SV=1
Thfi_0757	7,675	-0,678	0,016	0,052	153,35	142,62	151,14	311,7	293,31	250,51	tr|K7R0T4|K7R0T4_THEOS Geranylgeranyl pyrophosphate synthase OS=Thermus oshimai JL-2 GN=Theos_1886
Thfi_0758	7,657	-1,640	0,000	0,000	153,96	83,52	112,6	557,03	310,95	310,98	tr|E8PLD4|E8PLD4_THESS Transporter OS=Thermus scotoductus
Thfi_0759	10,410	-0,964	0,000	0,001	866,39	853,65	818,84	2567,18	1915,49	1946,53	tr|K7RKG4|K7RKG4_THEOS Molybdenum cofactor biosynthesis protein A OS=Thermus oshimai JL-2
Thfi_0760	6,024	-0,947	0,034	0,091	108,19	112,69	113,88	345,11	258,46	298,58	tr|F2NNN3|F2NNN3_MARHT Dihydroneopterin aldolase OS=Marinithermus hydrothermalis
Thfi_0765	11,226	0,625	0,005	0,020	2031,39	2753,51	2785,77	2455,75	1892,3	1705,62	tr|B7A8B7|B7A8B7_THEAQ TRAP dicarboxylate transporter-DctP subunit (Precursor)
Thfi_0766	7,247	-0,629	0,033	0,091	348,15	239,46	405,48	458,41	480	574,86	tr|F6DIA2|F6DIA2_THETG Putative lipoprotein OS=Thermus thermophilus (strain SG0.5JP17-16)
Thfi_0769	5,388	-2,888	0,000	0,000	47,44	21,84	19,88	193,82	283,92	86,61	tr|Q0RL52|Q0RL52_FRAAA Enoyl-CoA hydratase-isomerase, phenylacetic acid degradation OS=Frankia alni
Thfi_0771	7,106	0,591	0,050	0,124	405,33	161,59	270,24	154,15	212,84	54,45	tr|E8PQJ2|E8PQJ2_THESS Uncharacterized protein OS=Thermus scotoductus
Thfi_0773	9,431	-0,722	0,001	0,007	511,06	532,55	554	991,53	939,4	1293,82	tr|B7A8I8|B7A8I8_THEAQ Methionyl-tRNA formyltransferase OS=Thermus aquaticus Y51MC23
Thfi_0776	7,426	-0,900	0,007	0,025	154,03	85,69	104,63	268	144,66	188,66	tr|B7A8H1|B7A8H1_THEAQ Uracil-xanthine permease OS=Thermus aquaticus Y51MC23
Thfi_0781	8,584	-0,469	0,030	0,085	213,89	185,23	157	263,54	278,5	319,78	tr|Q5SH08|Q5SH08_THET8 Uncharacterized protein OS=Thermus thermophilus (strain HB8 / ATCC 27634 / DSM 579) GN=TTHA1922 PE=4 SV=1
Thfi_0782	8,569	0,715	0,001	0,006	471,36	403,73	430,05	324,99	306,23	214,55	tr|H9ZTF4|H9ZTF4_THETH Aspartate/tyrosine/aromatic aminotransferase OS=Thermus thermophilus JL-18
Thfi_0789	11,048	1,751	0,000	0,000	2633,34	3680,74	2808,74	878,46	1176,78	990,2	tr|H7GDK0|H7GDK0_9DEIN NAD(P) transhydrogenase subunit beta OS=Thermus sp.
Thfi_0790	5,261	1,562	0,010	0,034	312,04	384,36	245,93	105,12	149,36	90,68	tr|B7A900|B7A900_THEAQ NAD(P) transhydrogenase subunit beta OS=Thermus aquaticus Y51MC23 GN=TaqDRAFT_4710 PE=3 SV=1

					FPKM						
Gene code	logCPM	logFC	PValue	FDR	63 degrees			77 degrees			Top Hit Uniprot
Thfi_0792	8,327	0,997	0,000	0,000	564,87	523,04	559,12	297,45	332,97	375,66	tr|E8PQK2|E8PQK2_THESS Enoyl-[acyl-carrier-protein] reductase [NADH] OS=Thermus scotoductus
Thfi_0793	9,573	1,078	0,000	0,000	929,13	1103,41	913,7	451,25	521,94	552,07	tr|B7A8Z8|B7A8Z8_THEAQ Alanine dehydrogenase/PNT domain protein OS=Thermus aquaticus Y51MC23
Thfi_0796	5,344	-2,436	0,001	0,005	92,83	28,77	139,2	466,66	252,41	153,46	tr|G8NCG1|G8NCG1_9DEIN Glutaredoxin OS=Thermus sp. CCB_US3_UF1 GN=TCCBUS3UF1_21920 PE=4 SV=1
Thfi_0797	6,121	-1,133	0,003	0,014	75,29	42,85	39,22	112,94	91,72	70,08	tr|B7A8I2|B7A8I2_THEAQ AFG1-family ATPase OS=Thermus aquaticus Y51MC23
Thfi_0799	9,832	0,453	0,047	0,120	1229,34	949,32	1065,09	856,83	763,17	690,56	tr|E8PQJ4|E8PQJ4_THESS Phosphopentomutase OS=Thermus scotoductus
Thfi_0802	7,781	-0,583	0,024	0,071	461,33	509,22	534,29	656,72	1052,93	1103,83	tr|Q1PZQ0|Q1PZQ0_9BACT Uncharacterized protein OS=Candidatus Kuenenia stuttgartiensis
Thfi_0807	4,450	-2,124	0,004	0,015	22,01	7,42	0	33,62	37,16	58,39	tr|D7BGX2|D7BGX2_MEISD Phosphonate ABC transporter, ATPase subunit OS=Meiothermus silvanus
Thfi_0809	6,281	-0,797	0,019	0,060	222,94	143,33	110,87	237,83	300,1	206,12	tr|E7F3M3|E7F3M3_DANRE Uncharacterized protein OS=Danio rerio GN=CU074314.1 PE=4 SV=1
Thfi_0814	7,041	0,827	0,018	0,058	258,92	248,51	236,31	115,4	181,29	156,4	tr|D4ZPR2|D4ZPR2_ARTPN Putative XRE family transcriptional regulator OS=Arthrospira platensis
Thfi_0816	7,272	0,954	0,005	0,021	203,53	151,3	173,54	70,71	111,12	155,85	tr|B7AC53|B7AC53_THEAQ Beta lactamase-related protein, putative (Precursor)
Thfi_0818	8,052	1,109	0,000	0,000	552,14	917,85	772,35	458,2	524,16	418,91	tr|E8PM32|E8PM32_THESS Long-chain-fatty-acid--CoA ligase OS=Thermus scotoductus
Thfi_0819	7,263	-0,695	0,013	0,043	386,38	394,43	318,86	639,89	843,38	796,21	tr|Q5SJW8|Q5SJW8_THET8 Probable transposase OS=Thermus thermophilus
Thfi_0820	5,143	-1,854	0,002	0,009	0	73,72	106,84	361,69	490,39	475,05	tr|F6DEZ7|F6DEZ7_THETG Transposase OS=Thermus thermophilus (strain SG0.5JP17-16)
Thfi_0822	12,878	-0,705	0,001	0,006	5002,09	5022,62	5099,52	10298	9257,5	7754,05	tr|E8PJW4|E8PJW4_THESS Elongation factor Tu OS=Thermus scotoductus
Thfi_0823	8,822	-0,884	0,039	0,102	194,06	241,37	720,65	365,41	1305,15	1220,59	tr|Q1AV63|Q1AV63_RUBXD Phenylacetic acid catabolic OS=Rubrobacter xylanophilus
Thfi_0824	9,078	1,149	0,000	0,001	833,79	768,06	726,15	203,67	505,58	509,57	tr|H9ZP19|H9ZP19_THETH PAPS reductase/FAD synthetase family protein
Thfi_0826	9,441	0,969	0,004	0,016	1381,18	1318,75	1451,52	394,56	799,35	1103,86	tr|H9ZP18|H9ZP18_THETH Uncharacterized protein OS=Thermus thermophilus JL-18
Thfi_0827	10,427	1,046	0,003	0,012	1354,65	1485,58	1469,31	341,41	894,43	1171,03	tr|F6DHY7|F6DHY7_THETG Uncharacterized protein OS=Thermus thermophilus
Thfi_0833	10,677	-0,636	0,004	0,016	469,07	436,56	541,76	935,8	819,87	727,9	tr|F6DID5|F6DID5_THETG Leucine--tRNA ligase OS=Thermus thermophilus
Thfi_0837	8,570	-0,510	0,044	0,112	91,8	78,3	102,97	114,43	113,8	169,87	tr|G8NCJ8|G8NCJ8_9DEIN Putative uncharacterized protein OS=Thermus sp.
Thfi_0840	6,708	-1,078	0,004	0,018	46,56	77,08	51,97	105,49	212,91	254,96	tr|S5Z4F4|S5Z4F4_9BACI ABC transporter permease OS=Geobacillus sp. JF8
Thfi_0841	4,760	-2,377	0,000	0,002	8,49	13,46	12,29	42,05	94,11	132,66	tr|G8NDV5|G8NDV5_9DEIN ABC transporter protein
Thfi_0848	9,055	1,844	0,000	0,000	2610,96	2867,84	2574,77	497,68	1134,82	972,14	tr|B7A609|B7A609_THEAQ Putative uncharacterized protein (Precursor) OS=Thermus aquaticus Y51MC23 GN=TaqDRAFT_4878 PE=4 SV=1
Thfi_0851	6,187	-1,466	0,001	0,004	50,77	68,08	25,76	93,02	166,15	240	tr|K7RLE0|K7RLE0_THEOS ABC-type branched-chain amino acid transport system, periplasmic component (Precursor) OS=Thermus oshimai JL-2

					FPKM						
Gene code	logCPM	logFC	PValue	FDR	63 degrees			77 degrees			Top Hit Uniprot
Thfi_0852	5,856	-2,208	0,000	0,001	24,76	39,75	108,61	153,38	354,75	393,64	tr|Q1AV69|Q1AV69_RUBXD Lactaldehyde dehydrogenase OS=Rubrobacter xylanophilus
Thfi_0853	10,608	0,742	0,033	0,090	639,57	919,28	775,78	249,6	621,5	839,22	tr|G2SLH7|G2SLH7_RHOMR DNA methylase N-4/N-6 domain protein
Thfi_0856	5,428	1,159	0,049	0,122	145,16	101,54	123,61	38,47	65,56	53,39	tr|F6DF04|F6DF04_THETG Regulatory protein TetR OS=Thermus thermophilus
Thfi_0857	4,843	1,693	0,001	0,006	359,62	127,39	173,51	55,13	69,54	0	tr|B7AAX1|B7AAX1_THEAQ Putative uncharacterized protein OS=Thermus aquaticus Y51MC23
Thfi_0858	7,674	1,218	0,000	0,000	240	398,03	386,95	216,88	183,79	158,56	tr|G8NCN1|G8NCN1_9DEIN Iron(III) dicitrate transport ATP-binding protein fecE OS=Thermus sp.
Thfi_0859	8,393	1,187	0,000	0,000	349,18	421,27	451,79	193,11	271,63	235,22	tr|F6DFT7|F6DFT7_THETG ABC-type transporter, integral membrane subunit (Precursor) OS=Thermus thermophilus
Thfi_0860	10,550	1,451	0,000	0,000	2963,25	2632,52	2686,43	953,37	1387,29	1041,35	tr|K7QUT6|K7QUT6_THEOS ABC-type Fe3+-hydroxamate transport system, periplasmic component
Thfi_0861	4,899	-2,208	0,001	0,004	119,86	44,34	40,2	270,5	292,8	177,79	tr|D9PLG3|D9PLG3_9ZZZZ Transcriptional modulator of MazE/toxin, MazF OS=sediment metagenome
Thfi_0863	14,855	1,813	0,000	0,000	5085,07	81704,9	41636,2	20552,1	13503,5	30873,3	tr|T3MXP3|T3MXP3_CLODI Cell wall-associated hydrolase domain protein OS=Clostridium difficile DA00132
Thfi_0865	6,587	-2,085	0,000	0,000	47,54	78,36	22,9	163,73	417,91	345,9	tr|Q1AV69|Q1AV69_RUBXD Lactaldehyde dehydrogenase OS=Rubrobacter xylanophilus
Thfi_0868	10,035	0,655	0,015	0,050	1773,99	1699,32	1456,66	1088,42	996,21	920,93	tr|H9ZTP2|H9ZTP2_THETH Branched-chain amino acid aminotransferase, group I
Thfi_0869	8,216	-0,789	0,004	0,017	197,38	140,86	193,51	405,56	285,5	333,73	tr|G8N8L2|G8N8L2_9DEIN Folyl-polyglutamate synthetase OS=Thermus sp. CCB_US3_UF1
Thfi_0872	8,147	0,512	0,028	0,080	375,87	290,55	367,32	298,83	233,18	203,62	tr|E8PQX8|E8PQX8_THESS Phenylalanine--tRNA ligase alpha subunit OS=Thermus scotoductus
Thfi_0873	9,043	0,510	0,017	0,056	341,5	295,25	316,71	223,2	276,46	234,6	tr|B7ABK3|B7ABK3_THEAQ Phenylalanine--tRNA ligase beta subunit OS=Thermus aquaticus Y51MC23
Thfi_0876	8,588	1,394	0,000	0,000	363,03	574,3	647,97	244,68	245,94	295,72	tr|K7QYQ2|K7QYQ2_THEOS 6-phosphofructokinase OS=Thermus oshimai JL-2 GN=pfkA PE=3 SV=1
Thfi_0877	9,036	1,096	0,000	0,000	1201,54	985,01	1126	549,53	502,75	446,9	tr|G8NCV1|G8NCV1_9DEIN Ribosomal RNA small subunit methyltransferase I OS=Thermus sp. CCB_US3_UF1
Thfi_0878	7,294	0,641	0,042	0,109	217,74	234,93	250,95	167,53	209,67	270,09	tr|B7AC86|B7AC86_THEAQ Short-chain dehydrogenase/reductase SDR
Thfi_0884	6,069	-1,353	0,001	0,008	23,3	20,14	11,07	68,03	45,13	39,43	tr|F2NRB7|F2NRB7_MARHT DNA internalization-related competence protein ComEC/Rec2
Thfi_0890	9,618	-0,563	0,013	0,043	615,58	477,34	530,15	879,83	835,25	699,71	tr|B7ABI9|B7ABI9_THEAQ Chromosomal replication initiator protein DnaA OS=Thermus aquaticus Y51MC23
Thfi_0891	7,796	0,564	0,020	0,062	238,1	191,96	221,48	196,14	171,32	106,71	tr|G8NDC2|G8NDC2_9DEIN DNA polymerase III subunit beta OS=Thermus sp. CCB_US3_UF1
Thfi_0892	10,238	0,617	0,020	0,063	1158,84	1302,76	1136,68	658,68	831,27	1155,85	tr|F6DH47|F6DH47_THETG Enolase OS=Thermus thermophilus (strain SG0.5JP17-16) GN=eno PE=3 SV=1
Thfi_0893	10,115	1,196	0,000	0,000	1269,87	1165,41	1008,67	508,67	564,2	544,15	tr|F6DH48|F6DH48_THETG Pyruvate kinase OS=Thermus thermophilus (strain SG0.5JP17-16)
Thfi_0899	9,749	0,863	0,001	0,006	1843,12	2083,85	1985,18	1206,16	1093,09	1058,1	tr|E8PR20|E8PR20_THESS Phage shock protein A OS=Thermus scotoductus (strain ATCC 700910 / SA-01) GN=TSC_c00270 PE=4 SV=1
Thfi_0901	7,638	0,660	0,014	0,046	1005,24	464,56	596,24	359,23	367,43	315,14	tr|B7ABY5|B7ABY5_THEAQ Deoxycytidine triphosphate deaminase OS=Thermus aquaticus Y51MC23 GN=dcd PE=3 SV=1

					FPKM						
Gene code	logCPM	logFC	PValue	FDR	63 degrees			77 degrees			Top Hit Uniprot
Thfi_0902	6,898	0,875	0,014	0,047	273,38	238,23	389,38	160,17	195,47	98,83	tr|F6DD61|F6DD61_THETG Peptidyl-prolyl cis-trans isomerase cyclophilin type
Thfi_0903	8,412	0,809	0,003	0,012	648,31	428,73	480,78	270,16	284,44	208,65	tr|G8NAL4|G8NAL4_9DEIN ATP phosphoribosyltransferase regulatory subunit
Thfi_0905	6,859	-0,736	0,037	0,097	185,64	167,18	122,12	311,57	345,35	158,22	tr|K7QVL6|K7QVL6_THEOS rRNA methylase OS=Thermus oshimai JL-2 GN=Theos_0240 PE=4 SV=1
Thfi_0907	7,995	-0,690	0,022	0,067	497,66	226,59	288,26	619,24	396,3	387,49	tr|D3PMD6|D3PMD6_MEIRD Periplasmic binding protein OS=Meiothermus ruber
Thfi_0909	9,971	1,032	0,000	0,001	712,84	1199,2	856,44	571,56	466,64	590,62	tr|F6DHZ4|F6DHZ4_THETG Dihydrolipoyl dehydrogenase OS=Thermus thermophilus
Thfi_0910	9,515	1,346	0,000	0,000	621,99	743,04	753,92	397,45	330,46	287,65	tr|H9ZP26|H9ZP26_THETH Pyruvate/2-oxoglutarate dehydrogenase complex, dihydrolipoamide acyltransferase component OS=Thermus thermophilus JL-18
Thfi_0911	9,379	1,250	0,000	0,000	785,93	1020,84	858,75	564,03	482,15	324,18	tr|F6DHZ8|F6DHZ8_THETG 3-methyl-2-oxobutanoate dehydrogenase (2-methylpropanoyl-transferring)
Thfi_0912	9,865	1,738	0,000	0,000	1253,02	1287,86	1410,82	538,05	446,98	320,2	tr|B7A915|B7A915_THEAQ Pyruvate dehydrogenase (Acetyl-transferring) OS=Thermus aquaticus Y51MC23
Thfi_0918	8,056	0,881	0,001	0,004	506,32	338,84	413,3	314,51	237,42	170,71	tr|B7A6F4|B7A6F4_THEAQ Putative uncharacterized protein (Precursor) OS=Thermus aquaticus Y51MC23
Thfi_0924	10,259	0,885	0,000	0,001	709,89	801,3	856,63	596,84	438,57	514,31	tr|E8PJE7|E8PJE7_THESS 2-oxoacid:ferredoxin oxidoreductase, subunit alpha OS=Thermus scotoductus
Thfi_0926	7,025	1,335	0,000	0,000	195,18	176,21	276,37	135,22	58,43	65,93	tr|K7R198|K7R198_THEOS BirA, biotin-(Acetyl-CoA-carboxylase) ligase OS=Thermus oshimai JL-2
Thfi_0927	7,071	1,040	0,002	0,010	280,6	342,11	326,58	199,44	172,28	72,87	tr|B7A7G8|B7A7G8_THEAQ BioY protein (Precursor) OS=Thermus aquaticus Y51MC23
Thfi_0928	6,478	0,755	0,027	0,078	204,34	150,69	158,79	98,39	109,63	100,49	tr|H9ZPJ0|H9ZPJ0_THETH Putative divalent heavy-metal cations transporter OS=Thermus thermophilus JL-18
Thfi_0933	10,076	0,543	0,034	0,092	1149,2	1001,73	1344,2	1234,06	822,47	1138,54	tr|E8PK17|E8PK17_THESS Lipoyl synthase OS=Thermus scotoductus (strain ATCC 700910 / SA-01)
Thfi_0934	10,415	-0,489	0,033	0,091	2117,45	1979,59	2005,43	3531,69	2580,37	2998,13	tr|H9ZP13|H9ZP13_THETH Octanoyltransferase OS=Thermus thermophilus JL-18 GN=lipB PE=3 SV=1
Thfi_0935	10,849	0,552	0,011	0,039	7195,37	5610,7	5785,57	5109,33	4180,63	3828,19	tr|F6DHY0|F6DHY0_THETG 50S ribosomal protein L9 OS=Thermus thermophilus (strain SG0.5JP17-16)
Thfi_0939	6,922	0,795	0,022	0,066	150,57	208,37	242,52	139,39	132,04	93,1	tr|G8N8Q8|G8N8Q8_9DEIN Putative uncharacterized protein OS=Thermus sp. CCB_US3_UF1
Thfi_0941	5,476	0,877	0,021	0,065	78,25	155,03	167,2	105,33	112,1	45,58	tr|B3VH91|B3VH91_9DEIN Methylglyoxal synthase OS=Thermus sp. GH5 GN=mgsA PE=1 SV=1
Thfi_0956	7,349	-0,763	0,006	0,022	56,21	62,58	36,24	99,15	105,41	116,02	tr|B7A8D1|B7A8D1_THEAQ Primosomal protein N' OS=Thermus aquaticus Y51MC23
Thfi_0966	10,117	0,629	0,008	0,029	1240,74	816,85	1100,04	616,51	669,86	609,94	tr|F6DFV9|F6DFV9_THETG Glycoside hydrolase family 57 OS=Thermus thermophilus (strain SG0.5JP17-16)
Thfi_0968	10,317	0,497	0,017	0,055	1423,88	1378,4	1621,27	1246,09	1188,09	1085,99	tr|K7QWA1|K7QWA1_THEOS N-acetyl-gamma-glutamyl-phosphate/N-acetyl-gamma-aminoadipyl-phosphate reductase OS=Thermus oshimai JL-2
Thfi_0973	7,045	-1,671	0,000	0,000	167,95	141,96	73,99	517,67	551,22	352,62	tr|K7R0W7|K7R0W7_THEOS 3-isopropylmalate dehydratase small subunit
Thfi_0974	7,536	-1,590	0,000	0,000	89,52	62,73	78,34	252,46	271,25	178,87	tr|G8NBZ8|G8NBZ8_9DEIN 3-isopropylmalate dehydratase large subunit
Thfi_0977	9,425	-1,800	0,000	0,000	299,13	227,36	320,29	1164,34	1125,71	923,1	tr|E8PJX5|E8PJX5_THESS Homocitrate synthase OS=Thermus scotoductus

					FPKM						
Gene code	logCPM	logFC	PValue	FDR	63 degrees			77 degrees			Top Hit Uniprot
Thfi_0981	12,477	3,280	0,000	0,000	13175	8445,68	7574,69	809,34	851,25	643,98	tr|F6DIU2|F6DIU2_THETG Transposase OS=Thermus thermophilus (strain SG0.5JP17-16)
Thfi_0985	4,673	-1,883	0,005	0,020	7,36	7,18	0	32,41	18,43	22,53	tr|E8PLN1|E8PLN1_THESS Sensor histidine kinase OS=Thermus scotoductus
Thfi_0989	8,013	-0,823	0,005	0,020	365,1	419,73	373,48	847,95	1066,27	1237,11	tr|B7A5P7|B7A5P7_THEAQ OsmC family protein OS=Thermus aquaticus Y51MC23
Thfi_0993	8,462	0,723	0,004	0,017	875,28	595,56	574,26	331,82	450,43	417,45	tr|B7A5Q1|B7A5Q1_THEAQ Signal peptidase I OS=Thermus aquaticus Y51MC23
Thfi_0994	5,407	1,137	0,033	0,090	115,13	98,39	89,81	35,96	75,66	55,45	tr|E8PNC4|E8PNC4_THESS Uncharacterized protein OS=Thermus scotoductus
Thfi_0995	7,923	0,750	0,004	0,016	174,14	205,46	223,09	121,53	181,57	129,24	tr|G8NAK2|G8NAK2_9DEIN Iron-sulfur cluster-binding protein OS=Thermus sp.
Thfi_1000	7,944	0,786	0,005	0,020	191,98	366,58	241,58	231,92	227,59	129,52	tr|C6KVJ4|C6KVJ4_9BACT Catechol 2,3-dioxygenase OS=uncultured bacterium PE=4 SV=1
Thfi_1002	4,649	-1,792	0,018	0,057	6,32	9,94	0	30,96	58,65	58,65	tr|B8G996|B8G996_CHLAD Short-chain dehydrogenase/reductase SDR
Thfi_1011	6,302	0,807	0,032	0,089	108,41	120,76	95,28	67,02	96,49	93,1	
Thfi_1015	6,034	-0,783	0,034	0,092	53,5	59,11	82,31	105,34	145,11	199,49	tr|Q746P8|Q746P8_THET2 Cobalamin synthase OS=Thermus thermophilus
Thfi_1018	8,594	0,790	0,002	0,010	1181,56	883,86	844,57	507,89	601,97	432,26	tr|F6DIL5|F6DIL5_THETG High-affinity nickel-transporter OS=Thermus thermophilus
Thfi_1020	8,342	1,318	0,000	0,000	747,91	701,17	874,36	363,55	320,96	235,34	tr|F6DJT2|F6DJT2_THETG Precorrin-8X methylmutase CbiC/CobH OS=Thermus thermophilus
Thfi_1022	10,181	0,836	0,000	0,002	1253,85	1360,19	1273,96	799,53	771,78	794,05	tr|F6DJT1|F6DJT1_THETG Precorrin-6y C5,15-methyltransferase (Decarboxylating), CbiE subunit OS=Thermus thermophilus
Thfi_1023	7,062	0,905	0,007	0,025	223,38	264,47	166,31	174,17	164,94	134,37	tr|Q53WA8|Q53WA8_THET8 Precorrin-2 methylase OS=Thermus thermophilus
Thfi_1024	6,332	1,838	0,000	0,000	196,07	146,78	185,1	51,6	32,58	119,47	tr|B7A777|B7A777_THEAQ Uroporphyrin-III C/tetrapyrrole (Corrin/Porphyrin) methyltransferase
Thfi_1025	10,122	1,375	0,000	0,000	1678,39	2369,32	1823,27	740,13	856,95	1008,3	tr|H9ZUQ0|H9ZUQ0_THETH Precorrin-3B C17-methyltransferase OS=Thermus thermophilus JL-18
Thfi_1026	9,603	1,438	0,000	0,000	844,63	1252,2	1151,05	426,59	497,22	419,84	tr|Q53WA5|Q53WA5_THET8 Cobalamin biosynthesis protein CbiG OS=Thermus thermophilus
Thfi_1027	6,780	1,515	0,000	0,000	185,32	130,2	184,77	58,79	66,15	25,54	tr|Q53WA4|Q53WA4_THET8 Cobalamin biosynthesis protein CbiX OS=Thermus thermophilus
Thfi_1028	9,658	2,622	0,000	0,000	3585,43	5450,1	4583,18	875,66	946,72	817,87	tr|H9ZUQ3|H9ZUQ3_THETH Uncharacterized protein OS=Thermus thermophilus JL-18 GN=TtJL18_2228
Thfi_1029	6,361	2,882	0,000	0,000	199,34	209,64	252,11	31,28	23,7	65,16	tr|Q746N6|Q746N6_THET2 Uroporphyrin-III C-methyltransferase OS=Thermus thermophilus
Thfi_1030	6,386	0,907	0,007	0,025	99,6	112,95	143,06	73,71	74,49	85,36	tr|E8PQC4|E8PQC4_THESS Cobalamin biosynthesis protein CobD OS=Thermus scotoductus (strain ATCC 700910 / SA-01) GN=cobD PE=3 SV=1
Thfi_1048	9,948	-2,728	0,000	0,000	210,26	147,03	162,48	1417,35	1171,14	1476,71	tr|F2NQK2|F2NQK2_MARHT Uncharacterized protein OS=Marinithermus hydrothermalis (strain DSM 14884 / JCM 11576 / T1)
Thfi_1054	7,925	1,045	0,000	0,000	210,12	254	255,19	143,22	122,59	149,9	tr|K7QW97|K7QW97_THEOS 4-aminobutyrate aminotransferase family protein OS=Thermus oshimai JL-2 GN=Theos_0621 PE=3 SV=1

					FPKM						
Gene code	logCPM	logFC	PValue	FDR	63 degrees			77 degrees			Top Hit Uniprot
Thfi_1056	9,048	0,949	0,000	0,000	641,62	599	577,36	330,91	414,71	346,27	tr|H9ZQP2|H9ZQP2_THETH Putative ABC-type transport system, periplasmic component/surface lipoprotein (Precursor) OS=Thermus thermophilus JL-18
Thfi_1059	8,739	1,264	0,000	0,000	567,12	702,53	602,92	262,48	344,31	389,72	tr|K7R0G3|K7R0G3_THEOS Fructose-1,6-bisphosphate aldolase, class II OS=Thermus oshimai JL-2
Thfi_1061	5,996	0,854	0,014	0,048	157,73	96,19	124,1	89,84	54,7	66,84	tr|E8PN70|E8PN70_THESS Ribulose-phosphate 3-epimerase OS=Thermus scotoductus
Thfi_1062	5,360	-1,229	0,011	0,038	28,95	22,67	13,83	53,38	68,78	44,51	tr|K7RK40|K7RK40_THEOS Phosphoribulokinase OS=Thermus oshimai JL-2 GN=Theos_1732 PE=3 SV=1
Thfi_1064	4,122	-1,365	0,030	0,084	18,25	24,4	0	16,74	84,46	77,32	tr|K7R749|K7R749_THEOS Ribulose bisphosphate carboxylase small subunit OS=Thermus oshimai JL-2
Thfi_1066	3,799	-2,831	0,027	0,078	7,09	0	6,78	12,55	11,89	29,07	tr|K7QVX3|K7QVX3_THEOS Fructose-1,6-bisphosphatase OS=Thermus oshimai JL-2 GN=Theos_1736 PE=3 SV=1
Thfi_1069	5,318	-2,601	0,001	0,003	42,07	21,38	37,26	76,35	134,97	454,27	tr|K7R883|K7R883_THEOS Transposase OS=Thermus oshimai JL-2 GN=Theos_2258 PE=4 SV=1
Thfi_1070	5,401	-1,260	0,007	0,026	79,13	63,3	16,48	108,38	156,29	250,44	tr|Q1AV60|Q1AV60_RUBXD Benzoate-CoA ligase OS=Rubrobacter xylanophilus
Thfi_1071	6,374	-1,732	0,000	0,002	9,46	20,89	13,51	76,17	68,25	173,34	tr|Q1AV59|Q1AV59_RUBXD Succinate-semialdehyde dehydrogenase (NAD(P)+) OS=Rubrobacter xylanophilus
Thfi_1072	6,693	-1,348	0,000	0,002	62,99	156,84	165,88	300,9	591,3	561,32	tr|U2MVM4|U2MVM4_9ACTO Uncharacterized protein OS=Actinomadura madurae
Thfi_1075	7,104	-2,854	0,000	0,000	58,37	65,44	68,15	475,14	656,73	1184,12	tr|H7GHW1|H7GHW1_9DEIN Transposase OS=Thermus sp. RL GN=RLTM_05796 PE=4 SV=1
Thfi_1076	8,321	0,814	0,022	0,066	769,45	762	1208,74	466,47	623,47	408,04	tr|F6DJ48|F6DJ48_THETG Helix-turn-helix domain protein OS=Thermus thermophilus
Thfi_1077	10,163	1,350	0,000	0,000	1029,59	1276,85	1195,28	406,56	703,45	621,01	tr|K7QWQ5|K7QWQ5_THEOS Uncharacterized protein OS=Thermus oshimai JL-2 GN=Theos_2255 PE=4 SV=1
Thfi_1078	8,635	0,518	0,036	0,096	794,63	794,1	753,74	540,29	688,21	504,61	tr|F6DGK7|F6DGK7_THETG Polyamine-transporting ATPase OS=Thermus thermophilus
Thfi_1085	10,333	1,271	0,000	0,000	3885,78	4032,79	3289,38	1199	2202,57	1790,76	tr|K7R1Q2|K7R1Q2_THEOS Uncharacterized protein (Precursor) OS=Thermus oshimai JL-2 GN=Theos_2254
Thfi_1087	7,683	0,725	0,034	0,093	144,34	87,79	122,13	42,57	98,47	94,77	tr|E8PLJ1|E8PLJ1_THESS Ggdef domain protein OS=Thermus scotoductus
Thfi_1090	12,810	-0,589	0,026	0,077	4580,66	5109,29	6255,29	6612,25	9951,06	8666,57	tr|K7QUM3|K7QUM3_THEOS ABC-type transport system, involved in lipoprotein release, permease component (Precursor) OS=Thermus oshimai JL-2
Thfi_1093	5,833	-1,667	0,000	0,001	74,06	50,14	83,09	203,17	216,69	288,61	tr|H7GIN9|H7GIN9_9DEIN Integrase catalytic subunit OS=Thermus sp. RL GN=RLTM_11018 PE=4 SV=1
Thfi_1094	5,912	-1,175	0,020	0,061	17,95	10,57	14,28	12,5	27,27	60,9	tr|I4F7B6|I4F7B6_MICAE Uncharacterized protein OS=Microcystis aeruginosa PCC 9432
Thfi_1096	5,886	-3,880	0,000	0,001	6,36	2,97	3,62	11,13	63,32	201,33	tr|E8PL10|E8PL10_THESS Uncharacterized protein OS=Thermus scotoductus
Thfi_1097	6,615	1,791	0,000	0,002	128,46	151,99	77,94	36,01	26	83,45	tr|H9ZUC7|H9ZUC7_THETH Uncharacterized protein containing a von Willebrand factor type A (VWA) domain
Thfi_1102	4,649	-1,671	0,034	0,092	19,39	19,29	0	26,36	108,11	121,88	tr|Q1AV74|Q1AV74_RUBXD Adenine deaminase OS=Rubrobacter xylanophilus
Thfi_1106	5,842	2,283	0,000	0,000	137,6	131,49	177,62	19,45	49,13	45,03	tr|E8PR69|E8PR69_THESS Nitrilase/cyanide hydratase and apolipoprotein N-acyltransferase
Thfi_1108	9,277	1,026	0,000	0,000	506,93	463,32	443,27	247,16	288,5	262,61	tr|E8PR67|E8PR67_THESS Tungsten-containing aldehyde ferredoxin oxidoreductase

					FPKM						
Gene code	logCPM	logFC	PValue	FDR	63 degrees			77 degrees			Top Hit Uniprot
Thfi_1112	6,063	-1,189	0,004	0,017	14,67	12,64	11,59	24,87	30,99	64,27	tr|D7BCR2|D7BCR2_MEISD Conserved repeat domain protein (Precursor) OS=Meiothermus silvanus
Thfi_1115	5,429	-2,495	0,001	0,006	4,81	3,11	4,56	9,78	26,49	63,19	tr|Q53VY9|Q53VY9_THET8 Uncharacterized protein OS=Thermus thermophilus
Thfi_1116	8,921	2,357	0,000	0,000	651,69	501,43	716,98	93,48	151,03	213,08	tr|G8NDA7|G8NDA7_9DEIN 4-aminobutyrate aminotransferase OS=Thermus sp. CCB_US3_UF1
Thfi_1117	9,123	1,884	0,000	0,000	628,96	498,64	533,75	122,42	247,87	212,81	tr|E8PR76|E8PR76_THESS Betaine aldehyde dehydrogenase OS=Thermus scotoductus
Thfi_1118	7,663	2,401	0,000	0,000	187,04	149,75	264,74	42,95	75,79	41,19	tr|E8PR75|E8PR75_THESS Aminotransferase OS=Thermus scotoductus
Thfi_1119	6,870	1,641	0,000	0,000	170,14	140,12	173,16	45,5	63,72	109,99	tr|G8NDA8|G8NDA8_9DEIN Spermidine/putrescine transport system ATP-binding protein OS=Thermus sp.
Thfi_1122	7,874	2,443	0,000	0,000	210,17	380,18	343,16	65,91	90,83	111,05	tr|E8PR71|E8PR71_THESS Spermidine/putrescine-binding periplasmic protein OS=Thermus scotoductus
Thfi_1123	7,288	2,798	0,000	0,000	113,43	184,78	149,93	23,81	45,13	31,04	tr|G8NDB2|G8NDB2_9DEIN 4-aminobutyrate aminotransferase OS=Thermus sp. CCB_US3_UF1 GN=TCCBUS3UF1_12090 PE=3 SV=1
Thfi_1133	7,755	0,780	0,026	0,077	146,41	141,51	137,93	65,53	86,01	147,26	tr|Q746E5|Q746E5_THET2 Uncharacterized protein OS=Thermus thermophilus
Thfi_1135	9,477	1,191	0,000	0,000	1458,94	891,61	1175,92	451,33	566,54	388,77	tr|H9ZSL3|H9ZSL3_THETH Tetratricopeptide repeat protein (Precursor) OS=Thermus thermophilus JL-18
Thfi_1136	10,401	1,024	0,000	0,000	2130,32	1509,71	1629,55	739,7	926,51	793,74	tr|B7AAK1|B7AAK1_THEAQ Heat shock protein HslVU, ATPase subunit HslU OS=Thermus aquaticus Y51MC23
Thfi_1138	7,719	1,713	0,000	0,000	1194,13	577,41	1020,33	225,98	293,16	116,14	tr|B7AAK0|B7AAK0_THEAQ 20S proteasome A and B subunits OS=Thermus aquaticus Y51MC23
Thfi_1139	10,884	-0,546	0,027	0,078	766,68	884,77	1071,45	2165,33	1436,9	1893,2	tr|B7AAJ9|B7AAJ9_THEAQ Magnesium-chelatase subunit ChlI OS=Thermus aquaticus Y51MC23
Thfi_1140	6,751	-1,356	0,000	0,002	198,72	301,9	253,1	883,88	675,74	493,81	tr|Q72KZ6|Q72KZ6_THET2 Nucleotidyltransferase OS=Thermus thermophilus
Thfi_1142	10,372	-0,779	0,007	0,026	390,83	786,69	534,7	1939,63	1538,48	1179,02	tr|F6DFA4|F6DFA4_THETG von Willebrand factor type A OS=Thermus thermophilus
Thfi_1145	6,409	-1,129	0,003	0,015	95,09	33,04	54,45	108,16	95,42	155,55	tr|E8PPF0|E8PPF0_THESS Glycosyltransferase OS=Thermus scotoductus
Thfi_1146	12,937	0,670	0,001	0,004	4378,33	3751,66	4010,73	2669,77	2942,34	2746,34	tr|B7AAG6|B7AAG6_THEAQ Lon protease OS=Thermus aquaticus Y51MC23 GN=lon PE=3 SV=1
Thfi_1147	6,613	0,908	0,006	0,023	198,76	215,74	236,49	129,46	159,03	48,58	tr|Q5SJA2|Q5SJA2_THET8 Uncharacterized protein OS=Thermus thermophilus
Thfi_1156	8,517	0,519	0,033	0,091	822,03	547,46	543,57	455,99	400,15	333,5	tr|F6DH30|F6DH30_THETG Bifunctional protein FolD OS=Thermus thermophilus (strain SG0.5JP17-16) GN=folD PE=3 SV=1
Thfi_1157	6,581	0,684	0,036	0,095	455,78	278,06	265,89	182,15	246,24	180,38	tr|G8N7W1|G8N7W1_9DEIN N utilization substance protein B homolog OS=Thermus sp. CCB_US3_UF1
Thfi_1158	8,522	0,630	0,011	0,040	2002,78	1449,21	1545,02	1323,03	1577,75	832,01	tr|G8N7W2|G8N7W2_9DEIN Putative uncharacterized protein OS=Thermus sp. CCB_US3_UF1
Thfi_1160	8,861	0,483	0,025	0,073	362,32	374	442,22	331,97	368,46	259,93	tr|E8PPD8|E8PPD8_THESS Acetyl-CoA carboxylase, biotin carboxylase subunit OS=Thermus scotoductus
Thfi_1172	9,185	1,520	0,000	0,000	972,07	1740,08	1627,79	637,85	953,7	801,41	tr|F6DH44|F6DH44_THETG Cytochrome C oxidase subunit IIa transmembrane OS=Thermus thermophilus
Thfi_1173	10,750	1,174	0,000	0,000	759,9	1361,17	1149,79	528,11	989,1	599,97	tr|K7RJC0|K7RJC0_THEOS Heme/copper-type cytochrome/quinol oxidase, subunit 1 (Precursor)

					FPKM						
Gene code	logCPM	logFC	PValue	FDR	63 degrees			77 degrees			Top Hit Uniprot
Thfi_1174	5,484	-1,404	0,008	0,030	42,85	29,93	93,57	117,04	156,92	236,71	tr|H9ZR64|H9ZR64_THETH Uncharacterized protein OS=Thermus thermophilus JL-18
Thfi_1178	6,280	0,774	0,045	0,114	83,71	47,72	51,19	32,79	49,72	36,48	tr|E8PMN0|E8PMN0_THESS Exopolyphosphatase OS=Thermus scotoductus
Thfi_1179	6,550	-0,816	0,023	0,070	89,27	59,6	37,41	123,06	123,89	106,91	tr|K7R647|K7R647_THEOS Tellurite resistance protein-like permease (Precursor) OS=Thermus oshimai JL-2
Thfi_1184	6,936	1,512	0,000	0,001	107,06	90,75	142,49	48,75	58,51	79,08	tr|G8N8F8|G8N8F8_9DEIN Histidinol dehydrogenase OS=Thermus sp. CCB_US3_UF1 GN=hisD PE=3 SV=1
Thfi_1187	7,378	0,638	0,031	0,087	553,5	445,35	868,9	436,98	436,4	420,43	tr|E8PNK6|E8PNK6_THESS Uncharacterized protein OS=Thermus scotoductus
Thfi_1189	4,865	-1,421	0,023	0,069	54,29	10,65	23,39	45,78	36,52	50,22	tr|E8PKK0|E8PKK0_THESS Molybdate ABC transporter, periplasmic molybdate-binding protein
Thfi_1195	8,408	0,606	0,027	0,079	428,26	302,87	385,5	184,45	276,63	301,06	tr|E8PKK4|E8PKK4_THESS Histidine--tRNA ligase OS=Thermus scotoductus
Thfi_1197	7,346	0,842	0,033	0,091	393,7	236,74	278,77	100,09	264,63	48,52	tr|B7A668|B7A668_THEAQ Phenazine biosynthesis protein PhzF family OS=Thermus aquaticus Y51MC23
Thfi_1200	6,807	-0,765	0,024	0,071	163,58	126,29	133,52	283,23	300,34	235,89	tr|B7A671|B7A671_THEAQ Glutamine amidotransferase subunit PdxT OS=Thermus aquaticus Y51MC23
Thfi_1201	7,612	-1,099	0,001	0,004	85,12	42,37	52,83	148,79	128,39	132,69	tr|Q5SKD7|Q5SKD7_THET8 Cation-transporting ATPase OS=Thermus thermophilus
Thfi_1204	9,957	0,797	0,001	0,003	1060,19	1228,79	1399,58	983,14	886,59	1083,76	tr|E8PKL9|E8PKL9_THESS Pyridoxal biosynthesis lyase PdxS OS=Thermus scotoductus
Thfi_1210	8,555	0,872	0,000	0,001	1268	913,82	1038,29	550,1	604,58	587,33	tr|G8N9F9|G8N9F9_9DEIN Single-stranded nucleic acid binding R3H domain protein
Thfi_1212	4,429	-2,111	0,006	0,023	64,22	32,02	38,7	148,69	211,19	85,52	tr|G8N9F7|G8N9F7_9DEIN Putative membrane protein insertion efficiency factor
Thfi_1213	6,796	-0,743	0,027	0,079	382,51	216,85	189	484,65	326,12	335,91	tr|H9ZT49|H9ZT49_THETH Ribonuclease P protein component OS=Thermus thermophilus JL-18
Thfi_1215	9,181	-0,654	0,005	0,020	453,84	593,57	612,56	998,59	1373,85	968,72	tr|F6DE47|F6DE47_THETG Monosaccharide-transporting ATPase OS=Thermus thermophilus
Thfi_1216	9,745	-0,607	0,015	0,048	254,52	299,79	291,37	491,97	705,28	608,01	tr|F6DE48|F6DE48_THETG Long-chain-fatty-acid--CoA ligase (Precursor) OS=Thermus thermophilus
Thfi_1220	11,065	0,532	0,031	0,087	1241,47	2475,23	1753,4	1345,88	1884,38	1871,27	tr|K7QY28|K7QY28_THEOS ABC-type branched-chain amino acid transport system, periplasmic component
Thfi_1223	7,072	-0,755	0,016	0,053	158,31	210,54	215,02	504,12	354,43	432,82	tr|B7AAY7|B7AAY7_THEAQ Arsenite oxidase, small subunit (Precursor) OS=Thermus aquaticus Y51MC23
Thfi_1224	11,637	-1,426	0,000	0,000	314,7	571,61	401,36	2285,79	1662,85	1987,1	tr|Q53W39|Q53W39_THET8 Arsenite oxidase, large subunit OS=Thermus thermophilus
Thfi_1226	9,379	1,159	0,000	0,000	327,88	451,67	423,66	310,75	300,35	239,17	tr|G8NCP0|G8NCP0_9DEIN Isopentenyl-diphosphate delta-isomerase OS=Thermus sp. CCB_US3_UF1
Thfi_1227	9,155	1,116	0,000	0,001	454,82	775,83	511,92	439,48	418,42	481,42	tr|G8NCP1|G8NCP1_9DEIN Phytoene dehydrogenase OS=Thermus sp. CCB_US3_UF1
Thfi_1228	8,724	0,681	0,003	0,012	299,77	290,78	432,88	244,41	282,95	284,93	tr|D7BGJ5|D7BGJ5_MEISD Phosphoglucomutase/phosphomannomutase alpha/beta/alpha domain I OS=Meiothermus silvanus
Thfi_1236	7,667	1,069	0,001	0,007	276,82	319,04	570,51	275,68	214,53	393,15	tr|G8NCQ0|G8NCQ0_9DEIN Transcriptional regulator, Crp OS=Thermus sp. CCB_US3_UF1
Thfi_1238	6,869	-1,455	0,000	0,001	71,66	49,97	68,57	233,08	182,89	212,66	tr|Q746K1|Q746K1_THET2 Probable UV endonuclease OS=Thermus thermophilus

					FPKM						
Gene code	logCPM	logFC	PValue	FDR	63 degrees			77 degrees			Top Hit Uniprot
Thfi_1241	7,391	0,793	0,013	0,043	283,96	312,86	555,64	300,29	284,22	423,02	tr|G8NCQ8|G8NCQ8_9DEIN Flavin reductase domain protein FMN-binding protein OS=Thermus sp.
Thfi_1243	8,202	1,046	0,001	0,003	282,38	193,22	231,59	131,48	147,98	180,95	tr|B7A678|B7A678_THEAQ NmrA family protein OS=Thermus aquaticus Y51MC23
Thfi_1246	10,441	2,390	0,000	0,000	3039,88	3541,22	3927,27	743,81	1055	659,76	tr|K7QXH2|K7QXH2_THEOS Uncharacterized protein (Precursor) OS=Thermus oshimai JL-2
Thfi_1247	11,257	3,541	0,000	0,000	711,37	1833,3	1563,68	60,13	340,54	112,62	tr|E8PK48|E8PK48_THESS Molybdopterin oxidoreductase OS=Thermus scotoductus
Thfi_1248	8,726	3,596	0,000	0,000	415,74	1085,29	1189,77	65,01	168,48	213,78	tr|E8PK48|E8PK48_THESS Molybdopterin oxidoreductase OS=Thermus scotoductus
Thfi_1249	10,224	2,600	0,000	0,000	958,3	2756,29	1760,29	174,77	685,9	641,81	tr|E8PK47|E8PK47_THESS 4Fe-4S ferredoxin iron-sulfur binding domain protein OS=Thermus scotoductus
Thfi_1251	7,324	-0,736	0,026	0,076	133	181,06	132,52	228,88	209,98	418,49	tr|E8PK46|E8PK46_THESS Phosphonate ABC transporter, periplasmic phosphonate-binding protein OS=Thermus scotoductus
Thfi_1254	6,765	-1,909	0,000	0,000	202,4	115,53	133,89	456,8	591,41	666,21	tr|B7AA44|B7AA44_THEAQ Disulphide bond formation protein DsbB (Precursor)
Thfi_1255	9,162	0,582	0,029	0,082	933,25	471,74	863,35	589,8	543,78	643,8	tr|F2NM48|F2NM48_MARHT Signal recognition particle receptor FtsY OS=Marinithermus hydrothermalis
Thfi_1259	4,957	-1,951	0,007	0,025	11,22	22,42	32,7	46,07	145,31	248,38	tr|Q1AV68|Q1AV68_RUBXD Carbonic anhydrases/acetyltransferases isoleucine patch superfamily-like protein OS=Rubrobacter xylanophilus
Thfi_1260	7,307	-1,944	0,000	0,000	141,69	105,41	115,47	447,53	416,12	942,73	tr|H9ZSG3|H9ZSG3_THETH Transposase OS=Thermus thermophilus JL-18 GN=TtJL18_1389 PE=4 SV=1
Thfi_1267	7,164	0,564	0,034	0,092	611,21	667,42	746,29	583,01	559,54	350,6	tr|E8PR36|E8PR36_THESS FUN14 family
Thfi_1269	11,503	1,473	0,000	0,000	6957,29	3020,81	3418,65	842,1	1387,26	1014,46	tr|F6DIU2|F6DIU2_THETG Transposase OS=Thermus thermophilus (strain SG0.5JP17-16)
Thfi_1274	13,154	-1,273	0,000	0,002	3355,14	2652,29	2974,64	14612,9	5193,59	6726,71	tr|K7QXH6|K7QXH6_THEOS 60 kDa chaperonin OS=Thermus oshimai JL-2 GN=groL PE=3 SV=1
Thfi_1275	10,075	-1,145	0,003	0,014	3932	2680	2884,99	12976,5	3648	5052,15	tr|E8PJF5|E8PJF5_THESS 10 kDa chaperonin OS=Thermus scotoductus (
Thfi_1280	10,254	0,873	0,001	0,004	5057,25	4714,84	3847,27	2257,58	2524,1	2631,84	tr|B7ABH4|B7ABH4_THEAQ Peptidyl-prolyl cis-trans isomerase OS=Thermus aquaticus Y51MC23
Thfi_1282	7,754	-0,974	0,005	0,019	294,22	152,7	216,2	560,66	412,15	251,87	tr|K7RL96|K7RL96_THEOS 5'-nucleotidase SurE OS=Thermus oshimai JL-2 GN=surE PE=3 SV=1
Thfi_1285	7,028	0,874	0,003	0,012	280,53	245,8	279,58	167,2	152,49	129,01	tr|E8PR32|E8PR32_THESS Putative tetratricopeptide repeat family protein OS=Thermus
Thfi_1288	6,237	0,642	0,045	0,114	112,26	163,16	170,12	150,42	159,13	30,69	tr|F2NLA3|F2NLA3_MARHT CRISPR-associated protein, Cse2 family OS=Marinithermus hydrothermalis
Thfi_1290	8,531	-1,433	0,000	0,000	1689,67	1783,66	1563,58	4669,34	5323,15	5559,55	
Thfi_1291	8,856	1,133	0,000	0,000	268,61	222,42	213,05	97,95	123,82	130,5	tr|F2NLA1|F2NLA1_MARHT CRISPR-associated helicase Cas3 OS=Marinithermus hydrothermalis
Thfi_1300	6,041	-1,787	0,000	0,001	119,66	62,35	69,91	361,69	207,42	189,9	tr|E8PPN2|E8PPN2_THESS Uncharacterized protein OS=Thermus scotoductus
Thfi_1301	7,174	-1,034	0,005	0,020	94,56	146,49	102,49	449,45	247,97	417,63	tr|F6DFD9|F6DFD9_THETG Thiamine-phosphate synthase OS=Thermus thermophilus (strain SG0.5JP17-16) GN=thiE PE=3 SV=1

					FPKM						
Gene code	logCPM	logFC	PValue	FDR	63 degrees			77 degrees			Top Hit Uniprot
Thfi_1302	4,212	-1,499	0,031	0,087	53,7	75,6	0	212,05	33,55	365,53	tr|F6DFE0|F6DFE0_THETG Thiamine biosynthesis protein ThiS OS=Thermus thermophilus
Thfi_1303	5,410	-1,098	0,036	0,096	25,39	22,16	32,43	67,69	47,5	121,91	tr|H9ZSG9|H9ZSG9_THETH Thiazole synthase OS=Thermus thermophilus JL-18 GN=thiG PE=3 SV=1
Thfi_1304	4,148	-2,033	0,043	0,110	0	3,9	0	22,03	16,7	30,62	tr|H7GG23|H7GG23_9DEIN Oxidoreductase OS=Thermus sp. RL GN=RLTM_05019 PE=4 SV=1
Thfi_1305	8,806	-1,330	0,000	0,001	108,3	162,11	114,8	694,36	433,84	501,99	tr|F6DFE3|F6DFE3_THETG Phosphomethylpyrimidine synthase OS=Thermus thermophilus
Thfi_1306	6,507	-1,998	0,000	0,000	30,63	50,59	17,62	237,33	175,7	189,48	tr|G8NDY3|G8NDY3_9DEIN Phosphomethylpyrimidine kinase OS=Thermus sp. CCB_US3_UF1 GN=TCCBUS3UF1_13420 PE=4 SV=1
Thfi_1307	6,342	-2,066	0,000	0,000	13,92	10,12	9,9	53,1	44,59	58,05	tr|G8N8V2|G8N8V2_9DEIN Diguanylate cyclase/phosphodiesterase with GAF sensor
Thfi_1309	6,094	-1,130	0,012	0,042	156,71	65,68	86,46	101,23	129,71	268,79	tr|E8PMI6|E8PMI6_THESS Methyltransferase OS=Thermus scotoductus (strain ATCC 700910 / SA-01)
Thfi_1311	10,261	1,202	0,000	0,000	1560	1454,63	1385,48	704,05	620,84	590,79	tr|H9ZQJ9|H9ZQJ9_THETH Citrate synthase OS=Thermus thermophilus JL-18 GN=TtJL18_0706 PE=3 SV=1
Thfi_1314	11,647	0,992	0,000	0,002	1762,64	2661,21	2113,15	1000,11	1259,64	1407,75	tr|K7R3G6|K7R3G6_THEOS Small GTP-binding protein domain protein OS=Thermus oshimai JL-2 GN=Theos_0369
Thfi_1315	7,505	1,466	0,000	0,000	302,54	268,56	380,96	110,65	151,66	114,51	tr|Q72IJ7|Q72IJ7_THET2 MoxR-like ATPase OS=Thermus thermophilus (strain HB27 / ATCC BAA-163 / DSM 7039)
Thfi_1316	10,142	0,746	0,010	0,034	516,51	761,51	513,89	316,03	476,87	391,98	tr|K7QTT7|K7QTT7_THEOS Phosphoenolpyruvate synthase OS=Thermus oshimai JL-2
Thfi_1317	7,937	-1,129	0,000	0,001	171,91	108,74	117,14	330,32	294,19	401,5	tr|F6DE56|F6DE56_THETG Cysteine desulfurase OS=Thermus thermophilus (strain SG0.5JP17-16)
Thfi_1319	8,108	0,491	0,045	0,116	659,6	529,06	506,74	410,72	461,88	334,2	tr|G8NA19|G8NA19_9DEIN Two component transcriptional regulator, winged helix OS=Thermus sp. CCB_US3_UF1
Thfi_1321	5,931	-1,275	0,004	0,016	175,97	124,45	43,13	373,9	231,52	188,27	tr|E8PP42|E8PP42_THESS Uncharacterized protein OS=Thermus scotoductus
Thfi_1323	5,844	-1,098	0,006	0,023	162,97	101,83	130,79	219,94	324,63	285,49	tr|F6DDS0|F6DDS0_THETG Uncharacterized protein OS=Thermus thermophilus
Thfi_1324	5,454	-0,937	0,025	0,074	89,6	37,79	27,64	65,63	97,3	79,28	tr|F6DDS1|F6DDS1_THETG Cytochrome c assembly protein (Precursor) OS=Thermus thermophilus
Thfi_1325	8,573	-0,672	0,009	0,032	303,76	317,55	270,21	436,28	528,34	478,18	tr|G8NA12|G8NA12_9DEIN Glutamyl-tRNA reductase OS=Thermus sp. CCB_US3_UF1 GN=hemA PE=3 SV=1
Thfi_1330	11,086	3,285	0,000	0,000	4259,65	3801,48	3169,31	271,41	390,29	274,97	tr|F6DIU2|F6DIU2_THETG Transposase OS=Thermus thermophilus (strain SG0.5JP17-16)
Thfi_1331	5,293	-1,943	0,000	0,002	11,34	6,86	3,59	28,69	35,56	30,7	tr|E8PQP1|E8PQP1_THESS Amylo-alpha-1,6-glucosidase OS=Thermus scotoductus
Thfi_1332	6,108	-2,014	0,000	0,000	8,41	18,35	0	90,13	75,61	71,91	tr|G8ND41|G8ND41_9DEIN Binding-protein-dependent transport system inner membrane component
Thfi_1333	7,328	-2,106	0,000	0,000	33,41	45,7	41,85	287,45	202,54	294,59	tr|G8ND42|G8ND42_9DEIN Binding-protein-dependent transport system inner membrane component
Thfi_1335	6,631	-1,491	0,005	0,019	54,56	22,29	47,61	142,72	135,22	247,96	tr|E8PQP5|E8PQP5_THESS Transcriptional regulator, LacI family OS=Thermus scotoductus
Thfi_1339	4,667	-1,581	0,029	0,083	14,87	11,69	8,55	39,69	50,13	18,38	tr|K7R0L0|K7R0L0_THEOS ABC-type Mn2+/Zn2+ transport system, permease component (Precursor)
Thfi_1340	7,804	-0,604	0,026	0,077	52,5	55,57	46,24	69,56	109,91	125,48	tr|G8NCJ8|G8NCJ8_9DEIN Putative uncharacterized protein OS=Thermus sp. CCB_US3_UF1 GN=TCCBUS3UF1_22290 PE=4 SV=1

					FPKM						
Gene code	logCPM	logFC	PValue	FDR	63 degrees			77 degrees			Top Hit Uniprot
Thfi_1346	6,203	-0,794	0,039	0,102	27,36	42,63	22,98	60,78	91,09	39,31	tr|E8PPX8|E8PPX8_THESS Putative lipoprotein OS=Thermus scotoductus
Thfi_1355	4,368	-1,771	0,009	0,032	16,94	7,58	6,94	15	24,36	74,44	tr|E8PPX0|E8PPX0_THESS Binding-protein-dependent transport systems inner membrane component
Thfi_1356	5,772	-1,884	0,000	0,001	7,18	11,2	15,39	66,33	62,86	65,88	tr|E8PPW9|E8PPW9_THESS Multiple sugar transport system substrate-binding protein
Thfi_1357	4,557	-1,894	0,034	0,092	4,48	3,49	0	24,92	9,94	18,24	tr|E8PPW8|E8PPW8_THESS Beta-N-acetylglucosaminidase OS=Thermus scotoductus (strain ATCC 700910 / SA-01) GN=TSC_c10830 PE=4 SV=1
Thfi_1358	4,600	-2,355	0,004	0,017	18,07	4,74	8,66	45,57	20,31	93,1	tr|E8PPW7|E8PPW7_THESS N-acetylmuramic acid 6-phosphate etherase OS=Thermus scotoductus
Thfi_1368	3,919	-3,124	0,003	0,014	0	2,49	0	30,96	10,66	19,55	tr|Q53W91|Q53W91_THET8 Uncharacterized protein OS=Thermus thermophilus
Thfi_1370	6,431	0,863	0,007	0,025	240,35	177,66	193,59	113,25	134,04	73,7	tr|K7R242|K7R242_THEOS Uncharacterized protein (Precursor) OS=Thermus oshimai JL-2
Thfi_1372	9,175	0,623	0,020	0,063	679,55	885,25	594,12	490,84	598,21	481,26	tr|H7GF80|H7GF80_9DEIN Ferredoxin--NADP reductase OS=Thermus sp. RL GN=RLTM_03851 PE=3 SV=1
Thfi_1374	10,025	0,545	0,028	0,081	1210,12	934,16	1103,18	638,01	781,36	698,84	tr|A4BB90|A4BB90_9GAMM Putative uncharacterized protein OS=Reinekea blandensis MED297
Thfi_1376	5,736	-1,621	0,032	0,089	55,32	37,66	164,21	503,58	213,56	120,07	tr|G8N862|G8N862_9DEIN Antibiotic biosynthesis monooxygenase OS=Thermus sp. CCB_US3_UF1
Thfi_1378	6,148	-2,501	0,000	0,000	22,87	19,92	14,58	211,64	63,99	78,23	tr|G8N864|G8N864_9DEIN Hemin-binding periplasmic protein hmuT OS=Thermus sp. CCB_US3_UF1
Thfi_1380	5,245	-4,208	0,000	0,000	4,52	1,77	6,47	83,88	37,85	55,52	tr|Q53VW0|Q53VW0_THET8 Hemin ABC transporter, permease protein OS=Thermus thermophilus
Thfi_1381	6,594	-2,536	0,000	0,000	42,7	33,58	26,32	323,19	138,92	188,65	tr|Q745X8|Q745X8_THET2 Transporter OS=Thermus thermophilus
Thfi_1387	4,911	-1,425	0,038	0,099	13,93	6,22	28,46	36,83	29,92	24,38	tr|B7A8Q8|B7A8Q8_THEAQ Putative uncharacterized protein (Precursor) OS=Thermus aquaticus Y51MC23 GN=TaqDRAFT_4011 PE=4 SV=1
Thfi_1394	7,262	-0,979	0,009	0,033	91,85	61,1	118,44	253,75	188,49	211,63	tr|K7QW65|K7QW65_THEOS Uncharacterized protein
Thfi_1396	5,226	-2,017	0,000	0,002	10,29	9,65	5,89	50,84	41,29	63,1	tr|B7A8A3|B7A8A3_THEAQ Putative uncharacterized protein OS=Thermus aquaticus Y51MC23
Thfi_1400	8,850	0,710	0,003	0,014	1363,27	1307,8	1329,98	928,99	893,56	1302,18	tr|G8N8W3|G8N8W3_9DEIN Alkyl hydroperoxide reductase/ Thiol specific antioxidant/ Mal allergen
Thfi_1404	8,126	0,848	0,001	0,004	354,01	343	272,58	217,33	197,28	190,42	tr|Q53VX9|Q53VX9_THET8 Uncharacterized protein OS=Thermus thermophilus
Thfi_1405	6,071	-1,799	0,001	0,007	115,07	149,15	85,54	190,18	736,84	688,66	tr|Q1AV64|Q1AV64_RUBXD Putative uncharacterized protein OS=Rubrobacter xylanophilus
Thfi_1408	6,229	-1,170	0,003	0,015	63,39	72,1	57,26	138,81	262,88	172,95	tr|Q1AV67|Q1AV67_RUBXD Phenylacetic acid catabolic OS=Rubrobacter xylanophilus
Thfi_1411	8,569	-1,450	0,000	0,000	90,37	81,18	112,73	251,86	279,1	314,61	tr|B7A6J1|B7A6J1_THEAQ Helicase superfamily 1 and 2 ATP-binding OS=Thermus aquaticus Y51MC23
Thfi_1417	9,793	-0,717	0,002	0,008	1303,3	1052,07	910,22	1622,27	1707,21	2241,27	tr|E8PM08|E8PM08_THESS Probable transcriptional regulatory protein TSC_c18130
Thfi_1418	8,735	-0,641	0,006	0,025	226,5	169,49	229,32	356,31	408,16	347,6	tr|E8PM07|E8PM07_THESS Glutathione-regulated potassium-efflux system protein KefC
Thfi_1419	7,907	1,076	0,000	0,001	682,01	431,49	810,82	276,42	337,94	291,47	tr|G8N8Z2|G8N8Z2_9DEIN Thiol:disulfide interchange protein dsbA

					FPKM						
Gene code	logCPM	logFC	PValue	FDR	63 degrees			77 degrees			Top Hit Uniprot
Thfi_1424	10,433	1,504	0,000	0,000	6899,02	4764,01	5609,55	1510,27	1947,93	2577,01	tr|F6DG85|F6DG85_THETG Outer membrane chaperone Skp (OmpH) (Precursor)
Thfi_1425	7,187	1,225	0,002	0,008	742,59	556,42	771,51	236,43	383,5	117,03	tr|E8PM01|E8PM01_THESS Uncharacterized protein OS=Thermus scotoductus
Thfi_1427	8,928	-0,525	0,024	0,072	777,09	443,17	454,99	818,79	843,48	817,68	tr|B7A6H6|B7A6H6_THEAQ Prephenate dehydratase OS=Thermus aquaticus Y51MC23
Thfi_1432	5,460	-1,115	0,009	0,033	34,43	29,56	36,03	75,31	79,26	96,87	tr|K7RJV8|K7RJV8_THEOS Mg-dependent DNase OS=Thermus oshimai JL-2 GN=Theos_1654 PE=4 SV=1
Thfi_1433	8,083	0,675	0,008	0,028	467,7	429,34	384,92	303,53	271,44	269,93	tr|G8N8Y1|G8N8Y1_9DEIN Putative uncharacterized protein OS=Thermus sp. CCB_US3_UF1
Thfi_1434	5,452	-1,506	0,001	0,004	38,66	22,23	29,59	66,26	77,92	63,5	tr|H9ZR99|H9ZR99_THETH Uncharacterized protein (Precursor) OS=Thermus thermophilus JL-18
Thfi_1435	8,514	1,180	0,000	0,000	465,36	295,73	398,43	179,13	177,27	119,07	tr|G8N8X9|G8N8X9_9DEIN ABC transporter protein
Thfi_1436	11,207	2,176	0,000	0,000	10782,1	11243,2	12164,7	3074,08	2741,36	2184,06	tr|E8PLZ2|E8PLZ2_THESS Membrane lipoprotein OS=Thermus scotoductus
Thfi_1437	10,804	1,975	0,000	0,000	5873,98	5292,19	5531,5	1486,32	1249,05	1417,72	tr|B7A6I3|B7A6I3_THEAQ Basic membrane lipoprotein
Thfi_1443	7,848	0,620	0,027	0,078	404,08	314,96	309,42	219,94	221,95	332,21	tr|H9ZQS8|H9ZQS8_THETH 3-hydroxyacyl-CoA dehydrogenase
Thfi_1446	8,462	0,697	0,002	0,010	773,44	607,42	621,32	464,46	514,66	438,79	tr|B7A6G0|B7A6G0_THEAQ Ribose-5-phosphate isomerase A
Thfi_1447	10,100	-0,522	0,018	0,057	510,86	425,9	567,23	757,52	688,21	897,59	tr|F6DI12|F6DI12_THETG Methionine--tRNA ligase OS=Thermus thermophilus
Thfi_1448	8,503	-1,370	0,000	0,000	1677,33	691,65	1001,09	2054,11	2293,8	2564,59	tr|Q72J49|Q72J49_THET2 Uncharacterized protein OS=Thermus thermophilus
Thfi_1449	12,314	-0,553	0,016	0,053	2405,58	3143,39	2726,61	5133,24	4288,09	6445,94	tr|E8PLY1|E8PLY1_THESS Carboxyl-protease OS=Thermus scotoductus
Thfi_1450	8,567	0,838	0,003	0,014	976,32	845,03	767,47	417,93	473,82	550,8	tr|H9ZQP7|H9ZQP7_THETH Cell division ATP-binding protein FtsE OS=Thermus thermophilus JL-18 GN=TtJL18_0754 PE=3 SV=1
Thfi_1451	10,725	1,349	0,000	0,000	6306,47	6082,76	5081,18	2260,04	2120,09	2333,69	tr|B7A6F1|B7A6F1_THEAQ Sigma 54 modulation protein/ribosomal protein S30EA
Thfi_1453	9,531	1,142	0,000	0,000	861,98	713,84	864,67	323,17	408,38	341,34	tr|F6DHQ7|F6DHQ7_THETG 4-alpha-glucanotransferase OS=Thermus thermophilus
Thfi_1457	9,355	0,821	0,002	0,010	706,06	1287,28	1627,88	619,29	1006,24	1086,29	tr|R6S6T5|R6S6T5_9BACE TPR-domain containing protein OS=Bacteroides finegoldii CAG:203
Thfi_1459	5,851	-1,182	0,013	0,043	140,95	141,21	383,95	492,81	622,54	472,27	tr|F6DF67|F6DF67_THETG Preprotein translocase, SecG subunit OS=Thermus thermophilus
Thfi_1460	7,498	-1,019	0,002	0,010	153,73	108,3	119,66	233,35	407,11	272,91	tr|G8NC94|G8NC94_9DEIN Ornithine carbamoyltransferase OS=Thermus sp. CCB_US3_UF1
Thfi_1463	7,481	-1,020	0,001	0,005	94,3	117,55	68,89	162,74	271,54	307,41	tr|E8PKJ6|E8PKJ6_THESS Arginine biosynthesis bifunctional protein ArgJ
Thfi_1464	9,722	1,179	0,000	0,003	5770,26	2909,18	4444,09	1330,03	1844,76	1266,99	tr|K7QZG3|K7QZG3_THEOS Uncharacterized protein (Precursor)
Thfi_1466	7,108	-0,937	0,004	0,016	382,18	371,05	437,63	987,97	1057,03	1112,58	tr|Q72JE0|Q72JE0_THET2 Uncharacterized protein OS=Thermus thermophilus (strain HB27 / ATCC BAA-163 / DSM 7039) GN=TT_C0832 PE=4 SV=1
Thfi_1470	8,501	-2,866	0,000	0,000	117,25	59,26	112,18	961,12	757,32	658,18	tr|F6DG56|F6DG56_THETG Diguanylate cyclase OS=Thermus thermophilus

					FPKM						
Gene code	logCPM	logFC	PValue	FDR	63 degrees			77 degrees			Top Hit Uniprot
Thfi_1478	8,498	-0,928	0,001	0,003	147,15	139,74	143,07	261,5	329,21	213,15	tr|K7RIN4|K7RIN4_THEOS Membrane carboxypeptidase (Penicillin-binding protein) (Precursor)
Thfi_1481	8,978	-3,751	0,000	0,000	59,87	51,83	67,35	949,46	987,29	1062,73	tr|E8PMZ6|E8PMZ6_THESS Prephenate dehydrogenase OS=Thermus scotoductus
Thfi_1485	5,800	0,828	0,030	0,084	195,95	63,74	104,55	69,63	28,27	34,55	tr|K7QV18|K7QV18_THEOS Pseudouridine-5'-phosphate glycosidase (Precursor)
Thfi_1486	6,331	0,849	0,006	0,022	189,44	101,29	134,06	80,45	64,66	67,75	tr|K7QZE3|K7QZE3_THEOS Uncharacterized protein OS=Thermus oshimai JL-2 GN=Theos_1193 PE=4 SV=1
Thfi_1487	9,464	-0,671	0,002	0,009	777,3	384,15	469,18	746,59	733,74	801,04	tr|K7R5M3|K7R5M3_THEOS Ribosomal protein S12 methylthiotransferase RimO
Thfi_1488	9,256	-1,045	0,000	0,000	310,55	280,49	305,42	687,7	658,81	757,16	tr|E8PK93|E8PK93_THESS Potassium transporter peripheral membrane component
Thfi_1489	7,704	-0,896	0,002	0,009	92,2	74,2	105,27	210,4	204,52	168,81	tr|G8NCB9|G8NCB9_9DEIN Trk system potassium uptake protein OS=Thermus sp. CCB_US3_UF1
Thfi_1490	9,823	0,957	0,000	0,000	588,68	446,13	546,32	246,97	286,32	306,41	tr|E8PK91|E8PK91_THESS Phosphorylase OS=Thermus scotoductus (strain ATCC 700910 / SA-01)
Thfi_1491	9,898	1,374	0,000	0,000	1997,56	1995,92	1838,5	952,46	852,18	655,78	tr|B7A9Q3|B7A9Q3_THEAQ Extracellular solute-binding protein family 3 (Precursor) OS=Thermus aquaticus
Thfi_1492	9,627	-3,923	0,000	0,000	95,96	96,02	70,32	1603,06	1666,5	1726,76	tr|Q5SK52|Q5SK52_THET8 Phospho-2-dehydro-3-deoxyheptonate aldolase OS=Thermus thermophilus
Thfi_1493	7,720	0,996	0,000	0,001	310,17	326,76	363,79	225,17	172,66	242,07	tr|B7A9Q2|B7A9Q2_THEAQ Polar amino acid ABC transporter, inner membrane subunit
Thfi_1494	9,638	2,050	0,000	0,000	1430,48	1624,03	1521,78	425,95	332,83	396,7	tr|H9ZR39|H9ZR39_THETH TRAP transporter solute receptor, TAXI family (Precursor)
Thfi_1496	7,183	-0,869	0,009	0,031	125,36	106,29	148,08	272,35	249,81	398,23	tr|K7R4P8|K7R4P8_THEOS ABC-type polar amino acid transport system, ATPase component
Thfi_1498	11,020	2,975	0,000	0,000	8825,15	3798,62	3320,76	365,11	463,34	452,49	tr|F6DDV3|F6DDV3_THETG Transposase OS=Thermus thermophilus (strain SG0.5JP17-16)
Thfi_1507	11,154	-1,067	0,000	0,000	1561,37	1559,69	1232,48	3836,3	3070,58	3458,92	tr|Q72K76|Q72K76_THET2 Mrp protein
Thfi_1508	7,958	-0,905	0,000	0,003	387,79	267,58	410,25	709,42	611,26	703,39	tr|B7A9N7|B7A9N7_THEAQ Transcriptional regulator, TrmB OS=Thermus aquaticus Y51MC23
Thfi_1509	7,712	-1,001	0,005	0,019	213,49	158,31	228,13	594,79	298,41	282,98	
Thfi_1511	7,254	0,689	0,026	0,076	149,85	129,08	169,29	124,12	66,8	95,89	tr|B7A7X1|B7A7X1_THEAQ Peptidase U62 modulator of DNA gyrase OS=Thermus aquaticus Y51MC23
Thfi_1514	12,566	0,501	0,029	0,083	13415,8	21557,5	19028,3	19433	17773,1	12950,2	tr|B7A7V2|B7A7V2_THEAQ Putative uncharacterized protein (Precursor) OS=Thermus aquaticus Y51MC23
Thfi_1517	8,903	1,618	0,000	0,000	984,28	685,38	986,18	288	309,21	400,2	tr|G8NC60|G8NC60_9DEIN Succinyl-CoA ligase [ADP-forming] subunit alpha
Thfi_1518	10,311	0,865	0,001	0,003	1630,85	1773,68	1372,26	952,76	963,68	818,56	tr|H9ZSV6|H9ZSV6_THETH Succinyl-CoA ligase [ADP-forming] subunit beta
Thfi_1519	8,875	-0,988	0,000	0,000	421,01	311,36	346,66	773,42	701,61	686,19	tr|E8PNF8|E8PNF8_THESS Pin/tram domain protein OS=Thermus scotoductus
Thfi_1520	8,684	-1,336	0,000	0,000	184,47	207,42	206,78	606,37	358,95	641,75	tr|E8PNF9|E8PNF9_THESS DNA repair protein radA OS=Thermus scotoductus
Thfi_1521	12,960	-0,602	0,005	0,019	2838,39	2812,04	3003,78	5810,86	4372,79	4863,89	tr|B7A9W8|B7A9W8_THEAQ ATPase AAA-2 domain protein OS=Thermus aquaticus Y51MC23 GN=TaqDRAFT_3595 PE=4 SV=1

					FPKM						
Gene code	logCPM	logFC	PValue	FDR	63 degrees			77 degrees			Top Hit Uniprot
Thfi_1523	9,164	0,784	0,001	0,004	651,07	613,82	936,39	499,45	559,25	387,27	tr|H7GFF6|H7GFF6_9DEIN Aspartate-semialdehyde dehydrogenase OS=Thermus sp. RL GN=asd PE=3 SV=1
Thfi_1525	12,719	0,485	0,036	0,096	20782	17977,4	18422,1	14537,4	14794	11566,4	tr|F6DG60|F6DG60_THETG YceI family protein OS=Thermus thermophilus
Thfi_1527	4,975	-1,674	0,001	0,006	41,88	33,57	34,96	115,08	114,08	113,94	tr|K7R4L5|K7R4L5_THEOS Uncharacterized protein (Precursor)
Thfi_1528	7,209	0,934	0,003	0,014	146,65	192,06	172,33	102,13	120,95	162,65	tr|K7RJU5|K7RJU5_THEOS Fructose-1,6-bisphosphatase OS=Thermus oshimai JL-2 GN=Theos_1644 PE=3 SV=1
Thfi_1540	8,471	0,690	0,003	0,012	400,12	343,13	523,58	286,78	316,72	250,81	tr|E8PLP8|E8PLP8_THESS Putative lipoprotein OS=Thermus scotoductus
Thfi_1542	5,431	-1,039	0,024	0,071	16,07	26,96	13,16	50,75	69,24	42,33	tr|E8PLQ0|E8PLQ0_THESS ABC transporter, permease protein OS=Thermus scotoductus
Thfi_1543	9,184	0,956	0,000	0,000	326,76	495,32	393,12	297,69	266,81	268,52	tr|E8PLQ1|E8PLQ1_THESS Dipeptide-binding protein OS=Thermus scotoductus
Thfi_1547	7,875	1,736	0,000	0,000	215,16	338,8	393,13	138,05	114,95	116,29	tr|B7AA14|B7AA14_THEAQ TRAP transporter solute receptor, TAXI family
Thfi_1548	7,538	0,758	0,004	0,018	193,64	225,61	201,28	175,68	170,5	119,11	tr|B7A5T0|B7A5T0_THEAQ Inner-membrane translocator (Precursor) OS=Thermus aquaticus Y51MC23
Thfi_1549	11,379	1,647	0,000	0,000	2801,9	3590,72	3313,58	1215,61	1483,16	1136,39	tr|K7QW00|K7QW00_THEOS ABC-type branched-chain amino acid transport system, periplasmic component
Thfi_1551	9,949	1,789	0,000	0,000	960,08	947,3	1129,2	322	265,78	314	tr|B7AA05|B7AA05_THEAQ 5'-Nucleotidase domain protein
Thfi_1554	6,145	-0,859	0,031	0,087	34,2	37,08	27,17	88,68	66,6	69,79	tr|F6DI40|F6DI40_THETG Sulfite oxidase (Precursor) OS=Thermus thermophilus
Thfi_1563	7,860	-0,798	0,002	0,011	240,82	182,38	200,18	430,87	386,15	448,09	tr|F2NPD8|F2NPD8_MARHT Uncharacterized protein OS=Marinithermus hydrothermalis
Thfi_1568	8,961	0,814	0,000	0,001	1146,14	796,63	861,18	551,92	601,84	467,54	tr|B7A7U4|B7A7U4_THEAQ 5-oxopent-3-ene-1,2,5-tricarboxylate decarboxylase
Thfi_1569	8,414	-1,168	0,000	0,000	151,98	127,55	162,99	383,17	513,74	418,76	tr|K7QVE3|K7QVE3_THEOS Argininosuccinate synthase OS=Thermus oshimai JL-2 GN=argG PE=3 SV=1
Thfi_1570	7,912	0,757	0,005	0,019	224,62	316,58	284,68	234,27	166,47	232,59	tr|E8PLS2|E8PLS2_THESS Immunogenic protein OS=Thermus scotoductus
Thfi_1571	8,231	0,995	0,000	0,000	660,62	415,87	451,23	238,69	308,96	246,31	tr|Q72KR0|Q72KR0_THET2 Metallo-beta-lactamase protein OS=Thermus thermophilus
Thfi_1577	7,902	0,824	0,003	0,013	131,64	127,48	229,83	91,8	142,78	106,4	tr|F6DG77|F6DG77_THETG Putative sodium symporter protein OS=Thermus thermophilus
Thfi_1580	8,342	-1,066	0,000	0,000	52,83	71,01	82,65	144,38	235,89	192,34	tr|E8PN20|E8PN20_THESS Acetyl-coenzyme A synthetase OS=Thermus scotoductus
Thfi_1582	9,358	0,676	0,004	0,017	429,54	328,36	482,92	233,39	328,52	313,52	tr|H9ZQU3|H9ZQU3_THETH Acetyl-coenzyme A synthetase
Thfi_1583	6,982	0,872	0,017	0,055	552,58	473,33	425,75	229,7	338,03	486,07	tr|H9ZQU4|H9ZQU4_THETH Protein with protein kinase II-like association domain OS=Thermus thermophilus JL-18 GN=TtJL18_0801 PE=4 SV=1
Thfi_1591	7,366	-1,105	0,000	0,001	153,16	124,51	117,83	354,52	266,83	236,19	tr|E8PN30|E8PN30_THESS Spermidine/putrescine transport system permease protein PotB
Thfi_1593	6,825	-1,704	0,000	0,000	67,38	57,82	70,5	226,41	222,21	360,02	tr|E8PN31|E8PN31_THESS Spermidine/putrescine ABC transporter, permease protein OS=Thermus scotoductus
Thfi_1594	8,490	0,454	0,039	0,102	420,74	395,09	462,67	375,91	354,27	265,45	tr|B7A7R9|B7A7R9_THEAQ Extracellular solute-binding protein family 1 (Precursor) OS=Thermus aquaticus Y51MC23

					FPKM						
Gene code	logCPM	logFC	PValue	FDR	63 degrees			77 degrees			Top Hit Uniprot
Thfi_1599	9,251	-0,790	0,001	0,005	745,17	871,63	832,37	1862,27	2060,01	1480,77	tr|Q5SIY3|Q5SIY3_THET8 Uncharacterized protein OS=Thermus thermophilus
Thfi_1600	9,938	-0,931	0,000	0,001	662,81	762,96	524,23	1474,89	1546,93	1301,92	tr|H9ZQW0|H9ZQW0_THETH 3-isopropylmalate dehydrogenase
Thfi_1601	8,202	-0,849	0,001	0,003	425,43	388,1	281,21	768,7	717,48	859,76	tr|H7GEM6|H7GEM6_9DEIN 3-isopropylmalate dehydratase small subunit
Thfi_1602	11,335	-1,084	0,000	0,000	897,53	1103,42	1008,63	3239,19	2432,4	2804,36	tr|E8PN40|E8PN40_THESS 3-isopropylmalate dehydratase large subunit OS=Thermus scotoductus
Thfi_1603	7,572	0,680	0,009	0,031	295,83	176,74	272,23	177,16	141,36	103,7	tr|H9ZQN0|H9ZQN0_THETH UDP-N-acetylmuramyl pentapeptide phosphotransferase/UDP-N-acetylglucosamine-1-phosphate transferase
Thfi_1604	9,155	-1,355	0,000	0,000	330,12	288,15	308,82	914,82	992,77	827,53	tr|E8PN43|E8PN43_THESS Tryptophan--tRNA ligase OS=Thermus scotoductus
Thfi_1605	6,548	-1,497	0,000	0,000	114,57	75,89	64,01	221,89	213,26	344,9	tr|E8PN44|E8PN44_THESS Uncharacterized protein OS=Thermus scotoductus (strain ATCC 700910 / SA-01) GN=TSC_c07690 PE=4 SV=1
Thfi_1606	9,234	0,502	0,048	0,121	506,37	628,37	704,88	464,75	478,98	507,03	tr|E8PN49|E8PN49_THESS Acetyl-CoA acyltransferase OS=Thermus scotoductus
Thfi_1608	10,032	0,911	0,000	0,000	886,64	620,57	648,42	364,52	446,2	379,33	tr|Q5SKT2|Q5SKT2_THET8 Outer membrane protein OS=Thermus thermophilus
Thfi_1609	6,059	0,959	0,019	0,061	527,79	206,81	215,3	123,84	106,53	234,05	tr|F6DEV9|F6DEV9_THETG Surface antigen (D15) (Precursor) OS=Thermus thermophilus
Thfi_1610	8,724	0,771	0,001	0,005	922,66	542,58	875,77	423,13	527,9	394,32	tr|H9ZST1|H9ZST1_THETH Purine nucleoside phosphorylase OS=Thermus thermophilus JL-18
Thfi_1612	7,977	0,761	0,009	0,031	450,51	526,55	823,14	462,13	423,86	693,81	tr|E8PN56|E8PN56_THESS Cell division initiation protein DivIVA OS=Thermus scotoductus
Thfi_1617	5,853	-1,307	0,002	0,009	89,93	148,42	168,32	322,16	467,53	741,72	tr|F6DEW5|F6DEW5_THETG Acylphosphatase OS=Thermus thermophilus
Thfi_1619	7,684	0,935	0,002	0,009	266,4	292,49	256,53	148,36	153,69	178,73	tr|H7GFH7|H7GFH7_9DEIN L-threonine 3-dehydrogenase OS=Thermus sp. RL GN=tdh PE=3 SV=1
Thfi_1623	7,122	-0,706	0,035	0,093	501,46	305,69	278,27	731,51	414,06	562,96	tr|G8NBX3|G8NBX3_9DEIN Putative uncharacterized protein OS=Thermus sp. CCB_US3_UF1
Thfi_1625	6,327	1,298	0,004	0,018	99,86	126,96	211,12	62,71	54,45	90,75	tr|K7RGA5|K7RGA5_THEOS Phosphotransferase family protein (Precursor)
Thfi_1627	13,007	0,973	0,000	0,000	4058,38	9372,49	8082,4	4745,38	6827,5	6078,57	tr|K7RHG9|K7RHG9_THEOS Uncharacterized protein (Precursor)
Thfi_1632	6,158	-1,807	0,000	0,000	24,37	38,18	20,97	127,28	89,93	179,9	tr|F6DIS5|F6DIS5_THETG Uncharacterized protein OS=Thermus thermophilus (strain SG0.5JP17-16)
Thfi_1634	6,905	1,011	0,006	0,023	648,86	571,69	727,27	238,62	467,05	455,3	tr|G8N7Q8|G8N7Q8_9DEIN UPF0145 protein TCCBUS3UF1_1260
Thfi_1635	6,275	1,298	0,020	0,062	148,2	107,77	76,58	16,34	61,93	75,72	tr|B4D042|B4D042_9BACT Beta-lactamase OS=Chthoniobacter flavus Ellin428
Thfi_1642	9,486	1,578	0,000	0,000	562,08	675,99	521,25	178,08	231,09	258,03	tr|Q745W6|Q745W6_THET2 Uncharacterized protein OS=Thermus thermophilus
Thfi_1644	4,189	-3,347	0,003	0,012	9,21	2,87	0	4,86	18,43	78,87	tr|U2BT87|U2BT87_9BACE Collagen triple helix repeat protein (Fragment)
Thfi_1645	4,935	-2,930	0,000	0,001	22,91	7,73	0	46,74	77,46	121,72	
Thfi_1649	8,724	-1,291	0,000	0,000	132,43	118,5	144,75	420,86	588,07	429,45	tr|H7GDL4|H7GDL4_9DEIN Argininosuccinate lyase OS=Thermus sp. RL GN=argH PE=3 SV=1

					FPKM						
Gene code	logCPM	logFC	PValue	FDR	63 degrees			77 degrees			Top Hit Uniprot
Thfi_1650	5,815	-1,640	0,001	0,007	29,97	23,52	39,13	125,77	87,07	50,41	tr|Q5SMF1|Q5SMF1_THET8 Uncharacterized protein OS=Thermus thermophilus
Thfi_1651	8,321	-1,713	0,000	0,000	376,6	313,21	337,87	1331,82	835,43	1151,64	tr|K7QW23|K7QW23_THEOS Molybdopterin-guanine dinucleotide biosynthesis protein A
Thfi_1652	13,371	-0,447	0,038	0,101	3167,5	3040,55	3654,12	6281,41	4985,86	5735,84	tr|G8N996|G8N996_9DEIN Lon protease OS=Thermus sp. CCB_US3_UF1 GN=lon PE=3 SV=1
Thfi_1653	6,258	0,811	0,049	0,123	180,6	143,74	326,07	123,87	125,63	153,44	tr|G8N995|G8N995_9DEIN Putative uncharacterized protein OS=Thermus sp. CCB_US3_UF1
Thfi_1657	6,269	-0,982	0,034	0,092	100,52	40,42	59,17	148,51	90,91	95,26	tr|G8N991|G8N991_9DEIN Aspartate carbamoyltransferase OS=Thermus sp. CCB_US3_UF1 GN=pyrB PE=3 SV=1
Thfi_1659	10,307	-1,153	0,000	0,000	5619,89	2295,66	3281,3	9298,76	6566,68	6650,5	tr|E8PM24|E8PM24_THESS SPW repeat protein
Thfi_1664	7,423	-1,524	0,000	0,000	90,47	54,93	52,52	161,49	196,42	224,6	tr|K7QWI4|K7QWI4_THEOS Integral membrane protein MviN (Precursor)
Thfi_1668	9,494	0,557	0,023	0,071	860,35	1493,81	1354,75	949,79	1057,47	1247,68	tr|F6DHS7|F6DHS7_THETG UPF0173 metal-dependent hydrolase Ththe16_1295
Thfi_1673	8,076	1,018	0,000	0,000	3856	1488,86	1465,93	819,6	863,29	876,5	tr|K7QYU4|K7QYU4_THEOS Uncharacterized protein OS=Thermus oshimai JL-2 GN=Theos_0815 PE=4 SV=1
Thfi_1674	10,218	1,098	0,000	0,000	1131,89	871,31	926,41	456,23	441,98	398,41	tr|H9ZQR4|H9ZQR4_THETH Archaeal/vacuolar-type H+-ATPase subunit I OS=Thermus thermophilus JL-18 GN=TtJL18_0771 PE=4 SV=1
Thfi_1676	7,294	2,552	0,000	0,000	394,08	354,9	692,83	87,91	105,92	138,64	tr|H7GGU9|H7GGU9_9DEIN V-type proton ATPase subunit E OS=Thermus sp. RL GN=atpE PE=3 SV=1
Thfi_1677	8,720	2,005	0,000	0,000	854,83	673,66	914,12	225,35	223,86	136,83	tr|G8N8E1|G8N8E1_9DEIN V-type ATP synthase subunit C OS=Thermus sp. CCB_US3_UF1 GN=atpC PE=3 SV=1
Thfi_1678	5,601	1,843	0,001	0,004	508,57	335,87	233,77	115,2	46,71	56,91	tr|K7QYU6|K7QYU6_THEOS Archaeal/vacuolar-type H+-ATPase subunit F (Precursor) OS=Thermus oshimai JL-2 GN=Theos_0820 PE=4 SV=1
Thfi_1679	11,428	1,672	0,000	0,000	2078,11	2390,75	2265,83	839,72	952,54	755,59	tr|F6DHR7|F6DHR7_THETG V-type ATP synthase alpha chain OS=Thermus thermophilus
Thfi_1680	10,519	1,353	0,000	0,000	897,48	1410,61	1089,77	641,23	706,16	606,7	tr|E8PNV8|E8PNV8_THESS V-type ATP synthase beta chain OS=Thermus scotoductus
Thfi_1681	9,411	1,649	0,000	0,000	1478,36	1760,15	1728,27	586,18	746,39	482,86	tr|G8N8D7|G8N8D7_9DEIN V-type ATP synthase subunit D OS=Thermus sp. CCB_US3_UF1 GN=atpD PE=3 SV=1
Thfi_1683	7,065	0,640	0,047	0,119	140,94	145,28	181,79	122,58	94,49	158,83	tr|K7RIW9|K7RIW9_THEOS Pectinacetylesterase (Precursor) OS=Thermus oshimai JL-2 GN=Theos_1287
Thfi_1689	7,647	-0,722	0,004	0,018	169,68	175,29	141,86	279,35	276,52	333,22	tr|G8N9D0|G8N9D0_9DEIN Putative uncharacterized protein OS=Thermus sp. CCB_US3_UF1
Thfi_1692	9,574	0,483	0,027	0,078	442,05	433,16	468,93	426,7	344,69	358,18	tr|E8PMF0|E8PMF0_THESS Aldehyde:ferredoxin oxidoreductase OS=Thermus scotoductus
Thfi_1699	8,499	0,620	0,037	0,097	1317,6	1171,64	935,72	555,95	895,38	1014,46	tr|G8NC74|G8NC74_9DEIN Translation initiation factor IF-3 OS=Thermus sp. CCB_US3_UF1 GN=infC PE=3 SV=1
Thfi_1703	8,525	-0,825	0,007	0,026	145,65	124,96	155,28	407,93	291,68	199,08	tr|E8PNI4|E8PNI4_THESS Hypothetical membrane spanning protein OS=Thermus scotoductus
Thfi_1704	10,916	1,050	0,000	0,000	1368,43	1720,74	1561,18	772,9	1065,55	775,08	tr|G8NBH4|G8NBH4_9DEIN Formate--tetrahydrofolate ligase OS=Thermus sp. CCB_US3_UF1 GN=fhs
Thfi_1705	6,524	-1,425	0,002	0,008	63,82	65,25	119,24	323,11	159,36	163,57	tr|F6DEV2|F6DEV2_THETG Futalosine nucleosidase OS=Thermus thermophilus (strain SG0.5JP17-16)
Thfi_1706	11,848	-0,685	0,002	0,011	4595,28	5031,74	5281,97	11374,7	8005,15	8622,87	tr|H9ZST6|H9ZST6_THETH Superoxide dismutase OS=Thermus thermophilus JL-18 GN=TtJL18_1518

					FPKM						
Gene code	logCPM	logFC	PValue	FDR	63 degrees			77 degrees			Top Hit Uniprot
Thfi_1707	9,234	0,700	0,001	0,007	569,63	490,83	529,85	337,42	401,08	387,71	tr|Q5SKT5|Q5SKT5_THET8 Fumarate hydratase class II OS=Thermus thermophilus
Thfi_1709	6,668	-0,701	0,022	0,066	96,82	73,94	76,35	115,69	162,38	178,66	tr|E8PNI9|E8PNI9_THESS Thioredoxin reductase OS=Thermus scotoductus
Thfi_1710	10,653	-3,125	0,000	0,000	216,4	169,36	190,45	1895,74	1978,75	1912,52	tr|Q5SJ01|Q5SJ01_THET8 Acetolactate synthase OS=Thermus thermophilus
Thfi_1711	8,584	-3,481	0,000	0,000	87,86	120,43	141,77	1526,29	1901,17	1841,28	tr|E8PNJ1|E8PNJ1_THESS Acetolactate synthase, small subunit OS=Thermus scotoductus
Thfi_1712	9,020	-2,160	0,000	0,000	170,57	177,97	156,39	850,32	1005,66	1061,8	tr|F6DHK9|F6DHK9_THETG Ketol-acid reductoisomerase OS=Thermus thermophilus
Thfi_1713	10,806	-2,309	0,000	0,000	394,4	360,25	311,43	1928,64	2390,49	2219,04	tr|H9ZQY3|H9ZQY3_THETH 2-isopropylmalate synthase OS=Thermus thermophilus JL-18 GN=leuA PE=3 SV=1
Thfi_1714	9,882	-2,310	0,000	0,000	186,11	192,38	182,37	1093,62	1234,86	996,13	tr|K7QX64|K7QX64_THEOS 2-isopropylmalate synthase/homocitrate synthase family protein
Thfi_1716	7,541	-1,599	0,000	0,000	181,76	159,79	208,28	645,35	721,58	570,88	tr|H9ZQY6|H9ZQY6_THETH Uncharacterized protein OS=Thermus thermophilus JL-18 GN=TtJL18_0844
Thfi_1717	7,324	-3,526	0,000	0,000	39,82	31,32	52,87	480,11	387,58	416,86	tr|Q72JD2|Q72JD2_THET2 Integral membrane protein OS=Thermus thermophilus
Thfi_1719	6,673	-0,681	0,029	0,083	153,15	108,41	105,75	139,12	217,04	227,38	tr|D3PQ25|D3PQ25_MEIRD Uncharacterized protein OS=Meiothermus ruber
Thfi_1729	4,706	-2,229	0,001	0,005	37,85	30,96	28,12	196,42	84,47	185,18	tr|Q72HJ7|Q72HJ7_THET2 Initial dioxygenase ferredoxin subunit OS=Thermus thermophilus
Thfi_1730	10,680	-0,962	0,007	0,025	668,89	619,99	630,46	2844,41	1433,18	1349,1	tr|K7R2R8|K7R2R8_THEOS FeS assembly protein SufD OS=Thermus oshimai JL-2 GN=Theos_0111 PE=4 SV=1
Thfi_1731	12,269	-0,915	0,010	0,036	2106,56	1971,64	1788,03	8270,73	3354,57	3824,13	tr|B7A612|B7A612_THEAQ FeS assembly protein SufB OS=Thermus aquaticus Y51MC23
Thfi_1735	6,091	-0,717	0,038	0,101	92,29	55,38	54,57	113,24	86,73	117,18	tr|B7A593|B7A593_THEAQ Putative uncharacterized protein (Precursor) OS=Thermus aquaticus Y51MC23
Thfi_1741	8,063	-0,599	0,041	0,107	119,35	105,2	152,43	252,31	250,89	220,51	tr|B7A5A7|B7A5A7_THEAQ Alpha amylase catalytic region OS=Thermus aquaticus Y51MC23
Thfi_1742	8,158	0,687	0,005	0,019	736,69	570,28	679,46	373	526,45	390,83	tr|G8N9Z1|G8N9Z1_9DEIN Guanylate kinase OS=Thermus sp. CCB_US3_UF1 GN=gmk PE=3 SV=1
Thfi_1743	5,649	1,207	0,011	0,039	378	271,16	301,05	95,51	229,99	0	tr|B7A5A9|B7A5A9_THEAQ DNA-directed RNA polymerase subunit omega OS=Thermus aquaticus Y51MC23
Thfi_1745	8,196	0,961	0,000	0,001	819,58	1048,9	1005,47	583,19	634,91	465,11	tr|E8PP68|E8PP68_THESS Arginine repressor OS=Thermus scotoductus
Thfi_1748	8,833	0,605	0,019	0,061	636,23	432,83	614,1	292,36	407,41	370,61	tr|E8PP66|E8PP66_THESS Ggdef domain protein OS=Thermus scotoductus
Thfi_1752	6,313	-0,933	0,033	0,090	35,14	23,48	62,13	63,23	91,98	92,02	tr|B7A5N2|B7A5N2_THEAQ RNA methylase, NOL1/NOP2/sun family OS=Thermus aquaticus Y51MC23
Thfi_1757	7,932	-1,084	0,000	0,000	307,73	152,52	158,55	438,3	366,89	340,08	tr|G8N9X7|G8N9X7_9DEIN Dimethylallyltranstransferase OS=Thermus sp. CCB_US3_UF1
Thfi_1758	9,287	1,153	0,000	0,000	456,76	551,71	772,99	382,71	286,49	402,46	tr|G8N9X8|G8N9X8_9DEIN Glutamate dehydrogenase OS=Thermus sp. CCB_US3_UF1
Thfi_1759	9,980	1,113	0,000	0,000	1212,14	1050,34	1115,62	529,3	453,83	788,55	tr|E8PP83|E8PP83_THESS Glutamate dehydrogenase OS=Thermus scotoductus
Thfi_1761	7,737	1,237	0,000	0,000	475,09	335,91	402,36	174,94	165,73	127,95	tr|E8PP81|E8PP81_THESS D-isomer specific 2-hydroxyacid dehydrogenase NAD-binding protein OS=Thermus scotoductus (strain ATCC 700910 / SA-01)

					FPKM						
Gene code	logCPM	logFC	PValue	FDR	63 degrees			77 degrees			Top Hit Uniprot
Thfi_1763	10,988	-0,654	0,005	0,020	1940,58	1528,62	2033,03	2913,38	2855,5	2771,24	tr|E8PP79|E8PP79_THESS Deoxyhypusine synthase-like protein OS=Thermus scotoductus
Thfi_1764	6,890	-1,818	0,000	0,000	203,65	99,3	120,83	368,27	483,31	377,45	tr|B7AA71|B7AA71_THEAQ Transposase IS4 family protein OS=Thermus aquaticus Y51MC23
Thfi_1767	8,803	2,292	0,000	0,000	3501,47	2829,24	2590,17	341,18	901,03	639,6	tr|B7A609|B7A609_THEAQ Putative uncharacterized protein (Precursor) OS=Thermus aquaticus Y51MC23
Thfi_1768	6,563	0,929	0,014	0,048	271,58	200,1	198,52	100,51	122,82	135,08	tr|D7BJ44|D7BJ44_MEISD Uncharacterized protein OS=Meiothermus silvanus
Thfi_1769	6,231	0,966	0,038	0,101	240,97	279,99	106,7	128,64	117,24	132,15	tr|G8N7R9|G8N7R9_9DEIN Chromosome partitioning protein parB
Thfi_1772	6,361	-0,860	0,043	0,111	111,29	103,12	47,14	81,79	215,79	243,44	tr|A6MN83|A6MN83_9DEIN Tyrosine recombinase XerC OS=Thermus sp. 4C GN=int PE=3 SV=1
Thfi_1776	8,976	0,835	0,000	0,003	930,27	876,57	1153,51	852,43	639,14	579,68	tr|K7QXZ2|K7QXZ2_THEOS 30S ribosomal protein S4 OS=Thermus oshimai JL-2 GN=rpsD PE=3 SV=1
Thfi_1777	8,793	0,467	0,047	0,119	1498,24	1510,6	1425,2	1541,03	1087,46	1312,25	tr|E8PP97|E8PP97_THESS 30S ribosomal protein S11 OS=Thermus scotoductus
Thfi_1778	7,736	0,916	0,000	0,002	993,1	812,66	910,24	547,17	628,57	315,76	tr|E8PP98|E8PP98_THESS 30S ribosomal protein S13 OS=Thermus scotoductus
Thfi_1782	8,708	1,167	0,000	0,001	703,96	643,62	1342,85	651,53	555,88	530,23	tr|F6DEN1|F6DEN1_THETG Adenylate kinase OS=Thermus thermophilus
Thfi_1784	8,373	0,748	0,004	0,016	755,51	844,65	895,82	791,38	753,61	374,91	tr|E8PPA3|E8PPA3_THESS 50S ribosomal protein L15 OS=Thermus scotoductus
Thfi_1786	7,412	0,798	0,005	0,019	414,13	284,94	387,68	192,67	286,7	238,86	tr|H9ZPN7|H9ZPN7_THETH Redox-sensing transcriptional repressor rex
Thfi_1787	6,937	1,754	0,000	0,002	135,94	178,08	522,69	222,96	103,16	137,42	tr|F6DEN5|F6DEN5_THETG 30S ribosomal protein S5 OS=Thermus thermophilus
Thfi_1799	8,623	0,620	0,009	0,032	460,12	522,8	710,85	544,83	490,63	516,9	tr|K7R3A3|K7R3A3_THEOS 30S ribosomal protein S3 OS=Thermus oshimai JL-2 GN=rpsC PE=3 SV=1
Thfi_1807	8,272	0,990	0,000	0,001	278,61	249,2	283,22	180,32	176,58	156,71	tr|B7A589|B7A589_THEAQ Tetratricopeptide TPR_2 repeat protein (Precursor) OS=Thermus aquaticus Y51MC23
Thfi_1809	7,398	-0,599	0,027	0,079	171,72	165,51	169,57	294,62	222,33	346,93	tr|B7A586|B7A586_THEAQ Putative uncharacterized protein (Precursor)
Thfi_1811	8,795	1,059	0,000	0,000	2362,34	1937,75	1982,04	1293,65	1062,41	1033,19	tr|B7A584|B7A584_THEAQ 50S ribosomal protein L17 OS=Thermus aquaticus Y51MC23 GN=rplQ PE=3 SV=1
Thfi_1819	5,684	-1,978	0,000	0,002	12,98	12,21	22,35	85,17	104,69	63,98	tr|H7GHB0|H7GHB0_9DEIN Transposase OS=Thermus sp. RL GN=RLTM_08204 PE=4 SV=1
Thfi_1821	8,053	-0,883	0,001	0,004	402,7	436,36	540,63	886,81	897,07	943,67	tr|H9ZRP9|H9ZRP9_THETH Uncharacterized protein OS=Thermus thermophilus JL-18 GN=TtJL18_0228
Thfi_1823	5,662	-0,887	0,048	0,121	86,1	60,87	55,54	147,26	131,2	120,19	tr|B7A8G0|B7A8G0_THEAQ Putative transcriptional regulator OS=Thermus aquaticus Y51MC23 GN=TaqDRAFT_3913 PE=4 SV=1
Thfi_1827	5,390	-1,620	0,006	0,022	269,41	112,8	0	394,14	525,77	302,11	tr|D3PMY8|D3PMY8_MEIRD Uncharacterized protein OS=Meiothermus ruber
Thfi_1828	9,662	-0,901	0,000	0,001	700,66	451,55	656,23	1242,25	1207,12	1089,58	tr|E8PQM4|E8PQM4_THESS Probable dual-specificity RNA methyltransferase RlmN
Thfi_1832	5,699	-0,733	0,047	0,120	58,57	29,96	38,72	53,75	64,13	96,86	tr|E8PJH5|E8PJH5_THESS DNA replication and repair protein RecF OS=Thermus scotoductus
Thfi_1833	6,223	-1,575	0,001	0,004	249,77	95,25	146,12	418,52	249,53	238,35	tr|Q5SHI5|Q5SHI5_THET8 Uncharacterized protein OS=Thermus thermophilus

					FPKM						
Gene code	logCPM	logFC	PValue	FDR	63 degrees			77 degrees			Top Hit Uniprot
Thfi_1834	8,102	-1,025	0,000	0,001	228,53	183,9	267,53	546,5	517,7	435,41	tr|H9ZNY7|H9ZNY7_THETH Uncharacterized protein OS=Thermus thermophilus JL-18
Thfi_1835	5,856	-1,837	0,000	0,001	47,31	31,61	52,51	126,88	191,37	90,52	tr|B7A8N0|B7A8N0_THEAQ Sugar fermentation stimulation protein OS=Thermus aquaticus Y51MC23
Thfi_1839	10,497	-0,467	0,026	0,077	584,3	524,8	542,86	915,6	835,85	799,22	tr|B7A923|B7A923_THEAQ (P)ppGpp synthetase I, SpoT/RelA OS=Thermus aquaticus Y51MC23
Thfi_1841	6,913	-0,681	0,015	0,050	196,57	114,14	139,18	210	198,91	261,82	tr|G8NBJ7|G8NBJ7_9DEIN Putative uncharacterized protein
Thfi_1843	8,376	0,873	0,000	0,001	924,91	917,55	1298,28	747,53	686,21	773,19	tr|G8NBK0|G8NBK0_9DEIN Putative uncharacterized protein
Thfi_1848	6,308	-1,750	0,000	0,001	77,32	28,05	76,97	187,88	155,41	110,29	tr|H9ZU71|H9ZU71_THETH Putative divalent heavy-metal cations transporter (Precursor)
Thfi_1858	7,648	0,903	0,001	0,006	159,75	218,03	284,56	141,4	174,56	208,44	tr|G8NBY0|G8NBY0_9DEIN Alcohol dehydrogenase, zinc-binding protein
Thfi_1860	10,311	-0,927	0,010	0,034	250,09	317,31	272,51	1229,48	876,58	932,72	tr|E8PR43|E8PR43_THESS Tungsten-containing aldehyde ferredoxin oxidoreductase OS=Thermus scotoductus
Thfi_1866	9,342	0,758	0,001	0,006	4113,27	2750,55	2689,48	1687,12	2107,57	1488,56	tr|F2NKR8|F2NKR8_MARHT RNA binding S1 domain protein OS=Marinithermus hydrothermalis
Thfi_1867	7,978	0,685	0,008	0,030	253,39	252,48	279,72	188,2	163,33	244,53	tr|Q72IM4|Q72IM4_THET2 Na(+)/H(+) antiporter OS=Thermus thermophilus
Thfi_1868	7,535	0,572	0,033	0,091	626,7	542,45	481,93	411,14	433,39	468,99	tr|Q72IM3|Q72IM3_THET2 Uncharacterized protein OS=Thermus thermophilus
Thfi_1869	6,323	-2,670	0,000	0,000	62,76	26,02	19,03	232,96	201,09	143,36	tr|B7A8Y2|B7A8Y2_THEAQ Glucose-inhibited division protein A
Thfi_1870	6,989	-1,280	0,000	0,001	107,35	62,11	80,26	218,77	207,27	129,09	tr|B7A8Y1|B7A8Y1_THEAQ HhH-GPD family protein OS=Thermus aquaticus Y51MC23
Thfi_1871	11,305	0,753	0,001	0,005	4992,43	5259,41	4916,4	4383,91	3742,59	3019,16	tr|D3PLS4|D3PLS4_MEIRD Uncharacterized protein OS=Meiothermus ruber
Thfi_1873	7,109	0,870	0,011	0,038	234,22	159,82	168,23	151,08	107,93	137,66	tr|F6DFV7|F6DFV7_THETG NH(3)-dependent NAD(+) synthetase OS=Thermus thermophilus
Thfi_1876	4,223	-2,218	0,001	0,007	9,97	11,91	0	49,73	42,79	62,71	tr|H9ZRH3|H9ZRH3_THETH Uncharacterized protein (Precursor)
Thfi_1878	8,300	1,251	0,000	0,000	587,65	666,1	548,56	279,38	343,72	280,06	tr|H5SNC0|H5SNC0_9DEIN Acetylornithine aminotransferase
Thfi_1883	10,659	-1,060	0,000	0,000	2859,77	2835,79	3117,66	7819,64	7028,68	7619,79	tr|K7QWB0|K7QWB0_THEOS Uncharacterized protein (Precursor)
Thfi_1886	10,379	-0,897	0,000	0,001	315,17	354,31	294,85	836,62	633,42	664,06	tr|Q72H73|Q72H73_THET2 ATP-binding motif-containing protein pilF OS=Thermus thermophilus (strain HB27 / ATCC BAA-163 / DSM 7039)
Thfi_1887	9,556	-0,770	0,008	0,030	236,66	593	320,62	1236,39	816,37	933,28	tr|D3PKU4|D3PKU4_MEIRD Twitching motility protein OS=Meiothermus ruber
Thfi_1892	7,192	-0,701	0,020	0,062	109,08	104,9	113,78	212,98	232,98	183,09	tr|B7A8V4|B7A8V4_THEAQ Methylenetetrahydrofolate reductase OS=Thermus aquaticus Y51MC23
Thfi_1896	9,480	-0,826	0,002	0,011	929,03	509,97	1017,64	1492,95	1327,19	1221,2	tr|K7R0Y2|K7R0Y2_THEOS Histidinol phosphate phosphatase HisJ family OS=Thermus oshimai JL-2
Thfi_1898	10,977	-0,610	0,003	0,014	2980,72	2974,02	2814,73	4961,81	5223,13	4873,8	tr|H7GIZ2|H7GIZ2_9DEIN Sulfite dehydrogenase OS=Thermus sp. RL GN=RLTM_11628 PE=4 SV=1
Thfi_1899	7,841	-1,143	0,003	0,012	629,95	360,61	500,73	1793,66	1126,43	730,1	tr|B7A8U8|B7A8U8_THEAQ Putative uncharacterized protein OS=Thermus aquaticus Y51MC23

					FPKM						
Gene code	logCPM	logFC	PValue	FDR	63 degrees			77 degrees			Top Hit Uniprot
Thfi_1900	6,782	-1,433	0,000	0,001	205,29	148,15	194,1	632,24	565,95	423,6	tr|D3PMB8|D3PMB8_MEIRD Putative fluoride ion transporter CrcB OS=Meiothermus ruber
Thfi_1901	6,068	-1,839	0,002	0,008	22,64	20,91	17,67	45,39	110,11	201,93	tr|B7A637|B7A637_THEAQ Putative uncharacterized protein (Precursor)
Thfi_1902	6,316	-1,104	0,006	0,022	42,4	22,02	44,83	78,59	67,95	86,29	tr|E8PQZ9|E8PQZ9_THESS Uncharacterized protein OS=Thermus scotoductus
Thfi_1908	7,359	-0,562	0,042	0,108	133,7	93,94	114,71	161,51	159,42	257,3	tr|B7A8K3|B7A8K3_THEAQ L-carnitine dehydratase/bile acid-inducible protein F OS=Thermus aquaticus Y51MC23 GN=TaqDRAFT_3956 PE=4 SV=1
Thfi_1920	6,724	0,759	0,023	0,068	114,23	87,71	103,66	55,85	78,63	77,65	tr|K7QXH8|K7QXH8_THEOS Glucose-6-phosphate isomerase OS=Thermus oshimai JL-2 GN=pgi PE=3 SV=1
Thfi_1921	8,251	-0,584	0,016	0,053	164,58	100,8	129,82	153,24	175,63	222,83	tr|E8PJG1|E8PJG1_THESS 6-carboxyhexanoate-CoA ligase OS=Thermus scotoductus
Thfi_1923	5,672	-1,755	0,020	0,063	23,64	20,36	33,89	23,01	55,49	290,74	tr|B7A887|B7A887_THEAQ Putative uncharacterized protein OS=Thermus aquaticus Y51MC23
Thfi_1924	6,293	-1,447	0,000	0,002	29,01	47,87	25,02	167,7	141,75	125,47	tr|B7A886|B7A886_THEAQ Transposase IS116/IS110/IS902 family protein
Thfi_1925	8,120	0,600	0,027	0,079	160,37	168,23	235,74	178,47	145,36	203,6	tr|D3PR67|D3PR67_MEIRD Probable cytosol aminopeptidase OS=Meiothermus ruber
Thfi_1926	11,349	1,796	0,000	0,000	9167,33	11943,5	10709,1	3259,27	4184,07	3426,06	tr|F6DHW7|F6DHW7_THETG Ferric uptake regulator, Fur family OS=Thermus thermophilus
Thfi_1929	9,645	-1,363	0,000	0,000	185,45	173,06	136,04	415,59	535,48	498,84	tr|H9ZPB1|H9ZPB1_THETH Uncharacterized protein OS=Thermus thermophilus JL-18 GN=TtJL18_0257
Thfi_1930	8,859	-0,819	0,002	0,010	427,03	353,15	460,7	830,27	590,64	693,48	tr|H9ZU48|H9ZU48_THETH Thioredoxin reductase OS=Thermus thermophilus JL-18 GN=TtJL18_2001
Thfi_1931	7,471	-1,334	0,000	0,000	134,59	66,2	99,46	291,36	217,95	279,78	tr|D7BGQ6|D7BGQ6_MEISD Peptidase M29 aminopeptidase II OS=Meiothermus silvanus
Thfi_1932	10,524	-1,076	0,000	0,000	3550,07	2006,18	2157,17	7310,07	4371,7	5525,48	tr|E8PPR4|E8PPR4_THESS Small heat shock protein OS=Thermus scotoductus
Thfi_1933	7,563	-1,735	0,000	0,000	114,7	55,85	117,75	428,04	162,96	292,2	tr|K7QTW0|K7QTW0_THEOS Bifunctional PLP-dependent enzyme with beta-cystathionase and maltose regulon repressor activities
Thfi_1934	7,245	-1,501	0,001	0,005	114,84	64,56	71,61	404,67	180,17	138,3	tr|F6DEA7|F6DEA7_THETG tRNA (guanine-N(7)-)-methyltransferase OS=Thermus thermophilus
Thfi_1941	4,999	-0,957	0,047	0,119	51,85	71,88	21,8	109,97	117,04	237,91	tr|B7A9J4|B7A9J4_THEAQ DNA polymerase beta domain protein region OS=Thermus aquaticus Y51MC23
Thfi_1942	12,273	-0,564	0,010	0,035	3644,92	2438,28	2251,54	4360,53	4679,86	3480,11	tr|Q83YV9|Q83YV9_THETH 30S ribosomal protein S1 OS=Thermus thermophilus GN=rpsA PE=3 SV=1
Thfi_1943	7,710	-0,772	0,007	0,026	318,52	217,9	203,53	451,29	362,87	291,63	tr|E8PPQ5|E8PPQ5_THESS Pseudouridine synthase OS=Thermus scotoductus
Thfi_1950	6,092	0,639	0,040	0,106	680,72	437,56	425,75	421,27	328,52	85,52	tr|F6DDR1|F6DDR1_THETG Glutaredoxin 2 OS=Thermus thermophilus (strain SG0.5JP17-16)
Thfi_1951	7,851	1,230	0,000	0,000	534,07	328,49	524,02	178,61	225,61	115,83	tr|G8N983|G8N983_9DEIN Prolipoprotein diacylglyceryl transferase OS=Thermus sp. CCB_US3_UF1
Thfi_1952	8,243	0,832	0,001	0,004	359,72	272,62	326,69	167,51	201,55	162,05	tr|K7RJN4|K7RJN4_THEOS Bifunctional protein GlmU (Precursor) OS=Thermus oshimai JL-2
Thfi_1959	7,384	-1,055	0,000	0,002	192,97	159	114,56	365,54	366,91	227,38	tr|G8N912|G8N912_9DEIN Putative uncharacterized protein OS=Thermus sp. CCB_US3_UF1
Thfi_1962	5,959	-1,400	0,001	0,006	108,17	53,9	57,92	198,04	129,56	124,97	tr|G8N909|G8N909_9DEIN Putative uncharacterized protein OS=Thermus sp. CCB_US3_UF1

					FPKM						
Gene code	logCPM	logFC	PValue	FDR	63 degrees			77 degrees			Top Hit Uniprot
Thfi_1963	7,092	-0,989	0,001	0,005	583,75	716,1	610,54	1737,17	1585,83	1356,22	tr|B7A9D5|B7A9D5_THEAQ Putative uncharacterized protein OS=Thermus aquaticus Y51MC23
Thfi_1966	9,460	-1,020	0,000	0,000	320,38	174,84	219,44	440,65	447,55	529,12	tr|B7A9F0|B7A9F0_THEAQ Endonuclease MutS2 OS=Thermus aquaticus Y51MC23 GN=mutS2 PE=3 SV=1
Thfi_1967	7,187	0,859	0,007	0,025	91,76	103,51	121,58	65,64	60,07	70,84	tr|Q72I49|Q72I49_THET2 Maltodextrin glucosidase OS=Thermus thermophilus 1
Thfi_1968	7,913	0,905	0,001	0,005	137,32	231,8	218,54	117,7	156,45	180,67	tr|K7QXZ9|K7QXZ9_THEOS ABC-type maltose transport systems, permease component
Thfi_1969	9,356	1,194	0,000	0,000	393,11	581,03	581,08	285,5	398,73	344,77	tr|G8N925|G8N925_9DEIN Fructose-bisphosphate aldolase OS=Thermus sp. CCB_US3_UF1
Thfi_1970	11,548	1,729	0,000	0,000	3814,81	4591,58	3729,88	1163,98	1441,92	1442,45	tr|H7GHT0|H7GHT0_9DEIN Maltose ABC transporter substrate-binding protein OS=Thermus sp. RL
Thfi_1979	7,863	-0,640	0,010	0,034	123,39	83,21	109,44	142,54	175,64	169,96	tr|H9ZUR1|H9ZUR1_THETH Cobyric acid synthase OS=Thermus thermophilus JL-18 GN=cobQ PE=3 SV=1
Thfi_1983	9,864	0,436	0,043	0,111	1523,9	1252,45	1546,52	1203,17	1201,74	961,79	tr|B7ABV3|B7ABV3_THEAQ Putative uncharacterized protein OS=Thermus aquaticus Y51MC23
Thfi_1987	7,955	0,590	0,027	0,079	1117,38	769,4	591,34	698,69	510,89	476,96	tr|K7R4D1|K7R4D1_THEOS Uncharacterized protein (Precursor) OS=Thermus oshimai JL-2
Thfi_1990	10,372	0,558	0,019	0,061	2244,9	2721,21	2090,56	2344,77	1855,89	1939,49	tr|B7ABU6|B7ABU6_THEAQ Putative uncharacterized protein OS=Thermus aquaticus Y51MC23
Thfi_1991	9,227	0,819	0,002	0,009	1442,52	1674,62	1898,43	1730,18	1368,76	1042,45	tr|F6DDH6|F6DDH6_THETG Heat shock protein Hsp20 OS=Thermus thermophilus
Thfi_1992	9,866	1,020	0,000	0,001	1089,85	819,25	946,82	707,79	543,04	521,68	tr|E8PNA5|E8PNA5_THESS Uncharacterized protein OS=Thermus scotoductus
Thfi_1994	12,673	0,678	0,016	0,052	2287,91	2553,27	2190,59	2591,04	1724,05	2171,43	tr|K7QWD3|K7QWD3_THEOS ATP-dependent chaperone ClpB OS=Thermus oshimai JL-2 GN=Theos_0686
Thfi_1998	13,628	0,557	0,031	0,086	6975,48	7434,41	6776,41	8043,12	4801,15	5861,72	tr|B7A6Y3|B7A6Y3_THEAQ Chaperone protein DnaK OS=Thermus aquaticus Y51MC23 GN=dnaK PE=3 SV=1
Thfi_2002	12,212	2,145	0,000	0,000	34514,6	43047,6	32618,3	7598,23	10391	10181,7	tr|B7ABS8|B7ABS8_THEAQ Histone family protein DNA-binding protein OS=Thermus aquaticus Y51MC23
Thfi_2003	5,861	-1,480	0,001	0,007	70,92	34,29	68,33	162,79	107,23	196,53	tr|G8NA88|G8NA88_9DEIN 1-acyl-sn-glycerol-3-phosphate acyltransferase OS=Thermus sp. CCB_US3_UF1
Thfi_2005	7,323	1,029	0,001	0,005	296,05	184,62	365,61	147,43	130,35	153,64	tr|B7ABT1|B7ABT1_THEAQ Putative uncharacterized protein OS=Thermus aquaticus Y51MC23
Thfi_2006	8,801	0,919	0,000	0,002	974,79	947,65	926,58	511,56	498,67	581,72	tr|G8NA85|G8NA85_9DEIN Mannose-6-phosphate isomerase OS=Thermus sp. CCB_US3_UF1
Thfi_2009	6,442	-0,666	0,046	0,117	133,06	85,61	60,89	148,08	163,21	130,91	tr|H9ZT36|H9ZT36_THETH Phosphatidylglycerophosphate synthase OS=Thermus thermophilus JL-18
Thfi_2010	8,465	0,608	0,023	0,069	255,52	207,25	239,22	239,83	129,03	112,71	tr|E8PQI4|E8PQI4_THESS Glutamine--fructose-6-phosphate aminotransferase [isomerizing]
Thfi_2016	9,359	0,537	0,013	0,043	627,57	485,21	564,15	420,58	407,81	443,98	tr|K7RK64|K7RK64_THEOS Proline--tRNA ligase OS=Thermus oshimai JL-2 GN=proS PE=3 SV=1
Thfi_2019	7,123	-0,605	0,050	0,124	72,85	53,71	57,28	109,95	87,54	99,41	tr|F6DD75|F6DD75_THETG ABC transporter related protein OS=Thermus thermophilus (strain SG0.5JP17-16)
Thfi_2021	7,425	0,877	0,007	0,025	615,71	617,47	843,07	416,84	334,6	612,39	tr|D7BDB9|D7BDB9_MEISD S23 ribosomal protein OS=Meiothermus silvanus
Thfi_2023	9,287	-1,574	0,000	0,000	453,47	294,03	312,67	1043,76	950,16	818,56	tr|E8PN77|E8PN77_THESS Major facilitator superfamily MFS_1 OS=Thermus scotoductus

					FPKM						
Gene code	logCPM	logFC	PValue	FDR	63 degrees			77 degrees			Top Hit Uniprot
Thfi_2024	11,869	-1,140	0,000	0,000	2317,06	1338,6	1748,58	3178,14	4308,29	3658,8	tr|D3PP22|D3PP22_MEIRD DEAD/DEAH box helicase OS=Meiothermus ruber
Thfi_2027	7,837	-1,090	0,000	0,001	107,71	50,29	89,51	151,42	146,7	121,54	tr|E8PPM9|E8PPM9_THESS ATP-dependent helicase HrpB OS=Thermus scotoductus
Thfi_2028	10,753	-0,528	0,010	0,034	811,69	713,81	837,64	1186,83	1319,2	1232,25	tr|E8PPM8|E8PPM8_THESS DNA gyrase, subunit B OS=Thermus scotoductus
Thfi_2029	6,045	-1,421	0,003	0,015	69,75	78,75	122,87	322,33	365,92	133,93	tr|F2NNJ5|F2NNJ5_MARHT Uncharacterized protein OS=Marinithermus hydrothermalis
Thfi_2030	6,375	-0,933	0,040	0,105	119,47	58,47	65,08	184,33	158,22	100,02	tr|E8PPM6|E8PPM6_THESS Modification methylase TaqI OS=Thermus scotoductus
Thfi_2032	14,474	0,762	0,010	0,036	3250,8	7739,98	5809,15	6476,58	6806,39	5326,37	tr|F6DFV1|F6DFV1_THETG S-layer domain-containing protein (Precursor) OS=Thermus thermophilus
Thfi_2033	10,597	0,690	0,006	0,023	3356,17	2485,75	2593,88	1656,61	1611,46	1461,15	tr|H9ZPW2|H9ZPW2_THETH Uncharacterized protein OS=Thermus thermophilus JL-18 GN=TtJL18_0464
Thfi_2034	5,929	0,849	0,042	0,109	121,34	104,53	116,74	62,59	74,87	114,36	tr|H7GHL4|H7GHL4_9DEIN GntR family transcriptional regulator OS=Thermus sp. RL GN=RLTM_08814
Thfi_2035	8,097	1,469	0,000	0,000	597,07	405,49	506,67	163,05	246,33	91,87	tr|E8PPM1|E8PPM1_THESS Proline dehydrogenase/delta-1-pyrroline-5-carboxylate dehydrogenase
Thfi_2036	9,089	1,393	0,000	0,000	680,54	530,98	481,27	156,7	263,87	270,48	tr|E8PPM0|E8PPM0_THESS Delta-1-pyrroline-5-carboxylate dehydrogenase
Thfi_2037	8,465	-1,103	0,000	0,000	137,97	145,93	182,94	405,5	358,32	411,39	tr|F6DFJ7|F6DFJ7_THETG Anthranilate synthase component I OS=Thermus thermophilus
Thfi_2046	7,233	1,532	0,000	0,000	348,29	212,49	278,31	112,38	96,03	30,62	tr|K7R1A7|K7R1A7_THEOS tRNA pseudouridine synthase B OS=Thermus oshimai JL-2 GN=truB PE=3 SV=1
Thfi_2047	8,212	1,030	0,000	0,001	332,05	326,45	334,77	200,85	164,07	268,97	tr|K7QWF5|K7QWF5_THEOS Alanine dehydrogenase OS=Thermus oshimai JL-2 GN=Theos_2115 PE=3 SV=1
Thfi_2049	9,395	0,600	0,018	0,056	422,72	453,23	676,83	424,89	322,64	403,32	tr|H5SND6|H5SND6_9DEIN Dak phosphatase OS=uncultured Thermus/Deinococcus group bacterium GN=HGMM_F51G12C41 PE=4 SV=1
Thfi_2050	7,579	0,821	0,003	0,012	244,95	263,96	321,85	247,69	214,21	93,51	tr|K7R7V5|K7R7V5_THEOS Uncharacterized protein (Precursor) OS=Thermus oshimai JL-2
Thfi_2053	9,732	-0,538	0,015	0,050	1022,93	559,29	699,57	1017,59	868,67	1070,02	tr|E8PQ14|E8PQ14_THESS S-adenosylmethionine synthase OS=Thermus scotoductus
Thfi_2054	10,948	-0,505	0,019	0,060	778,43	749,5	858,87	1438,19	1092,1	1351,47	tr|F6DFV0|F6DFV0_THETG UvrABC system protein B OS=Thermus thermophilus
Thfi_2055	8,078	-0,675	0,011	0,038	254,41	192,05	268,51	396,33	354,97	328,91	tr|G8N932|G8N932_9DEIN GGDEF domain protein OS=Thermus sp. CCB_US3_UF1
Thfi_2059	7,519	-0,665	0,040	0,106	154,78	109,56	157,55	267,57	284,92	245,86	tr|H7GHR7|H7GHR7_9DEIN Ribose-phosphate pyrophosphokinase OS=Thermus sp.
Thfi_2061	11,994	-0,823	0,000	0,001	10748,4	10020,6	10008,3	22636	19352,8	18019,2	tr|K7RFX9|K7RFX9_THEOS Iron-sulfur cluster assembly accessory protein OS=Thermus oshimai JL-2
Thfi_2062	13,604	0,846	0,000	0,001	6400,37	8886,12	7227,12	5955,25	5115,79	4976,86	tr|Q5SHU6|Q5SHU6_THET8 Peptide ABC transporter, peptide-binding protein OS=Thermus thermophilus
Thfi_2065	8,627	0,461	0,048	0,122	434,03	290,29	384,15	325,85	344,53	274,21	tr|F2NLS0|F2NLS0_MARHT E3 binding domain protein OS=Marinithermus hydrothermalis (strain DSM 14884 / JCM 11576 / T1)
Thfi_2066	5,676	-1,426	0,005	0,020	83,35	26,27	57,64	122,07	101,51	62,03	tr|K7QTV4|K7QTV4_THEOS tRNA pseudouridine synthase A OS=Thermus oshimai JL-2 GN=truA PE=3 SV=1

FPKM											
Gene code	logCPM	logFC	PValue	FDR	63 degrees			77 degrees			Top Hit Uniprot
Thfi_2067	7,855	-1,468	0,000	0,000	144,18	91,66	148,45	422,05	343,3	318,24	tr|F6DEB8|F6DEB8_THETG Fe(3+)-transporting ATPase OS=Thermus thermophilus (strain SG0.5JP17-16)
Thfi_2068	6,776	-1,850	0,000	0,001	22,01	18,28	33,49	151,87	60,99	134,25	tr|E8PQ01|E8PQ01_THESS Iron ABC transporter, permease protein OS=Thermus scotoductus
Thfi_2070	4,759	-2,740	0,000	0,000	36,91	9,68	0	46,58	41,52	114,19	tr|E8PPZ9|E8PPZ9_THESS Metalloenzyme superfamily protein OS=Thermus scotoductus
Thfi_2071	7,949	-0,899	0,000	0,003	237,72	266,44	366,47	697,63	586,42	592,97	tr|I0U9F3|I0U9F3_GEOTM Uncharacterized protein OS=Geobacillus thermoglucosidans TNO-09.020
Thfi_2072	8,565	1,517	0,000	0,000	1369,11	1249,43	1618,41	730,8	559,53	463,92	tr|G8N948|G8N948_9DEIN Osmotically inducible protein C OS=Thermus sp. CCB_US3_UF1
Thfi_2075	6,995	0,913	0,011	0,040	231,03	141,94	244,8	176,07	126,5	126,48	tr|Q72I74|Q72I74_THET2 Thiosulfate sulfurtransferase OS=Thermus thermophilus
Thfi_2076	9,223	1,297	0,000	0,000	183,92	488,37	284,66	231,28	215,94	232,07	tr|G8NBH9|G8NBH9_9DEIN Putative uncharacterized protein OS=Thermus sp. CCB_US3_UF1
Thfi_2077	11,094	-1,923	0,000	0,000	134,64	173,21	193,89	567,65	1021,76	952,86	tr|K7R0A8|K7R0A8_THEOS Glutamate synthase family protein OS=Thermus oshimai JL-2 GN=Theos_1674
Thfi_2078	6,592	1,257	0,000	0,001	94,2	95,95	131,76	65,78	69,66	13,45	tr|K7R0P1|K7R0P1_THEOS Threonine synthase OS=Thermus oshimai JL-2 GN=Theos_1818 PE=3 SV=1
Thfi_2079	7,579	0,617	0,044	0,112	1131,55	1020,48	883,96	606,76	856,8	939,09	tr|F6DEG5|F6DEG5_THETG Uncharacterized protein OS=Thermus thermophilus (strain SG0.5JP17-16)
Thfi_2082	7,964	-0,485	0,049	0,122	124,75	156,55	120,29	214,9	205,01	306,76	tr|H9ZSZ9|H9ZSZ9_THETH 2-phosphoglycerate kinase (Precursor) OS=Thermus thermophilus JL-18
Thfi_2083	7,733	-1,359	0,000	0,000	123,15	151,59	209,05	388,43	581,19	469,26	tr|F2NLR5|F2NLR5_MARHT Metal dependent phosphohydrolase OS=Marinithermus hydrothermalis
Thfi_2087	8,415	0,650	0,033	0,091	650,8	404,58	468,57	236,46	311,29	263,49	tr|B7A5P0|B7A5P0_THEAQ Type IV pilus assembly protein PilM (Precursor) OS=Thermus aquaticus Y51MC23
Thfi_2088	8,635	-0,547	0,021	0,064	1373,02	1859,7	1695,83	3663,04	2942,67	3400,03	tr|Q5SHC7|Q5SHC7_THET8 Pterin-4-alpha-carbinolamine dehydratase OS=Thermus thermophilus
Thfi_2089	6,504	1,121	0,002	0,008	378,03	181,84	259,01	83,98	152,4	72,87	tr|G8NAI9|G8NAI9_9DEIN Putative uncharacterized protein OS=Thermus sp. CCB_US3_UF1 GN=TCCBUS3UF1_6350 PE=4 SV=1
Thfi_2090	6,365	0,804	0,041	0,107	96,15	206,09	115,83	122,42	109,1	99,98	tr|E8PND8|E8PND8_THESS Competence protein PilO OS=Thermus scotoductus (strain ATCC 700910 / SA-01)
Thfi_2092	7,130	1,001	0,000	0,002	67,04	103,22	130,46	70,86	73,5	46,49	tr|E8PNE0|E8PNE0_THESS General secretion pathway protein OS=Thermus scotoductus
Thfi_2095	6,666	-0,860	0,025	0,074	74,11	65,01	77,2	150,82	154,18	68,96	tr|G8NAE0|G8NAE0_9DEIN Putative uncharacterized protein
Thfi_2096	10,243	-0,887	0,000	0,001	602,44	420,25	639,91	944,35	984,81	1384,38	tr|K7QXU1|K7QXU1_THEOS CTP synthase OS=Thermus oshimai JL-2 GN=pyrG PE=3 SV=1
Thfi_2099	4,474	-3,193	0,000	0,001	44,88	10,31	0	82,55	89,26	122,56	tr|G8NAD4|G8NAD4_9DEIN Putative uncharacterized protein OS=Thermus sp. CCB_US3_UF1 GN=TCCBUS3UF1_5800 PE=4 SV=1
Thfi_2100	4,493	2,305	0,003	0,014	37,1	35,91	83,47	14,83	0	25,74	tr|E8PNS2|E8PNS2_THESS Uncharacterized protein OS=Thermus scotoductus
Thfi_2101	10,149	1,156	0,000	0,000	294,84	765,47	542,21	426,94	337,1	377	tr|Q5SLK7|Q5SLK7_THET8 Serine protease, subtilase family OS=Thermus thermophilus
Thfi_2107	6,986	-0,688	0,040	0,104	126,63	69,54	130,2	127,31	152,04	181,85	tr|E6SLU3|E6SLU3_THEM7 Probable tRNA sulfurtransferase OS=Thermaerobacter marianensis
Thfi_2109	8,389	0,898	0,000	0,002	525,54	394,86	459,37	220,98	296,27	347,71	tr|B7A5H4|B7A5H4_THEAQ Delta-aminolevulinic acid dehydratase OS=Thermus aquaticus Y51MC23

					FPKM						
Gene code	logCPM	logFC	PValue	FDR	63 degrees			77 degrees			Top Hit Uniprot
Thfi_2112	9,712	0,471	0,031	0,087	625,16	626,47	732,17	597,28	520,6	636,58	tr|F6DHT7|F6DHT7_THETG Dihydrolipoyl dehydrogenase OS=Thermus thermophilus
Thfi_2115	4,068	1,889	0,017	0,054	79,86	51,84	47,14	22,34	14,09	0	tr|G8NA45|G8NA45_9DEIN Putative uncharacterized protein OS=Thermus sp. CCB_US3_UF1
Thfi_2116	8,346	0,800	0,002	0,008	3991,52	2081,27	2714,44	1533,32	1346,19	1611,34	tr|B7A5G8|B7A5G8_THEAQ Putative uncharacterized protein OS=Thermus aquaticus Y51MC23
Thfi_2120	6,483	-0,997	0,003	0,012	233,59	141,31	149,56	312,26	275,79	468,99	tr|B7A5G4|B7A5G4_THEAQ Putative uncharacterized protein (Precursor) OS=Thermus aquaticus Y51MC23
Thfi_2122	10,401	-0,584	0,025	0,075	1088,57	1058,09	1363,14	2763,99	1536,14	1810,78	tr|E8PNU1|E8PNU1_THESS Transporter, stomatin/podocin/band 7/nephrosis.2/spfh
Thfi_2124	6,311	-1,610	0,000	0,002	325,61	226,1	163,96	1064,35	547,65	634,76	tr|G8NA37|G8NA37_9DEIN Putative uncharacterized protein OS=Thermus sp. CCB_US3_UF1
Thfi_2127	7,800	0,602	0,016	0,053	190,04	134,97	216,96	132,08	123,92	139,16	tr|B7A5F9|B7A5F9_THEAQ S-layer domain protein (Precursor) OS=Thermus aquaticus Y51MC23 GN=TaqDRAFT_5066 PE=4 SV=1
Thfi_2128	8,313	0,839	0,000	0,003	869,5	816,15	758,5	593,56	488,57	566,93	tr|F6DEA1|F6DEA1_THETG Phosphoribosyltransferase OS=Thermus thermophilus
Thfi_2132	8,788	-0,631	0,005	0,019	372,74	220,68	271,18	408,17	471,66	516,94	tr|E8PNV0|E8PNV0_THESS Uncharacterized protein OS=Thermus scotoductus
Thfi_2133	12,108	-2,345	0,000	0,000	268,09	244,32	251,72	1785,3	1488,02	1062,46	tr|K7QY19|K7QY19_THEOS Ribonucleoside-diphosphate reductase OS=Thermus oshimai JL-2 GN=Theos_0365
Thfi_2135	7,965	-0,824	0,002	0,008	379,08	455,02	682,31	1201,28	1008,96	976,47	tr|H9ZPZ7|H9ZPZ7_THETH Uncharacterized protein OS=Thermus thermophilus JL-18 GN=TtJL18_0499
Thfi_2136	9,808	1,195	0,000	0,000	1753,71	1376,08	1655,41	805,66	643,2	780,7	tr|B7AA36|B7AA36_THEAQ Putative uncharacterized protein OS=Thermus aquaticus Y51MC23
Thfi_2137	9,789	0,598	0,007	0,026	1228,58	1298,79	1337,17	1017,28	941,44	1210,96	tr|G8N9Q4|G8N9Q4_9DEIN Enoyl-CoA hydratase/isomerase OS=Thermus sp. CCB_US3_UF1
Thfi_2138	7,358	0,796	0,012	0,040	366,93	192,83	421,05	200,35	184	231,89	tr|B7AA34|B7AA34_THEAQ Purine or other phosphorylase family 1 OS=Thermus aquaticus Y51MC23
Thfi_2142	9,397	0,479	0,034	0,092	524,14	480,22	716,68	553,68	449,76	433,6	tr|K7RKA8|K7RKA8_THEOS Acetylornithine deacetylase/succinyldiaminopimelate desuccinylase-like deacylase
Thfi_2143	8,289	-0,546	0,031	0,087	220,58	423,96	387,5	705,49	501,87	748,54	tr|B7AA29|B7AA29_THEAQ Transcriptional regulator, MerR family OS=Thermus aquaticus Y51MC23
Thfi_2144	4,060	-2,452	0,017	0,054	15,45	2,43	0	24,77	20,85	38,23	tr|B7AA28|B7AA28_THEAQ Transcriptional regulator, IclR family OS=Thermus aquaticus Y51MC23
Thfi_2146	9,330	-0,748	0,004	0,016	369,56	312,37	300,66	746,92	460,75	501,8	tr|E8PLU1|E8PLU1_THESS Malate synthase OS=Thermus scotoductus (strain ATCC 700910 / SA-01)
Thfi_2150	6,791	-1,041	0,007	0,025	61,87	45,37	58,97	158,49	84,48	149,21	tr|H7GFB2|H7GFB2_9DEIN Glycerate dehydrogenase/hydroxypyruvate reductase
Thfi_2154	8,818	-0,489	0,028	0,080	368,16	451,74	399,63	643,94	711,81	612,47	tr|B7A609|B7A609_THEAQ Putative uncharacterized protein (Precursor) OS=Thermus aquaticus Y51MC23
Thfi_2157	9,006	-0,733	0,001	0,005	233,65	227,29	195,87	353,26	412,6	448,79	tr|H7GHI4|H7GHI4_9DEIN UvrABC system protein C OS=Thermus sp. RL GN=uvrC PE=3 SV=1
Thfi_2164	8,808	-0,836	0,000	0,002	274,37	317,65	344,16	727,9	743,31	837,45	tr|Q72GH3|Q72GH3_THET2 Galactoside O-acetyltransferase OS=Thermus thermophilus
Thfi_2165	8,117	-0,657	0,022	0,066	487,83	189,21	371,8	436,8	405,29	438,07	tr|G8NAM1|G8NAM1_9DEIN GTPase Era OS=Thermus sp. CCB_US3_UF1 GN=era PE=3 SV=1
Thfi_2174	8,109	0,536	0,030	0,084	174,37	269,27	241,25	201,41	212,77	218,07	tr|K7R0S6|K7R0S6_THEOS Glucose-1-phosphate adenylyltransferase (Precursor)

					FPKM						
Gene code	logCPM	logFC	PValue	FDR	63 degrees			77 degrees			Top Hit Uniprot
Thfi_2175	8,755	-0,565	0,015	0,049	181,35	139,99	208,37	263,17	247,6	309,4	tr|E8PLC2|E8PLC2_THESS ATP-dependent protease La OS=Thermus scotoductus
Thfi_2178	6,671	-1,063	0,009	0,032	189,49	78,81	196,18	330,05	262,31	254,46	tr|B7ABV9|B7ABV9_THEAQ Putative uncharacterized protein
Thfi_2179	7,557	-0,646	0,012	0,042	257,78	190,5	244,31	308,22	392,79	389,24	tr|F6DJB4|F6DJB4_THETG Uncharacterized protein OS=Thermus thermophilus
Thfi_2184	6,218	0,780	0,022	0,067	158,18	132,62	116,38	87,18	102,49	41,75	tr|H7GF99|H7GF99_9DEIN Phosphoesterase-like protein OS=Thermus sp. RL GN=RLTM_03946 PE=4 SV=1
Thfi_2186	4,914	-1,530	0,013	0,045	60,99	32,75	39,75	87,53	165,62	129,91	tr|H9ZT07|H9ZT07_THETH Uncharacterized protein (Precursor)
Thfi_2187	5,600	-0,932	0,024	0,071	152,09	172,98	167,24	362,05	431,9	555,19	tr|Q72LE5|Q72LE5_THET2 Uncharacterized protein OS=Thermus thermophilus
Thfi_2189	10,649	1,091	0,000	0,001	455,13	1138,79	982,86	716,01	582,03	916,33	tr|D3DJ29|D3DJ29_HYDTT Polymorphic outer membrane protein OS=Hydrogenobacter thermophilus
Thfi_2195	8,059	0,664	0,030	0,084	152,64	301,07	173,54	203,5	176,49	227,78	tr|B7A763|B7A763_THEAQ Extracellular ligand-binding receptor (Precursor) OS=Thermus aquaticus Y51MC23
Thfi_2198	8,069	0,913	0,003	0,014	341,66	257,63	138,06	149,29	135	142,85	tr|K7QZ08|K7QZ08_THEOS 4-hydroxyphenylacetate 3-monooxygenase, oxygenase component
Thfi_2199	7,352	0,899	0,005	0,019	226,77	141,2	100,6	97,28	97,78	71,74	tr|F6DGL4|F6DGL4_THETG 5-carboxymethyl-2-hydroxymuconate semialdehyde dehydrogenase
Thfi_2202	5,834	1,245	0,002	0,010	174,42	122,6	100,79	66,11	46,12	72,46	tr|Q72K26|Q72K26_THET2 2-hydroxyhepta-2,4-diene-1,7-dioate isomerase/5-carboxymethyl-2-oxo-hex-3-ene-1,7-dioate decarboxylase
Thfi_2203	6,147	0,961	0,024	0,071	143,31	74,95	152,38	47,09	66,91	81,79	tr|K7RHY0|K7RHY0_THEOS 4-hydroxy-tetrahydrodipicolinate synthase
Thfi_2206	5,676	-1,099	0,029	0,082	16,55	33,32	27,11	33,47	95,13	130,83	tr|G8NDU0|G8NDU0_9DEIN Putative uncharacterized protein OS=Thermus sp. CCB_US3_UF1
Thfi_2216	6,851	0,834	0,021	0,066	326,67	224,67	228,25	130,07	144,62	78,56	tr|E8PPG6|E8PPG6_THESS Formate dehydrogenase, subunit FdhD OS=Thermus scotoductus
Thfi_2217	6,701	-1,929	0,000	0,000	65,31	39,53	54,28	159,89	147,98	193,85	tr|B7AB14|B7AB14_THEAQ Putative uncharacterized protein OS=Thermus aquaticus Y51MC23
Thfi_2219	4,289	-1,927	0,024	0,071	14,07	14,91	0	46,66	64,25	0	tr|K7QXJ4|K7QXJ4_THEOS Putative periplasmic protein (Precursor) OS=Thermus oshimai JL-2 GN=Theos_0060
Thfi_2220	5,741	-0,906	0,017	0,055	45,94	45,77	52,87	81,84	87,85	151,59	tr|E8PKC3|E8PKC3_THESS ApbE family OS=Thermus scotoductus (strain ATCC 700910 / SA-01)
Thfi_2229	8,431	0,750	0,001	0,005	259,55	345,8	379,98	255,45	292,49	197,3	tr|F6DH72|F6DH72_THETG Acyl-CoA dehydrogenase OS=Thermus thermophilus (strain SG0.5JP17-16)
Thfi_2230	8,635	1,092	0,000	0,000	565,72	738,97	805,19	381,3	385,58	517,7	tr|K7QXJ7|K7QXJ7_THEOS Electron transfer flavoprotein, beta subunit OS=Thermus oshimai JL-2 GN=Theos_1510
Thfi_2231	8,955	1,220	0,000	0,000	523,1	792,59	654,22	313,97	282,9	595,04	tr|E8PR95|E8PR95_THESS Electron transfer flavoprotein, subunit alpha OS=Thermus scotoductus
Thfi_2232	6,220	0,817	0,038	0,100	332,28	232,98	259,93	114,07	226,17	112,95	tr|E8PR96|E8PR96_THESS Uncharacterized protein OS=Thermus scotoductus
Thfi_2233	7,508	-0,683	0,042	0,109	193,47	194,72	200,86	421,31	364,23	176,75	tr|F6DGP6|F6DGP6_THETG Phenylacetate-CoA oxygenase, PaaI subunit OS=Thermus thermophilus (strain SG0.5JP17-16)
Thfi_2235	8,245	-2,190	0,000	0,000	405,88	260,7	328,78	1370,22	1757,56	1668,48	tr|D3PL27|D3PL27_MEIRD MarR family transcriptional regulator OS=Meiothermus ruber

					FPKM						
Gene code	logCPM	logFC	PValue	FDR	63 degrees			77 degrees			Top Hit Uniprot
Thfi_2236	9,280	-0,683	0,004	0,016	222,91	222,92	191,42	338,86	430,95	320,91	tr|D3PL28|D3PL28_MEIRD Drug resistance transporter, EmrB/QacA subfamily OS=Meiothermus ruber
Thfi_2244	6,775	-0,790	0,021	0,066	267,28	152,82	136,06	360,59	289,13	235,45	tr|F6DGP7|F6DGP7_THETG Phenylacetic acid degradation B
Thfi_2245	9,895	-1,304	0,000	0,000	382,26	610,07	523,89	2125,56	1265,96	1478,62	tr|H9ZRL3|H9ZRL3_THETH Phenylacetate-CoA oxygenase, PaaG subunit
Thfi_2246	7,535	-2,246	0,000	0,000	173,91	100,82	102,37	694,66	489,46	286,67	tr|K7RHZ8|K7RHZ8_THEOS Transcriptional regulator OS=Thermus oshimai JL-2 GN=Theos_0989 PE=4 SV=1
Thfi_2251	8,081	-0,974	0,000	0,000	140,36	136,17	133,73	285	303,1	396,29	tr|K7R6Y6|K7R6Y6_THEOS Aspartyl-tRNA synthetase, archaeal type
Thfi_2253	7,872	1,062	0,001	0,007	527,15	324,88	783,94	267,91	263,56	410,61	tr|K7R6Z5|K7R6Z5_THEOS Putative phosphoribosyltransferase
Thfi_2261	4,917	1,506	0,007	0,027	58,03	27,68	57,91	20,12	8,47	15,53	tr|B7A841|B7A841_THEAQ PfkB domain protein OS=Thermus aquaticus Y51MC23 GN=TaqDRAFT_4237
Thfi_2271	7,403	0,839	0,002	0,010	92,87	88,6	120,57	78,15	54,58	71,52	tr|B7A850|B7A850_THEAQ Tetratricopeptide TPR_2 repeat protein OS=Thermus aquaticus Y51MC23
Thfi_2272	8,200	-1,309	0,000	0,000	153,09	134,5	160,91	396,22	287,48	419,66	tr|E8PM87|E8PM87_THESS Putative lipoprotein OS=Thermus scotoductus (strain ATCC 700910 / SA-01)
Thfi_2273	11,223	0,534	0,037	0,099	770,34	1350,08	1225,41	1400,2	1156,29	1237,97	tr|K7QVQ7|K7QVQ7_THEOS Succinate dehydrogenase, flavoprotein subunit (Precursor) OS=Thermus oshimai JL-2
Thfi_2275	8,868	0,535	0,015	0,049	1121,24	899,62	939,09	690,51	856,03	765,92	tr|B7A856|B7A856_THEAQ Rad52/22 double-strand break repair protein OS=Thermus aquaticus Y51MC23
Thfi_2279	5,642	1,032	0,005	0,019	295,01	183,68	245,04	147,59	106,37	0	tr|B7A859|B7A859_THEAQ NADH-quinone oxidoreductase subunit A OS=Thermus aquaticus Y51MC23 GN=nuoA
Thfi_2280	8,830	0,923	0,000	0,000	1476,46	1191,59	1194,86	824,42	641,77	754,9	tr|G8NBB2|G8NBB2_9DEIN NADH-quinone oxidoreductase subunit B OS=Thermus sp. CCB_US3_UF1 GN=nuoB
Thfi_2281	8,327	0,699	0,004	0,017	886,53	716,88	683,28	516,69	569,66	294,8	tr|E8PM80|E8PM80_THESS NADH-quinone oxidoreductase subunit C OS=Thermus scotoductus
Thfi_2282	9,867	0,602	0,010	0,036	703,17	956,59	798,65	828,26	675,47	581,61	tr|K7R4F8|K7R4F8_THEOS NADH-quinone oxidoreductase subunit D OS=Thermus oshimai JL-2 GN=nuoD PE=3 SV=1
Thfi_2283	9,187	1,036	0,000	0,000	1622,1	1658,63	1589,97	1011,62	883,39	716,22	tr|E8PM78|E8PM78_THESS NADH-quinone oxidoreductase, subunit E OS=Thermus scotoductus
Thfi_2284	8,504	0,929	0,000	0,001	1335,87	1427,03	1161,33	965,64	925,29	600,26	tr|K7RJW6|K7RJW6_THEOS Succinate dehydrogenase, hydrophobic anchor subunit OS=Thermus oshimai JL-2
Thfi_2285	10,459	0,806	0,000	0,002	1278,17	1488,8	1223,81	930,15	881,49	858,74	tr|K7RGS6|K7RGS6_THEOS NADH-quinone oxidoreductase, F subunit OS=Thermus oshimai JL-2
Thfi_2286	10,117	0,683	0,004	0,016	464,85	535,49	465,31	438,11	423,18	334,79	tr|H9ZTK0|H9ZTK0_THETH NADH-quinone oxidoreductase, chain G (Precursor) OS=Thermus thermophilus JL-18
Thfi_2288	7,320	0,996	0,000	0,003	426,79	450,71	394,91	262,51	248,51	170,76	tr|E8PM74|E8PM74_THESS NADH-quinone oxidoreductase subunit I OS=Thermus scotoductus
Thfi_2292	8,362	0,908	0,000	0,003	295,15	290,31	285,54	155,83	252,41	118,2	tr|E8PM70|E8PM70_THESS NADH-quinone oxidoreductase, subunit M OS=Thermus scotoductus
Thfi_2293	7,521	1,052	0,000	0,000	174,74	194,9	186,73	109,95	128,24	82,31	tr|G8NBA0|G8NBA0_9DEIN NADH-quinone oxidoreductase subunit N OS=Thermus sp. CCB_US3_UF1 GN=nuoN PE=3 SV=1
Thfi_2294	7,529	0,839	0,008	0,029	282,86	245,2	224,33	164,96	149,48	249,16	tr|K7QWC7|K7QWC7_THEOS Arginase OS=Thermus oshimai JL-2 GN=Theos_0676 PE=4 SV=1
Thfi_2295	8,679	0,854	0,000	0,002	2163,74	1590,23	1708,18	1064,09	1305,88	1194,32	tr|G8N9D6|G8N9D6_9DEIN Succinate dehydrogenase, cytochrome subunit OS=Thermus sp. CCB_US3_UF1 GN=TCCBUS3UF1_16710 PE=4 SV=1

					FPKM						
Gene code	logCPM	logFC	PValue	FDR	63 degrees			77 degrees			Top Hit Uniprot
Thfi_2296	10,937	-1,203	0,000	0,000	3004,77	2613,91	3135,46	5768,07	6229,99	7921,75	tr|K7RGN4|K7RGN4_THEOS Putative metal-binding protein, possibly nucleic-acid binding protein
Thfi_2299	8,166	0,645	0,007	0,025	443,67	297,84	438,99	286,99	312,57	219,83	tr|E8PM63|E8PM63_THESS Malonyl CoA-acyl carrier protein transacylase OS=Thermus scotoductus
Thfi_2300	8,129	1,278	0,000	0,000	613,02	533,82	663,17	234,39	306,96	261,27	tr|B7AA64|B7AA64_THEAQ 3-oxoacyl-(Acyl-carrier-protein) reductase OS=Thermus aquaticus Y51MC23
Thfi_2301	10,312	1,380	0,000	0,000	12304,4	12465,2	13159,4	4919	4974,8	5045,97	tr|K7RGN2|K7RGN2_THEOS Acyl carrier protein OS=Thermus oshimai JL-2 GN=acpP PE=3 SV=1
Thfi_2315	9,758	-0,799	0,000	0,003	828,17	747,65	710,37	1337,22	1368,77	1344,61	tr|B7A6N0|B7A6N0_THEAQ D-alanine--D-alanine ligase OS=Thermus aquaticus Y51MC23 GN=ddl PE=3 SV=1
Thfi_2316	7,872	0,533	0,049	0,123	568,47	394,05	784,72	513,41	393,46	339,28	tr|B7A6N1|B7A6N1_THEAQ Peptidyl-tRNA hydrolase OS=Thermus aquaticus Y51MC23 GN=pth PE=3 SV=1
Thfi_2318	9,902	0,695	0,002	0,008	2745,65	1887,01	2427,89	1633,73	1294,16	1507,14	tr|K7QWB6|K7QWB6_THEOS 50S ribosomal protein L25 OS=Thermus oshimai JL-2 GN=rplY PE=3 SV=1
Thfi_2320	5,571	0,940	0,032	0,087	91,45	66,43	116,13	39,32	74,47	45,5	tr|Q5SI30|Q5SI30_THET8 5'-methylthioadenosine/S-adenosylhomocysteine nucleosidase
Thfi_2321	9,164	0,889	0,000	0,001	2613,32	1802,73	2207,27	1192,57	1114,04	1206,44	tr|H9ZPZ2|H9ZPZ2_THETH S-ribosylhomocysteine lyase OS=Thermus thermophilus JL-18 GN=luxS PE=3 SV=1
Thfi_2322	8,581	0,595	0,007	0,026	240,18	281,08	285,23	212,02	233,2	236,63	tr|E8PMT4|E8PMT4_THESS GMP synthase [glutamine-hydrolyzing] OS=Thermus scotoductus
Thfi_2327	7,535	0,803	0,004	0,017	697,98	660,51	834,81	393,89	579,68	433,04	tr|F6DDU5|F6DDU5_THETG Uncharacterized protein OS=Thermus thermophilus
Thfi_2332	7,410	-0,579	0,035	0,094	173,06	118,22	131,76	226,37	216,32	188,27	tr|B7A7Z2|B7A7Z2_THEAQ tRNA pseudouridine synthase D OS=Thermus aquaticus Y51MC23 GN=truD PE=3 SV=1
Thfi_2338	9,524	1,364	0,000	0,000	1117,29	1004,3	740,8	242,47	418,08	388,52	tr|H9ZTH3|H9ZTH3_THETH Transposase, IS605 OrfB family, central region
Thfi_2339	8,509	-1,360	0,000	0,000	185,21	175,63	293,52	763,7	486,46	629,67	tr|B7A827|B7A827_THEAQ ABC-2 type transporter OS=Thermus aquaticus Y51MC23
Thfi_2340	11,537	-1,029	0,000	0,000	1030,9	785,54	919,85	1836,33	1905,78	1708,08	tr|H9ZQI7|H9ZQI7_THETH DNA gyrase subunit A OS=Thermus thermophilus JL-18 GN=gyrA PE=3 SV=1
Thfi_2341	6,517	-1,052	0,006	0,022	527,94	185,8	297,07	565,25	583,36	414,57	tr|K7RG66|K7RG66_THEOS Uncharacterized protein involved in tolerance to divalent cations
Thfi_2342	8,479	-3,089	0,000	0,000	255,55	140,37	143,09	1639,2	1039,35	1235,53	tr|G8NAT3|G8NAT3_9DEIN Transcriptional regulator, FNR/CRP
Thfi_2343	8,494	-2,264	0,000	0,000	196,18	182,96	164,63	1334,34	967,37	775,79	tr|F6DI73|F6DI73_THETG Uncharacterized protein (Precursor) OS=Thermus thermophilus
Thfi_2344	7,472	2,156	0,000	0,000	258,88	333,47	268,51	37,46	85,94	123,34	tr|L7E4S6|L7E4S6_MICAE Uncharacterized protein OS=Microcystis aeruginosa TAIHU98
Thfi_2345	6,629	2,256	0,000	0,000	343,07	343,03	271,15	24,13	91,38	195,35	tr|D3DG57|D3DG57_HYDTT Uncharacterized protein OS=Hydrogenobacter thermophilus
Thfi_2346	8,258	1,341	0,000	0,000	244,12	244,03	225,58	75,29	147,25	149,6	tr|K7QWR9|K7QWR9_THEOS Uncharacterized protein (Precursor) OS=Thermus oshimai JL-2
Thfi_2347	9,529	0,829	0,004	0,018	334,81	329,18	334,69	126,85	231,31	298,99	tr|D7BJ12|D7BJ12_MEISD Uncharacterized protein OS=Meiothermus silvanus
Thfi_2355	5,535	3,252	0,000	0,000	486,98	401,55	331,22	21,12	79,96	72,95	tr|D7BJ20|D7BJ20_MEISD Uncharacterized protein OS=Meiothermus silvanus
Thfi_2356	9,122	0,741	0,016	0,052	711,28	861,65	741,11	317,77	655,21	763,05	tr|G2SLI1|G2SLI1_RHOMR Uncharacterized protein OS=Rhodothermus marinus SG0.5JP17-172 GN=Rhom172_2840 PE=4 SV=1

					FPKM						
Gene code	logCPM	logFC	PValue	FDR	63 degrees			77 degrees			Top Hit Uniprot
Thfi_2357	9,156	0,818	0,005	0,020	490,34	530,69	563,17	217,71	367,74	514,88	tr|B9LF22|B9LF22_CHLSY Restriction modification system DNA specificity domain protein OS=Chloroflexus aurantiacus
Thfi_2358	5,422	1,231	0,027	0,079	365,78	282,91	329,87	117,18	133,12	323,6	tr|B7J9I4|B7J9I4_ACIF2 Putative uncharacterized protein OS=Acidithiobacillus ferrooxidans
Thfi_2359	8,917	0,689	0,005	0,020	370,69	350,99	373,92	195,23	304,5	300,75	tr|H5SL04|H5SL04_9BACT N-6 DNA methylase OS=uncultured candidate division OP1 bacterium
Thfi_2360	7,456	0,758	0,020	0,062	271,75	272,68	241,65	137,32	191,59	234,36	tr|G8N7R9|G8N7R9_9DEIN Chromosome partitioning protein parB OS=Thermus sp. CCB_US3_UF1 GN=TCCBUS3UF1_1370 PE=4 SV=1
Thfi_2364	5,869	-1,422	0,003	0,014	46,72	20,88	44,61	86,48	93,12	40,98	tr|K7R5Y6|K7R5Y6_THEOS Putative dehydrogenase (Precursor) OS=Thermus oshimai JL-2
Thfi_2366	6,188	2,102	0,000	0,000	142,46	288,93	223,49	69,92	66,17	103,89	tr|G8NDS2|G8NDS2_9DEIN Putative uncharacterized protein
Thfi_2368	11,113	1,330	0,000	0,000	2317,8	2897,51	2561,1	992,11	1122,89	1307,61	tr|K7R721|K7R721_THEOS Isocitrate dehydrogenase [NADP] OS=Thermus oshimai JL-2 GN=Theos_1703
Thfi_2372	5,792	-2,492	0,000	0,000	9,12	9,47	0	56,04	58,17	83,5	tr|Q53W24|Q53W24_THET8 Glycerol kinase OS=Thermus thermophilus
Thfi_2373	4,520	-3,234	0,000	0,001	0	1,71	0	28,93	29,24	40,22	tr|F6DGP1|F6DGP1_THETG Galactose-1-phosphate uridylyltransferase OS=Thermus thermophilus
Thfi_2374	4,808	-6,512	0,000	0,000	0	0	0	40,53	18,54	29,15	tr|Q53W51|Q53W51_THET8 Alpha-galactosidase OS=Thermus thermophilus
Thfi_2375	5,107	-6,938	0,000	0,000	0	0	0	32,26	19,11	49,09	tr|Q0GA06|Q0GA06_THETH Beta-galactosidase OS=Thermus thermophilus PE=3 SV=1
Thfi_2377	7,571	1,382	0,000	0,000	283,24	203,16	327,54	105,3	127,7	160,99	tr|D7BJ15|D7BJ15_MEISD Uncharacterized protein OS=Meiothermus silvanus
Thfi_2378	6,980	-1,574	0,000	0,000	66,22	34,78	48,35	164,9	102,48	131,59	tr|G9MBD6|G9MBD6_THET8 Xylulokinase OS=Thermus thermophilus
Thfi_2379	8,172	-1,620	0,000	0,001	159,83	64,73	95,96	420,86	270,26	628,64	tr|G9MBD7|G9MBD7_THET8 Xylose isomerase OS=Thermus thermophilus
Thfi_2380	6,931	-1,570	0,000	0,000	83,19	39,63	63,87	195,04	111,91	236,33	tr|K7QXA4|K7QXA4_THEOS Transcriptional regulator/sugar kinase OS=Thermus oshimai JL-2 GN=Theos_1294
Thfi_2381	7,130	-1,344	0,000	0,000	159,29	80,25	137,57	318,14	279,81	315,67	tr|G9MBD9|G9MBD9_THET8 ABC transporter-like protein OS=Thermus thermophilus
Thfi_2382	7,885	-0,759	0,006	0,024	197,9	104,46	172,47	242,33	251,66	357,7	tr|G9MBE0|G9MBE0_THET8 Permease protein, ABC-type xylose transporter OS=Thermus thermophilus
Thfi_2387	5,620	-1,200	0,029	0,082	11,97	17,14	22,83	68,59	26,67	97,81	tr|D7BCN4|D7BCN4_MEISD D-galactarate dehydratase/Altronate hydrolase domain protein OS=Meiothermus silvanus
Thfi_2388	5,966	3,753	0,000	0,000	526,31	275,81	294,05	14,52	27,48	33,55	tr|D7BJ21|D7BJ21_MEISD Uncharacterized protein OS=Meiothermus silvanus
Thfi_2399	8,326	1,558	0,000	0,000	79,85	93,47	84,22	18,95	46	47,48	tr|D7BJ19|D7BJ19_MEISD Uncharacterized protein OS=Meiothermus silvanus (strain ATCC 700542 / DSM 9946 / VI-R2) GN=Mesil_3363 PE=4 SV=1
Thfi_2400	5,323	1,476	0,015	0,048	84	61,95	42,52	10,94	41,46	15,2	tr|D7BJ18|D7BJ18_MEISD Uncharacterized protein OS=Meiothermus silvanus (strain ATCC 700542 / DSM 9946 / VI-R2) GN=Mesil_3362 PE=4 SV=1

FPKM: Fragments per kilobase of exon per million fragments mapped; CPM: counts per million reads; FC: Fold change; FDR: false discovery rate.

Table S4: Genes differently expressed in hydrogen peroxide assay.

					FPKM						
Gene code	**logCPM**	**logFC**	**PValue**	**FDR**	**Without H_2O_2**			**With H_2O_2**			**Top Hit Uniprot**
Thfi_0025	7,764	-0,590	0,048	0,751	319,29	181,11	228,44	105,97	194,23	171,37	tr|H7GDU4|H7GDU4_9DEIN Bifunctional purine biosynthesis protein PurH OS=Thermus sp. RL GN=purH PE=3 SV=1
Thfi_0035	9,097	0,529	0,015	0,497	168,63	192,77	203,15	316,75	236,26	245,9	tr|G8N7Y4|G8N7Y4_9DEIN Cation-transporting ATPase OS=Thermus sp. CCB_US3_UF1 GN=TCCBUS3UF1_14100 PE=3 SV=1
Thfi_0065	6,176	-1,015	0,038	0,720	110,89	34,43	93,45	34,92	49,55	28,23	tr|G8NCZ8|G8NCZ8_9DEIN 30S ribosomal protein S16 OS=Thermus sp. CCB_US3_UF1 GN=rpsP PE=3 SV=1
Thfi_0069	6,104	-1,391	0,007	0,451	133,97	74,74	84,63	63,25	14,97	27,29	tr|H0BHA6|H0BHA6_9ACTO Putative integral membrane protein OS=Streptomyces sp. W007 GN=SPW_4644 PE=4 SV=1
Thfi_0070	8,930	0,490	0,027	0,629	433,02	493,5	472,2	547,38	621,4	769,27	tr|E8PMK5|E8PMK5_THESS LAO/AO transport system ATPase OS=Thermus scotoductus
Thfi_0084	6,504	1,066	0,014	0,460	183,43	83,12	166,76	178,03	343,81	365,27	tr|B7A843|B7A843_THEAQ Imidazoleglycerol-phosphate dehydratase OS=Thermus aquaticus Y51MC23 GN=hisB PE=3 SV=1
Thfi_0085	7,877	0,830	0,007	0,451	249,64	223,83	307,87	360,15	352,33	651,9	tr|G8NB16|G8NB16_9DEIN ABC transporter, permease protein OS=Thermus sp. CCB_US3_UF1
Thfi_0087	5,849	1,509	0,009	0,451	67,61	29,26	33,34	99,73	175,92	107,56	tr|E8PMX8|E8PMX8_THESS Glutamine-fructose-6-phosphate transaminase OS=Thermus scotoductus
Thfi_0091	7,472	0,668	0,018	0,539	322,98	383,92	415,91	530,19	608,25	643,23	tr|B7A624|B7A624_THEAQ Putative Holliday junction resolvase OS=Thermus aquaticus Y51MC23 GN=TaqDRAFT_4893 PE=3 SV=1
Thfi_0103	5,597	-1,474	0,045	0,739	144,5	57,41	236,16	81,85	52,64	15,98	tr|F6DHW4|F6DHW4_THETG tRNA-specific 2-thiouridylase MnmA OS=Thermus thermophilus
Thfi_0104	4,810	-1,804	0,044	0,739	11,87	38,2	43,31	8,09	0	15,72	tr|E8PQF6|E8PQF6_THESS Uncharacterized protein OS=Thermus scotoductus
Thfi_0113	8,586	0,504	0,030	0,653	315,43	376,04	511,53	501,78	568,71	611,23	tr|E8PJH7|E8PJH7_THESS Phosphate ABC transporter, ATP-binding protein OS=Thermus scotoductus
Thfi_0200	6,464	2,257	0,000	0,005	41,17	49,24	74,94	154,03	269,74	382,22	tr|Q5SIP2|Q5SIP2_THET8 Uncharacterized protein OS=Thermus thermophilus
Thfi_0202	7,304	0,847	0,005	0,413	87,08	89,53	93,96	140,45	178,16	162,44	tr|E8PLH0|E8PLH0_THESS 16S rRNA M OS=Thermus scotoductus (strain ATCC 700910 / SA-01)
Thfi_0204	7,823	-0,973	0,001	0,189	1971,9	1458,33	1175,4	974,92	738,38	608,47	tr|E8PLH1|E8PLH1_THESS Stage V sporulation protein S OS=Thermus scotoductus (strain ATCC 700910 / SA-01) GN=TSC_c17060 PE=4 SV=1
Thfi_0205	7,815	0,727	0,018	0,539	229,77	648,28	441,05	607,17	837,29	779,45	tr|G8N8T2|G8N8T2_9DEIN Cyclase/dehydrase OS=Thermus sp. CCB_US3_UF1 GN=TCCBUS3UF1_15480 PE=4 SV=1
Thfi_0213	6,815	-0,951	0,003	0,372	116,84	77,81	119,26	51,6	49,88	54,58	tr|G8N8T9|G8N8T9_9DEIN SpoVR OS=Thermus sp. CCB_US3_UF1 GN=TCCBUS3UF1_15550 PE=4 SV=1
Thfi_0233	7,607	0,545	0,042	0,724	118,72	175,47	189,6	215,93	237,11	248,91	tr|H9ZRT7|H9ZRT7_THETH 33 kDa chaperonin
Thfi_0276	5,906	-1,329	0,036	0,709	128,94	180,76	58,75	87,82	0	53,41	tr|D7BIA8|D7BIA8_MEISD Dephospho-CoA kinase OS=Meiothermus silvanus
Thfi_0281	10,270	0,443	0,020	0,551	875,92	920,65	913	1211,31	1125,36	1282,61	tr|H9ZRS1|H9ZRS1_THETH Acetylornithine/acetyl-lysine aminotransferase
Thfi_0344	7,503	-0,704	0,013	0,460	184,64	173,11	168,6	100,8	134,02	83,09	tr|G8N8D1|G8N8D1_9DEIN Putative uncharacterized protein

FPKM											
Gene code	logCPM	logFC	PValue	FDR	Without H_2O_2			With H_2O_2			Top Hit Uniprot
Thfi_0351	5,985	0,990	0,046	0,744	19,87	20,12	13,61	23,74	36,03	46	tr|K7QZ72|K7QZ72_THEOS Uncharacterized protein OS=Thermus oshimai JL-2 GN=Theos_1080 PE=4 SV=1
Thfi_0375	8,198	-0,598	0,021	0,557	554,28	588,7	573,49	489,85	348,57	277,94	tr|Q5SJV6|Q5SJV6_THET8 Zn-dependent protease OS=Thermus thermophilus (strain HB8 / ATCC 27634 / DSM 579) GN=TTHA0896 PE=4 SV=1
Thfi_0380	6,116	-1,030	0,019	0,541	58,37	74,07	83,74	39,83	30,27	33,12	tr|B7ABE6|B7ABE6_THEAQ Major facilitator superfamily MFS_1 OS=Thermus aquaticus Y51MC23 GN=TaqDRAFT_4588 PE=4 SV=1
Thfi_0436	6,748	-0,981	0,005	0,413	94,83	106,14	113,24	34,85	63,54	57,93	tr|E8PKC6|E8PKC6_THESS Outer membrane efflux protein OS=Thermus scotoductus
Thfi_0439	6,613	-0,884	0,013	0,460	140,29	113	157,54	66,23	54,87	92,9	tr|D7BAB3|D7BAB3_MEISD Binding-protein-dependent transport systems inner membrane component
Thfi_0448	9,173	0,492	0,028	0,652	1553,93	1099,57	1170,4	1468,79	1822,18	2013,98	tr|G8N9G7|G8N9G7_9DEIN Phospho-2-dehydro-3-deoxyheptonate aldolase OS=Thermus sp. CCB_US3_UF1
Thfi_0460	8,880	-0,661	0,003	0,315	601,87	479,53	475,23	360,73	289,32	312,24	tr|F6DFL5|F6DFL5_THETG Extracellular solute-binding protein family 1 OS=Thermus thermophilus
Thfi_0465	8,939	-0,471	0,035	0,709	1130,54	826,65	1134,63	669,48	858,07	662,42	tr|G8N8R7|G8N8R7_9DEIN Quinol-cytochrome c reductase, Rieske iron-sulfur subunit OS=Thermus sp. CCB_US3_UF1
Thfi_0485	7,053	-0,706	0,035	0,709	181,55	102,54	182,28	92,89	112,05	72,11	tr|Q5SLX0|Q5SLX0_THET8 Aminotransferase, class V OS=Thermus thermophilus
Thfi_0490	4,851	2,865	0,008	0,451	0	0	17,87	80,15	28,58	52,07	tr|G8NB72|G8NB72_9DEIN Putative uncharacterized protein OS=Thermus sp. CCB_US3_UF1
Thfi_0520	7,771	0,512	0,050	0,751	141,34	190,01	197,8	269,96	266,87	212,1	tr|E8PLA1|E8PLA1_THESS ABC transporter OS=Thermus scotoductus (strain ATCC 700910 / SA-01)
Thfi_0523	5,439	-1,664	0,012	0,460	74,12	118,46	101,25	25,22	0	61,43	tr|H9ZTW0|H9ZTW0_THETH Ribulose-5-phosphate 4-epimerase-like epimerase or aldolase
Thfi_0535	8,747	0,624	0,005	0,413	208,8	197,21	233,11	308,85	374,53	283,98	tr|H5SA76|H5SA76_9DEIN Hypothetical conserved protein OS=uncultured Thermus/Deinococcus group bacterium
Thfi_0571	11,651	0,898	0,000	0,001	2516,04	2482,78	2764,43	4811,54	4163,51	5242,6	tr|R5RG01|R5RG01_9BACE UDP-3-O-acylglucosamine N-acyltransferase
Thfi_0585	9,137	-0,424	0,045	0,739	2812,78	3479,56	2783,42	2137,05	2466,41	2188,45	tr|E8PNN6|E8PNN6_THESS 30S ribosomal protein S20 OS=Thermus scotoductus
Thfi_0599	5,293	1,728	0,032	0,677	17,55	0	47,95	71,67	51,06	93,05	tr|G8NBZ6|G8NBZ6_9DEIN Putative uncharacterized protein OS=Thermus sp. CCB_US3_UF1 GN=TCCBUS3UF1_21050 PE=4 SV=1
Thfi_0610	4,851	2,863	0,007	0,451	18,3	0	0	37,37	39,95	72,8	tr|Q5SIF1|Q5SIF1_THET8 Putative cytochrome c OS=Thermus thermophilus
Thfi_0620	6,764	1,101	0,001	0,189	270,41	460,28	293,42	656,82	909,81	720,76	tr|G8NA52|G8NA52_9DEIN Protein serine/threonine phosphatase
Thfi_0623	5,598	1,317	0,034	0,707	28,63	30,79	0	32,55	62,38	56,87	tr|Q72KZ6|Q72KZ6_THET2 Nucleotidyltransferase OS=Thermus thermophilus
Thfi_0654	5,447	2,453	0,010	0,451	0	0	52,93	26,37	141,03	141,32	tr|G8N8S8|G8N8S8_9DEIN Putative uncharacterized protein
Thfi_0660	6,760	1,193	0,001	0,189	50,29	121,29	57,33	154,25	210,14	174,88	tr|F2NQ38|F2NQ38_MARHT Uncharacterized protein OS=Marinithermus hydrothermalis
Thfi_0684	7,435	0,731	0,041	0,724	480,97	216,27	685,91	722,11	576,75	936,12	tr|F6DHY7|F6DHY7_THETG Uncharacterized protein OS=Thermus thermophilus
Thfi_0730	8,484	0,633	0,009	0,451	937,96	686,11	606,08	1123,96	1187,08	1097,47	tr|F6DD49|F6DD49_THETG Uncharacterized protein OS=Thermus thermophilus

					FPKM						
Gene code	logCPM	logFC	PValue	FDR	Without H_2O_2			With H_2O_2			Top Hit Uniprot
Thfi_0731	9,639	0,452	0,036	0,709	1162,05	999,07	885,01	1462,62	1232,27	1403,82	tr|G8NAC2|G8NAC2_9DEIN Putative uncharacterized protein OS=Thermus sp. CCB_US3_UF1
Thfi_0773	9,265	0,751	0,000	0,059	577,09	498,26	479,57	822,27	860,77	887,04	tr|B7A8I8|B7A8I8_THEAQ Methionyl-tRNA formyltransferase OS=Thermus aquaticus Y51MC23 GN=fmt PE=3 SV=1
Thfi_0783	5,827	-1,330	0,012	0,454	94,38	59,14	76,55	28,61	53,33	6,94	tr|K7QYD9|K7QYD9_THEOS Sphingosine/diacylglycerol kinase-like enzyme (Precursor) OS=Thermus oshimai JL-2
Thfi_0791	7,864	0,929	0,016	0,497	210,33	887,57	952,92	797,09	1598,13	1595,22	tr|D3PT69|D3PT69_MEIRD Pyruvate kinase OS=Meiothermus ruber (strain ATCC 35948 / DSM 1279 / VKM B-1258 / 21)
Thfi_0803	7,199	0,672	0,047	0,751	523,72	493,68	946,54	823,74	1106,96	1202,7	tr|E8PRA0|E8PRA0_THESS Uncharacterized protein OS=Thermus scotoductus (strain ATCC 700910 / SA-01)
Thfi_0822	12,846	0,645	0,011	0,454	4473,35	6673,98	4596,38	9700,82	8998,51	5469,56	tr|E8PJW4|E8PJW4_THESS Elongation factor Tu OS=Thermus scotoductus (strain ATCC 700910 / SA-01) GN=tuf1 PE=3 SV=1
Thfi_0831	9,459	0,610	0,016	0,497	258,8	523,06	538,31	520,07	714,83	756,47	tr|E8PL68|E8PL68_THESS Coenzyme A disulfide reductase OS=Thermus scotoductus (strain ATCC 700910 / SA-01)
Thfi_0862	10,551	0,401	0,048	0,751	1580,62	2019,94	1996,69	2269,36	2222,21	2797,77	tr|B8HJZ9|B8HJZ9_CYAP4 Uncharacterized protein OS=Cyanothece sp. (strain PCC 7425 / ATCC 29141)
Thfi_0879	8,877	0,654	0,008	0,451	665,73	787,04	1094,48	964,03	1516,87	1495,65	tr|K7R1I7|K7R1I7_THEOS Uncharacterized protein OS=Thermus oshimai JL-2 GN=Theos_2197 PE=4 SV=1
Thfi_0881	8,167	0,519	0,039	0,724	430,75	437,75	377,38	496,4	554,35	713,74	tr|E8PQY5|E8PQY5_THESS Glycerophosphoryl diester phosphodiesterase OS=Thermus scotoductus
Thfi_0892	10,340	0,518	0,007	0,451	959,41	818,06	917,42	1216,66	1354,43	1214,96	tr|F6DH47|F6DH47_THETG Enolase OS=Thermus thermophilus (strain SG0.5JP17-16) GN=eno PE=3 SV=1
Thfi_0909	10,455	0,486	0,019	0,541	769,78	1089,4	822,25	1229,06	1321,84	1150,74	tr|F6DHZ4|F6DHZ4_THETG Dihydrolipoyl dehydrogenase OS=Thermus thermophilus
Thfi_0934	10,233	0,492	0,019	0,541	1601,87	2109,55	1546,48	2214,42	2364,6	2753,8	tr|H9ZP13|H9ZP13_THETH Octanoyltransferase OS=Thermus thermophilus JL-18 GN=lipB PE=3 SV=1
Thfi_0936	9,601	-0,599	0,010	0,453	4054,23	5836,64	3712,38	2952,72	3028,01	3054,08	tr|B7A903|B7A903_THEAQ 30S ribosomal protein S18 OS=Thermus aquaticus Y51MC23 GN=rpsR PE=3 SV=1
Thfi_0939	6,854	0,907	0,010	0,452	101,87	81,89	116,13	182,26	138,81	227,74	tr|G8N8Q8|G8N8Q8_9DEIN Putative uncharacterized protein OS=Thermus sp. CCB_US3_UF1
Thfi_0954	4,852	2,862	0,008	0,451	16,03	0	0	65,51	23,32	42,5	tr|K7R0Q5|K7R0Q5_THEOS Uncharacterized protein OS=Thermus oshimai JL-2 GN=Theos_1844 PE=4 SV=1
Thfi_0971	9,468	1,437	0,000	0,001	1241,79	1399,02	2181,51	2812,23	5696,64	4541,96	tr|F6DDS0|F6DDS0_THETG Uncharacterized protein OS=Thermus thermophilus
Thfi_1049	6,587	-0,829	0,045	0,739	195,8	74,74	112,84	63,25	82,33	61,41	tr|E8PNX3|E8PNX3_THESS Sensory transduction protein kinase OS=Thermus scotoductus
Thfi_1050	7,428	0,664	0,039	0,724	279,51	136,91	226,43	317,31	406,54	267,55	tr|B7AA84|B7AA84_THEAQ L-serine dehydratase, iron-sulfur-dependent, beta subunit
Thfi_1090	12,045	0,428	0,049	0,751	3162,31	3068,95	3586,82	3176,13	4222,43	5601,25	tr|K7QUM3|K7QUM3_THEOS ABC-type transport system, involved in lipoprotein release, permease component
Thfi_1095	5,090	-2,422	0,003	0,372	17,06	34,43	54,51	5,82	6,19	5,65	tr|E8PL11|E8PL11_THESS ATPase associated with various cellular activities, AAA_3 OS=Thermus scotoductus
Thfi_1103	6,857	-0,760	0,023	0,577	298,16	188,64	214,51	128,26	125,54	145,59	tr|G2SLI0|G2SLI0_RHOMR Type III restriction protein res subunit OS=Rhodothermus marinus SG0.5JP17-172 GN=Rhom172_2839 PE=4 SV=1
Thfi_1112	5,763	-1,997	0,001	0,189	13,61	27,62	37,32	4,65	9,87	4,5	tr|D7BCR2|D7BCR2_MEISD Conserved repeat domain protein (Precursor) OS=Meiothermus silvanus

					FPKM						
Gene code	logCPM	logFC	PValue	FDR	Without H_2O_2			With H_2O_2			Top Hit Uniprot
Thfi_1117	9,404	-0,503	0,042	0,724	810,39	472,83	479,26	399	337,44	479,13	tr|E8PR76|E8PR76_THESS Betaine aldehyde dehydrogenase OS=Thermus scotoductus
Thfi_1129	7,270	0,904	0,005	0,413	101,78	75,32	100,66	162,03	141,63	202,11	tr|Q746D8|Q746D8_THET2 Hypothetical conserved protein OS=Thermus thermophilus
Thfi_1135	9,190	-0,559	0,007	0,451	781,13	704,33	637,47	501,51	487,13	425,86	tr|H9ZSL3|H9ZSL3_THETH Tetratricopeptide repeat protein (Precursor) OS=Thermus thermophilus JL-18 GN=TtJL18_1440 PE=4 SV=1
Thfi_1140	6,320	1,276	0,008	0,451	41,49	227,05	225,57	308,85	363,69	579,57	tr|K7R5E7|K7R5E7_THEOS UDP-N-acetylenolpyruvoylglucosamine reductase
Thfi_1141	8,314	-0,496	0,030	0,664	1149,28	1113,74	1200,89	741,32	712,39	973,04	tr|F6DFA3|F6DFA3_THETG Nucleotidyltransferase substrate binding protein, HI0074 family OS=Thermus thermophilus
Thfi_1145	6,354	0,932	0,033	0,704	62,21	43,03	32,45	72,76	90,34	94,13	tr|E8PPF0|E8PPF0_THESS Glycosyltransferase OS=Thermus scotoductus (strain ATCC 700910 / SA-01)
Thfi_1146	13,182	0,418	0,022	0,577	3848,47	3155,8	3316,97	4581,1	4044,21	4892,72	tr|B7AAG6|B7AAG6_THEAQ Lon protease OS=Thermus aquaticus Y51MC23 GN=lon PE=3 SV=1
Thfi_1185	6,803	0,737	0,029	0,652	143,76	172,41	114,57	220,19	287,66	214,43	tr|F2NLC3|F2NLC3_MARHT Uncharacterized protein OS=Marinithermus hydrothermalis
Thfi_1218	7,342	-0,658	0,029	0,652	276,83	222,9	191,94	128,36	176,97	124,66	tr|E8PM51|E8PM51_THESS Branched-chain amino acid ABC transporter, permease protein OS=Thermus scotoductus (strain ATCC 700910 / SA-01)
Thfi_1219	7,701	-0,640	0,011	0,454	245,84	227,74	265,95	173,92	138,84	150,69	tr|Q5SL43|Q5SL43_THET8 Branched-chain amino acid ABC transporter, permease protein OS=Thermus thermophilus
Thfi_1231	6,099	-0,994	0,040	0,724	189,96	82,06	106,56	89,6	31,87	58,09	tr|G8NCP4|G8NCP4_9DEIN Phytoene synthase-related protein OS=Thermus sp. CCB_US3_UF1
Thfi_1241	8,056	-0,723	0,003	0,315	663,42	774,73	925,64	481,24	434,84	498,76	tr|G8NCQ8|G8NCQ8_9DEIN Flavin reductase domain protein FMN-binding protein OS=Thermus sp. CCB_US3_UF1 GN=TCCBUS3UF1_10260 PE=4 SV=1
Thfi_1246	10,624	-0,652	0,002	0,206	3944,26	3086,78	3014,39	2316,39	1993,27	1975,77	tr|K7QXH2|K7QXH2_THEOS Uncharacterized protein (Precursor) OS=Thermus oshimai JL-2 GN=Theos_1458
Thfi_1251	7,035	0,853	0,015	0,497	57,29	138,33	114,97	203,1	133,19	227,63	tr|E8PK46|E8PK46_THESS Phosphonate ABC transporter, periplasmic phosphonate-binding protein
Thfi_1281	8,065	0,744	0,018	0,539	1392,78	1845,77	1255,99	3397,96	2630,15	1615,78	tr|E8PR29|E8PR29_THESS Cold shock protein, CSD family OS=Thermus scotoductus (strain ATCC 700910 / SA-01)
Thfi_1288	6,711	-0,765	0,042	0,724	250,46	316,15	246,97	227,18	136,77	110,74	tr|F2NLA3|F2NLA3_MARHT CRISPR-associated protein, Cse2 family OS=Marinithermus hydrothermalis
Thfi_1323	5,728	1,308	0,024	0,596	64,27	126,71	29,18	152,62	257,94	170,81	tr|B7AA29|B7AA29_THEAQ Transcriptional regulator, MerR family OS=Thermus aquaticus Y51MC23
Thfi_1334	9,849	-0,454	0,024	0,596	880,51	950,62	946,23	739,1	605,23	644,67	tr|G8ND43|G8ND43_9DEIN Extracellular solute-binding protein family 1
Thfi_1350	4,816	-2,452	0,023	0,577	40,27	32,35	48,96	9,15	0	8,89	tr|E8PMI3|E8PMI3_THESS Mn2+/Zn2+ ABC transporter, ATP-binding protein OS=Thermus scotoductus
Thfi_1361	9,444	0,397	0,049	0,751	644,84	619,51	623,15	756,82	729,97	954,28	tr|G8N9W8|G8N9W8_9DEIN Alcohol dehydrogenase OS=Thermus sp. CCB_US3_UF1
Thfi_1373	6,521	-0,879	0,022	0,577	186,46	208,58	254,71	164,99	81,42	98,9	tr|Q745Z1|Q745Z1_THET2 RNA polymerase sigma factor OS=Thermus thermophilus
Thfi_1419	7,645	-0,744	0,005	0,413	447,32	437,75	437,76	293,33	228,97	252,56	tr|G8N8Z2|G8N8Z2_9DEIN Thiol:disulfide interchange protein dsbA
Thfi_1424	10,041	-0,702	0,001	0,189	3905,91	2662,22	3227,14	1923,34	2256,25	1757,22	tr|F6DG85|F6DG85_THETG Outer membrane chaperone Skp (OmpH) (Precursor)

					FPKM						
Gene code	**logCPM**	**logFC**	**PValue**	**FDR**	**Without H_2O_2**			**With H_2O_2**			**Top Hit Uniprot**
Thfi_1431	7,182	-0,794	0,013	0,460	286,89	397,13	400,57	208,26	264,49	152,18	tr|H9ZR97|H9ZR97_THETH Uncharacterized protein (Precursor) OS=Thermus thermophilus JL-18 GN=TtJL18_0957 PE=4 SV=1
Thfi_1457	9,896	0,550	0,007	0,451	1081,35	1448,81	1421,96	1809,84	1999,61	1914,29	tr|R6S6T5|R6S6T5_9BACE TPR-domain containing protein OS=Bacteroides finegoldii CAG:203 GN=BN532_01025
Thfi_1459	6,188	2,515	0,000	0,001	125,89	48,37	170,52	508,6	783,14	713,83	tr|H7GI01|H7GI01_9DEIN Orotate phosphoribosyltransferase OS=Thermus sp. RL GN=pyrE PE=3 SV=1
Thfi_1463	7,205	0,688	0,040	0,724	92,77	115,76	76,99	132,34	116,33	206,55	tr|E8PKJ6|E8PKJ6_THESS Arginine biosynthesis bifunctional protein ArgJ OS=Thermus scotoductus
Thfi_1466	7,410	0,798	0,009	0,451	695,39	462,81	719,15	1174,21	1162,16	893,16	tr|Q72JE0|Q72JE0_THET2 Uncharacterized protein OS=Thermus thermophilus
Thfi_1517	9,117	-0,468	0,038	0,724	924,48	734,95	780,89	723,7	472,65	529,09	tr|G8NC60|G8NC60_9DEIN Succinyl-CoA ligase [ADP-forming] subunit alpha OS=Thermus sp. CCB_US3_UF1
Thfi_1549	12,136	-0,423	0,047	0,749	3573,95	5778,73	5087,2	3264,58	3925,1	3397,57	tr|K7QW00|K7QW00_THEOS ABC-type branched-chain amino acid transport system, periplasmic component (Precursor)
Thfi_1552	5,116	1,852	0,049	0,751	50,2	19,93	0	85,28	91,46	83,29	tr|F6DEW5|F6DEW5_THETG Acylphosphatase OS=Thermus thermophilus (strain SG0.5JP17-16)
Thfi_1606	9,362	0,462	0,019	0,541	412,54	509,61	553,89	645,78	704,68	653,21	tr|E8PN49|E8PN49_THESS Acetyl-CoA acyltransferase OS=Thermus scotoductus
Thfi_1617	5,867	1,785	0,001	0,189	99,34	154,27	44,95	234,84	363,17	496,2	tr|B7A5K4|B7A5K4_THEAQ Cytochrome c biogenesis protein transmembrane region OS=Thermus aquaticus Y51MC23
Thfi_1625	6,814	0,686	0,046	0,744	62,07	109,81	135,87	186,17	135,32	172,68	tr|K7RGA5|K7RGA5_THEOS Phosphotransferase family protein (Precursor) OS=Thermus oshimai JL-2 GN=Theos_0533
Thfi_1686	8,079	0,757	0,012	0,454	257,31	126,04	209,7	394,94	340,33	237,27	tr|E8PNF1|E8PNF1_THESS Zinc-dependent peptidase OS=Thermus scotoductus (strain ATCC 700910 / SA-01
Thfi_1689	7,498	0,629	0,035	0,709	99,26	184,05	144,94	169,26	252,33	243,17	tr|G8N9D0|G8N9D0_9DEIN Putative uncharacterized protein OS=Thermus sp. CCB_US3_UF1 GN=TCCBUS3UF1_16650
Thfi_1700	7,953	-0,749	0,012	0,454	1951,34	3317,6	1962,31	1612,84	1538,87	1253,51	tr|K7QWH2|K7QWH2_THEOS 50S ribosomal protein L35 OS=Thermus oshimai JL-2 GN=rpmI PE=3 SV=1
Thfi_1737	7,971	0,587	0,027	0,629	210,17	298,25	270,62	387,65	296,47	474,94	tr|G8N9Y5|G8N9Y5_9DEIN Menaquinone biosynthetic enzyme OS=Thermus sp. CCB_US3_UF1 GN=TCCBUS3UF1_5080
Thfi_1744	8,380	0,714	0,011	0,454	230,93	390,29	305,45	432,97	679,51	405,28	tr|G8N9Z3|G8N9Z3_9DEIN DNA/pantothenate metabolism flavoprotein OS=Thermus sp. CCB_US3_UF1
Thfi_1781	7,786	0,612	0,041	0,724	224,16	275,45	216,43	458,31	383,35	244,57	tr|G8N9N5|G8N9N5_9DEIN Methionine aminopeptidase OS=Thermus sp. CCB_US3_UF1 GN=map PE=3 SV=1
Thfi_1811	9,357	-0,500	0,013	0,460	2324,67	2956,16	3105,02	1982,1	1890,39	2030,2	tr|B7A584|B7A584_THEAQ 50S ribosomal protein L17 OS=Thermus aquaticus Y51MC23 GN=rplQ PE=3 SV=1
Thfi_1823	4,987	-1,717	0,037	0,720	81,77	48,91	74,43	0	44,65	13,56	tr|B7A8G0|B7A8G0_THEAQ Putative transcriptional regulator OS=Thermus aquaticus Y51MC23 GN=TaqDRAFT_3913
Thfi_1836	10,250	0,445	0,031	0,664	1408,84	1534,09	1716,87	1892,8	1851,19	2503,8	tr|E8PKB9|E8PKB9_THESS Chlorite dismutase OS=Thermus scotoductus (strain ATCC 700910 / SA-01)
Thfi_1868	7,902	0,780	0,024	0,596	612	427,8	311,69	549,06	588,63	1153,39	tr|Q72IM3|Q72IM3_THET2 Uncharacterized protein OS=Thermus thermophilus (strain HB27 / ATCC BAA-163 / DSM 7039) GN=TT_C1109 PE=4 SV=1
Thfi_1938	7,247	0,833	0,020	0,551	117,02	295,81	213,09	265,43	496,84	375,03	tr|B7A9J0|B7A9J0_THEAQ FAD-dependent pyridine nucleotide-disulphide oxidoreductase OS=Thermus aquaticus Y51MC23
Thfi_1987	8,146	-0,536	0,019	0,541	920,91	889,33	882,73	608,94	562,26	660,71	tr|K7R4D1|K7R4D1_THEOS Uncharacterized protein (Precursor) OS=Thermus oshimai JL-2 GN=Theos_0693 PE=4 SV=1
					FPKM						

Gene code	logCPM	logFC	PValue	FDR	Without H_2O_2			With H_2O_2			Top Hit Uniprot
Thfi_1992	10,325	-0,420	0,037	0,720	1472,14	1077,3	1470,25	926,79	1003,77	1012,1	tr|E8PNA5|E8PNA5_THESS Uncharacterized protein OS=Thermus scotoductus
Thfi_1997	9,818	0,762	0,001	0,151	1735,74	1354,51	1225,25	2495,02	2640,36	2082,06	tr|H9ZQ50|H9ZQ50_THETH Protein GrpE
Thfi_1998	14,132	0,382	0,042	0,724	9928,17	9009,38	7911,81	12827,97	10705,65	10801,2	tr|B7A6Y3|B7A6Y3_THEAQ Chaperone protein DnaK OS=Thermus aquaticus Y51MC23 GN=dnaK PE=3 SV=1
Thfi_2035	8,215	-0,610	0,010	0,451	398,51	422,46	401,89	207,4	312,31	270,81	tr|E8PPM1|E8PPM1_THESS Proline dehydrogenase/delta-1-pyrroline-5-carboxylate dehydrogenase
Thfi_2037	8,098	0,517	0,029	0,652	144,67	161,56	188,74	244,5	214,99	237,06	tr|F6DFJ7|F6DFJ7_THETG Anthranilate synthase component I OS=Thermus thermophilus
Thfi_2049	9,518	0,578	0,010	0,451	397,53	385,14	390,63	538,66	708,02	474,27	tr|H5SND6|H5SND6_9DEIN Dak phosphatase GN=HGMM_F51G12C41 PE=4 SV=1
Thfi_2072	8,941	-0,643	0,005	0,413	1834,3	1641,64	1691,42	1388,62	878,62	991,45	tr|G8N948|G8N948_9DEIN Osmotically inducible protein C OS=Thermus sp. CCB_US3_UF1
Thfi_2082	7,895	0,680	0,008	0,451	135,89	120,89	136,51	171,59	212,03	233,81	tr|H9ZSZ9|H9ZSZ9_THETH 2-phosphoglycerate kinase (Precursor) OS=Thermus thermophilus JL-18
Thfi_2089	6,422	-0,779	0,040	0,724	165,67	172,45	181,14	78,97	84,36	131,77	tr|G8NAI9|G8NAI9_9DEIN Putative uncharacterized protein OS=Thermus sp. CCB_US3_UF1
Thfi_2103	5,515	-1,317	0,044	0,739	47,58	88,96	115,62	10,8	46,14	42,04	tr|B7A7H2|B7A7H2_THEAQ Cell wall hydrolase/autolysin (Precursor) OS=Thermus aquaticus Y51MC23
Thfi_2105	7,566	1,060	0,000	0,086	159,65	171,01	169,84	326,4	290,1	414,22	tr|F6DF67|F6DF67_THETG Preprotein translocase, SecG subunit OS=Thermus thermophilus
Thfi_2126	5,727	-1,327	0,014	0,460	121,39	124,86	94,78	35,42	50,46	45,98	tr|E8PNU4|E8PNU4_THESS Hydrolase family protein OS=Thermus scotoductus
Thfi_2128	8,245	-0,565	0,033	0,704	994,79	712,54	683,81	635,38	546,85	403,91	tr|F6DEA1|F6DEA1_THETG Phosphoribosyltransferase OS=Thermus thermophilus
Thfi_2131	7,397	0,687	0,017	0,539	400,92	515,26	495,94	617,49	878,15	799,58	tr|Q5SHW3|Q5SHW3_THET8 Probable HIT family protein OS=Thermus thermophilus
Thfi_2135	7,752	0,670	0,042	0,724	459,71	545,51	469,91	448,69	796,2	1106,6	tr|H9ZPZ7|H9ZPZ7_THETH Uncharacterized protein OS=Thermus thermophilus JL-18 GN=TtJL18_0499
Thfi_2143	8,829	1,236	0,000	0,001	277,63	597,89	386,28	1095,07	924,29	958,5	tr|H7GF52|H7GF52_9DEIN Uncharacterized protein OS=Thermus sp. RL GN=RLTM_03696 PE=4 SV=1
Thfi_2155	8,598	0,462	0,050	0,751	1094,74	795,17	1236,42	1486,31	1251,63	1493,4	tr|B7A6R2|B7A6R2_THEAQ NADH dehydrogenase (Quinone) OS=Thermus aquaticus Y51MC23 GN=TaqDRAFT_4511
Thfi_2198	8,397	-0,519	0,023	0,577	300,85	275,13	274,77	169,64	204,09	207,74	tr|K7QZ08|K7QZ08_THEOS 4-hydroxyphenylacetate 3-monooxygenase, oxygenase component OS=Thermus oshimai
Thfi_2210	6,541	0,823	0,027	0,641	65,06	83,66	94,93	141,9	141,86	146,54	tr|D3PP09|D3PP09_MEIRD DeoR family transcriptional regulator OS=Meiothermus ruber
Thfi_2264	7,526	1,003	0,001	0,189	125,79	215,52	327,35	403,68	496,86	440,78	tr|H9ZTT4|H9ZTT4_THETH Transposase OS=Thermus thermophilus JL-18 GN=TtJL18_1880 PE=4 SV=1
Thfi_2296	9,987	0,551	0,009	0,451	1591,54	2111,43	1702,54	2869,75	2273,63	2704,47	tr|K7RGN4|K7RGN4_THEOS Putative metal-binding protein, possibly nucleic-acid binding protein
Thfi_2334	7,952	-0,725	0,009	0,451	528,32	315,52	518,77	304,64	206,78	287,17	tr|H9ZSF1|H9ZSF1_THETH 3-hydroxybutyrate dehydrogenase (Precursor) OS=Thermus thermophilus JL-18
Thfi_2343	7,168	-0,827	0,010	0,453	227	315,5	317,24	206,18	121,05	150,42	tr|F6DI73|F6DI73_THETG Uncharacterized protein (Precursor) OS=Thermus thermophilus
Thfi_2351	6,732	-0,726	0,038	0,720	461,73	322,78	296,24	166,03	257,41	216,37	tr|F6DIN0|F6DIN0_THETG Helix-turn-helix domain protein OS=Thermus thermophilus
Thfi_2402	6,508	-1,025	0,006	0,451	74,86	65,63	85,47	21,29	45,27	41,28	tr|E8PNS4|E8PNS4_THESS Two-component response regulator

FPKM: Fragments per kilobase of exon per million fragments mapped; CPM: counts per million reads; FC: Fold change; FDR: false discovery rate.

Table S5: Differently expressed proteins in temperature assay.

		Quantitative value						
Gene code	T Test (P-Value)	63 ºC			77 ºC			Top Hit Uniprot
Thfi_0025	95% (0,035)	0	2	2	4	4	3	tr|H7GDU4|H7GDU4_9DEIN Bifunctional purine biosynthesis protein PurH OS=Thermus sp. RL GN=purH PE=3 SV=1
Thfi_0031	95% (0,023)	0	0	0	9	3	7	tr|Q72JJ7|Q72JJ7_THET2 Metal dependent hydrolase OS=Thermus thermophilus (strain HB27 / ATCC BAA-163 / DSM 7039) GN=TT_C0775 PE=1 SV=1
Thfi_0063	95% (0,047)	2	1	2	0	0	1	tr|E4U6W5|E4U6W5_OCEP5 Alpha-glucosidase OS=Oceanithermus profundus (strain DSM 14977 / NBRC 100410 / VKM B-2274 / 506) GN=Ocepr_0509 PE=4 SV=1
Thfi_0069	95% (0,012)	0	1	4	11	17	22	tr|H0BHA6|H0BHA6_9ACTO Putative integral membrane protein OS=Streptomyces sp. W007 GN=SPW_4644 PE=4 SV=1
Thfi_0080	95% (0,033)	3	0	2	4	7	6	tr|K7R7Y9|K7R7Y9_THEOS Pyruvate/2-oxoglutarate dehydrogenase complex, dihydrolipoamide acyltransferase component OS=Thermus oshimai JL-2 GN=Theos_2160 PE=3 SV=1
Thfi_0090	95% (0,0022)	0	0	0	2	3	2	tr|E8PL75|E8PL75_THESS Putative membrane protein OS=Thermus scotoductus (strain ATCC 700910 / SA-01) GN=TSC_c04020 PE=4 SV=1
Thfi_0096	95% (0,026)	1	3	2	4	4	4	tr|E8PQ70|E8PQ70_THESS Universal stress protein OS=Thermus scotoductus (strain ATCC 700910 / SA-01) GN=TSC_c23890 PE=3 SV=1
Thfi_0136	95% (0,011)	12	19	12	5	2	1	tr|Q72KS1|Q72KS1_THET2 ABC transporter substrate-binding protein (Taurine) OS=Thermus thermophilus (strain HB27 / ATCC BAA-163 / DSM 7039) GN=TT_C0421 PE=4 SV=1
Thfi_0156	95% (0,013)	0	1	1	3	2	3	tr|E8PMF8|E8PMF8_THESS Uncharacterized protein OS=Thermus scotoductus (strain ATCC 700910 / SA-01) GN=TSC_c18860 PE=4 SV=1
Thfi_0201	95% (0,0075)	0	0	0	1	2	2	tr|H9ZRX7|H9ZRX7_THETH Pyrroline-5-carboxylate reductase OS=Thermus thermophilus JL-18 GN=TtJL18_1195 PE=3 SV=1
Thfi_0223	95% (0,016)	1	1	2	0	0	0	tr|F6DEZ9|F6DEZ9_THETG PpiC-type peptidyl-prolyl cis-trans isomerase (Precursor) OS=Thermus thermophilus (strain SG0.5JP17-16) GN=Ththe16_0606 PE=4 SV=1
Thfi_0232	95% (0,016)	0	0	0	1	1	2	tr|F6DGF5|F6DGF5_THETG Universal stress protein OS=Thermus thermophilus (strain SG0.5JP17-16) GN=Ththe16_0896 PE=3 SV=1
Thfi_0234	95% (0,0011)	2	2	1	5	6	6	tr|E8PRA8|E8PRA8_THESS Cysteine--tRNA ligase OS=Thermus scotoductus (strain ATCC 700910 / SA-01) GN=cysS PE=3 SV=1
Thfi_0266	95% (0,026)	4	2	3	1	1	1	tr|D7BGL6|D7BGL6_MEISD ABC-2 type transporter (Precursor) OS=Meiothermus silvanus (strain ATCC 700542 / DSM 9946 / VI-R2) GN=Mesil_1957 PE=4 SV=1
Thfi_0290	95% (0,021)	2	0	1	5	4	3	tr|G8N809|G8N809_9DEIN UPF0365 protein TCCBUS3UF1_14350 OS=Thermus sp. CCB_US3_UF1 GN=TCCBUS3UF1_14350 PE=3 SV=1
Thfi_0298	95% (0,047)	1	0	0	2	1	2	tr|E8PP08|E8PP08_THESS Anti-cleavage anti-GreA transcription factor Gfh1 OS=Thermus scotoductus (strain ATCC 700910 / SA-01) GN=TSC_c09290 PE=4 SV=1
Thfi_0309	95% (0,0058)	6	4	4	1	0	1	tr|F6DF87|F6DF87_THETG ATP-dependent Clp protease ATP-binding subunit ClpX OS=Thermus thermophilus (strain SG0.5JP17-16) GN=clpX PE=3 SV=1
Thfi_0324	95% (0,00012)	10	8	13	35	34	37	tr|Q72GH6|Q72GH6_THET2 Pseudocatalase OS=Thermus thermophilus (strain HB27 / ATCC BAA-163 / DSM 7039) GN=TT_C1872 PE=4 SV=1
Thfi_0325	95% (0,030)	3	3	4	18	14	32	tr|K7QTP0|K7QTP0_THEOS Mn-containing catalase OS=Thermus oshimai JL-2 GN=Theos_0243 PE=4 SV=1
Thfi_0335	95% (0,047)	0	0	1	2	1	2	tr|E8PK21|E8PK21_THESS Glutamyl-tRNA(Gln) amidotransferase subunit A OS=Thermus scotoductus (strain ATCC 700910 / SA-01) GN=gatA PE=3 SV=1
Thfi_0344	95% (0,026)	0	0	0	3	2	1	tr|G8N8D1|G8N8D1_9DEIN Putative uncharacterized protein OS=Thermus sp. CCB_US3_UF1 GN=TCCBUS3UF1_14760 PE=4 SV=1
Thfi_0345	95% (0,024)	0	1	1	2	3	2	tr|B7AA76|B7AA76_THEAQ Putative uncharacterized protein (Precursor) OS=Thermus aquaticus Y51MC23 GN=TaqDRAFT_3843 PE=4 SV=1
Thfi_0346	95% (0,016)	0	0	0	5	2	5	tr|F2NMA1|F2NMA1_MARHT Efflux transporter, RND family, MFP subunit OS=Marinithermus hydrothermalis (strain DSM 14884 / JCM 11576 / T1) GN=Marky_1047 PE=4 SV=1
Thfi_0350	95% (0,0083)	14	20	17	44	44	31	tr|K7QVD4|K7QVD4_THEOS Aconitate hydratase 1 OS=Thermus oshimai JL-2 GN=Theos_1424 PE=4 SV=1

		Quantitative value						
Gene code	T Test (P-Value)	63 °C			77 °C			Top Hit Uniprot
Thfi_0414	95% (0,024)	1	1	2	3	5	6	tr|B7A6T1|B7A6T1_THEAQ Oligopeptide/dipeptide ABC transporter, ATPase subunit OS=Thermus aquaticus Y51MC23 GN=TaqDRAFT_4530 PE=3 SV=1
Thfi_0423	95% (0,016)	1	2	1	0	0	0	tr|E8PMZ1|E8PMZ1_THESS Type 4 fimbrial assembly protein PilC OS=Thermus scotoductus (strain ATCC 700910 / SA-01) GN=pilC PE=3 SV=1
Thfi_0428	95% (0,0033)	3	4	4	7	9	9	tr|H7GHA4|H7GHA4_9DEIN Long-chain-fatty-acid-CoA ligase OS=Thermus sp. RL GN=RLTM_08162 PE=4 SV=1
Thfi_0429	95% (0,0078)	0	0	1	3	2	3	tr|E8PMH9|E8PMH9_THESS Long-chain-fatty-acid--CoA ligase OS=Thermus scotoductus (strain ATCC 700910 / SA-01) GN=TSC_c19070 PE=4 SV=1
Thfi_0431	95% (0,047)	0	1	0	1	2	2	tr|E8PKD1|E8PKD1_THESS Uncharacterized protein OS=Thermus scotoductus (strain ATCC 700910 / SA-01) GN=TSC_c02630 PE=4 SV=1
Thfi_0435	95% (0,015)	0	1	0	17	16	7	tr|E8PKC7|E8PKC7_THESS Outer membrane efflux protein OS=Thermus scotoductus (strain ATCC 700910 / SA-01) GN=TSC_c02590 PE=4 SV=1
Thfi_0436	95% (0,047)	0	1	1	3	2	5	tr|E8PKC6|E8PKC6_THESS Outer membrane efflux protein OS=Thermus scotoductus (strain ATCC 700910 / SA-01) GN=TSC_c02580 PE=4 SV=1
Thfi_0499	95% (0,00045)	2	3	2	7	8	7	tr|Q9RHA2|Q9RHA2_THEAQ Fructose-1,6-bisphosphate aldolase OS=Thermus aquaticus PE=1 SV=1
Thfi_0517	95% (0,025)	6	7	6	4	3	5	tr|K7QV57|K7QV57_THEOS Prepilin-type N-terminal cleavage/methylation domain-containing protein (Precursor) OS=Thermus oshimai JL-2 GN=Theos_1240 PE=4 SV=1
Thfi_0529	95% (0,033)	0	2	4	5	7	8	tr|B7A503|B7A503_THEAQ Cell shape determining protein, MreB/Mrl family OS=Thermus aquaticus Y51MC23 GN=TaqDRAFT_4910 PE=4 SV=1
Thfi_0538	95% (0,0011)	5	5	4	1	0	1	tr|G8NCJ8|G8NCJ8_9DEIN Putative uncharacterized protein OS=Thermus sp. CCB_US3_UF1 GN=TCCBUS3UF1_22290 PE=4 SV=1
Thfi_0574	95% (0,024)	1	1	0	2	3	2	tr|D7BFA0|D7BFA0_MEISD Cytochrome c class I (Precursor) OS=Meiothermus silvanus (strain ATCC 700542 / DSM 9946 / VI-R2) GN=Mesil_1563 PE=4 SV=1
Thfi_0602	95% (0,016)	0	0	0	1	1	2	tr|E8PNQ1|E8PNQ1_THESS Sulfide dehydrogenase flavocytochrome C OS=Thermus scotoductus (strain ATCC 700910 / SA-01) GN=TSC_c21020 PE=4 SV=1
Thfi_0621	95% (0,033)	4	12	5	16	16	14	tr|K7R067|K7R067_THEOS Inosine-5'-monophosphate dehydrogenase OS=Thermus oshimai JL-2 GN=guaB PE=3 SV=1
Thfi_0653	95% (0,016)	0	0	0	2	1	1	tr|E8PKV7|E8PKV7_THESS Orotidine 5'-phosphate decarboxylase OS=Thermus scotoductus (strain ATCC 700910 / SA-01) GN=pyrF PE=3 SV=1
Thfi_0672	95% (0,047)	0	0	1	1	2	2	tr|B7A6J9|B7A6J9_THEAQ RNA polymerase sigma factor OS=Thermus aquaticus Y51MC23 GN=TaqDRAFT_4448 PE=3 SV=1
Thfi_0690	95% (0,037)	10	22	16	39	27	29	tr|B7A552|B7A552_THEAQ Elongation factor G OS=Thermus aquaticus Y51MC23 GN=fusA PE=3 SV=1
Thfi_0728	95% (0,013)	0	1	0	3	2	2	tr|G8NC04|G8NC04_9DEIN 50S ribosomal protein L10 OS=Thermus sp. CCB_US3_UF1 GN=rplJ PE=3 SV=1
Thfi_0747	95% (0,0075)	0	2	2	7	12	9	tr|Q5SHD3|Q5SHD3_THET8 Probable amidase OS=Thermus thermophilus (strain HB8 / ATCC 27634 / DSM 579) GN=TTHA1797 PE=1 SV=1
Thfi_0774	95% (0,014)	8	6	6	2	4	3	tr|E8PQK3|E8PQK3_THESS 4-hydroxy-3-methylbut-2-en-1-yl diphosphate synthase OS=Thermus scotoductus (strain ATCC 700910 / SA-01) GN=ispG PE=3 SV=1
Thfi_0793	95% (0,035)	2	4	5	6	9	10	tr|B7A8Z8|B7A8Z8_THEAQ Alanine dehydrogenase/PNT domain protein OS=Thermus aquaticus Y51MC23 GN=TaqDRAFT_4708 PE=4 SV=1
Thfi_0805	95% (0,031)	7	11	12	2	3	6	tr|G8ND83|G8ND83_9DEIN Pyruvate-flavodoxin oxidoreductase OS=Thermus sp. CCB_US3_UF1 GN=TCCBUS3UF1_11800 PE=3 SV=1
Thfi_0822	95% (0,028)	42	63	72	94	99	84	tr|E8PJW4|E8PJW4_THESS Elongation factor Tu OS=Thermus scotoductus (strain ATCC 700910 / SA-01) GN=tuf1 PE=3 SV=1
Thfi_0827	95% (0,010)	5	7	5	2	2	0	tr|F6DHY7|F6DHY7_THETG Uncharacterized protein OS=Thermus thermophilus (strain SG0.5JP17-16) GN=Ththe16_0149 PE=4 SV=1
Thfi_0830	95% (0,039)	0	0	0	1	3	4	tr|F6DFI9|F6DFI9_THETG Isocitrate lyase OS=Thermus thermophilus (strain SG0.5JP17-16) GN=Ththe16_1853 PE=4 SV=1

Quantitative value								
Gene code	T Test (P-Value)	63 °C			77 °C			Top Hit Uniprot
Thfi_0835	95% (0,00048)	2	2	2	8	7	9	tr|F6DFY3|F6DFY3_THETG Gamma-glutamyl phosphate reductase OS=Thermus thermophilus (strain SG0.5JP17-16) GN=proA PE=3 SV=1
Thfi_0843	95% (0,016)	0	0	0	1	1	2	tr|F6DIS5|F6DIS5_THETG Uncharacterized protein OS=Thermus thermophilus (strain SG0.5JP17-16) GN=Ththe16_2388 PE=4 SV=1
Thfi_0844	95% (0,0021)	1	2	1	5	4	5	tr|U2E7Z2|U2E7Z2_9FIRM CDP-glycerol:poly(Glycerophosphate) glycerophosphotransferase OS=Blautia sp. KLE 1732 GN=HMPREF1547_03339 PE=4 SV=1
Thfi_0872	95% (0,016)	4	2	2	0	0	0	tr|E8PQX8|E8PQX8_THESS Phenylalanine--tRNA ligase alpha subunit OS=Thermus scotoductus (strain ATCC 700910 / SA-01) GN=pheS PE=3 SV=1
Thfi_0891	95% (0,041)	2	5	2	7	6	10	tr|G8NDC2|G8NDC2_9DEIN DNA polymerase III subunit beta OS=Thermus sp. CCB_US3_UF1 GN=TCCBUS3UF1_20 PE=3 SV=1
Thfi_0892	95% (0,0097)	9	11	10	6	2	4	tr|F6DH47|F6DH47_THETG Enolase OS=Thermus thermophilus (strain SG0.5JP17-16) GN=eno PE=3 SV=1
Thfi_0893	95% (0,024)	2	3	2	0	1	1	tr|F6DH48|F6DH48_THETG Pyruvate kinase OS=Thermus thermophilus (strain SG0.5JP17-16) GN=Ththe16_0004 PE=3 SV=1
Thfi_0899	95% (0,033)	0	1	0	5	3	2	tr|E8PR20|E8PR20_THESS Phage shock protein A OS=Thermus scotoductus (strain ATCC 700910 / SA-01) GN=TSC_c00270 PE=4 SV=1
Thfi_0911	95% (0,047)	4	5	4	0	3	2	tr|F6DHZ8|F6DHZ8_THETG 3-methyl-2-oxobutanoate dehydrogenase (2-methylpropanoyl-transferring) OS=Thermus thermophilus (strain SG0.5JP17-16) GN=Ththe16_0161 PE=4 SV=1
Thfi_0918	95% (0,016)	3	2	3	4	4	4	tr|B7A6F4|B7A6F4_THEAQ Putative uncharacterized protein (Precursor) OS=Thermus aquaticus Y51MC23 GN=TaqDRAFT_4403 PE=4 SV=1
Thfi_0968	95% (0,0075)	0	1	0	2	2	2	tr|K7QWA1|K7QWA1_THEOS N-acetyl-gamma-glutamyl-phosphate/N-acetyl-gamma-aminoadipyl-phosphate reductase OS=Thermus oshimai JL-2 GN=argC PE=3 SV=1
Thfi_0977	95% (0,025)	1	1	0	2	4	3	tr|E8PJX5|E8PJX5_THESS Homocitrate synthase OS=Thermus scotoductus (strain ATCC 700910 / SA-01) GN=lysS1 PE=3 SV=1
Thfi_1019	95% (0,025)	0	0	0	3	3	1	tr|Q53WB1|Q53WB1_THET8 Putative cobalt-precorrin-6A synthase [deacetylating] OS=Thermus thermophilus (strain HB8 / ATCC 27634 / DSM 579) GN=cbiD PE=3 SV=1
Thfi_1028	95% (0,047)	2	2	1	0	1	0	tr|H9ZUQ3|H9ZUQ3_THETH Uncharacterized protein OS=Thermus thermophilus JL-18 GN=TtJL18_2228 PE=4 SV=1
Thfi_1032	95% (0,016)	1	1	1	2	3	2	tr|Q53VT9|Q53VT9_THET8 5-carboxy-2-hydroxymuconate semialdehyde dehydrogenase OS=Thermus thermophilus (strain HB8 / ATCC 27634 / DSM 579) GN=TTHB240 PE=3 SV=1
Thfi_1109	95% (0,024)	1	0	1	2	3	2	tr|G8NAQ3|G8NAQ3_9DEIN (S)-2-hydroxy-acid oxidase chain D OS=Thermus sp. CCB_US3_UF1 GN=TCCBUS3UF1_19020 PE=4 SV=1
Thfi_1123	95% (0,0075)	2	2	2	1	0	0	tr|G8NDB2|G8NDB2_9DEIN 4-aminobutyrate aminotransferase OS=Thermus sp. CCB_US3_UF1 GN=TCCBUS3UF1_12090 PE=3 SV=1
Thfi_1146	95% (0,011)	7	9	15	21	24	28	tr|B7AAG6|B7AAG6_THEAQ Lon protease OS=Thermus aquaticus Y51MC23 GN=lon PE=3 SV=1
Thfi_1181	95% (0,013)	0	0	1	2	3	2	tr|G8NDY0|G8NDY0_9DEIN CRISPR-associated protein, TIGR02710 OS=Thermus sp. CCB_US3_UF1 GN=TCCBUS3UF1_13390 PE=4 SV=1
Thfi_1184	95% (0,047)	0	0	1	1	2	2	tr|G8N8F8|G8N8F8_9DEIN Histidinol dehydrogenase OS=Thermus sp. CCB_US3_UF1 GN=hisD PE=3 SV=1
Thfi_1197	95% (0,047)	1	0	0	2	1	2	tr|B7A668|B7A668_THEAQ Phenazine biosynthesis protein PhzF family OS=Thermus aquaticus Y51MC23 GN=TaqDRAFT_4317 PE=4 SV=1
Thfi_1224	95% (0,0015)	12	19	19	70	52	66	tr|Q53W39|Q53W39_THET8 Arsenite oxidase, large subunit OS=Thermus thermophilus (strain HB8 / ATCC 27634 / DSM 579) GN=TTHB127 PE=4 SV=1
Thfi_1242	95% (0,022)	5	1	3	8	13	9	tr|H9ZSC2|H9ZSC2_THETH Uncharacterized protein (Precursor) OS=Thermus thermophilus JL-18 GN=TtJL18_1345 PE=4 SV=1
Thfi_1247	95% (0,0064)	32	40	46	18	9	15	tr|E8PK48|E8PK48_THESS Molybdopterin oxidoreductase OS=Thermus scotoductus (strain ATCC 700910 / SA-01) GN=TSC_c14620 PE=3 SV=1
Thfi_1274	95% (0,0014)	153	212	239	593	727	573	tr|K7QXH6|K7QXH6_THEOS 60 kDa chaperonin OS=Thermus oshimai JL-2 GN=groL PE=3 SV=1

		Quantitative value						
Gene code	T Test (P-Value)	63 °C			77 °C			Top Hit Uniprot
Thfi_1311	95% (0,035)	10	4	4	15	14	11	tr|H9ZQJ9|H9ZQJ9_THETH Citrate synthase OS=Thermus thermophilus JL-18 GN=TtJL18_0706 PE=3 SV=1
Thfi_1314	95% (0,026)	14	21	18	28	37	27	tr|K7R3G6|K7R3G6_THEOS Small GTP-binding protein domain protein OS=Thermus oshimai JL-2 GN=Theos_0369 PE=4 SV=1
Thfi_1334	95% (0,013)	5	2	5	11	8	10	tr|G8ND43|G8ND43_9DEIN Extracellular solute-binding protein family 1 OS=Thermus sp. CCB_US3_UF1 GN=TCCBUS3UF1_11400 PE=4 SV=1
Thfi_1374	95% (0,0053)	0	1	0	5	4	3	tr|A4BB90|A4BB90_9GAMM Putative uncharacterized protein OS=Reinekea blandensis MED297 GN=MED297_11825 PE=4 SV=1
Thfi_1419	95% (0,0065)	2	2	2	6	4	5	tr|G8N8Z2|G8N8Z2_9DEIN Thiol:disulfide interchange protein dsbA OS=Thermus sp. CCB_US3_UF1 GN=TCCBUS3UF1_16080 PE=4 SV=1
Thfi_1420	95% (0,0072)	0	2	3	7	8	6	tr|K7QW86|K7QW86_THEOS Spermidine synthase OS=Thermus oshimai JL-2 GN=speE PE=3 SV=1
Thfi_1481	95% (0,00056)	0	0	0	3	4	3	tr|E8PMZ6|E8PMZ6_THESS Prephenate dehydrogenase OS=Thermus scotoductus (strain ATCC 700910 / SA-01) GN=tyrA PE=4 SV=1
Thfi_1492	95% (0,0011)	3	2	2	10	12	9	tr|Q5SK52|Q5SK52_THET8 Phospho-2-dehydro-3-deoxyheptonate aldolase OS=Thermus thermophilus (strain HB8 / ATCC 27634 / DSM 579) GN=TTHA0800 PE=4 SV=1
Thfi_1528	95% (0,039)	1	1	1	4	2	5	tr|K7RJU5|K7RJU5_THEOS Fructose-1,6-bisphosphatase OS=Thermus oshimai JL-2 GN=Theos_1644 PE=3 SV=1
Thfi_1533	95% (0,016)	0	0	0	1	1	2	tr|B7A5R7|B7A5R7_THEAQ Two component transcriptional regulator, LuxR family OS=Thermus aquaticus Y51MC23 GN=TaqDRAFT_5174 PE=4 SV=1
Thfi_1558	95% (0,016)	1	1	2	0	0	0	tr|G8NAW5|G8NAW5_9DEIN Transporter OS=Thermus sp. CCB_US3_UF1 GN=TCCBUS3UF1_6860 PE=4 SV=1
Thfi_1559	95% (0,024)	1	0	0	5	2	4	tr|S4XQ54|S4XQ54_SORCE Ribonuclease OS=Sorangium cellulosum So0157-2 GN=SCE1572_38265 PE=3 SV=1
Thfi_1600	95% (0,049)	4	2	4	9	10	5	tr|H9ZQW0|H9ZQW0_THETH 3-isopropylmalate dehydrogenase OS=Thermus thermophilus JL-18 GN=leuB PE=3 SV=1
Thfi_1602	95% (0,013)	3	7	5	10	12	14	tr|E8PN40|E8PN40_THESS 3-isopropylmalate dehydratase large subunit OS=Thermus scotoductus (strain ATCC 700910 / SA-01) GN=leuC PE=3 SV=1
Thfi_1610	95% (0,038)	2	3	2	6	8	4	tr|H9ZST1|H9ZST1_THETH Purine nucleoside phosphorylase OS=Thermus thermophilus JL-18 GN=TtJL18_1513 PE=3 SV=1
Thfi_1627	95% (0,0094)	3	3	6	13	9	12	tr|K7RHG9|K7RHG9_THEOS Uncharacterized protein (Precursor) OS=Thermus oshimai JL-2 GN=Theos_0757 PE=4 SV=1
Thfi_1666	95% (0,015)	1	3	1	5	8	9	tr|K7R4N3|K7R4N3_THEOS Acyl-CoA synthetase/AMP-acid ligase OS=Thermus oshimai JL-2 GN=Theos_0809 PE=4 SV=1
Thfi_1687	95% (0,0031)	1	0	0	3	3	4	tr|H7GGU2|H7GGU2_9DEIN Zinc protease OS=Thermus sp. RL GN=RLTM_07213 PE=3 SV=1
Thfi_1706	95% (0,016)	3	9	8	28	26	16	tr|H9ZST6|H9ZST6_THETH Superoxide dismutase OS=Thermus thermophilus JL-18 GN=TtJL18_1518 PE=3 SV=1
Thfi_1710	95% (0,047)	1	0	0	2	2	1	tr|Q5SJ01|Q5SJ01_THET8 Acetolactate synthase OS=Thermus thermophilus (strain HB8 / ATCC 27634 / DSM 579) GN=TTHA1213 PE=3 SV=1
Thfi_1713	95% (0,0020)	5	5	3	12	15	12	tr|H9ZQY3|H9ZQY3_THETH 2-isopropylmalate synthase OS=Thermus thermophilus JL-18 GN=leuA PE=3 SV=1
Thfi_1783	95% (0,047)	8	8	6	6	4	4	tr|E8PPA2|E8PPA2_THESS Protein translocase subunit SecY OS=Thermus scotoductus (strain ATCC 700910 / SA-01) GN=secY PE=3 SV=1
Thfi_1860	95% (0,023)	1	2	2	3	5	5	tr|E8PR43|E8PR43_THESS Tungsten-containing aldehyde ferredoxin oxidoreductase OS=Thermus scotoductus (strain ATCC 700910 / SA-01) GN=aor PE=4 SV=1
Thfi_1862	95% (0,035)	3	5	3	1	1	2	tr|Q72GY3|Q72GY3_THET2 Thermostable carboxypeptidase 1 OS=Thermus thermophilus (strain HB27 / ATCC BAA-163 / DSM 7039) GN=TT_C1715 PE=1 SV=1
Thfi_1878	95% (0,026)	1	3	2	0	0	0	tr|H5SNC0|H5SNC0_9DEIN Acetylornithine aminotransferase OS=uncultured Thermus/Deinococcus group bacterium GN=argD PE=3 SV=1

Quantitative value								
Gene code	T Test (P-Value)	63 °C			77 °C			Top Hit Uniprot
Thfi_1881	95% (0,013)	3	2	2	0	0	1	tr|K7R0Y0|K7R0Y0_THEOS Putative exonuclease of the beta-lactamase fold involved in RNA processing OS=Thermus oshimai JL-2 GN=Theos_1956 PE=4 SV=1
Thfi_1894	95% (0,013)	0	0	1	2	3	2	tr|G8NC13|G8NC13_9DEIN Isochorismatase hydrolase OS=Thermus sp. CCB_US3_UF1
Thfi_1919	95% (0,013)	5	3	3	10	8	7	tr|E8PJG3|E8PJG3_THESS Phosphoenolpyruvate carboxykinase [ATP]
Thfi_1924	95% (0,016)	1	2	1	0	0	0	tr|B7A886|B7A886_THEAQ Transposase IS116/IS110/IS902 family protein
Thfi_1926	95% (0,034)	0	3	0	5	4	4	tr|F6DHW7|F6DHW7_THETG Ferric uptake regulator, Fur family OS=Thermus thermophilus (strain SG0.5JP17-16) GN=Ththe16_0129 PE=4 SV=1
Thfi_1930	95% (0,026)	0	0	0	2	3	1	tr|H9ZU48|H9ZU48_THETH Thioredoxin reductase OS=Thermus thermophilus JL-18 GN=TtJL18_2001 PE=3 SV=1
Thfi_1932	95% (0,026)	0	0	0	6	4	2	tr|E8PPR4|E8PPR4_THESS Small heat shock protein OS=Thermus scotoductus (strain ATCC 700910 / SA-01) GN=TSC_c23100 PE=3 SV=1
Thfi_1935	95% (0,047)	2	3	3	2	1	1	tr|E8PPP7|E8PPP7_THESS Menaquinone biosynthesis decarboxylase, family OS=Thermus scotoductus (strain ATCC 700910 / SA-01) GN=TSC_c22930 PE=4 SV=1
Thfi_1946	95% (0,016)	1	2	1	0	0	0	tr|F6DDB6|F6DDB6_THETG DNA topoisomerase OS=Thermus thermophilus (strain SG0.5JP17-16) GN=Ththe16_0312 PE=3 SV=1
Thfi_1956	95% (0,0075)	2	2	1	0	0	0	tr|Q5SGY1|Q5SGY1_THET8 Uncharacterized protein OS=Thermus thermophilus (strain HB8 / ATCC 27634 / DSM 579) GN=TTHA1949 PE=4 SV=1
Thfi_1968	95% (0,025)	8	6	7	2	3	5	tr|K7QXZ9|K7QXZ9_THEOS ABC-type maltose transport systems, permease component (Precursor)
Thfi_1987	95% (0,025)	0	0	0	3	1	3	tr|K7R4D1|K7R4D1_THEOS Uncharacterized protein (Precursor)
Thfi_1992	95% (0,041)	1	3	4	7	5	9	tr|E8PNA5|E8PNA5_THESS Uncharacterized protein OS=Thermus scotoductus
Thfi_1994	95% (0,0030)	12	11	16	43	54	38	tr|K7QWD3|K7QWD3_THEOS ATP-dependent chaperone ClpB OS=Thermus oshimai JL-2 GN=Theos_0686 PE=3 SV=1
Thfi_1998	95% (0,0090)	5	10	6	20	28	19	tr|B7A6Y3|B7A6Y3_THEAQ Chaperone protein DnaK OS=Thermus aquaticus Y51MC23 GN=dnaK
Thfi_2037	95% (0,047)	0	1	0	2	1	2	tr|F6DFJ7|F6DFJ7_THETG Anthranilate synthase component I OS=Thermus thermophilus (strain SG0.5JP17-16) GN=Ththe16_1861 PE=4 SV=1
Thfi_2050	95% (0,019)	6	8	16	21	22	22	tr|K7R7V5|K7R7V5_THEOS Uncharacterized protein (Precursor) OS=Thermus oshimai JL-2 GN=Theos_2118 PE=4 SV=1
Thfi_2065	95% (0,026)	0	0	0	1	3	2	tr|F2NLS0|F2NLS0_MARHT E3 binding domain protein OS=Marinithermus hydrothermalis (strain DSM 14884 / JCM 11576 / T1) GN=Marky_0137 PE=4 SV=1
Thfi_2073	95% (0,047)	2	1	1	2	3	3	tr|Q72I72|Q72I72_THET2 Uncharacterized protein OS=Thermus thermophilus (strain HB27 / ATCC BAA-163 / DSM 7039) GN=TT_C1260 PE=4 SV=1
Thfi_2076	95% (0,0028)	46	44	46	35	31	28	tr|G8NBH9|G8NBH9_9DEIN Putative uncharacterized protein OS=Thermus sp. CCB_US3_UF1
Thfi_2086	95% (0,0029)	1	2	0	5	6	5	tr|G8NAJ1|G8NAJ1_9DEIN Homoisocitrate dehydrogenase OS=Thermus sp. CCB_US3_UF1
Thfi_2145	95% (0,0048)	1	0	1	4	3	3	tr|G8NBI4|G8NBI4_9DEIN Enoyl-CoA hydratase OS=Thermus sp. CCB_US3_UF1 GN=TCCBUS3UF1_20220 PE=4 SV=1
Thfi_2146	95% (0,011)	4	5	2	8	8	10	tr|E8PLU1|E8PLU1_THESS Malate synthase OS=Thermus scotoductus
Thfi_2230	95% (0,019)	0	0	0	2	5	3	tr|K7QXJ7|K7QXJ7_THEOS Electron transfer flavoprotein, beta subunit OS=Thermus oshimai JL-2 GN=Theos_1510 PE=4 SV=1
Thfi_2302	95% (0,015)	2	3	4	6	7	9	tr|K7QU85|K7QU85_THEOS 3-oxoacyl-[acyl-carrier-protein] synthase 2 (Precursor)
Thfi_2310	95% (0,016)	3	5	4	1	1	2	tr|H9ZT87|H9ZT87_THETH 3-methyl-2-oxobutanoate hydroxymethyltransferase
Thfi_2340	95% (0,042)	2	6	5	11	10	7	tr|H9ZQI7|H9ZQI7_THETH DNA gyrase subunit A OS=Thermus thermophilus JL-18
Thfi_2354	95% (0,024)	2	2	3	1	1	0	tr|H5SLU5|H5SLU5_9ZZZZ Type I restriction enzyme, R subunit
Thfi_2383	95% (0,00020)	1	1	1	6	5	5	tr|G9MBE1|G9MBE1_THET8 D-xylose ABC transporter periplasmic substrate-binding protein OS=Thermus thermophilus (strain HB8 / ATCC 27634 / DSM 579) GN=TTHV089 PE=4 SV=1

Table S6: Differently expressed proteins in hydrogen peroxide assay.

		Quantitative value						
Gene code	**T Test (P-Value)**	**Without H_2O_2**			**With H_2O_2**			**Top Hit Uniprot**
Thfi_0064	95% (0,025)	31	26	32	18	24	20	tr|H9ZT91|H9ZT91_THETH ATP-dependent zinc metalloprotease FtsH (Precursor) OS=Thermus thermophilus JL-18 GN=ftsH PE=3 SV=1
Thfi_0089	95% (0,0060)	23	26	22	8	6	14	tr|H9ZTY0|H9ZTY0_THETH Alanine--tRNA ligase OS=Thermus thermophilus JL-18 GN=alaS PE=3 SV=1
Thfi_0098	95% (0,016)	2	1	1	0	0	0	tr|Q72H05|Q72H05_THET2 Deacetylase OS=Thermus thermophilus (strain HB27 / ATCC BAA-163 / DSM 7039) GN=TT_C1690 PE=4 SV=1
Thfi_0110	95% (0,039)	3	2	5	8	6	6	tr|E8PQK3|E8PQK3_THESS 4-hydroxy-3-methylbut-2-en-1-yl diphosphate synthase OS=Thermus scotoductus (strain ATCC 700910 / SA-01) GN=ispG PE=3 SV=1
Thfi_0247	95% (0,038)	0	2	4	9	5	7	tr|G8N8P3|G8N8P3_9DEIN Putative uncharacterized protein OS=Thermus sp. CCB_US3_UF1 GN=TCCBUS3UF1_3040 PE=4 SV=1
Thfi_0254	95% (0,018)	8	5	6	3	2	3	tr|B7A7E3|B7A7E3_THEAQ Mandelate racemase/muconate lactonizing protein OS=Thermus aquaticus Y51MC23 GN=TaqDRAFT_5346 PE=4 SV=1
Thfi_0435	95% (0,025)	4	4	5	1	3	2	tr|E8PKC7|E8PKC7_THESS Outer membrane efflux protein OS=Thermus scotoductus (strain ATCC 700910 / SA-01) GN=TSC_c02590 PE=4 SV=1
Thfi_0460	95% (0,047)	2	2	1	1	0	0	tr|F6DJ48|F6DJ48_THETG Helix-turn-helix domain protein OS=Thermus thermophilus (strain SG0.5JP17-16) GN=Ththe16_2059 PE=4 SV=1
Thfi_0526	95% (0,043)	33	35	27	21	17	26	tr|K7RFC6|K7RFC6_THEOS DNA-directed RNA polymerase subunit beta OS=Thermus oshimai JL-2 GN=rpoB PE=3 SV=1
Thfi_0569	95% (0,0022)	1	0	1	3	3	3	tr|K7R3E0|K7R3E0_THEOS Phosphoribosylformylglycinamidine synthase 2 OS=Thermus oshimai JL-2 GN=purL PE=3 SV=1
Thfi_0717	95% (0,026)	7	3	7	14	16	10	tr|E8PLJ1|E8PLJ1_THESS Ggdef domain protein OS=Thermus scotoductus (strain ATCC 700910 / SA-01) GN=TSC_c17260 PE=4 SV=1
Thfi_0727	95% (0,032)	28	24	18	13	15	9	tr|G8NC05|G8NC05_9DEIN 50S ribosomal protein L1 OS=Thermus sp. CCB_US3_UF1 GN=rplA PE=3 SV=1
Thfi_0774	95% (0,039)	6	5	7	8	8	10	tr|E8PJI0|E8PJI0_THESS Phosphate-binding protein OS=Thermus scotoductus (strain ATCC 700910 / SA-01) GN=pstS PE=3 SV=1
Thfi_0792	95% (0,0075)	2	2	2	0	1	0	tr|Q53WA4|Q53WA4_THET8 Cobalamin biosynthesis protein CbiX OS=Thermus thermophilus (strain HB8 / ATCC 27634 / DSM 579) GN=TTHB058 PE=4 SV=1
Thfi_1024	95% (0,016)	1	1	1	2	3	2	tr|D3PL28|D3PL28_MEIRD Drug resistance transporter
Thfi_1027	95% (0,0075)	3	3	3	1	1	2	tr|G8NAB2|G8NAB2_9DEIN Replicative DNA helicase DnaB OS=Thermus sp. CCB_US3_UF1 GN=TCCBUS3UF1_18380 PE=4 SV=1
Thfi_1059	95% (0,047)	2	2	1	0	1	0	tr|F6DFL5|F6DFL5_THETG Extracellular solute-binding protein family 1 OS=Thermus thermophilus (strain SG0.5JP17-16) GN=Ththe16_1881 PE=4 SV=1
Thfi_1076	95% (0,047)	0	0	1	1	2	2	tr|B7A9F0|B7A9F0_THEAQ Endonuclease MutS2 OS=Thermus aquaticus Y51MC23 GN=mutS2 PE=3 SV=1
Thfi_1087	95% (0,026)	2	1	3	0	0	0	tr|B7AAU3|B7AAU3_THEAQ DOMON domain protein (Precursor) OS=Thermus aquaticus Y51MC23 GN=TaqDRAFT_5509 PE=4 SV=1
Thfi_1136	95% (0,039)	3	1	3	6	5	4	tr|B7AAK1|B7AAK1_THEAQ Heat shock protein HslVU
Thfi_1139	95% (0,015)	17	18	18	14	9	9	tr|B7AAJ9|B7AAJ9_THEAQ Magnesium-chelatase subunit ChlI OS=Thermus aquaticus Y51MC23 GN=TaqDRAFT_3484 PE=4 SV=1
Thfi_1246	95% (0,016)	1	1	1	2	3	2	tr|G8ND96|G8ND96_9DEIN Sensory transduction histidine kinase OS=Thermus sp. CCB_US3_UF1 GN=TCCBUS3UF1_11930 PE=4 SV=1
Thfi_1584	95% (0,021)	3	4	5	1	2	0	tr|H9ZQU5|H9ZQU5_THETH Methylmalonyl-CoA mutase family protein OS=Thermus thermophilus JL-18 GN=TtJL18_0802 PE=4 SV=1

Quantitative value								
Gene code	T Test (P-Value)	Without H_2O_2			With H_2O_2			Top Hit Uniprot
Thfi_1619	95% (0,024)	1	0	1	2	2	3	tr|H9ZQ50|H9ZQ50_THETH Protein GrpE OS=Thermus thermophilus JL-18 GN=grpE PE=3 SV=1
Thfi_1679	95% (0,000044)	28	29	29	19	20	20	tr|F6DHR7|F6DHR7_THETG V-type ATP synthase alpha chain OS=Thermus thermophilus (strain SG0.5JP17-16) GN=atpA PE=3 SV=1
Thfi_1733	95% (0,0078)	3	3	2	0	0	1	tr|G8NB20|G8NB20_9DEIN Putative uncharacterized protein OS=Thermus sp. CCB_US3_UF1 GN=TCCBUS3UF1_19390 PE=4 SV=1
Thfi_1798	95% (0,026)	0	0	0	1	3	2	tr|G8N9M0|G8N9M0_9DEIN 50S ribosomal protein L16 OS=Thermus sp. CCB_US3_UF1 GN=rplP PE=3 SV=1
Thfi_1836	95% (0,028)	1	2	2	9	7	4	tr|E8PKB9|E8PKB9_THESS Chlorite dismutase OS=Thermus scotoductus (strain ATCC 700910 / SA-01) GN=TSC_c02510 PE=4 SV=1
Thfi_1837	95% (0,016)	1	1	2	0	0	0	tr|B7A777|B7A777_THEAQ Uroporphyrin-III C/tetrapyrrole (Corrin/Porphyrin) methyltransferase OS=Thermus aquaticus Y51MC23 GN=TaqDRAFT_5280 PE=3 SV=1
Thfi_1925	95% (0,0013)	9	9	9	7	6	6	tr|D3PR67|D3PR67_MEIRD Probable cytosol aminopeptidase OS=Meiothermus ruber (strain ATCC 35948 / DSM 1279 / VKM B-1258 / 21) GN=pepA PE=3 SV=1
Thfi_1953	95% (0,0075)	1	2	2	0	0	0	tr|E8PQK2|E8PQK2_THESS Enoyl-[acyl-carrier-protein] reductase [NADH] OS=Thermus scotoductus (strain ATCC 700910 / SA-01) GN=TSC_c24440 PE=3 SV=1
Thfi_1966	95% (0,047)	1	2	2	0	0	1	tr|K7R0G3|K7R0G3_THEOS Fructose-1
Thfi_1997	95% (0,024)	1	0	1	2	3	2	tr|H7GFH7|H7GFH7_9DEIN L-threonine 3-dehydrogenase OS=Thermus sp. RL GN=tdh PE=3 SV=1
Thfi_2025	95% (0,0075)	0	1	0	2	2	2	tr|H7GE63|H7GE63_9DEIN Molybdopterin biosynthesis MoeA OS=Thermus sp. RL GN=RLTM_01740 PE=4 SV=1
Thfi_2226	95% (0,016)	2	1	1	0	0	0	tr|K7QXH2|K7QXH2_THEOS Uncharacterized protein (Precursor) OS=Thermus oshimai JL-2 GN=Theos_1458 PE=4 SV=1
Thfi_2236	95% (0,016)	1	1	2	0	0	0	tr|E8PKB8|E8PKB8_THESS Mechanosensitive ion channel OS=Thermus scotoductus (strain ATCC 700910 / SA-01) GN=TSC_c02500 PE=4 SV=1
Thfi_2271	95% (0,013)	4	3	3	2	1	1	tr|B7A850|B7A850_THEAQ Tetratricopeptide TPR_2 repeat protein OS=Thermus aquaticus Y51MC23 GN=TaqDRAFT_4246 PE=4 SV=1
Thfi_2275	95% (0,0075)	0	0	0	1	2	2	tr|B7A856|B7A856_THEAQ Rad52/22 double-strand break repair protein OS=Thermus aquaticus Y51MC23 GN=TaqDRAFT_4252 PE=4 SV=1
Thfi_2282	95% (0,033)	0	1	1	5	2	4	tr|K7R4F8|K7R4F8_THEOS NADH-quinone oxidoreductase subunit D OS=Thermus oshimai JL-2 GN=nuoD PE=3 SV=1
Thfi_2286	95% (0,019)	18	19	17	14	16	14	tr|H9ZTK0|H9ZTK0_THETH NADH-quinone oxidoreductase
Thfi_2314	95% (0,025)	4	3	3	2	1	0	tr|B7ABE7|B7ABE7_THEAQ PpiC-type peptidyl-prolyl cis-trans isomerase (Precursor) OS=Thermus aquaticus Y51MC23 GN=TaqDRAFT_4589 PE=4 SV=1

Table S7: Top enriched biological process for statistically different expressed proteins comparing conditions with and without H_2O_2.

Gene	Protein	Top enriched Biological Process	p-value	Uniprot ID	Cellular component	Regulation with H_2O_2	Fig. 5A*
purL	Phosphoribosylformylglycinamidine synthase 2	_de novo_ IMP biosynthetic process	0.15877697314	K7R3E0	cytoplasm	up	
alaS	Alanine - tRNA ligase	alanyl-tRNA aminoacylation	0.033625876414	H9ZTY0	cytoplasm	down	
TtJL18_1792	NADH-quinone oxidoreductase, chain G	ATP synthesis coupled electron transport	0.07990207710	H9ZTK0		down	
TTHB058	Cobalamin biosynthesis protein CbiX	cobalamin biosynthetic process	0.18675934150	Q53WA4		down	
TSC_c17260	Ggdef domain protein	cyclic nucleotide biosynthetic process	0.10813523080	E8PLJ1		up	
TCCBUS3UF1_18380	Replicative DNA helicase DnaB	DNA duplex unwinding	0.033625876414	G8NAB2		down	
TaqDRAFT_4252	Rad52/22 double-strand break repair protein	DNA recombination	0.21213051721	B7A856		up	
TSC_c24440	Enoyl-[acyl-carrier-protein] reductase [NADH]	fatty acid biosynthetic process	0.17588928316	E8PQK2		down	
Theos_1730	Fructose-1,6-bisphosphate aldolase, class II	fructose 1,6-bisphosphate metabolic process	0.017099735812	K7R0G3		down	
ispG	4-hydroxy-3-methylbut-2-en-1-yl diphosphate synthase	isopentenyl diphosphate biosynthetic process, mevalonate-independent pathway	0.10126593858	E8PQK3		up	
tdh	L-threonine 3-dehydrogenase	L-threonine catabolic process to glycine	0.017099735812	H7GFH7	cytoplasm	up	
mutS2	Endonuclease MutS2	maintenance of fidelity involved in DNA-dependent DNA replication	0.025433618145	B7A9F0		up	
RLTM_01740	Molybdopterin biosynthesis MoeA	Mo-molybdopterin cofactor biosynthetic process	0.094271710999	H7GE63		up	
pstS	Phosphate-binding protein	phosphate ion transmembrane transport	0.017099735812	E8PJI0		up	
TCCBUS3UF1_11930	Sensory transduction histidine kinase	phosphorelay signal transduction system	0.072523440983	G8ND96		up	
nuoD	NADH-quinone oxidoreductase subunit	photosynthesis, light reaction	0.10813523080	K7R4F8	plasma membrane	up	
atpA	V-type ATP synthase alpha chain	plasma membrane ATP synthesis coupled proton transport	0.094271710999	F6DHR7		down	
TaqDRAFT_5280	Uroporphyrin-III C/tetrapyrrole (Corrin/Porphyrin) methyltransferase	porphyrin-containing compound biosynthetic process	0.10813523080	B7A777		down	
ftsH	ATP-dependent zinc metalloprotease FtsH	protein catabolic process	0.033625876414	H9ZT91	plasma membrane	down	

Gene	Protein	Top enriched Biological Process	p-value	Uniprot ID	Cellular component	Regulation with H_2O_2	Fig. 5A*
TaqDRAFT_4589	PpiC-type peptidyl-prolyl cis-trans isomerase	protein folding	0.015438924074	B7ABE7		down	3
grpE	Protein GrpE	protein folding	0.015438924074	H9ZQ50	cytoplasm	up	3
pepA	MEIRD Probable cytosol aminopeptidase	proteolysis	0.11991957939	D3PR67	cytoplasm	down	
TaqDRAFT_3484	Magnesium-chelatase subunit ChlI	regulation of transcription, DNA-dependent	0.10778502538	B7AAJ9		down	5
rplA	50S ribosomal protein L1	regulation of translation	0.025433618145	G8NC05		down	
TaqDRAFT_3486	Heat shock protein HslVU, ATPase subunit HslU	response to stress	0.032868991839	B7AAK1	cytoplasm	up	
rpoB	DNA-directed RNA polymerase subunit beta	transcription, DNA-dependent	0.34589175148	K7RFC6		down	
rplP	50S ribosomal protein L16	translation	0.23010519510	G8N9M0	cytoplasm	up	6
TSC_c02500	Mechanosensitive ion channel	transmembrane transport	0.050326842730	E8PKB8		down	4
Mrub_0144	Drug resistance transporter, EmrB/QacA subfamily	transmembrane transport	0.050326842730	D3PL28	plasma membrane	up	4

*Numebered according to the Biological Process shown in Figure 5A.

Table S8: Top enriched biological process for statistically different expressed transcripts comparing conditions with and without H_2O_2.

Gene	Protein	Top enriched Biological Process	p-value	Uniprot ID	Cellular component	Regulation with H_2O_2	Fig. 5A*
purH	Bifunctional purine biosynthesis protein PurH	_de novo_ IMP biosynthetic process	0.34093431742	H7GDU4		down	
Theos_0514	ABC-type branched-chain amino acid transport system, periplasmic component	amino acid transport	0.079729623745	K7QW00		down	
argJ	Arginine biosynthesis bifunctional protein ArgJ	arginine biosynthetic process	0.12323188935	E8PKJ6	cytoplasm	down	
argD	Acetylornithine/acetyl-lysine aminotransferase	arginine biosynthetic process	0.12323188935	H9ZRS1	cytoplasm	up	
TSC_c19110	Mn2+/Zn2+ ABC transporter, ATP-binding protein	ATP catabolic process	0.22852516282	E8PMI3		down	1
TSC_c16200	ATPase associated with various cellular activities, AAA_3	ATP catabolic process	0.22852516282	E8PL11		down	1
pstB	Phosphate ABC transporter, ATP-binding protein	ATP catabolic process	0.22852516282	E8PJH7	plasma membrane	up	1
TSC_c09910	Glycosyltransferase	biosynthetic process	0.37398714575	E8PPF0		up	
glmS1	Glutamine-fructose-6-phosphate transaminase	carbohydrate metabolic process	0.332302293902	E8PMX8		up	
TCCBUS3UF1_16650	Putative uncharacterized protein	carotenoid biosynthetic process	0.10333623104	G8N9D0		up	
cdr	Coenzyme A disulfide reductase	cell redox homeostasis	0.070018186961	E8PL68	cytoplasm	up	
Ththe16_0157	Dihydrolipoyl dehydrogenase	cell redox homeostasis	0.070018186961	F6DHZ4	cytoplasm	up	
TCCBUS3UF1_4850	Methionine aminopeptidase	cellular process	0.166095464554	G8N9N5		up	
TCCBUS3UF1_4170	Phospho-2-dehydro-3-deoxyheptonate aldolase	chorismate metabolic process	0.079729623745	G8N9G7		up	
coaE	Dephospho-CoA kinase	coenzyme A biosynthetic process	0.018576466430	D7BIA8	cytoplasm	down	
TCCBUS3UF1_5160	DNA/pantothenate metabolism flavoprotein	coenzyme A biosynthetic process	0.018576466430	G8N9Z3		up	
TaqDRAFT_5111	Cytochrome c biogenesis protein transmembrane region	cytochrome complex assembly	0.21792333211	B7A5K4		up	
TaqDRAFT_4893	Putative Holliday junction resolvase	DNA repair	0.29873805213	B7A624	cytoplasm	up	

Gene	Protein	Top enriched Biological Process	p-value	Uniprot ID	Cellular component	Regulation with H_2O_2	Fig. 5A*
TT_P0164	RNA polymerase sigma factor	DNA-dependent transcription, initiation	0.12556084577	Q745Z1		down	
TaqDRAFT_3851	L-serine dehydratase, iron-sulfur-dependent, beta subunit	gluconeogenesis	0.272346059952	B7AA84		up	
HGMM_F51G12C41	Dak phosphatase	glycerol metabolic process	0.007218886081	H5SND6		up	
TSC_c24980	Glycerophosphoryl diester phosphodiesterase	glycerol metabolic process	0.0072188860811	E8PQY5		up	
eno	Enolase	glycolysis	0.3348262451	F6DH47	extracellular	up	
tuf1	Elongation factor Tu	GTP catabolic process	0.34643449515	E8PJW4	cytoplasm	up	
hisB	Imidazoleglycerol-phosphate dehydratase	histidine biosynthetic process	0.34093431742	B7A843	cytoplasm	up	
TaqDRAFT_4511	NADH dehydrogenase (Quinone)	iron-sulfur cluster assembly	0.21792333211	B7A6R2		up	
lipB	Octanoyltransferase	lipoate biosynthetic process	0.054680405382	H9ZP13	cytoplasm	up	
TSC_c08000	Zinc-dependent peptidase	metabolic process	0.04048031282	E8PNF1		up	2
TTHA1327	Uncharacterized protein	metabolic process	0.04048031282	Q5SIP2		up	2
TTHA1617	Probable HIT family protein	metabolic process	0.04048031282	Q5SHW3		up	2
TCCBUS3UF1_5750	Protein serine/threonine phosphatase	metabolic process	0.04048031282	G8NA52		up	2
TaqDRAFT_3451	Lon protease	misfolded or incompletely synthesized protein catabolic process	0.166095464	B7AAG6	cytoplasm	up	
Ththe16_1633	Phosphoribosyltransferase	nucleoside metabolic process	0.3557263668	F6DEA1		down	
murB	UDP-N-acetylenolpyruvoylglucosamine reductase (Precursor)	peptidoglycan biosynthetic process	0.3513558633	K7R5E7	cytoplasm	up	
TaqDRAFT_5375	Cell wall hydrolase/autolysin	peptidoglycan catabolic process	0.10333623104	B7A7H2		down	
Theos_0972	4-hydroxyphenylacetate 3-monooxygenase, oxygenase component	phenylacetate catabolic process	0.10333623104	K7QZ08		down	
TSC_c22670	Proline dehydrogenase/delta-1-pyrroline-5-carboxylate dehydrogenase	proline catabolic process	0.054680405382	E8PPM1		down	
hslO	33 kDa chaperonin	protein folding	0.022044360933	H9ZRT7	cytoplasm	up	3
dnaK	Chaperone protein DnaK	protein folding	0.022044360933	B7A6Y3		up	3

Gene	Protein	Top enriched Biological Process	p-value	Uniprot ID	Cellular component	Regulation with H_2O_2	Fig. 5A*
grpE	Protein GrpE	protein folding	0.015438924074	H9ZQ50	cytoplasm	up	3
Theos_2007	Sphingosine/diacylglycerol kinase-like enzyme	protein kinase C-activating G-protein coupled receptor signaling pathway	0.054680405382	K7QYD9		down	
Ththe16_1801	Preprotein translocase, SecG subunit	protein secretion	0.28362872783	F6DF67		up	
TTHA0896	Zn-dependent protease	proteolysis	0.27200642469	Q5SJV6		down	
pyrE	Orotate phosphoribosyltransferase	pyrimidine nucleobase biosynthetic process	0.079729623745	H7GI01		up	
TSC_c21260	Two-component response regulator	regulation of transcription, DNA-dependent	0.19174334941	E8PNS4		down	5
TSC_c00360	Cold shock protein, CSD family	regulation of transcription, DNA-dependent	0.19174334941	E8PR29	nucleus	up	5
TSC_c17050	16S rRNA M	regulation of transcription, DNA-dependent	0.19174334941	E8PLH0		up	5
TCCBUS3UF1_3770	Osmotically inducible protein C	response to stress	0.0581760018	G8N948		down	
TSC_c08940	Sensory transduction protein kinase	signal transduction by phosphorylation	0.34093431742	E8PNX3		down	
TSC_c04280	ABC transporter	thiamine transport	0.054680405382	E8PLA1		up	
Mrub_2807	Transcriptional regulator, DeoR family	transcription, DNA-dependent	0.25129231678	D3PP09		up	
rpsP	30S ribosomal protein S16	translation	0.16509790954	G8NCZ8	cytoplasm	down	6
rplQ	50S ribosomal protein L17	translation	0.16509790954	B7A584	cytoplasm	down	6
rpmI	50S ribosomal protein L35	translation	0.16509790954	K7QWH2	cytoplasm	down	6
rpsT	30S ribosomal protein S20	translation	0.16509790954	E8PNN6	cytoplasm	down	6
rpsR	30S ribosomal protein S18	translation	0.16509790954	B7A903	cytoplasm	down	6
fmt	Methionyl-tRNA formyltransferase	translational initiation	0.079729623745	B7A8I8		up	
TaqDRAFT_4588	Major facilitator superfamily MFS_1	transmembrane transport	0.36194743038	B7ABE6		down	4
mnmA	tRNA-specific 2-thiouridylase MnmA	tRNA modification	0.18451582622	F6DHW4	cytoplasm	down	
Ththe16_1861	Anthranilate synthase component I	tryptophan biosynthetic process	0.26017642449	F6DFJ7		up	

*Numebered according to the Biological Process shown in Figure 5A.

Table S9: Top enriched biological process for statistically different expressed proteins comparing conditions at 77 and 63 °C.

Gene	Protein	Top enriched Biological Process	p-value	Uniprot ID	Cellular component	Regulation at 77 °C	Fig. 5B*
purH	Bifunctional purine biosynthesis protein PurH	_de novo_ IMP biosynthetic process	0.331527130931597	H7GDU4		up	
pyrF	Orotidine 5'-phosphate decarboxylase	_de novo_ pyrimidine nucleobase biosynthetic process	0.138146540694358	E8PKV7		up	
argD	Acetylornithine aminotransferase	arginine biosynthetic process	0.0835603667586405	H5SNC0	cytoplasm	down	4
argC	N-acetyl-gamma-glutamyl-phosphate/N-acetyl-gamma-aminoadipyl-phosphate reductase	arginine biosynthetic process	0.0835603667586405	K7QWA1	cytoplasm	up	4
TTHA0800	Phospho-2-dehydro-3-deoxyheptonate aldolase	aromatic amino acid family biosynthetic process	0.206028291459765	Q5SK52		up	
TaqDRAFT_4530	Oligopeptide/dipeptide ABC transporter, ATPase subunit	ATP catabolic process	0.18695618368922	B7A6T1		up	1
TaqDRAFT_4317	Phenazine biosynthesis protein PhzF family	biosynthetic process	0.135963833690532	B7A668		up	5
Ocepr_0509	Alpha-glucosidase	carbohydrate metabolic process	0.0735585834754744	E4U6W5		down	6
Ththe16_1853	Isocitrate lyase	carboxylic acid metabolic process	0.0511853879369035	F6DFI9		up	
TaqDRAFT_4910	Cell shape determining protein, MreB/Mrl family	cell morphogenesis	0.118207263666517	B7A503		up	
TtJL18_0706	Citrate synthase	cellular carbohydrate metabolic process	0.276719408966394	H9ZQJ9	cytoplasm	up	
cbiD	Putative cobalt-precorrin-6A synthase [deacetylating]	corrin biosynthetic process	0.0511853879369035	Q53WB1		up	
cysS	Cysteine-tRNA ligase	cysteinyl-tRNA aminoacylation	0.0511853879369035	E8PRA8	cytoplasm	up	
Ththe16_2388	Uncharacterized protein	DNA recombination	0.179036870842999	F6DIS5		up	
TaqDRAFT_4282	Transposase IS116/IS110/IS902 family protein	DNA repair	0.0451192309149931	B7A886		down	2
TCCBUS3UF1_20	DNA polymerase III subunit beta	DNA replication	0.0609959896993388	G8NDC2	nucleus	up	
HGMM_F47C12C08	Type I restriction enzyme, R subunit	DNA restriction-modification system	0.118207263666517	H5SLU5		down	
Ththe16_0312	DNA topoisomerase	DNA topological change	0.0249988193687379	F6DDB6	cytoplasm	down	

Gene	Protein	Top enriched Biological Process	p-value	Uniprot ID	Cellular component	Regulation at 77 °C	Fig. 5B*
gyrA	DNA gyrase subunit A	DNA topological change	0.298622505706405	H9ZQI7	cytoplasm	up	
TaqDRAFT_4448	RNA polymerase sigma factor	DNA-dependent transcription, initiation	0.407312468518377	B7A6J9		up	
TTHV089	D-xylose ABC transporter periplasmic substrate-binding protein	D-xylose transport	0.0262779716690618	G9MBE1		up	
TCCBUS3UF1_11800	Pyruvate-flavodoxin oxidoreductase	electron transport chain	0.301612704977513	G8ND83		down	
Theos_0669	3-oxoacyl-[acyl-carrier-protein] synthase 2 (Precursor)	fatty acid biosynthetic process	0.347896908793974	K7QU85		up	
pckA	Phosphoenolpyruvate carboxykinase [ATP]	gluconeogenesis	0.0455104945148549	E8PJG3	cytoplasm	up	
Theos_1644	Fructose-1,6-bisphosphatase	glycerol metabolic process	0.0395204522226343	K7RJU5		up	
Ththe16_0004	Pyruvate kinase	glycolysis	0.0171743908879947	F6DH48		down	14
eno	Enolase	glycolysis	0.0171743908879947	F6DH47	extracellular	down	14
Q9RHA2	Fructose-1,6-bisphosphate aldolase	glycolysis	0.0171743908879947	Q9RHA2		up	14
aceB	Malate synthase	glyoxylate cycle	0.0801839902230023	E8PLU1		up	
guaB	Inosine-5'-monophosphate dehydrogenase	GMP biosynthetic process	0.131443763759153	K7R067		up	
tuf1	Elongation factor Tu	GTP catabolic process	0.118717834921604	E8PJW4	cytoplasm	up	3
fusA	Elongation factor G	GTP catabolic process	0.118717834921604	B7A552	cytoplasm	up	3
Theos_0369	Small GTP-binding protein domain protein	GTP catabolic process	0.118717834921604	K7R3G6		up	3
hisD	Histidinol dehydrogenase	histidine biosynthetic process	0.216274227272425	G8N8F8		up	
TTHA1213	Acetolactate synthase	isoleucine biosynthetic process	0.175495689431207	Q5SJ01		up	
ispG	4-hydroxy-3-methylbut-2-en-1-yl diphosphate synthase	isopentenyl diphosphate biosynthetic process, mevalonate-independent pathway	0.248695143254404	E8PQK3		down	
leuB	3-isopropylmalate dehydrogenase	leucine biosynthetic process	0.0165352937609784	H9ZQW0	cytoplasm	up	15
leuA	2-isopropylmalate synthase	leucine biosynthetic process	0.0165352937609784	H9ZQY3		up	15
leuC	3-isopropylmalate dehydratase	leucine biosynthetic process	0.0165352937609784	E8PN40		up	15

Gene	Protein	Top enriched Biological Process	p-value	Uniprot ID	Cellular component	Regulation at 77 °C	Fig. 5B*
proA	Gamma-glutamyl phosphate reductase	L-proline biosynthetic process	0.00925543926365451	F6DFY3	cytoplasm	up	
TtJL18_1195	Pyrroline-5-carboxylate reductase	L-proline biosynthetic process	0.400482074471707	H9ZRX7		up	
lysS1	Homocitrate synthase	lysine biosynthetic process via aminoadipic acid	0.242646331189368	E8PJX5		up	
TCCBUS3UF1_12090	4-aminobutyrate aminotransferase	metabolic process	0.113352313672226	G8NDB2		down	16
Theos_1424	Aconitate hydratase 1	metabolic process	0.240229026098881	K7QVD4		up	16
TaqDRAFT_3451	Lon protease	misfolded or incompletely synthesized protein catabolic process	0.0929510257131942	B7AAG6	cytoplasm	up	
TtJL18_1513	Purine nucleoside phosphorylase	nucleoside metabolic process	0.0413018244604076	H9ZST1		up	18
TtJL18_1345	Uncharacterized protein	oxidation-reduction process	0.367785768384358	H9ZSC2		up	18
panB	3-methyl-2-oxobutanoate hydroxymethyltransferase	pantothenate biosynthetic process	0.138146540694358	H9ZT87	cytoplasm	down	
pheS	Phenylalanine-tRNA ligase alpha subunit	phenylalanyl-tRNA aminoacylation	0.220732219375865	E8PQX8	cytoplasm	down	
Ththe16_0606	PpiC-type peptidyl-prolyl cis-trans isomerase	protein folding	0.027838062936008	F6DEZ9		down	21
clpX	ATP-dependent Clp protease ATP-binding subunit ClpX	protein folding	0.027838062936008	F6DF87		down	21
dnaK	Chaperone protein DnaK	protein folding	0.027838062936008	B7A6Y3		up	21
Theos_0686	ATP-dependent chaperone ClpB	protein processing	0.296106066284261	K7QWD3	cytoplasm	up	
groL	60 kDa chaperonin	protein refolding	0.296106066284261	K7QXH6	cytoplasm	up	
pilC	Type 4 fimbrial assembly protein PilC	protein secretion	0.272147084216211	E8PMZ1		down	
secY	Protein translocase subunit SecY	protein transport by the Sec complex	0.0747754496601345	E8PPA2	plasma membrane	down	
TT_C1715	Thermostable carboxypeptidase 1	proteolysis	0.193464376137058	Q72GY3		down	22
RLTM_07213	Zinc protease	proteolysis	0.193464376137058	H7GGU2		up	22
TaqDRAFT_4708	Alanine dehydrogenase/PNT domain protein	proton transport	0.296106066284261	B7A8Z8		up	
TtJL18_2001	Thioredoxin reductase	removal of superoxide radicals	0.296106066284261	H9ZU48	cytoplasm	up	

Gene	Protein	Top enriched Biological Process	p-value	Uniprot ID	Cellular component	Regulation at 77 °C	Fig. 5B*
TSC_c23890	Universal stress protein family	response to stress	0.0106859264862616	E8PQ70		up	24
TSC_c23100	Small heat shock protein	response to stress	0.160048502958006	E8PPR4		up	24
Ththe16_0896	UspA domain-containing protein	response to stress	0.0106859264862616	F6DGF5		up	24
speE	Spermidine synthase	spermidine biosynthetic process	0.174703168305732	K7QW86		up	
TtJL18_1518	Superoxide dismutase	superoxide metabolic process	0.296106066284261	H9ZST6		up	
TaqDRAFT_5174	Two component transcriptional regulator, LuxR family	transcription, DNA-dependent	0.276460601710911	B7A5R7		up	26
TSC_c09290	Anti-cleavage anti-GreA transcription factor Gfh1	transcription, DNA-dependent	0.0698494597069458	E8PP08		up	26
rplJ	50S ribosomal protein L10	translation	0.00588933923984203	G8NC04	cytoplasm	up	27
gatA	Glutamyl-tRNA(Gln) amidotransferase subunit A	translation	0.157031344561381	E8PK21		up	27
Ththe16_1861	Anthranilate synthase component I	tryptophan biosynthetic process	0.214853543666316	F6DFJ7		up	
tyrA	Prephenate dehydrogenase	tyrosine biosynthetic process	0.296106066284261	E8PMZ6		up	

*Numebered according to the Biological Process shown in Figure 5B.

Table S10: Top enriched biological process for statistically different expressed transcripts comparing conditions at 77 and 63 °C.

Gene	Protein	Top enriched Biological Process	p-value	Uniprot ID	Cellular component	Regulation at 77°C	Fig. 5B*
asd	Aspartate-semialdehyde dehydrogenase	_de novo_ L-methionine biosynthetic process	0.0801839902230	H7GFF6	cytoplasm	down	
TaqDRAFT_5358	O-acetylhomoserine/O-acetylserine sulfhydrylase	_de novo_ L-methionine biosynthetic process	0.0801839902230	B7A7F5		up	
pyrE	Orotate phosphoribosyltransferase	_de novo_ UMP biosynthetic process	0.245962185014	H7GI01		up	
TT_C0592	2-hydroxyhepta-2,4-diene-1,7-dioate isomerase/5-carboxymethyl-2-oxo-hex-3-ene-1,7-dioate decarboxylase	4-hydroxyphenylacetate catabolic process	0.131443763759	Q72K26		down	
Ththe16_0955	5-carboxymethyl-2-hydroxymuconate semialdehyde dehydrogenase	4-hydroxyphenylacetate catabolic process	0.131443763759	F6DGL4		down	
deoB	Phosphopentomutase	5-phosphoribose 1-diphosphate biosynthetic process	0.131443763759	E8PQJ4	cytoplasm	down	
acsA	Acetyl-coenzyme A synthetase	acetyl-CoA biosynthetic process from acetate	0.397670969765	H9ZQU3		down	
alaS	Alanine-tRNA ligase	alanyl-tRNA aminoacylation	0.397670969765	H9ZTY0	cytoplasm	up	
Theos_0514	ABC-type branched-chain amino acid transport system, periplasmic component	amino acid transport	0.0801839902230	K7QW00		down	
TaqDRAFT_5266	Extracellular ligand-binding receptor	amino acid transport	0.0801839902230	B7A763		down	
TSC_c10820	N-acetylmuramic acid 6-phosphate etherase	amino sugar catabolic process	0	E8PPW7		up	
adk	Adenylate kinase	AMP salvage	0.296106066284	F6DEN1	cytoplasm	down	
argH	Argininosuccinate lyase	arginine biosynthetic process via ornithine	0.296106066284	H7GDL4	cytoplasm	up	
Theos_0676	Arginase	arginine metabolic process	0.296106066284	K7QWC7		down	
TCCBUS3UF1_4170	Phospho-2-dehydro-3-deoxyheptonate aldolase	aromatic amino acid family biosynthetic process	0.206028291459	G8N9G7		up	
TTHA0800	Phospho-2-dehydro-3-deoxyheptonate aldolase	aromatic amino acid family biosynthetic process	0.206028291459	Q5SK52		up	
Theos_1657	Aspartyl-tRNA synthetase, archaeal type	aspartyl-tRNA aminoacylation	0.400482074471	K7R6Y6	cytoplasm	up	
Mesil_1956	ABC transporter related protein	ATP catabolic process	0.08856520199680	D7BGL5		down	1

Gene	Protein	Top enriched Biological Process	p-value	Uniprot ID	Cellular component	Regulation at 77°C	Fig. 5B*
TaqDRAFT_3486	Heat shock protein HslVU, ATPase subunit HslU	ATP catabolic process	0.08856520199680	B7AAK1	cytoplasm	down	1
moxR	MoxR-like ATPase	ATP catabolic process	0.08856520199680	Q72IJ7		down	1
TCCBUS3UF1_9990	Iron(III) dicitrate transport ATP-binding protein fecE	ATP catabolic process	0.08856520199680	G8NCN1		down	1
TaqDRAFT_4887	ABC transporter related	ATP catabolic process	0.08856520199680	B7A618		down	1
Ththe16_0948	Polyamine-transporting ATPase	ATP catabolic process	0.08856520199680	F6DGK7		down	1
Ocepr_1433	ABC transporter related protein	ATP catabolic process	0.08856520199680	E4U959		down	1
TCCBUS3UF1_12050	Spermidine/putrescine transport system ATP-binding protein	ATP catabolic process	0.08856520199680	G8NDA8		down	1
TCCBUS3UF1_15950	ABC transporter protein	ATP catabolic process	0.08856520199680	G8N8X9		down	1
TCCBUS3UF1_13140	ABC transporter protein	ATP catabolic process	0.08856520199680	G8NDV5		up	1
macB1	Macrolide export ATP-binding/permease protein MacB	ATP catabolic process	0.08856520199680	E8PKC9		up	1
Theos_0842	ABC-type polar amino acid transport system, ATPase component	ATP catabolic process	0.08856520199680	K7R4P8		up	1
Ththe16_0271	ABC transporter related protein	ATP catabolic process	0.08856520199680	F6DD75		up	1
Ththe16_0447	Monosaccharide-transporting ATPase	ATP catabolic process	0.08856520199680	F6DE47		up	1
Mesil_0181	Phosphonate ABC transporter, ATPase subunit	ATP catabolic process	0.08856520199680	D7BGX2	plasma membrane	up	1
TT_P0177	Transporter	ATP catabolic process	0.08856520199680	Q745X8		up	1
TTHV087	ABC transporter-like protein	ATP catabolic process	0.08856520199680	G9MBD9		up	1
Ththe16_1650	Fe(3+)-transporting ATPase	ATP catabolic process	0.08856520199680	F6DEB8		up	1
TSC_c04350	ABC transporter, permease/ATP-binding protein, HlyB family	ATP catabolic process	0.08856520199680	E8PLA7		up	1
TCCBUS3UF1_10090	Phytoene dehydrogenase	carotenoid biosynthetic process	0.25325449169829	G8NCP1		down	
TCCBUS3UF1_16650	Putative uncharacterized protein	carotenoid biosynthetic process	0.25325449169829	G8N9D0		up	

Gene	Protein	Top enriched Biological Process	p-value	Uniprot ID	Cellular component	Regulation at 77°C	Fig. 5B*
TaqDRAFT_4252	Rad52/22 double-strand break repair protein	DNA repair	0.04511923091499	B7A856		down	2
radA	DNA repair protein radA	DNA repair	0.04511923091499	E8PNF9		up	2
TaqDRAFT_5398	DNA repair protein RecO	DNA repair	0.04511923091499	B7A7J5		up	2
recA	Protein RecA	DNA repair	0.04511923091499	E7CG24	nucleus	up	2
TaqDRAFT_4282	Transposase IS116/IS110/IS902 family protein	DNA repair	0.04511923091499	B7A886		up	2
recF	DNA replication and repair protein RecF	DNA repair	0.04511923091499	E8PJH5	nucleus	up	2
TaqDRAFT_3067	Histone family protein DNA-binding protein	chromosome condensation	0.29610606628426	B7ABS8		down	
TTHA0899	Chromosome segregation SMC protein	chromosome organization	0.29610606628426	Q5SJV3	cytoplasm	down	
Theos_0369	Small GTP-binding protein domain protein	GTP catabolic process	0.11871783492160	K7R3G6		down	3
Mrub_0318	GTP-binding protein TypA	GTP catabolic process	0.11871783492160	D3PLY5		up	3
obg	GTPase obg	GTP catabolic process	0.11871783492160	B7A5T8	cytoplasm	up	3
tuf1	Elongation factor Tu	GTP catabolic process	0.11871783492160	E8PJW4	cytoplasm	up	3
era	GTPase Era	GTP catabolic process	0.11871783492160	G8NAM1	Plasma membrane	up	3
fusA	Elongation factor G	GTP catabolic process	0.11871783492160	B7A552	cytoplasm	up	3
TtJL18_0706	Citrate synthase	cellular carbohydrate metabolic process	0.27671940896639	H9ZQJ9	cytoplasm	down	
argD	Acetylornithine aminotransferase	arginine biosynthetic process	0.08356036675864	H5SNC0	cytoplasm	down	4
argC	N-acetyl-gamma-glutamyl-phosphate/N-acetyl-gamma-aminoadipyl-phosphate reductase	arginine biosynthetic process	0.08356036675864	K7QWA1	cytoplasm	down	4
argG	Argininosuccinate synthase	arginine biosynthetic process	0.08356036675864	K7QVE3	cytoplasm	up	4
argJ	Arginine biosynthesis bifunctional protein ArgJ	arginine biosynthetic process	0.08356036675864	E8PKJ6	cytoplasm	up	4
carB	Carbamoyl-phosphate synthase large chain (Precursor)	arginine biosynthetic process	0.0835603667586405	K7QZP1		up	4

Gene	Protein	Top enriched Biological Process	p-value	Uniprot ID	Cellular component	Regulation at 77°C	Fig. 5B*
HMPREF1013_01460	Putative uncharacterized protein	biosynthetic process	0.13596383369053	E5WG85		down	5
RLTM_00865	Lipopolysaccharide core biosynthesis protein rfaG	biosynthetic process	0.13596383369053	H7GDR7		down	5
Tlie_1812	Glycosyl transferase group 1	biosynthetic process	0.13596383369053	G7V8Z4		down	5
TtJL18_1745	Aspartate/tyrosine/aromatic aminotransferase	biosynthetic process	0.13596383369053	H9ZTF4		down	5
TaqDRAFT_4317	Phenazine biosynthesis protein PhzF family	biosynthetic process	0.13596383369053	B7A668		down	5
Theos_0412	Bifunctional PLP-dependent enzyme with beta-cystathionase and maltose regulon repressor activities	biosynthetic process	0.13596383369053	K7QTW0		up	5
TTHA0620	Alternative anthranilate synthase component I+II (TrpEG)	biosynthetic process	0.13596383369053	Q5SKM3		up	5
TSC_c09910	Glycosyltransferase	biosynthetic process	0.13596383369053	E8PPF0		up	5
ilvN	Acetolactate synthase, small subunit	branched-chain amino acid biosynthetic process	0.29610606628426	E8PNJ1		up	
TtJL18_1837	Branched-chain amino acid aminotransferase, group I	branched-chain amino acid metabolic process	0.29610606628426	H9ZTP2		down	
Ththe16_1904	Glycoside hydrolase family 57	carbohydrate metabolic process	0.07355858347547	F6DFV9		down	6
TaqDRAFT_3070	Putative uncharacterized protein	carbohydrate metabolic process	0.07355858347547	B7ABT1		down	6
Mesil_1936	Phosphoglucomutase/phosphomannomutase alpha/beta/alpha domain I	carbohydrate metabolic process	0.07355858347547	D7BGJ5		down	6
malP	Phosphorylase	carbohydrate metabolic process	0.07355858347547	E8PK91		down	6
Ocepr_0509	Alpha-glucosidase	carbohydrate metabolic process	0.07355858347547	E4U6W5		down	6
Mesil_1834	Polysaccharide deacetylase	carbohydrate metabolic process	0.07355858347547	D7BG08		down	6
TT_C1283	Maltodextrin glucosidase	carbohydrate metabolic process	0.07355858347547	Q72I49	cytoplasm	down	6
Theos_1732	Phosphoribulokinase	carbohydrate metabolic process	0.07355858347547	K7RK40		up	6
TTHB115	Alpha-galactosidase	carbohydrate metabolic process	0.07355858347547	Q53W51		up	6
glmM	Phosphoribulokinase	carbohydrate metabolic process	0.07355858347547	K7QYX6		up	6
TSC_c10830	Beta-N-acetylglucosaminidase	carbohydrate metabolic process	0.07355858347547	E8PPW8		up	6

Gene	Protein	Top enriched Biological Process	p-value	Uniprot ID	Cellular component	Regulation at 77°C	Fig. 5B*
TaqDRAFT_5014	Alpha amylase catalytic region	carbohydrate metabolic process	0.07355858347547	B7A5A7		up	6
Theos_0104	ABC-type sugar transport system, periplasmic component	carbohydrate transport	0.1498825669787	K7RF25		down	
Theos_2161	ABC-type sugar transport system, periplasmic component	carbohydrate transport	0.14988256697871	K7R1F0		down	
TSC_c10840	Multiple sugar transport system substrate-binding protein	carbohydrate transport	0.14988256697873	E8PPW9		up	
ftsZ	Cell division protein FtsZ	cell cycle	0.11569371283475	Q72JP4	cytoplasm	down	
divIVA	Cell division initiation protein DivIVA	cell division	0.06741337253062	E8PN56	cytoplasm	down	7
ftsA	Cell division protein ftsA	cell division	0.06741337253062	E8PK41		down	7
TtJL18_0754	Cell division ATP-binding protein FtsE	cell division	0.06741337253062	H9ZQP7		down	7
int	Tyrosine recombinase XerC	cell division	0.06741337253062	A6MN83	nucleus	up	7
TCCBUS3UF1_21920	Glutaredoxin	cell redox homeostasis	0.24679517466959	G8NCG1		up	
TCCBUS3UF1_5010	Glutamate dehydrogenase	cellular amino acid metabolic process	0.21334979867869	G8N9X8		down	8
gdhA1	Glutamate dehydrogenase	cellular amino acid metabolic process	0.21334979867867	E8PP83		down	8
Theos_1523	O-acetylhomoserine sulfhydrylase	cellular amino acid metabolic process	0.21334979867869	K7QVH5		down	8
pyrB	Aspartate carbamoyltransferase	cellular amino acid metabolic process	0.21334979867867	G8N991		up	8
bfr	Bacterioferritin	cellular iron ion homeostasis	0.39767096976508	E8PQQ9		down	
Theos_2104	BirA, biotin-(Acetyl-CoA-carboxylase) ligase	cellular protein modification process	0.29154671139448	K7R198		down	
lipB	Octanoyltransferase	cellular protein modification process	0.29154671139448	H9ZP13	cytoplasm	up	
TTHB054	Precorrin-2 methylase	cobalamin biosynthetic process	0.02641547902147	Q53WA8		down	9
cobD	Cobalamin biosynthesis protein CobD	cobalamin biosynthetic process	0.02641547902141	E8PQC4	plasma membrane	down	9
TTHB057	Cobalamin biosynthesis protein CbiG	cobalamin biosynthetic process	0.02641547902147	Q53WA5		down	9
TTHB058	Cobalamin biosynthesis protein CbiX	cobalamin biosynthetic process	0.02641547902147	Q53WA4		down	9

Gene	Protein	Top enriched Biological Process	p-value	Uniprot ID	Cellular component	Regulation at 77°C	Fig. 5B*
Ththe16_2318	Precorrin-6y C5,15-methyltransferase (Decarboxylating), CbiE subunit	cobalamin biosynthetic process	0.02641547902147	F6DJT1		down	9
Ththe16_2319	Precorrin-8X methylmutase CbiC/CobH	cobalamin biosynthetic process	0.02641547902147	F6DJT2		down	9
TtJL18_2225	Precorrin-3B C17-methyltransferase	cobalamin biosynthetic process	0.02641547902147	H9ZUQ0		down	9
cobQ	Cobyric acid synthase	cobalamin biosynthetic process	0.02641547902147	H9ZUR1		up	9
cobS	Cobalamin synthase	cobalamin biosynthetic process	0.02641547902147	Q746P8	plasma membrane	up	9
coaD	Phosphopantetheine adenylyltransferase	coenzyme A biosynthetic process	0.35843550942014	H9ZRR4	cytoplasm	up	
udk	Uridine kinase	CTP salvage	0.29610606628426	E8PJU2	cytoplasm	up	
TSC_c21880	Ggdef domain protein	cyclic nucleotide biosynthetic process	0.02109139582735	E8PP66		down	10
TSC_c17260	Ggdef domain protein	cyclic nucleotide biosynthetic process	0.02109139582735	E8PLJ1		down	10
TCCBUS3UF1_15680	Diguanylate cyclase/phosphodiesterase with GAF sensor	cyclic nucleotide biosynthetic process	0.02109139582735	G8N8V2		up	10
TSC_c08960	Diguanylate cyclase	cyclic nucleotide biosynthetic process	0.02109139582735	E8PNX5		up	10
TCCBUS3UF1_3620	GGDEF domain protein	cyclic nucleotide biosynthetic process	0.02109139582735	G8N932		up	10
Ththe16_0803	Diguanylate cyclase	cyclic nucleotide biosynthetic process	0.02109139582735	F6DG56		up	10
TCCBUS3UF1_6050	Cytochrome c-type biogenesis protein, heme exporter protein B	cytochrome complex assembly	0.29862250570640	G8NAF9		down	
dapA	4-hydroxy-tetrahydrodipicolinate synthase	diaminopimelate biosynthetic process	0.22073221937586	K7RHY0	cytoplasm	down	
Marky_1548	Integrase catalytic region	DNA integration	0.19777111431889	F2NQR9		up	
RLTM_11018	Integrase catalytic subunit	DNA integration	0.19777111431886	H7GIN9		up	
Rhom172_2836	DNA methylase N-4/N-6 domain protein	DNA methylation	0.36397510920339	G2SLH7		down	
HGMM_F43B07C24	N-6 DNA methylase	DNA methylation on adenine	0.29610606628426	H5SL04		down	

Gene	Protein	Top enriched Biological Process	p-value	Uniprot ID	Cellular component	Regulation at 77°C	Fig. 5B*
Chy400_1961	Restriction modification system DNA specificity domain protein	DNA modification	0	B9LF22		down	
Mesil_3363	Putative uncharacterized protein	DNA recombination	0.17903687084299	D7BJ19		down	
Ththe16_2388	Uncharacterized protein	DNA recombination	0.17903687084299	F6DIS5		up	
TtJL18_0771	Archaeal/vacuolar-type H+-ATPase subunit I	ATP hydrolysis coupled proton transport	0.10706497978868	H9ZQR4		down	
TtJL18_1792	NADH-quinone oxidoreductase, chain G	ATP synthesis coupled electron transport	0.17549568943120	H9ZTK0		down	
nuoM	NADH-quinone oxidoreductase, subunit M	ATP synthesis coupled electron transport	0.17549568943120	E8PM70		down	
TaqDRAFT_4691	HhH-GPD family protein	base-excision repair	0.35843550942014	B7A8Y1		up	
Ththe16_0098	Dihydrolipoyl dehydrogenase	cell redox homeostasis	0.24679517466959	F6DHT7	cytoplasm	down	
Ththe16_0157	Dihydrolipoyl dehydrogenase	cell redox homeostasis	0.24679517466959	F6DHZ4	cytoplasm	down	
TCCBUS3UF1_20	DNA polymerase III subunit beta	DNA replication	0.06099598969933	G8NDC2	nucleus	down	
tdk	Thymidine kinase	DNA replication	0.06099598969933	K7QZR4	cytoplasm	up	
Theos_0365	Ribonucleoside-diphosphate reductase	DNA replication	0.06099598969933	K7QY19	cytoplasm	up	
gyrB	DNA gyrase, subunit B	DNA topological change	0.29862250570640	E8PPM8	cytoplasm	up	
gyrA	DNA gyrase subunit A	DNA topological change	0.29862250570640	H9ZQI7	cytoplasm	up	
TaqDRAFT_4448	RNA polymerase sigma factor	DNA-dependent transcription, initiation	0.40731246851837	B7A6J9		up	
TaqDRAFT_4237	PfkB domain protein	D-ribose metabolic process	0.39767096976508	B7A841		down	
Ththe16_1143	Cytochrome C oxidase subunit IIa transmembrane	electron transport chain	0.20065454405306	F6DH44		down	11
Theos_1499	Heme/copper-type cytochrome/quinol oxidase, subunit 1	electron transport chain	0.20065454405306	K7RJC0		down	11
TaqDRAFT_3811	Disulphide bond formation protein DsbB	electron transport chain	0.20065454405306	B7AA44		up	11
rsmI	Ribosomal RNA small subunit methyltransferase I	enzyme-directed rRNA 2_-O-methylation	0.29610606628426	G8NCV1	cytoplasm	down	

Gene	Protein	Top enriched Biological Process	p-value	Uniprot ID	Cellular component	Regulation at 77°C	Fig. 5B*
Marky_2247	DNA internalization-related competence protein ComEC/Rec2	establishment of competence for transformation	0.180661055224	F2NRB7		up	
TSC_c24440	Enoyl-[acyl-carrier-protein] reductase [NADH]	fatty acid biosynthetic process	0.20569362928578	E8PQK2		down	
TaqDRAFT_3831	3-oxoacyl-(Acyl-carrier-protein) reductase	fatty acid biosynthetic process	0.20569362928578	B7AA64		down	
TtJL18_0785	3-hydroxyacyl-CoA dehydrogenase	fatty acid metabolic process	0.39767096976508	H9ZQS8		down	
Marky_0291	Dihydroneopterin aldolase	folic acid-containing compound metabolic process	0.29610606628426	F2NNN3		up	
Ththe16_0983	Galactose-1-phosphate uridylyltransferase	galactose metabolic process	0.27671940896639	F6DGP1		up	
Q0GA06	Beta-galactosidase	galactose metabolic process	0.27671940896639	Q0GA06		up	
TCCBUS3UF1_12040	4-aminobutyrate aminotransferase	gamma-aminobutyric acid metabolic process	0	G8NDA7		down	
Theos_0371	Phosphoenolpyruvate synthase	gluconeogenesis	0.06400535587079	K7QTT7		down	
Ththe16_0908	Glyceraldehyde-3-phosphate dehydrogenase, type I	glucose metabolic process	0.36397510920339	F6DGG7		down	
TSC_c22670	Proline dehydrogenase/delta-1-pyrroline-5-carboxylate dehydrogenase	glutamate biosynthetic process	0.13144376375915	E8PPM1		down	
Theos_1674	Glutamate synthase family protein	glutamate biosynthetic process	0.13144376375915	K7R0A8		up	
guaA	GMP synthase [glutamine-hydrolyzing]	glutamine metabolic process	0.10900415134619	E8PMT4		down	12
Mesil_0319	Peptidase C26	glutamine metabolic process	0.10900415134619	D7BHM2		down	12
glmS2	Glutamine--fructose-6-phosphate aminotransferase [isomerizing]	glutamine metabolic process	0.10900415134619	E8PQI4	cytoplasm	down	12
pyrG	CTP synthase	glutamine metabolic process	0.10900415134619	K7QXU1		up	12
glpK	Glycerol kinase	glycerol catabolic process	0.29610606628426	Q53W24		up	
Theos_1644	Fructose-1,6-bisphosphatase	glycerol metabolic process	0.03952045222263	K7RJU5		down	
HGMM_F51G12C41	Dak phosphatase	glycerol metabolic process	0.03952045222263	H5SND6		down	
Theos_1736	Fructose-1,6-bisphosphatase	glycerol metabolic process	0.03952045222263	K7QVX3		up	
Theos_0177	Folate-binding protein YgfZ	glycine catabolic process	0.3976709697650	K7R309	cytoplasm	up	

Gene	Protein	Top enriched Biological Process	p-value	Uniprot ID	Cellular component	Regulation at 77°C	Fig. 5B*
gcvPA	Probable glycine dehydrogenase [decarboxylating] subunit 1	glycine decarboxylation via glycine cleavage system	0.03351893484805	H7GFD6		down	
gcvPB	Probable glycine dehydrogenase [decarboxylating] subunit 2	glycine decarboxylation via glycine cleavage system	0.03351893484805	F6DEJ8		down	13
gcvH	Glycine cleavage system H protein	glycine decarboxylation via glycine cleavage system	0.03351893484805	B7A6K6	cytoplasm	down	13
gcvT	Aminomethyltransferase	glycine decarboxylation via glycine cleavage system	0.03351893484805	H9ZSX1	cytoplasm	down	13
glgC	Glucose-1-phosphate adenylyltransferase (Precursor)	glycogen biosynthetic process	0.17955248737595	K7R0S6		down	
TSC_c12030	Amylo-alpha-1,6-glucosidase	glycogen biosynthetic process	0.17955248737595	E8PQP1		up	
Q9RHA2	Fructose-1,6-bisphosphate aldolase	glycolysis	0.01717439088799	Q9RHA2		down	14
Ththe16_0004	Pyruvate kinase	glycolysis	0.01717439088799	F6DH48		down	14
eno	Enolase	glycolysis	0.01717439088799	F6DH47	extracellular	down	14
Theos_1730	Fructose-1,6-bisphosphate aldolase, class II	glycolysis	0.01717439088799	K7R0G3		down	14
tpiA	Triosephosphate isomerase	glycolysis	0.01717439088799	H7GG75	cytoplasm	down	14
pgi	Glucose-6-phosphate isomerase	glycolysis	0.01717439088799	K7QXH8	cytoplasm	down	14
pfkA	6-phosphofructokinase	glycolysis	0.0171743908879	K7QYQ2	cytosol	down	14
pgk	Phosphoglycerate kinase	glycolysis	0.01717439088799	B7A7G6	cytoplasm	down	14
Theos_1703	Isocitrate dehydrogenase [NADP]	glyoxylate cycle	0.08018399022300	K7R721		down	
aceB	Malate synthase	glyoxylate cycle	0.08018399022300	E8PLU1		up	
guaB	Inosine-5'-monophosphate dehydrogenase	GMP biosynthetic process	0.1314437637591	K7R067		up	
TaqDRAFT_4733	(P)ppGpp synthetase I, SpoT/RelA	guanosine tetraphosphate metabolic process	0.29610606628426	B7A923		up	
hisZ	ATP phosphoribosyltransferase regulatory subunit	histidine biosynthetic process	0.21627422727242	G8NAL4	cytoplasm	down	
hisD	Histidinol dehydrogenase	histidine biosynthetic process	0.21627422727242	G8N8F8		down	
Theos_1961	Histidinol phosphate phosphatase HisJ family	histidine biosynthetic process	0.21627422727242	K7R0Y2		up	

Gene	Protein	Top enriched Biological Process	p-value	Uniprot ID	Cellular component	Regulation at 77°C	Fig. 5B*
hisS	Histidine-tRNA ligase	histidyl-tRNA aminoacylation	0.29610606628426	E8PKK4	cytoplasm	down	
TtJL18_0257	Uncharacterized protein	intein-mediated protein splicing	0.14988256697871	H9ZPB1		up	
Ththe16_0848	Putative serine protein kinase, PrkA	intein-mediated protein splicing	0.14988256697871	F6DGA7		up	
Theos_1172	Protein-export membrane protein, SecD/SecF family	intracellular protein transport	0.29610606628426	K7R5J4	plasma membrane	down	
Theos_0820	Archaeal/vacuolar-type H+-ATPase subunit F	ion transmembrane transport	0	K7QYU6		down	
TaqDRAFT_4881	FeS assembly protein SufB	iron-sulfur cluster assembly	0.17549568943120	B7A612		up	
Theos_0397	Iron-sulfur cluster assembly accessory protein	iron-sulfur cluster assembly	0.17549568943120	K7RFX9		up	
Theos_0111	FeS assembly protein SufD	iron-sulfur cluster assembly	0.17549568943120	K7R2R8		up	
ilvC	Ketol-acid reductoisomerase	isoleucine biosynthetic process	0.17549568943120	F6DHK9		up	
TTHA1213	Acetolactate synthase	isoleucine biosynthetic process	0.17549568943120	Q5SJ01		up	
Theos_1886	Geranylgeranyl pyrophosphate synthase	isoprenoid biosynthetic process	0.12190649326266	K7R0T4		up	
TCCBUS3UF1_5000	Dimethylallyltranstransferase	isoprenoid biosynthetic process	0.12190649326266	G8N9X7		up	
TCCBUS3UF1_6480	Iron-sulfur cluster-binding protein	lactate oxidation	0.29610606628426	G8NAK2		down	
Theos_2115	Alanine dehydrogenase	L-alanine catabolic process	0.29610606628426	K7QWF5		down	
leuC	3-isopropylmalate dehydratase large subunit	leucine biosynthetic process	0.01653529376097	E8PN40		up	15
Theos_1227	2-isopropylmalate synthase/homocitrate synthase family protein	leucine biosynthetic process	0.01653529376097	K7QX64		up	15
leuA	2-isopropylmalate synthase	leucine biosynthetic process	0.01653529376097	H9ZQY3		up	15
leuB	3-isopropylmalate dehydrogenase	leucine biosynthetic process	0.01653529376097	H9ZQW0	cytoplasm	up	15
leuD	3-isopropylmalate dehydratase small subunit	leucine biosynthetic process	0.01653529376097	K7R0W7	cytosol	up	15
Ththe16_0982	Lipopolysaccharide biosynthesis protein	lipopolysaccharide biosynthetic process	0.25325449169829	F6DGP0		down	
Ththe16_04	Long-chain-fatty-acid--CoA ligase	long-chain fatty acid metabolic	0.39767096976508	F6DE48		up	

Gene	Protein	Top enriched Biological Process	p-value	Uniprot ID	Cellular component	Regulation at 77°C	Fig. 5B*
TaqDRAFT_4425	Prephenate dehydratase	L-phenylalanine biosynthetic process	0.1806610552248	B7A6H6		up	
TtJL18_1195	Pyrroline-5-carboxylate reductase	L-proline biosynthetic process	0.40048207447170	H9ZRX7		down	
TaqDRAFT_5222	D-3-phosphoglycerate dehydrogenase	L-serine biosynthetic process	0.29610606628426	B7A719		up	
tdh	L-threonine 3-dehydrogenase	L-threonine catabolic process to glycine	0.29610606628426	H7GFH7	cytoplasm	down	
lysS1	Homocitrate synthase	lysine biosynthetic process via aminoadipic acid	0.24264633118936	E8PJX5		up	
lysS2	Lysine--tRNA ligase OS=Thermus scotoductus	lysyl-tRNA aminoacylation	0.36397510920339	E8PP07	cytoplasm	up	
accD	Acetyl-coenzyme A carboxylase carboxyl transferase subunit beta	malonyl-CoA biosynthetic process	0.13144376375915	E8PKR7	cytoplasm	down	
accA	Acetyl-coenzyme A carboxylase carboxyl transferase subunit alpha	malonyl-CoA biosynthetic process	0.13144376375915	K7QTP7	cytoplasm	down	
TTHA1854	Ubiquinone/menaquinone biosynthesis methyltransferase	menaquinone biosynthetic process	0.33035327024904	Q5SH76		up	
luxS	S-ribosylhomocysteine lyase	metabolic process	0.11335231367222	H9ZPZ2		down	16
TaqDRAFT_3803	Putative uncharacterized protein	metabolic process	0.11335231367222	B7AA36		down	16
Marky_0976	CRISPR-associated helicase Cas3	metabolic process	0.11335231367222	F2NLA1		down	16
TCCBUS3UF1_12090	4-aminobutyrate aminotransferase	metabolic process	0.11335231367222	G8NDB2		down	16
Theos_0621	4-aminobutyrate aminotransferase family protein	metabolic process	0.11335231367222	K7QW97		down	16
Theos_1008	Thioredoxin domain protein	metabolic process	0.11335231367222	K7QUP2		up	16
Marky_0132	Metal dependent phosphohydrolase	metabolic process	0.11335231367222	F2NLR5		up	16
TTHA0706	Cation-transporting ATPase	metal ion transport	0.35843550942014	Q5SKD7		up	
TaqDRAFT_4664	Methylenetetrahydrofolate reductase	methionine biosynthetic process	0.12190649326266	B7A8V4	cytosol	up	
metX	Homoserine O-acetyltransferase	methionine biosynthetic process	0.12190649326266	H9ZS71	cytoplasm	up	
metG	Methionine-tRNA ligase	methionyl-tRNA aminoacylation	0.29610606628426	F6DI12	cytoplasm	up	
TCCBUS3UF1_20360	Putative uncharacterized protein	methylation	0.35843550942014	G8NBJ7		up	

Gene	Protein	Top enriched Biological Process	p-value	Uniprot ID	Cellular component	Regulation at 77°C	Fig. 5B*
mgsA	Methylglyoxal synthase	methylglyoxal biosynthetic process	0.29610606628426	B3VH91		down	
TaqDRAFT_3451	Lon protease	misfolded or incompletely synthesized protein catabolic process	0.09295102571319	B7AAG6	cytoplasm	down	
lon1	ATP-dependent protease La	misfolded or incompletely synthesized protein catabolic process	0.09295102571319	E8PLC2		up	
TCCBUS3UF1_16310	Lon protease	misfolded or incompletely synthesized protein catabolic process	0.09295102571319	G8N996	cytoplasm	up	
mutS2	Endonuclease MutS2	mismatch repair	0.35843550942014	B7A9F0		up	
Theos_1888	Molybdenum cofactor biosynthesis protein A	Mo-molybdopterin cofactor biosynthetic process	0.24212756907799	K7RKG4		up	
nadE	NH(3)-dependent NAD(+) synthetase	NAD biosynthetic process	0.29905935775708	F6DFV7		down	
Ththe16_1003	Nicotinate-nucleotide pyrophosphorylase	NAD biosynthetic process	0.29905935775708	F6DGR1		up	
Ththe16_2321	High-affinity nickel-transporter	nickel cation transmembrane transport	0.29610606628426	F6DIL5		down	
TaqDRAFT_5093	UvrD/REP helicase	nucleic acid phosphodiester bond hydrolysis	0.02245772252487	B7A5I6		down	17
uvrB	UvrABC system protein	nucleic acid phosphodiester bond hydrolysis	0.02245772252493	F6DFV0	nucleus	up	17
vapC	Probable ribonuclease VapC	nucleic acid phosphodiester bond hydrolysis	0.02245772252487	Q82UB3		up	17
rnpA	Ribonuclease P protein component	nucleic acid phosphodiester bond hydrolysis	0.02245772252489	H9ZT49		up	17
rnr	Ribonuclease R	nucleic acid phosphodiester bond hydrolysis	0.02245772252487	Q72K93	cytoplasm	up	17
TTHA1550	5'-methylthioadenosine/S-adenosylhomocysteine nucleosidase	Nucleoside catabolic process	0.29610606628426	Q5SI30		down	
Ththe16_1633	Phosphoribosyltransferase	nucleoside metabolic process	0.04130182446040	F6DEA1		down	18
TtJL18_1513	Purine nucleoside phosphorylase	nucleoside metabolic process	0.04130182446040	H9ZST1		down	18
Theos_1667	Putative phosphoribosyltransferase	nucleoside metabolic process	0.04130182446040	K7R6Z5		down	18
TaqDRAFT_3801	Purine or other phosphorylase family 1	nucleoside metabolic process	0.04130182446040	B7AA34		down	18
prs	Ribose-phosphate pyrophosphokinase	nucleoside metabolic process	0.04130182446040	H7GHR7	cytoplasm	up	18

Gene	Protein	Top enriched Biological Process	p-value	Uniprot ID	Cellular component	Regulation at 77°C	Fig. 5B*
TCCBUS3UF1_5230	Amidophosphoribosyltransferase	nucleoside metabolic process	0.04130182446040	G8NA00		up	18
Ththe16_0556	Futalosine nucleosidase	nucleoside metabolic process	0.04130182446040	F6DEV2		up	18
TaqDRAFT_3772	5'-Nucleotidase domain protein	nucleotide catabolic process	0.39767096976508	B7AA05		down	
uvrC	UvrABC system protein	nucleotide-excision repair	0.14988256697871	H7GHI4	nucleus	up	
TT_P0052	Probable UV endonuclease	nucleotide-excision repair	0.14988256697871	Q746K1		up	
fni	Isopentenyl-diphosphate delta-isomerase	oxidation-reduction process	0.04453233705376	G8NCP0	cytoplasm	down	19
TaqDRAFT_3003	Short-chain dehydrogenase/reductase SDR	oxidation-reduction process	0.04453233705376	B7AC86		down	19
TaqDRAFT_5111	Cytochrome c biogenesis protein transmembrane region	oxidation-reduction process	0.04453233705376	B7A5K4		up	19
RLTM_11628	Sulfite dehydrogenase	oxidation-reduction process	0.04453233705376	H7GIZ2		up	19
TaqDRAFT_3098	Putative uncharacterized protein	oxygen transport	0.29610606628426	B7ABV9		up	
rpe	Ribulose-phosphate 3-epimerase	pentose-phosphate shunt	0.19777111431889	E8PN70		down	
TTHV085	Xylose isomerase	pentose-phosphate shunt	0.19777111431889	G9MBD7	cytoplasm	up	
rpiA	Ribose-5-phosphate isomerase	pentose-phosphate shunt, non-oxidative branch	0.29610606628426	B7A6G0		down	
Theos_1200	Membrane carboxypeptidase (Penicillin-binding protein)	peptidoglycan biosynthetic process	0.21089838775232	K7RIN4	cell wall	up	
TaqDRAFT_5375	Cell wall hydrolase/autolysin	peptidoglycan catabolic process	0.39767096976508	B7A7H2		down	
TSC_c22010	Deoxyhypusine synthase-like protein	peptidyl-lysine modification to hypusine	0.36397510920339	E8PP79		up	
Theos_0972	4-hydroxyphenylacetate 3-monooxygenase, oxygenase component	phenylacetate catabolic process	0.39767096976504	K7QZ08		down	
pheS	Phenylalanine--tRNA ligase alpha subunit	phenylalanyl-tRNA aminoacylation	0.22073221937586	E8PQX8	cytoplasm	down	
pheT	Phenylalanine--tRNA ligase beta subunit	phenylalanyl-tRNA aminoacylation	0.22073221937586	B7ABK3	cytoplasm	down	

Gene	Protein	Top enriched Biological Process	p-value	Uniprot ID	Cellular component	Regulation at 77°C	Fig. 5B*
pstS	Phosphate-binding protein	phosphate ion transmembrane transport	0.29610606628426	E8PJI0		down	
TT_C0694	ADP-ribosylglycohydrolase	phosphate-containing compound metabolic process	0.36397510920339	Q72JS4	cytoplasm	down	
TtJL18_1622	Phosphatidylglycerophosphate synthase	phospholipid biosynthetic process	0.29403811421943	H9ZT36		up	
TSC_c08330	Hypothetical membrane spanning protein	phospholipid biosynthetic process	0.29403811421943	E8PNI4	plasma membrane	up	
nuoC	NADH-quinone oxidoreductase subunit C	photosynthesis, light reaction	0.02109139582735	E8PM80	plasma membrane	down	
nuoA	NADH-quinone oxidoreductase subunit A	photosynthesis, light reaction	0.02109139582735	B7A859	plasma membrane	down	
nuoD	NADH-quinone oxidoreductase subunit D	photosynthesis, light reaction	0.02109139582735	K7R4F8	plasma membrane	down	
nuoB	NADH-quinone oxidoreductase subunit B	photosynthesis, light reaction	0.02109139582735	G8NBB2	plasma membrane	down	
nuoI	NADH-quinone oxidoreductase subunit I	photosynthesis, light reaction	0.02109139582735	E8PM74	plasma membrane	down	
nuoN	NADH-quinone oxidoreductase subunit N	photosynthesis, light reaction	0.02109139582735	G8NBA0	plasma membrane	down	
atpB	V-type ATP synthase beta chain	plasma membrane ATP synthesis coupled proton transport	0.03766623385339	E8PNV8		down	20
atpE	V-type proton ATPase subunit E	plasma membrane ATP synthesis coupled proton transport	0.03766623385336	H7GGU9		down	20
atpD	V-type ATP synthase subunit D	plasma membrane ATP synthesis coupled proton transport	0.03766623385336	G8N8D7		down	20
atpA	V-type ATP synthase alpha chain	plasma membrane ATP synthesis coupled proton transport	0.03766623385336	F6DHR7		down	20
atpC	V-type ATP synthase subunit C	plasma membrane ATP synthesis coupled proton transport	0.03766623385336	G8N8E1		down	20
TaqDRAFT_4115	Extracellular solute-binding protein family 1	polyamine transport	0.03260802208266	B7A7R9		down	
TSC_c12800	Spermidine/putrescine-binding periplasmic protein	polyamine transport	0.03260802208266	E8PR71		down	
TT_P0017	Uroporphyrin-III C-methyltransferase	porphyrin-containing compound biosynthetic process	0.14547336020393	Q746N6		down	
TaqDRAFT_5280	Uroporphyrin-III C/tetrapyrrole (Corrin/Porphyrin) methyltransferase	porphyrin-containing compound biosynthetic process	0.14547336020393	B7A777		down	

Gene	Protein	Top enriched Biological Process	p-value	Uniprot ID	Cellular component	Regulation at 77°C	Fig. 5B*
TaqDRAFT_5081	Delta-aminolevulinic acid dehydratase	porphyrin-containing compound biosynthetic process	0.14547336020393	B7A5H4		down	
TSC_c15070	Potassium transporter peripheral membrane component	potassium ion transmembrane transport	0.29610606628426	E8PK93	plasma membrane	up	
kefC	Glutathione-regulated potassium-efflux system protein KefC	potassium ion transport	0.38281092298422	E8PM07		up	
TaqDRAFT_4400	Sigma 54 modulation protein/ribosomal protein S30EA	primary metabolic process	0.29610606628426	B7A6F1	cytoplasm	down	
TSC_c22660	Delta-1-pyrroline-5-carboxylate dehydrogenase	proline biosynthetic process	0.40731246851837	E8PPM0		down	
proS	Proline-tRNA ligase	prolyl-tRNA aminoacylation	0.29610606628426	K7RK64	cytoplasm	down	
Ththe16_0257	Peptidyl-prolyl cis-trans isomerase cyclophilin type	protein folding	0.02783806293600	F6DD61		down	21
TaqDRAFT_4616	Peptidyl-prolyl cis-trans isomerase	protein folding	0.02783806293600	B7ABH4		down	21
dnaK	Chaperone protein DnaK	protein folding	0.02783806293600	B7A6Y3		down	21
TaqDRAFT_4589	PpiC-type peptidyl-prolyl cis-trans isomerase	protein folding	0.02783806293600	B7ABE7		down	21
Ththe16_0606	PpiC-type peptidyl-prolyl cis-trans isomerase	protein folding	0.02783806293600	F6DEZ9		down	21
clpX	ATP-dependent Clp protease ATP-binding subunit ClpX	protein folding	0.02783806293600	F6DF87		up	21
hslO	33 kDa chaperonin	protein folding	0.02783806293600	H9ZRT7	cytoplasm	up	21
groS	10 kDa chaperonin	protein folding	0.02783806293600	E8PJF5	cytoplasm	up	21
lgt	Prolipoprotein diacylglyceryl transferase	protein lipoylation	0.22073221937586	G8N983	plasma membrane	down	
lipA	Lipoyl synthase	protein lipoylation	0.22073221937586	E8PK17	cytoplasm	down	
TaqDRAFT_3595	ATPase AAA-2 domain protein	protein metabolic process	0	B7A9W8		Up	
Theos_0873	Putative Ser protein kinase	protein phosphorylation	0.29610606628426	K7R4R6		up	
Theos_0686	ATP-dependent chaperone ClpB	protein processing	0.29610606628426	K7QWD3	cytoplasm	down	
groL	60 kDa chaperonin	protein refolding	0.29610606628426	K7QXH6	cytoplasm	up	
TSC_c20700	General secretion pathway protein	protein secretion	0.25723239902906	E8PNE0		down	

Gene	Protein	Top enriched Biological Process	p-value	Uniprot ID	Cellular component	Regulation at 77°C	Fig. 5B*
Ththe16_1801	Preprotein translocase, SecG subunit	protein secretion	0.25723239902906	F6DF67		up	
TaqDRAFT_4341	Peptidase M24	proteolysis	0.11027168548082	B7A692		down	22
pepA	Probable cytosol aminopeptidase	proteolysis	0.11027168548082	D3PR67	cytoplasm	down	22
TTHA0286	Serine protease, subtilase family	proteolysis	0.11027168548082	Q5SLK7		down	22
TaqDRAFT_5158	Signal peptidase I	proteolysis	0.11027168548082	B7A5Q1		down	22
Theos_1520	Leucyl aminopeptidase (Aminopeptidase T)	proteolysis	0.11027168548082	K7QXK2		down	22
pcp	Pyrrolidone-carboxylate peptidase	proteolysis	0.11027168548082	E8PRB6	cytoplasm	down	22
Theos_0798	Zn-dependent dipeptidase, microsomal dipeptidase	proteolysis	0.11027168548082	K7QWI0		down	22
TSC_c17860	Carboxyl-protease	proteolysis	0.11027168548082	E8PLY1		Up	22
Mesil_0115	Peptidase M29 aminopeptidase II	proteolysis	0.11027168548082	D7BGQ6		Up	22
TTHA0896	Zn-dependent protease	proteolysis	0.11027168548082	Q5SJV6		Up	22
TSC_c15690	Membrane metalloprotease	proteolysis	0.11027168548082	E8PKN3		Up	22
clpP	ATP-dependent Clp protease proteolytic subunit	proteolysis	0.11027168548082	F6DF86	cytoplasm	Up	22
TaqDRAFT_3485	20S proteasome A and B subunits	proteolysis involved in cellular protein catabolic process	0.29610606628426	B7AAK0	cytoplasm	down	
TaqDRAFT_4708	Alanine dehydrogenase/PNT domain protein	proton transport	0.29610606628426	B7A8Z8		down	
TSC_c12840	Aminotransferase	protoporphyrinogen IX biosynthetic process	0.27671940896639	E8PR75	cytoplasm	down	
hemA	Glutamyl-tRNA reductase	protoporphyrinogen IX biosynthetic process	0.27671940896639	G8NA12		Up	
rluA	Pseudouridine synthase	pseudouridine synthesis	0.40048207447177	E8PPQ5		Up	
metH	Methionine synthase	pteridine-containing compound metabolic process	0.36397510920339	E8PJR6		Up	
TCCBUS3UF1_5140	Guanylate kinase	purine nucleotide metabolic process	0.39767096976508	G8N9Z1	cytoplasm	down	
pdxS	Pyridoxal biosynthesis lyase PdxS	pyridoxal phosphate biosynthetic process	0.13144376375915	E8PKL9		down	

Gene	Protein	Top enriched Biological Process	p-value	Uniprot ID	Cellular component	Regulation at 77°C	Fig. 5B*
pdxT	Glutamine amidotransferase subunit PdxT	pyridoxal phosphate biosynthetic process	0.13144376375915	B7A671		Up	
dcd	Deoxycytidine triphosphate deaminase	pyrimidine ribonucleotide biosynthetic process	0.29610606628426	B7ABY5		down	
glmU	Bifunctional protein GlmU (Precursor)	regulation of cell shape	0.16436060135749	K7RJN4	cytoplasm	down	
ddl	D-alanine-D-alanine ligase	regulation of cell shape	0.16436060135741	B7A6N0	cell wall	Up	
uppP	Undecaprenyl-diphosphatase	regulation of cell shape	0.16436060135741	D7BBZ8	plasma membrane	Up	
dnaA	Chromosomal replication initiator protein DnaA	regulation of DNA replication	0.29610606628426	B7ABI9	cytoplasm	Up	
CU074314.1	Uncharacterized protein	regulation of Rho protein signal transduction	0	E7F3M3	cytoplasm	Up	
TCCBUS3UF1_5420	Two component transcriptional regulator, winged helix	regulation of transcription, DNA-dependent	0.11505841930103	G8NA19		down	23
TSC_c03290	Cold shock protein, CSD family	regulation of transcription, DNA-dependent	0.11505841930103	E8PKS4	nucleus	down	23
TaqDRAFT_4552	Response regulator receiver protein	regulation of transcription, DNA-dependent	0.11505841930103	B7A6V3		down	23
nusB	N utilization substance protein B homolog	regulation of transcription, DNA-dependent	0.11505841930103	G8N7W1		down	23
TSC_c07440	Acetyl-coenzyme A synthetase	regulation of transcription, DNA-dependent	0.11505841930103	E8PN20		up	23
TaqDRAFT_3484	Magnesium-chelatase subunit ChlI	regulation of transcription, DNA-dependent	0.11505841930103	B7AAJ9		up	23
rho	Transcription termination factor Rho	regulation of transcription, DNA-dependent	0.11505841930103	G8N8I1		up	23
leuS	Leucine-tRNA ligase	regulation of translational fidelity	0.29403811421943	F6DID5	cytoplasm	up	
ileS	Isoleucine--tRNA ligase	regulation of translational fidelity	0.29403811421943	H9ZRD2	cytoplasm	up	
TtJL18_2001	Thioredoxin reductase	removal of superoxide radicals	0.29610606628426	H9ZU48	cytoplasm	up	
Ththe16_1525	Cytochrome c assembly protein	respiratory chain complex IV assembly	0.40048207447170	F6DDS1		up	
Theos_0487	Uncharacterized protein involved in tolerance to divalent cations	response to metal ion	0.29610606628426	K7RG66		up	
Ththe16_1503	Heat shock protein Hsp20	response to stress	0.16004850295800	F6DDH6		down	24

Gene	Protein	Top enriched Biological Process	p-value	Uniprot ID	Cellular component	Regulation at 77°C	Fig. 5B*
TCCBUS3UF1_3770	Osmotically inducible protein C	response to stress	0.16004850295800	G8N948		down	24
TSC_c23100	Small heat shock protein	response to stress	0.16004850295800	E8PPR4		up	24
TaqDRAFT_5154	OsmC family protein	response to stress	0.16004850295800	B7A5P7		up	24
ribD	Riboflavin biosynthesis protein RibD	riboflavin biosynthetic process	0.30069863234195	Q72JR9		up	
rimP	Ribosome maturation factor RimP	ribosomal small subunit biogenesis	0.17955248737595	K7QZC0	cytoplasm	up	
der	GTPase Der	ribosome biogenesis	0.13144376375915	K7QY54		up	
trmB	tRNA (guanine-N(7)-)-methyltransferase	RNA (guanine-N7)-methylation	0.29610606628426	F6DEA7		up	
TT_C0162	Hypothetical cytosolic protein	RNA metabolic process	0.27671940896639	Q72L97		up	
TSC_c21520	Uncharacterized protein	RNA modification	0.13144376375915	E8PNV0		up	
rimO	Ribosomal protein S12 methylthiotransferase RimO	RNA modification	0.13144376375915	K7R5M3	cytoplasm	up	
pnp	Polyribonucleotide nucleotidyltransferase	RNA processing	0.24264633118936	E8PPC3	cytoplasm	up	
Theos_0240	rRNA methylase	RNA processing	0.24264633118936	K7QVL6		up	
TT_C1691	23S rRNA methyltransferase	RNA processing	0.24264633118936	Q72H04		up	
rlmN	Probable dual-specificity RNA methyltransferase RlmN	rRNA base methylation	0.39767096976508	E8PQM4	cytoplasm	up	
TtJL18_1131	N6-adenine-specific methylase	rRNA methylation	0.25325449169829	H9ZRR5		down	
Ththe16_0532	Methyltransferase small	rRNA methylation	0.25325449169829	F6DEK4		up	
metK	S-adenosylmethionine synthase	S-adenosylmethionine biosynthetic process	0.29610606628426	E8PQ14	cytoplasm	up	
TSC_c04840	Sensor histidine kinase	signal transduction by phosphorylation	0.06022236780272	E8PLN1		up	
ftsY	Signal recognition particle receptor FtsY	SRP-dependent cotranslational protein targeting to membrane	0.39767096976508	F2NM48	plasma membrane	down	
TtJL18_1518	Superoxide dismutase	superoxide metabolic process	0.29610606628426	H9ZST6		up	
TTHA1803	Pterin-4-alpha-carbinolamine dehydratase	tetrahydrobiopterin biosynthetic process	0.36397510920339	Q5SHC7		up	
glyA	Serine hydroxymethyltransferase	tetrahydrofolate interconversion	0.03952045222263	B7A5B7	cytoplasm	down	

Gene	Protein	Top enriched Biological Process	p-value	Uniprot ID	Cellular component	Regulation at 77°C	Fig. 5B*
folD	Bifunctional protein FolD	tetrahydrofolate interconversion	0.03952045222263	F6DH30		down	
fhs	Formate-tetrahydrofolate ligase	tetrahydrofolate interconversion	0.03952045222263	G8NBH4		down	
TCCBUS3UF1_2720	Folyl-polyglutamate synthetase	tetrahydrofolylpolyglutamate biosynthetic process	0.39767096976508	G8N8L2		up	
TCCBUS3UF1_13420	Phosphomethylpyrimidine kinase	thiamine biosynthetic process	0.12676859867092	G8NDY3		up	
thiC	Phosphomethylpyrimidine synthase	thiamine diphosphate biosynthetic process	0.06758896094216	F6DFE3		up	25
thiE	Thiamine-phosphate synthase	thiamine diphosphate biosynthetic process	0.06758896094216	F6DFD9		up	25
thiI	Probable tRNA sulfurtransferase	thiamine diphosphate biosynthetic process	0.06758896094216	E6SLU3	cytoplasm	up	25
thiG	Thiazole synthase	thiamine diphosphate biosynthetic process	0.06758896094216	H9ZSG9	cytoplasm	up	25
TSC_c04280	ABC transporter	thiamine transport	0.29610606628426	E8PLA1		up	
Theos_1818	Threonine synthase	threonine biosynthetic process	0.29403811421943	K7R0P1		down	
TCCBUS3UF1_19750	ATP/GTP hydrolase	threonylcarbamoyladenosine biosynthetic process	0.40048207447170	G8NB56		up	
RLTM_08814	GntR family transcriptional regulator	transcription, DNA-dependent	0.06984945970694	H7GHL4		down	26
rex	Redox-sensing transcriptional repressor rex	transcription, DNA-dependent	0.06984945970694	H9ZPN7	nucleus	down	26
rpoZ	DNA-directed RNA polymerase subunit omega	transcription, DNA-dependent	0.06984945970694	B7A5A9		down	26
TCCBUS3UF1_10180	Transcriptional regulator, Crp	transcription, DNA-dependent	0.06984945970694	G8NCQ0		down	26
argR	Arginine repressor Arginine repressor	transcription, DNA-dependent	0.06984945970694	E8PP68	nucleus	down	26
Ththe16_0611	Regulatory protein TetR	transcription, DNA-dependent	0.06984945970694	F6DF04		down	26
TSC_c12070	Transcriptional regulator, LacI family	transcription, DNA-dependent	0.06984945970694	E8PQP5		up	26
rpoC	DNA-directed RNA polymerase subunit beta'	transcription, DNA-dependent	0.06984945970694	H9ZTW1		up	26
rpoB	DNA-directed RNA polymerase subunit beta	transcription, DNA-dependent	0.06984945970694	K7RFC6		up	26
TaqDaft_3795	Transcriptional regulator, IclR family	transcription, DNA-dependent	0.06984945970694	B7AA28		up	26

Gene	Protein	Top enriched Biological Process	p-value	Uniprot ID	Cellular component	Regulation at 77°C	Fig. 5B*
TCCBUS3UF1_6540	Transcriptional regulator, FNR/CRP	transcription, DNA-dependent	0.06984945970694	G8NAT3		up	26
TSC_c09290	Anti-cleavage anti-GreA transcription factor Gfh1	transcription, DNA-dependent	0.06984945970694	E8PP08		up	26
TSC_c18130	Probable transcriptional regulatory protein TSC_c18130	transcription, DNA-dependent	0.06984945970694	E8PM08	nucleus	up	26
Theos_0989	Transcriptional regulator	transcription, DNA-dependent	0.06984945970694	K7RHZ8		up	26
greA	Transcription elongation factor GreA	transcription, DNA-dependent	0.06984945970694	Q8VQD6		up	26
TtJL18_1038	Transcriptional regulator	transcription, DNA-dependent	0.06984945970694	H9ZRH6		up	26
TaqDRAFT_3845	Transcriptional regulator, MarR family	transcription, DNA-dependent	0.06984945970694	B7AA78		up	26
rpsK	30S ribosomal protein S11	translation	0.00588933923984	E8PP97	cytoplasm	down	27
rpsC	30S ribosomal protein S3	translation	0.00588933923984	K7R3A3		down	27
rplI	50S ribosomal protein L9	translation	0.00588933923984	F6DHY0	cytoplasm	down	27
rpsD	30S ribosomal protein S4	translation	0.00588933923984	K7QXZ2		down	27
rplJ	50S ribosomal protein L10	translation	0.00588933923984	G8NC04	cytoplasm	down	27
rplY	50S ribosomal protein L25	translation	0.00588933923984	K7QWB6	cytoplasm	down	27
rpsE	30S ribosomal protein S5	translation	0.00588933923984	F6DEN5		down	27
rplQ	50S ribosomal protein L17	translation	0.00588933923984	B7A584	cytoplasm	down	27
rpsT	30S ribosomal protein S20	translation	0.00588933923984	E8PNN6	cytoplasm	down	27
rplO	50S ribosomal protein L15	translation	0.00588933923982	E8PPA3		down	27
pth	Peptidyl-tRNA hydrolase	translation	0.00588933923984	B7A6N1	cytoplasm	down	27
rplL	50S ribosomal protein L7/L12	translation	0.00588933923984	F6DI90	cytoplasm	down	27
rpsA	30S ribosomal protein S1	translation	0.00588933923984	Q83YV9	cytoplasm	up	27
rpmA	50S ribosomal protein L27	translation	0.00588933923984	K7RFL5	cytoplasm	up	27
rpsM	30S ribosomal protein S13	translation	0.00588933923984	E8PP98	cytoplasm	up	27
rpsO	30S ribosomal protein S15	translation	0.00588933923984	F2NM77	cytoplasm	up	27
fmt	Methionyl-tRNA formyltransferase	translational initiation	0.36397510920339	B7A8I8		up	

Gene	Protein	Top enriched Biological Process	p-value	Uniprot ID	Cellular component	Regulation at 77°C	Fig. 5B*
frr	Ribosome-recycling factor	translational termination	0.29610606628426	E8PLG3	cytoplasm	down	
Ththe16_0824	Putative sodium symporter protein	transmembrane transport	0.14721004982635	F6DG77		down	28
TaqDRAFT_3924	Uracil-xanthine permease	transmembrane transport	0.14721004982635	B7A8H1		up	28
Theos_1382	Tellurite resistance protein-like permease	transmembrane transport	0.14721004982635	K7R647		up	28
RLTM_04929	Uncharacterized protein	transmembrane transport	0.14721004982635	H7GG11		up	28
TSC_c20050	Major facilitator superfamily MFS_1	transmembrane transport	0.14721004982635	E8PN77		up	28
TaqDRAFT_4588	Major facilitator superfamily MFS_1	transmembrane transport	0.14721004982635	B7ABE6		up	28
Mrub_0144	Drug resistance transporter, EmrB/QacA subfamily	transmembrane transport	0.14721004982635	D3PL28	plasma membrane	up	28
TaqDRAFT_4068	TRAP dicarboxylate transporter-DctP subunit	transport	0.14115412319067	B7A8B7		down	
pilF	ATP-binding motif-containing protein pilF	transport	0.14115412319065	Q72H73		up	
Mrub_2215	Twitching motility protein	transport	0.14115412319067	D3PKU4		up	
TaqDRAFT_3838	Transposase IS4 family protein	transposition, DNA-mediated	0.13994323497076	B7AA71		up	29
RLTM_05796	Transposase	transposition, DNA-mediated	0.13994323497076	H7GHW1		up	29
TtJL18_1389	Transposase	transposition, DNA-mediated	0.13994323497076	H9ZSG3		up	29
RLTM_08204	Transposase	transposition, DNA-mediated	0.13994323497076	H7GHB0		up	29
mdh	Malate dehydrogenase	tricarboxylic acid cycle	0.08356036675864	E8PMQ8		down	30
sucC	Succinyl-CoA ligase [ADP-forming] subunit beta	tricarboxylic acid cycle	0.08356036675864	H9ZSV6		down	30
Theos_1659	Succinate dehydrogenase, flavoprotein subunit	tricarboxylic acid cycle	0.08356036675864	K7QVQ7		down	30
TCCBUS3UF1_16710	Succinate dehydrogenase, cytochrome subunit	tricarboxylic acid cycle	0.08356036675860	G8N9D6		down	30
fumC	Fumarate hydratase class II	tricarboxylic acid cycle	0.08356036675860	Q5SKT5	cytoplasm	down	30

Gene	Protein	Top enriched Biological Process	p-value	Uniprot ID	Cellular component	Regulation at 77°C	Fig. 5B*
TaqDRAFT_4692	Glucose-inhibited division protein A	tRNA processing	0.25325449169829	B7A8Y2		up	
truB	tRNA pseudouridine synthase B	tRNA pseudouridine synthesis	0.06479534891742	K7R1A7		down	
truD	tRNA pseudouridine synthase D	tRNA pseudouridine synthesis	0.06479534891742	B7A7Z2		up	
truA	tRNA pseudouridine synthase A	tRNA pseudouridine synthesis	0.06479534891742	K7QTV4		up	
Ththe16_1861	Anthranilate synthase component I	tryptophan biosynthetic process	0.21485354366631	F6DFJ7		up	
trpS	Tryptophan-tRNA ligase	tryptophanyl-tRNA aminoacylation	0.29610606628426	E8PN43	cytoplasm	up	
tyrA	Prephenate dehydrogenase	tyrosine biosynthetic process	0.29610606628426	E8PMZ6		up	
TTHV084	Xylulokinase	xylulose metabolic process	0.1806610552248	G9MBD6		up	

*Numebered according to the Biological Process shown in Figure 5B.

Table S11: Gene encoding aminoacyl-tRNA synthetases that presented duplication in *Thermus filfiromis*, and their regulation in sample cultivated at 77 °C for trancriptome and proteome analysis.

Gene Name	aminoacyl-tRNA synthetases	Transcriptome	Proteome
Thfi_0089	alanyl tRNA synthetase	+	nsd
Thfi_1940	alanyl tRNA synthetase	nsd	nsd
Thfi_2251	aspartyl-tRNA synthetase	+	nsd
Thfi_1196	aspartyl-tRNA synthetase	nsd	nsd
Thfi_0234	cysteinyl-tRNA synthetase	nsd	+
Thfi_1287	cysteinyl-tRNA synthetase	nsd	nsd
Thfi_1644	valyl-tRNA synthetase	+	nsd
Thfi_1505	valyl-tRNA synthetase	nsd	nsd

(+)Up-regulated at 77 °C , (nsd) no signifincant difference in expression between sample cultivated at 77 °C and 63 °C.

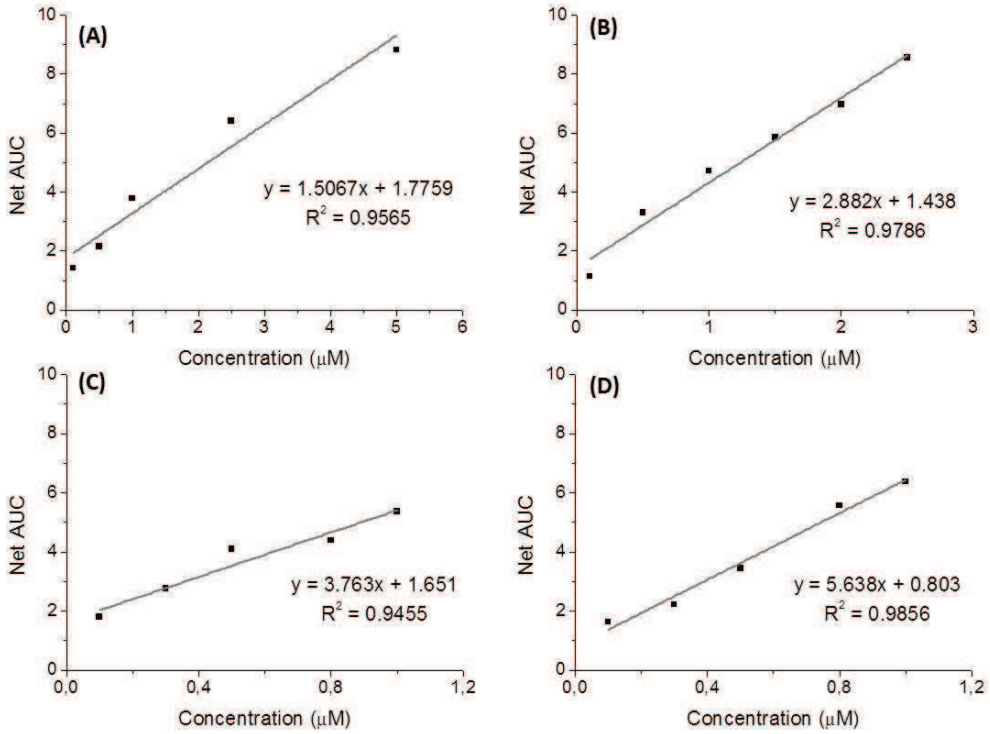

Figure SF1. Peroxyl radical scavenger capacity by carotenoid extracts of *Thermus filiformis*. Linear relationship between the carotenoid concentrations of samples cultivated at 63 °C (A), 70 °C (B), 77 °C (C) and 70 °C with 100 μM of H_2O_2 (D) and net AUC values from the fluorescence decay curves of C11–BODIPY581/591 oxidation.

APÊNDICE

Artigo publicado durante o período de Doutorado como autor principal sobre produção simultânea de xilooligossacarídeos e compostos antioxidantes através de hidrólise enzimática.

Reproduzido do periódico *Industrial Crops and Products*, volume 52, F. Mandelli, L.B. Brenelli, R.F. Almeida, R. Goldbeck, L.D. Wolf, Z.B. Hoffmam, R. Ruller, G.J.M. Rocha, A.Z. Mercadante, F.M. Squina, Simultaneous production of xylooligosaccharides and antioxidante compounds from sugarcane bagasse via enzymatic hydrolysis, 770-775,

Industrial Crops and Products 52 (2014) 770–775

Contents lists available at ScienceDirect

Industrial Crops and Products

journal homepage: www.elsevier.com/locate/indcrop

Simultaneous production of xylooligosaccharides and antioxidant compounds from sugarcane bagasse via enzymatic hydrolysis

F. Mandelli[a,b], L.B. Brenelli[a,c], R.F. Almeida[a], R. Goldbeck[a], L.D. Wolf[a], Z.B. Hoffmam[a,c], R. Ruller[a], G.J.M. Rocha[a], A.Z. Mercadante[b], F.M. Squina[a,*]

[a] Brazilian Bioethanol Science and Technology Laboratory (CTBE), Brazilian Centre of Research in Energy and Materials (CNPEM), Campinas, Brazil
[b] Department of Food Science, Faculty of Food Engineering, University of Campinas (UNICAMP), Campinas, Brazil
[c] Institute of Biology, University of Campinas (UNICAMP), Campinas, Brazil

ARTICLE INFO

Article history:
Received 12 July 2013
Received in revised form 17 October 2013
Accepted 1 December 2013

Keywords:
XynZ
Clostridium thermocellum
Xylooligosaccharides
Phenolic compounds
Peroxyl radical scavenger

ABSTRACT

Advances in industrial biotechnology offer potential opportunities for economic utilization of agro-industrial residues such as sugarcane bagasse, which is the major by-product of the sugarcane industry. Due to its abundant availability and despite the complex chemical composition, it can be considered an ideal substrate for microbial processes for the production of value-added products. In the present study we evaluated the enzymatic production of xylooligosaccharides (XOS) and antioxidant compounds from sugarcane bagasse using XynZ from *Clostridium thermocellum*, a naturally chimeric enzyme comprising activities of xylanase and feruloyl esterase along with a carbohydrate binding module (CBM6). In order to reveal the biotechnological potential of XynZ, the XOS released after enzymatic hydrolysis using different substrates were characterized by capillary electrophoresis and quantified by high performance anion exchange chromatography. In parallel, the antioxidant capacity related to the release of phenolic compounds was also determined. The results indicated noteworthy differences regarding the amount of XOS and antioxidant phenolic compounds produced, as well as the XOS profile, functions of the pre-treatment method employed. The ability of XynZ to simultaneously produce xylooligosaccharides, natural probiotics, phenolic compounds and antioxidant molecules from natural substrates such as sugarcane bagasse demonstrated the biotechnological potential of this enzyme. Production of value-added products from agro-industrial residues is of great interest not only for advancement in the biofuel field, but also for pharmaceutical and food industries.

1. Introduction

Large amounts of waste are generated every year from the industrial processing of agricultural raw materials. Most of these wastes are used as animal feed or burned as an alternative for elimination. However, such wastes may be a potential source of many interesting compound, such as antioxidant compounds and xylooligosaccharides (Sultana et al., 2008; Akpinar et al., 2009). Plant biomass, like sugarcane bagasse, is a cheap, abundant and renewable raw material that can be employed for sustainable production of biofuel, bioenergy and several value added biomolecules (Jayapal et al., 2013; Gonçalves et al., 2012; Damásio et al., 2012). Currently, sugarcane is used worldwide as a feedstock for ethanol and sugar production. After sugarcane is milled for juice extraction, bagasse is obtained as a residue, which corresponds to about 25% of the total fresh weight and contains 60%–80% of carbohydrates (Betancur and Pereira, 2010). Sugarcane bagasse is composed of cellulose, hemicellulose, lignin, and small amounts of extractives and mineral salts (Rezende et al., 2011). The enzymatic conversion of lignocellulosic biomass could significantly improve bioethanol productivity and sustainability, but instead it is discarded as agricultural waste or burned for energy supply in sugar and ethanol mills (Pandey et al., 2000; Rocha et al., 2012). The close association and complexity of the carbohydrate–lignin complex is the main obstacle in bioconversion. In this context, much has been invested in technology to make this process economically feasible, such as the development of an efficient pre-treatment step and optimization of enzymatic cocktails for cell wall deconstruction.

The employment of enzymes in bioconversion processes provides advantages when compared to chemical processes, such as mild reaction conditions. Moreover, product specificity and waste minimization are also advantages that make the enzymatic process eco-friendly (Rozzell, 1999). Xylanases (E.C. 3.2.1.8) are hemicellulases responsible for breaking down xylan, the major hemicellulosic component of plant cell walls, into short xylooligosaccharides by a

* Corresponding author at: Giuseppe Máximo Scolfaro Street, n° 10000, Campinas, SP 13083 970, Brazil. Tel.: +55 19 35183111; fax: +55 19 35183164.
E-mail address: fabio.squina@bioetanol.org.br (F.M. Squina).

0926-6690/$ – see front matter © 2013 Elsevier B.V. All rights reserved.
http://dx.doi.org/10.1016/j.indcrop.2013.12.005

general acid–base mechanism involving two glutamic acid residues (Davies and Henrissat, 1995). Ferulic acid esterase (FAE) is the biotechnological key to access ferulic acid (FA) in the plant cell wall. FAE belongs to carbohydrate esterase family 1 (EC 3.1.1.73), which is a subclass of the carboxylic esterases that catalyze the hydrolysis of FA ester linkages in lignin–carbohydrate complexes (Henrissat and Davies, 1997). The xylanase (XynZ) from *Clostridium thermocellum* ATCC 27405 is composed of a xylanolytic domain together with a C-terminal domain which has feruloyl esterase activity (Blum et al., 2000).

In this context, the aim of this work was to evaluate the ability of XynZ from *C. thermocellum* ATCC 27405 to produce antioxidant compounds and xylooligosaccharides from sugarcane bagasse. In order reveal the biotechnological potential of XynZ, the XOS (xylooligosaccharides) produced by hydrolysis of different substrates were identified and the antioxidant capacity (related to the released phenolic compounds) was determined.

2. Materials and methods

2.1. Cloning of XynZ from C. thermocellum

Genomic DNA of *Clostridium thermocellum* ATCC 27405 was purified using a previously described methodology (Blum et al., 2000) and stored at 4 °C without loss of integrity until the moment of use. The XynZ sequence (Cthe_1963 with NCBI-GI: 125974464), coding both xylanase and feruloyl esterase domains, was amplified from genomic DNA by means of standardized PCR reaction, adding 50 ng of the genomic DNA template from *C. thermocellum* ATCC 27405. The signal peptide was removed after sequence analysis using forward (5′-ATATATGCTAGCACCATGCCGCCTTCGGGATA-3′) and reverse (5′-TATATAGGATCCTCAATAGCCCATAAGAGCTT3-′) primers, where the NheI and BamHI endonucleases site are underlined, respectively. Remaining parameters were adjusted as recommended by the manufacturer of Phusion High-Fidelity DNA polymerase (New England BioLabs Inc., USA). The PCR reaction product was double digested with NheI and BamHI restriction enzymes and cloned into the pET28a vector, a plasmid that was optimized for protein expression in *Escherichia coli* (Novagen-USA). The *E. coli* strains DH5α and BL21 (DE3) were grown at 37 °C in Luria-Bertani (LB) medium and used as hosts for cloning and overexpression of XynZ, respectively.

2.2. Expression and purification of XynZ from E. coli

E. coli BL21 (DE3) was transformed with the pET28a/XynZ construct and plated on a selective solid LB medium containing kanamycin (50 μg/mg). A single colony was grown in liquid LB-kanamycin (50 μg/mg) for 16 h at 37 °C and 250 rpm. This pre-inoculum was inoculated in 500 mL of fresh LB-kanamycin medium and growing at the same conditions until reaching an optical density (OD 600 nm) equal to 0.6. Thus, recombinant protein expression was induced by adding IPTG (isopropyl β-D-1-thiogalactopyranoside) at final concentration of 0.5 mM. After 4 h, the cells were harvested at 8500 × *g* and stored at −20 °C.

Stored cells were re-suspended in a lysis buffer (20 mM sodium phosphate pH 7.5, 500 mM NaCl, 5 mM imidazole, 80 μg of egg lysozyme/mL and 5 mM PMSF) for 30 min in a Nutating Mixer (Labnet, USA). Cell disruption was performed in an ice bath using an ultrasonic processor (7 pulses for 10 s at 500 W; VC750 Ultrasonic Processor, Sonics Vibracell). The extract was centrifuged at 10,000 × *g* for 30 min at 4 °C and the supernatant was loaded onto a Ni^{2+}-chelating affinity column (GE Healthcare). Chromatography was carried out using a non-linear imidazole gradient from 5 to 0.5 M with 20 column volumes. To attain a homogenous sample, it was further loaded on a gel filtration Superdex 200 column (GE Healthcare), which was previously equilibrated with a 20 mM phosphate buffer (pH 7.4) containing 50 mM NaCl (Mandelli et al., 2013).

2.3. Enzymatic activity assay

The xylanase activity of xylan feruloyl esterase was evaluated according Gonçalves et al. (2012) with modifications. Enzymatic reaction mixtures consisted of 50 μL of xylan beechwood 0.5% at pH 6.0, 40 μL of citrate phosphate glycine buffer (0.1 M) and 10 μL of the purified enzyme. After 10 min the reaction was stopped by addition of 100 μL of 3,5-dinitrosalicylic acid, immediately boiled for 5 min at 99 °C and cooled (Miller, 1959). The solution was analyzed at 540 nm in an Infinite M200® spectrophotometer (Tecan-Switzerland) to measure the release of reducing sugars. Esterase activity of the purified enzyme was assessed against the substrate α-naphthylacetate according to the method previously described (Koseki et al., 2007).

2.4. Preparation of substrates for hydrolysis

Four different substrates were used in the analysis: insoluble wheat arabinoxylan (WA), purchased from Megazyme (lot 120801); *in natura* sugarcane bagasse (variety SP81-3250) (IN), graciously provided by the Usina Vale do Rosário (São Paulo, Brazil); steam-exploded sugarcane bagasse (SE), obtained from *in natura* sugarcane bagasse which was loaded into a custom-made stainless steel reactor with volume of 5 m^3, treated by saturated steam at 190 °C with a pressure of 13 $kgf\,cm^{-2}$ for 7 min and then exhaustively washed with water to remove the soluble compounds; and chemically treated sugarcane bagasse (CT) prepared by treating the *in natura* sugarcane bagasse with a 1:1 mixture of glacial acetic acid P.A. and hydrogen peroxide P.A. at 60 °C for 7 h.

2.5. Chemical composition determination

Cellulose, hemicellulose and lignin content in IN, SE and CT were determined according to Gouveia et al. (2009). Representative samples of 200 mg were hydrolyzed in two steps: 72% H_2SO_4 for 7 min at 45 °C followed by dilution to 3% H_2SO_4 for an additional 30 min at 121 °C. The samples were then quenched in ice and filtered. The cellulose and hemicellulose contents of the filtrates were determined by high-performance anion exchange-pulsed amperometric detection chromatography (HPAE–PAD) with a Dionex ICS-3000 (Thermo Fisher Scientific, USA) system using a CarboPac PA 10 column (4 mm × 250 mm Dionex, USA). The monosaccharide contents found in the hydrolysates were converted to percentage of polysaccharides. For determination of ash content, the sample was slowly calcined at 300 °C for 1 h followed by 2 h at 800 °C in a muffle. After cooling the crucible in a dissector, the ash mass was determined on an analytical balance (adequate from the standard ASTM, 1966). All these analyses were performed in triplicate.

2.6. Enzymatic hydrolysis

The capacity of XynZ to release phenolic compounds and oligosaccharides from WA, IN, SE and CT was evaluated using methods previously described (Bragatto et al., 2012; Gonçalves et al., 2012). Reaction mixtures contained 20 mg of each substrate, 0.08 mg/mL of the purified enzyme, and sodium phosphate buffer (0.1 M, pH 6.4) at the amount necessary to complete a final volume of 1 mL. The samples were incubated at 50 °C for 5 h and 1500 rpm.

After that the samples were centrifuged (12,000 × *g* for 15 min at 4 °C), and the supernatant collected for subsequent analysis. The control sample consisted of adding the inactivated enzyme (99 °C for 10 min) prior to the centrifugation step.

2.7. Capillary electrophoresis of oligosaccharides (CZE)

Oligosaccharides released by the enzyme action, as well as the standards purchased from Megazyme (xylose, xylobiose, xylotriose, xylotetraose, xylopentose and xylohexaose) were derivatized with 8-aminopyrene-1,3,6-trisulfonic acid (APTS) by reductive amination as described previously (Cota et al., 2011). Capillary electrophoresis of oligosaccharides was performed using a P/ACETM MDQ system (Beckman Coulter) with laser-induced fluorescence detection. A fused-silica capillary column (TSP050375, Polymicro Technologies) with 50 μm internal diameter and length of 31 cm was used for separation of the oligosaccharides. Samples were injected by application of 0.5 psi for 0.5 s. Electrophoresis conditions were 15 kV/70–100 μA with the cathode at the inlet, 0.1 M sodium phosphate pH 2.5 as running buffer and a controlled temperature of 20 °C. The capillary column was rinsed with 1 M NaOH followed by running the buffer with a dip-cycle to prevent carry over after injection. Oligomers labeled with APTS were excited at 488 nm and emission was collected through a 520 nm band pass filter (Gonçalves et al., 2012). Because of the small volumes of capillary electrophoresis combined with small variations in buffer strength, retention times varied slightly when comparing separate electrophoresis runs. The combined information obtained from the electrophoretic behavior and co-electrophoresis with mono and oligosaccharides standards (purchased from Megazyme) were used to identify the degradation products.

2.8. Oligosaccharides quantification

The supernatants that resulted from enzymatic hydrolysis of sugarcane pulp were analyzed by high performance anion exchange–pulsed amperometric detection (HPAE–PAD) to detect oligosaccharides released by XynZ. Separation was performed using a Dionex ICS 3000 instrument with a CarboPac PA100 column (4 mm × 250 mm) and CarboPac PA100 guard column (4 mm × 50 mm), adopting a linear gradient of A (NaOH 500 mM) and B (NaOAc 500 mM; NaOH 80 mM) and C (H_2O). Gradient program: 15% of A, 2% of B and 83% of C at 0–10 min, 15–50% of A, 2–20% of B and 83–30% of C at 10–20 min, with flow rate of 1.0 mL min^{-1}. The concentrations of each saccharide were calculated based on the construction of calibration curve with external standards (xylobiose, xylotriose, xylotetraose, xylopentaose, xylohexaose) purchased from Megazyme. The results are presented as the difference between the reaction samples and the control sample.

2.9. Quantification of total phenolic compounds

The folin–ciocalteau colorimetric method of Singleton et al. (1999) was adapted to a microplate reader (Synergy Mx; Biotek, USA). Reaction mixtures in the sample wells contained the following reagents: 150 μL of ultrapure water, 25 μL of extracts in four different concentrations (XynZ hydrolysis products), and 25 μL of the folin–ciocalteau reagent. The mixture was incubated in the microplate reader, shaken for 20 s, and then maintained at 25 °C for 5 min. This was followed by adding 100 μL of a 7% sodium carbonate solution. The absorbance signal was measured after 2 h at a wavelength of 765 nm. Results were expressed in milligrams of gallic acid equivalent per liter of extract.

2.10. Peroxyl radical scavenging assay

The peroxyl radical (ROO•) scavenging capacity was measured by monitoring fluorescence decay due to the oxidation of fluorescein according to the method of oxygen radical absorbance capacity (Damásio et al., 2012). The peroxyl radical scavenger capacity was calculated according to Ou et al. (2001). Briefly, the net protection provided by the extracts or Trolox (standard) was calculated using the difference between the area under the fluorescence decay curve in the presence of the sample (area under the curve $AUC_{extract}$) and in its absence (AUC_{blank}). Regression equations between net AUC and the sample concentrations were calculated for all extracts and Trolox. The results of the peroxyl radical scavenger capacity of the extracts were expressed as Trolox equivalents in micromoles per liter of extract.

3. Results and discussion

3.1. XynZ purification and activity

XynZ was expressed in *E. coli* BL21 (DE3) cells in the soluble fraction at 37 °C. Protein purification included two steps, first IMAC (immobilized metal ion affinity chromatography) followed by a size exclusion chromatography, which resulted in a highly purified enzyme suitable for biochemical assays. The specific activities of the protein were assayed against rye arabinoxylan and α-naphthylacetate. Values obtained were equal to 21 U/mg and 0.4 U/mg for xylanase and feruloyl esterase activity, respectively.

3.2. Substrates chemical composition

The cellulose crystalline arrangement and the lignin protective effects, as well as the hemicellulose content, together hamper enzyme access and make up an obstacle to conversion of bagasse polysaccharides into value-added products (Canettieri et al., 2007; Rocha et al., 2012). The pretreatment step of lignocellulosic biomass results in changes to the chemical composition and physical structure of substrates, including redistribution of hemicelluloses and lignin fractions, increasing the surface area and formation of pores (Grethlein, 1985). In this study, the *in natura* sugarcane bagasse was submitted to two different pretreatments strategies: steam explosion and chemical treatment.

Chemical composition of the four different substrates submitted to enzymatic hydrolysis is shown in Fig. 1. With exception of WA, which presented hemicellulose as a major compound, cellulose was the major constituent of IN, SE and CT. The lowest dry weight percentage of hemicellulose was observed in the SE substrate that also presented the highest dry weight percentage of lignin.

Rocha et al. (2012) determined the chemical composition for different varieties of sugarcane bagasse, reporting the contents of cellulose, hemicellulose and lignin as 43.1, 25.2 and 22.9%, respectively. The values showed in Fig. 1 are in full agreement with this previous report in literature. According to Rocha et al. (2012), steam explosion pretreatment removes significant amounts of hemicellulose, thus explaining the reduction in hemicellulose content described for SE bagasse in the present study. The peracetic mixture (acetic acid and hydrogen peroxide) employed in the CT pretreatment is not only considered environmentally friendly, but is a highly selective delignificant agent (Borges et al., 2001). Moreover, it can oxidize the aromatic rings of the lignin structure and expose hemicellulose and cellulose fibrils which facilitate enzymatic action (Bragatto et al., 2012, 2013).

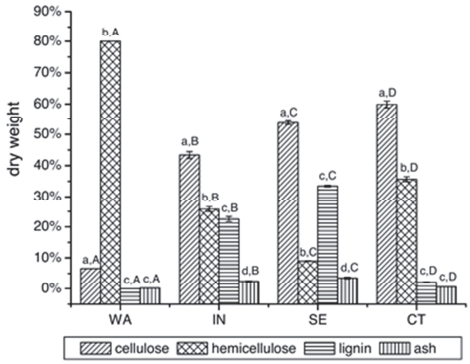

Fig. 1. Chemical composition of the substrates: wheat arabinoxylan (WA), *in natura* sugarcane bagasse (IN), steam exploded sugarcane bagasse (SE) and chemically treated sugarcane bagasse (CT). The chemical composition of WA was obtained from the specification sheet provided by Megazyme. Different letters correspond to mean values statically different by Tukey's test ($p < 0.05$), intra groups (lower case letters) and inter groups (capital letters).

3.3. XOS from enzymatic hydrolysis

The oligosaccharides present in the supernatants, after enzymatic hydrolysis using recombinant XynZ and WA, IN, SE and CT, were analyzed through capillary electrophoresis after APTS-labeling. Data shown in Fig. 2 underline the ability of XynZ to release xylose, xylobiose and short chain xylooligosaccharides from the different hemicellulosic substrates (Fig. 2). As shown in Fig. 2, the major saccharide detected after hydrolysis of WA, SE and CT was xylobiose (X2) while xylose (X1) was preferentially produced from IN. Some unidentified peaks can be attributed to oligosaccharides degradation products after APTS-labeling.

Supernatants were also analyzed by HPAE–PAD in order to quantify the xylose and XOS formed after enzymatic hydrolysis. The xylose/XOS conversion rate for each substrate was 8.6% for WA, 0.3% for IN, 2.3% for SE and 14.8% for CT. Previous studies have reported higher values of oligosaccharide production (Yoon et al., 2006; Reddy and Krishnan, 2010), however it is important to highlight that in those cases an enzymatic cocktail was used to achieve the increased conversion rates.

As shown in Fig. 3, the profile of the xylose/XOS produced was different for each substrate used, where the highest amount was obtained from hydrolysis of WA (4.52 mmol/L) followed by CT (2.98 mmol/L), SE (0.15 mmol/L) and IN (0.06 mmol/L). These results indicate that the greatest enzymatic conversion yield correlated to the lowest structural substrate complexity. Moreover, after removing lignin in the chemical treatment, the xylose-containing polysaccharides were exposed, leading the improvement of enzymatic hydrolysis and xylooligosaccharides production (Gonçalves et al., 2012; Bragatto et al., 2013).

XynZ efficiently formed xylose/XOS from all substrates; however it is important to highlight that different products were generated after enzymatic action on the different substrates. From WA the major compound released was xylobiose (67%), while from IN it was xylose (75%). Hydrolysis of SE released almost the same amount of xylose (42%) and xylobiose (45%). CT was the substrate that provided the greatest yield of xylo-oligos with high degree of

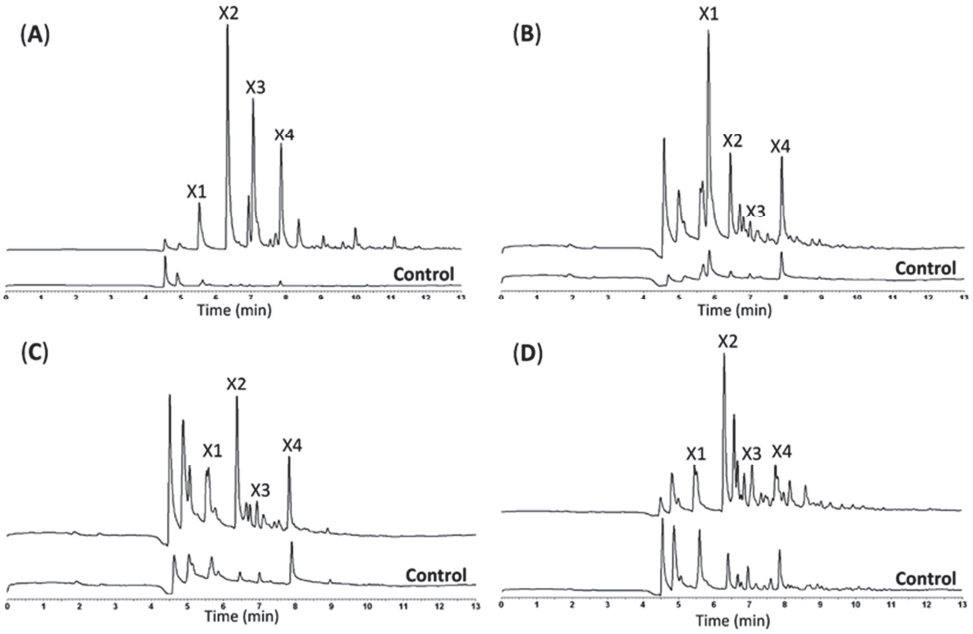

Fig. 2. Capillary electrophoresis of APTS-labeled oligosaccharide products released by XynZ after hydrolysis of the substrates: (A) wheat arabinoxylan; (B) *in natura* sugarcane bagasse; (C) steam exploded sugarcane bagasse; and (D) chemically treated sugarcane bagasse.

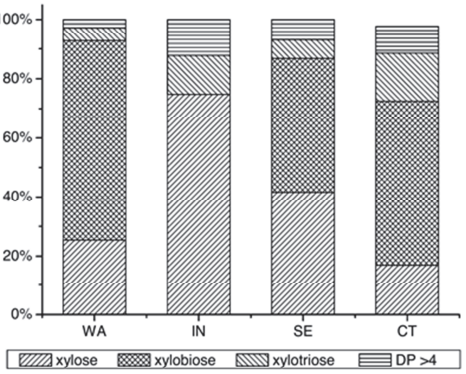

Fig. 3. HPAE–PAD analysis of xylose and oligosaccharides released from the substrates WA, IN, SE and CT after hydrolysis with XynZ. The concentrations were calculated using a standard curve of xylobiose, xylotriose, xylotetraose, xylopentaose and xylohexaose (Megazyme, USA). DP – degree of polymerization.

polymerization, up to 5%. Therefore, these experiments indicated an interesting strategy to direct the production of different types of XOS.

XOS have potential applications in a wide range of fields. In the food industry, XOS can be used in functional foods due to the positive effects that oligosaccharides have on gastrointestinal microbiota which promote several benefits to human health (Gullon et al., 2010; Teng et al., 2010; Yang et al., 2011). The preferred degree of the XOS polymerization ranges from 2 to 4 for food related applications (Loo et al., 1999). Xylobiose can also be employed as a sweetener due to its degree of sweetness of 30% when compared to sucrose and its low calorie characteristics (Toshio et al., 1990). In pharmaceuticals, XOS offers advantages when compared with other oligosaccharides in terms of stability and beneficial effects such as stimulating the growth of probiotics such as *Lactobacillus* spp., noncariogenicity and inhibiting the growth of pathogenic microorganisms, providing a number of benefits to the digestive and immune system (Chapla et al., 2012). XOS has acceptable organoleptic properties and does not exhibit toxicity or negative effects on human health (Nabarlatz et al., 2005).

3.4. Antioxidant capacity

Ferulic and ρ-coumaric acids are the major hydroxycinnamic acids of sugarcane (Xu et al., 2005). Although the alkali treatment is a simple and cheap method to extract hydroxycinnamic acids from plant biomass, other by-products are concurrently formed, and the salts produced after alkali neutralization impair the subsequent purification steps. As an alternative, feruloyl esterases can provide a clean and environmentally friendly route for the production of hydroxycinnamates from lignocellulosic materials (Fazary and Ju, 2008).

The use of XynZ allowed for the production of value added compounds, such as phenolic acids known for their antioxidant capacity, from agro-industrial by-products. Total phenolic compounds (TP) and ROO• scavenging capacity derived from XynZ treatment of WA, IN, SE and CT are shown in Table 1.

The best result for phenolic compounds and ROO• scavenging capacity was observed using WA as substrate compared to sugarcane bagasse. This was expected because WA is a commercial substrate which exhibits high purity, low cellulose content and no lignin, furthermore it is carefully extracted and purified from wheat to maintain the ferulic acid crosslinks in the native arabinoxylan.

Table 1
Total phenolic compounds and peroxyl scavenging capacity derived by XynZ treatment.

Substrate	Phenolic compounds (mg GAE/L)[a]	ROO• scavenger capacity (μmol TE/L)[a]
Wheat arabinoxylan	106.1 ± 8.4	2300.5 ± 190.5
In natura sugarcane bagasse	22.0 ± 2.7	400.6 ± 170.9
Steam exploded sugarcane bagasse	78.3 ± 2.7	320.0 ± 3.8
Chemically treated sugarcane bagasse	56.7 ± 1.5	695.8 ± 105.3

GAE, gallic acid equivalent; TE, trolox equivalent.

[a] Values shown are the difference between the reaction samples and the control sample (see Section 2.10). The values of the control samples were 24.97 ± 5.77 and 437.89 ± 62.63 for WA, 42.06 ± 4.61 and 821.94 ± 22.19 for IN, 146.9 ± 25.9 and 2080 ± 84.9 for SE and 85.52 ± 9.06 and 2063.78 ± 11.84 for CT, respectively, for phenolic compounds (mg GAE/L) and ROO• scavenger capacity (μmol TE/L).

It is important to highlight that XynZ efficiently released phenolic compounds from all substrates (Table 1), and as previously reported in many studies, a correlation was also found between TP and antioxidant capacity, since the main mechanism of ROO• scavenging is a hydrogen atom transfer by the phenolic compounds (Huang et al., 2005).

The values of TP and ROO• scavenging capacity were 2 times higher for WA and 4 times higher for CT than those obtained by Damásio et al. (2012) working with the enzyme AcFAE from *Aspergillus clavatus*. These results suggest that the association between xylanase and feruloyl esterase of the XynZ had a positive effect on the production of phenolic compounds with high antioxidant capacity from plant biomass.

Interest in the industrial use of hydroxycinnamic acids is growing due to their antioxidant capacity and health benefits. The extraction of these phenolic compounds from biomass via the breakdown of the ester linkages with polymers has allowed the exploitation of such compounds for pharmaceutical, industrial and food applications (Benoit et al., 2006).

4. Conclusions

Our findings demonstrated the biotechnological potential for use of XynZ from *C. thermocellum* ATCC 27405 in the hydrolysis of agro-industrial residue by-products such as sugarcane bagasse. The bi-functionality of XynZ allowed for simultaneous extraction of probiotic xylooligosaccharides and antioxidant compounds from plant biomass. Seeking out industrial applications and taking into account the difficulty in preparing efficient enzyme cocktails, chimeric enzymes such as XynZ are appealing for biomass to bioproducts applications, as previously described by others (Cota et al., 2013).

The highest xylose/XOS and phenolics production yield were observed after enzymatic hydrolysis of WA followed by CT, SE and IN. Therefore, as the substrate complexity decreases, greater was the ability of the enzyme to produce these higher-value compounds. In order for economically feasible production of antioxidant compounds and XOS from agricultural wastes, it is essential to determinate the optimal pre-treatment and the best enzyme:substrate combination to be used, as well as the additional enzymatic activities that would be needed. It was also observed that each substrate showed a different XOS profile, which might be of biotechnological interest for the development of new enzymatic routes for the production of higher-value bioproducts from plant structural polysaccharides.

Acknowledgments

This work was financially supported by grants from CNPq (474022/2011-4 and 310177/2011-1) and FAPESP (2008/58037-9). FM received fellowship from CNPq (142685/2010-0). ZBH, RG and LBB received a fellowship from FAPESP (2011/14200-6, 2012/18859-5 and 2013/03061-0, respectively).

References

Akpinar, O., Erdogan, K., Bostanci, S., 2009. Production of xylooligosaccharides by controlled acid hydrolysis of lignocellulosic materials. Carbohydr. Res. 344, 660–666.

Benoit, I., Navarro, D., Marnet, N., Rakotomanomana, N., Lesage-Meesen, L., Sigoillot, J.C., Asther, M., Asther, M., 2006. Feruloyl esterases as a tool for the release of phenolic compounds from agro-industrial by-products. Carbohydr. Res. 341, 1820–1827.

Betancur, G.J.V., Pereira Jr., N., 2010. Sugar cane bagasse as feedstock for second generation ethanol production. Part I: Diluted acid pretreatment optimization. Electron. J. Biotechnol. 13, 1–9.

Blum, D.L., Schubot, F.D., Ljungdahl, L.G., Rose, J.P., Wang, B.-C., 2000. Crystallization and preliminary X-ray analysis of the *Clostridium thermocellum* cellulosome xylanase Z feruloyl esterase domain. Acta Crystallogr. D 56, 1027–1029.

Borges, L., Colodette, J.L., Pilo-Veloso, D., 2001. A utilização de perácidos na deslignificação e no branqueamento de polpas celulósicas. Quim. Nova 24, 819–829.

Bragatto, J., Segato, F., Cota, J., Mello, D.B., Oliveira, M.M., Buckeridge, M.S., Squina, F.M., Driemeier, C., 2012. Insights on how the activity of an endoglucanase is affected by physical properties of insoluble celluloses. J. Phys. Chem. B 116, 6128–6136.

Bragatto, J., Segato, F., Squina, F.M., 2013. Production of xylooligosaccharides (XOS) from delignified sugarcanebagasse by peroxide-HAc process using recombinant xylanase from *Bacillus subtilis*. Ind. Crops Prod. 51, 123–129.

Canettieri, E., Rocha, G.J.M., de Carvalho, J.R., Silva, J.B.A., 2007. Optimization of acid hydrolysis from the hemicellulosic fraction of the *Eucalyptus grandis* residue using response surface methodology. Bioresour. Technol. 98, 422–428.

Chapla, D., Pandit, P., Shah, A., 2012. Production of xylooligosaccharides from corncob xylan by fungal xylanase and their utilization by probiotics. Bioresour. Technol. 115, 215–221.

Cota, J., Alvarez, T.M., Citadini, A.P., Santos, C.R., de Oliveira Neto, M., Oliveira, R.R., Pastore, G.M., Ruller, R., Prade, R.A., Murakami, M.T., Squina, F.M., 2011. Mode of operation and low-resolution structure of a multi-domain and hyperthermophilic endo-b-1,3-glucanase from *Thermotoga petrophila*. Biochem. Biophys. Res. Commun. 406, 590–594.

Cota, J., Oliveira, L.C., Damásio, A.R.L., Citadini, A.P., Hoffmam, Z.B., Alvarez, T.M., Codima, C.A., Leite, V.B.P., Pastore, G., Oliveira-Neto, M., Murakami, M.T., Ruller, R., Squina, F.M., 2013. Assembling a xylanase–lichenase chimera through all-atom molecular dynamics simulations. Biochim. Biophys. Acta 1834, 1492–1500.

Damásio, A.R., Braga, C.M., Brenelli, L.B., Citadini, A.P., Mandelli, F., Cota, J., de Almeida, R.F., Salvador, V.H., Paixao, D.A., Segato, F., Mercadante, A.Z., de Oliveira Neto, M., do Santos, W.D., Squina, F.M., 2012. Biomass-to-bio-products application of feruloyl esterase from *Aspergillus clavatus*. Appl. Microbiol. Biotechnol. 97, 6759–6767.

Davies, G., Henrissat, B., 1995. Structures and mechanisms of glycosyl hydrolases. Structure 3, 853–859.

Fazary, A.E., Ju, Y.H., 2008. The large-scale use of feruloyl esterases in industry. Biotechnol. Mol. Biol. Rev. 3, 95–110.

Gonçalves, T.A., Damásio, A.R.L., Segato, F., Alvarez, T.M., Bragatto, J., Brenelli, L.B., Citadini, A.P.S., Murakami, M.T., Ruller, R., Paes Leme, A.F., Prade, R.A., Squina, F.M., 2012. Functional characterization and synergic action of fungal xylanase and arabinofuranosidase for production of xylooligosaccharides. Bioresour. Technol. 119, 293–299.

Gouveia, E.R., Nascimento, R.T., Souto-Maior, A.M., Rocha, G.J.M., 2009. Avaliação de metodologia para a caracterização química do bagaço de cana-de-açúcar. Quim. Nova 32, 1500–1503.

Grethlein, H.E., 1985. The effect of pore size distribution on the rate of enzymatic hydrolysis of cellulosic substrates. Nat. Biotechnol. 3, 155–160.

Gullon, B., Yanez, R., Alonso, J.L., Parajo, J.C., 2010. Production of oligosaccharides and sugars from rye straw: a kinetic approach. Bioresour. Technol. 101, 6676–6684.

Henrissat, B., Davies, G., 1997. Structural and sequence-based classification of glycoside hydrolases. Curr. Opin. Struct. Biol. 7, 637–644.

Huang, D., Ou, B., Prior, R.L., 2005. The chemistry behind antioxidant capacity assays. J. Agric. Food Chem. 53, 1841–1856.

Jayapal, N., Samanta, A.K., Kolte, A.P., Senani, S., Sridhar, M., Suresh, K.P., Sampath, K.T., 2013. Value addition to sugarcane bagasse: xylan extraction and its process optimization for xylooligosaccharides production. Ind. Crops Prod. 42, 14–24.

Koseki, T., Mimasaka, N., Hashizume, K., Shiono, Y., Murayama, T., 2007. Stimulatory effect of ferulic acid on the production of extracellular xylanolytic enzymes by *Aspergillus kawachii*. Biosci. Biotechnol. Biochem. 71, 1785–1787.

Loo, J.V., Cummings, J., Delzenne, N., Englyst, H., Franck, A., Hopkins, M., Kok, N., Macfarlane, G., Newton, D., Quigley, M., Roberfroid, M., van Vliet, T., van den Heuvel, E., 1999. Functional food properties of nondigestible oligosaccharides: a consensus report from the ENDO Project (DGXII-AIRII-CT94-1095). Br. J. Nutr. 81, 121–132.

Mandelli, F., Franco Cairo, J.P.L., Citadini, A.P.S., Büchli, F., Alvarez, T.M., Oliveira, R.J., Leite, V.B.P., Paes Leme, A.F., Mercadante, A.Z., Squina, F.M., 2013. The characterization of a thermostable and cambialistic superoxide dismutase from *Thermus filiformis*. Lett. Appl. Microbiol. 57, 40–46.

Miller, G.L., 1959. Use of dinitrosalicylic acid reagent for determination of reducing sugar. Anal. Chem. 31, 426–428.

Nabarlatz, D., Farriol, X., Montane, D., 2005. Autohydrolysis of almond shells for the production of xylooligosaccharides: product characteristics and reaction kinetics. Ind. Eng. Chem. Res. 44, 7746–7755.

Ou, B., Hampsch-Woodill, M., Prior, R.L., 2001. Development and validation of an improved oxygen radical absorbance capacity assay using fluorescein as the fluorescent probe. J. Agric. Food Chem. 49, 4619–4626.

Pandey, A., Soccol, C.R., Nigam, P., Brand, D., Mohan, R., Roussous, S., 2000. Biotechnological potential of coffee pulp and coffee husk for bioprocesses. Biochem. Eng. J. 6, 153–162.

Reddy, S.S., Krishnan, C., 2010. Production of prebiotics and antioxidants as health food supplements from lignocellulosic materials using multi enzymatic hydrolysis. Int. J. Chem. Sci. 8, S535–S549.

Rezende, C.A., de Lima, M.A., Maziero, P., de Azevedo, E.R., Garcia, W., Polikarpov, I., 2011. Chemical and morphological characterization of sugarcane bagasse submitted to a delignification process for enhanced enzymatic digestibility. Biotechnol. Biofuels 54, 1–18.

Rocha, G.J.M., Gonçalves, A.R., Oliveira, B.R., Olivares, E.G., Rossell, C.E.V., 2012. Steam explosion pretreatment reproduction and alkaline delignification reactions performed on a pilot scale with sugarcane bagasse for bioethanol production. Ind. Crops Prod. 35, 274–279.

Rozzell, J.D., 1999. Commercial Scale biocatalysis: myths and realities. Bioorg. Med. Chem. 7, 2245–2261.

Singleton, V.L., Orthofer, R., Lamuela-Raventes, R.M., 1999. Analysis of total phenols and other oxidation substrates and antioxidants by means of folin–ciocalteu reagent. Methods Enzymol. 299, 152–178.

Sultana, B.B., Anwar, F., Asi, M.R., Chatha, S.A.S., 2008. Antioxidant potential of extracts from different agro wastes: stabilization of corn oil. Grasas Aceites 59, 205–217.

Teng, C., Yan, Q., Jiang, Z., Fan, G., Shi, B., 2010. Production of xylooligosaccharides from the steam explosion liquor of corncobs coupled with enzymatic hydrolysis using a thermostable xylanase. Bioresour. Technol. 101, 7679–7682.

Toshio, I., Noriyoshi, I., Toshiaki, K., Toshiyuki, N., Kunimasa, K., 1990. Production of xylobiose. Japanese Patent JP 2119790.

Xu, F., Sun, R.C., Sun, J.X., Liu, C.F., He, B.H., Fan, J.S., 2005. Determination of cell wall ferulic and p-coumaric acids in sugarcane bagasse. Anal. Chim. Acta 552, 207–217.

Yang, H., Wang, K., Song, X., Xu, F., 2011. Production of xylooligosaccharides by xylanase from *Pichia stipitis* based on xylan preparation from triploid *Populas tomentosa*. Bioresour. Technol. 102, 7171–7176.

Yoon, K.Y., Woodams, E.E., Hang, Y.D., 2006. Enzymatic production of pentoses from the hemicellulose fraction of corn residues. LWT - Food Sci. Technol. 39, 388–392.